



National Library
of Canada

Acquisitions and
Bibliographic Services Branch

395 Wellington Street
Ottawa, Ontario
K1A 0N4

Bibliothèque nationale
du Canada

Direction des acquisitions et
des services bibliographiques

395, rue Wellington
Ottawa (Ontario)
K1A 0N4

Your file Votre référence

Our file Notre référence

NOTICE

The quality of this microform is heavily dependent upon the quality of the original thesis submitted for microfilming. Every effort has been made to ensure the highest quality of reproduction possible.

If pages are missing, contact the university which granted the degree.

Some pages may have indistinct print especially if the original pages were typed with a poor typewriter ribbon or if the university sent us an inferior photocopy.

Reproduction in full or in part of this microform is governed by the Canadian Copyright Act, R.S.C. 1970, c. C-30, and subsequent amendments.

AVIS

La qualité de cette microforme dépend grandement de la qualité de la thèse soumise au microfilmage. Nous avons tout fait pour assurer une qualité supérieure de reproduction.

S'il manque des pages, veuillez communiquer avec l'université qui a conféré le grade.

La qualité d'impression de certaines pages peut laisser à désirer, surtout si les pages originales ont été dactylographiées à l'aide d'un ruban usé ou si l'université nous a fait parvenir une photocopie de qualité inférieure.

La reproduction, même partielle, de cette microforme est soumise à la Loi canadienne sur le droit d'auteur, SRC 1970, c. C-30, et ses amendements subséquents.

UNIVERSITY OF ALBERTA

EXPERIMENTAL INVESTIGATION OF FOAM FLOW IN POROUS MEDIA

by

NASSER SALIM ALBARTAMANI



A THESIS

**SUBMITTED TO THE FACULTY OF GRADUATE STUDIES AND RESEARCH
IN PARTIAL FULFILLMENT OF THE REQUIREMENTS FOR THE DEGREE OF
MASTER OF SCIENCE**

IN

PETROLEUM ENGINEERING

**DEPARTMENT OF MINING, METALLURGICAL AND PETROLEUM
ENGINEERING**

**EDMONTON, ALBERTA
SPRING, 1996**



National Library
of Canada

Acquisitions and
Bibliographic Services Branch

395 Wellington Street
Ottawa, Ontario
K1A 0N4

Bibliothèque nationale
du Canada

Direction des acquisitions et
des services bibliographiques

395, rue Wellington
Ottawa (Ontario)
K1A 0N4

Your file Votre référence

Our file Notre référence

The author has granted an irrevocable non-exclusive licence allowing the National Library of Canada to reproduce, loan, distribute or sell copies of his/her thesis by any means and in any form or format, making this thesis available to interested persons.

L'auteur a accordé une licence irrévocable et non exclusive permettant à la Bibliothèque nationale du Canada de reproduire, prêter, distribuer ou vendre des copies de sa thèse de quelque manière et sous quelque forme que ce soit pour mettre des exemplaires de cette thèse à la disposition des personnes intéressées.

The author retains ownership of the copyright in his/her thesis. Neither the thesis nor substantial extracts from it may be printed or otherwise reproduced without his/her permission.

L'auteur conserve la propriété du droit d'auteur qui protège sa thèse. Ni la thèse ni des extraits substantiels de celle-ci ne doivent être imprimés ou autrement reproduits sans son autorisation.

ISBN 0-612-10693-4

Canada

UNIVERSITY OF ALBERTA

RELEASE FORM

NAME OF AUTHOR: Nasser Salim Albartamani
TITLE OF THESIS: Experimental Investigation of Foam Flow in Porous Media
DEGREE : Master of Science
YEAR THIS DEGREE GRANTED: 1996

Permission is hereby granted to the University of Alberta Library to reproduce single copies of this thesis and to lend or sell such copies for private, scholarly, or scientific research purposes only.

The author reserves all other publication and other rights in association with the copyright in the thesis, and except as hereinbefore provided, neither the thesis nor any substantial portion thereof may be printed or otherwise reproduced in any material form whatever without the author's prior written permission.

..........

Permanent Address:

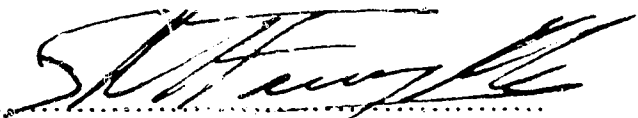
P.O. Box 768
Nizwa - 611
Sultanate of Oman

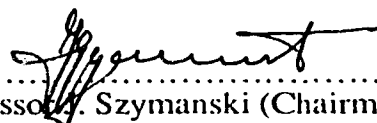
DATED: April 12, 1996

UNIVERSITY OF ALBERTA

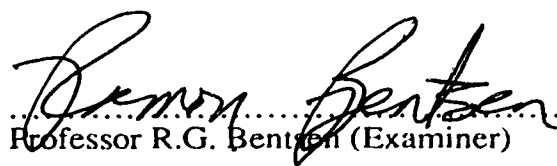
FACULTY OF GRADUATE STUDIES AND RESEARCH

The undersigned certify that they have read, and recommend to the Faculty of Graduate Studies and Research for acceptance, a thesis entitled EXPERIMENTAL INVESTIGATION OF FOAM FLOW IN POROUS MEDIA submitted by NASSER SALIM ALBARTAMANI in partial fulfillment of the requirements for the degree of Master of Science in Petroleum Engineering.


.....
Professor S.M. Farooq Ali (Supervisor)


.....
Professor A. Szymanski (Chairman)


.....
Professor J.D. Scott (External Examiner)


.....
Professor R.G. Benton (Examiner)

DATED: April 7, 76

Abstract

The main objective of this experimental work was to investigate the mechanisms of foam flow in porous media.

Investigations were directed towards the use of surfactant solutions along with a gas phase in order to displace oil from the reservoir. Foam was used as an oil-displacing fluid. However, when displacing oil, foam was not effective due to the detrimental effect of oil on the surfactant.

A series of experiments were performed to study the effect of slug size and gas flow rate and to investigate the different injection strategies in foam flooding. Results show that there was an optimum surfactant slug size of 20% pore volume in the case of two-phase water-gas displacement. The total foam mobility increased with increasing surfactant slug size. In experiments involving oil, no optimum surfactant slug was found in the range tested, 2.5 to 25% pore volume.

Two gas flow rates were investigated, 8 and 1.75 cc/min. Both flow rates gave almost the same recovery at gas breakthrough; however, the higher rate produced higher pressure gradients.

Pressure profiles in the core were monitored using five pressure transducers along the length of the core. Pressure distributions as a function of time were recorded by an Easy Sense data acquisition system. Higher pressure gradients were encountered in experiments performed with no oil present than in ones involving oil.

From the pressure responses, two foam flow regimes were identified. In experiments conducted in the absence of oil, foam propagates as a frontal movement rather than in situ foam mobilization. In experiments carried out in the presence of oil, foam tended to break and reform.

Acknowledgements

I wish to express my sincere appreciation to my academic supervisor, Dr. S.M. Farouq Ali for his guidance and support throughout the course of this study.

I am also grateful to Mr. John Czuroski for his help in obtaining the surfactants and for measuring the viscosity of the oil used in this study. I thank Mr. Robert Smith for his help in construction of the physical model. Also my thanks go to Dr. S. Thomas for her help in the calibration of the spectrophotometer instrument for measuring the surfactant concentration.

I am indebted to Petroleum Development Oman Company (PDO) for funding this study.

I wish to thank all the staff at the Scholars Administration in Shell Oil Co, Houston who helped me directly or indirectly during my stay in Edmonton. In particular, I would like to thank Mr. B. E. Stubbs for his support and encouragement.

Finally, I would like to thank my family and my parents for their enduring patience, and support.

Table of Contents

Chapter 1: Introduction	1
Chapter 2: Review of the Literature	2
2.1 Foam Application in the Oilfield.....	2
2.2 Foam Characterization	3
2.2.1 Quality.....	3
2.2.2 Texture.....	3
2.2.3 Foam Stability and Resiliency.....	4
2.3 Foam Rheology.....	6
2.4 Mechanisms of Foam Generation in Porous Media	9
2.4.1 Leave-behind Mechanism	10
2.4.2 Snap-off Mechanism.....	10
2.4.3 Lamella Division Mechanism	11
2.5 Foam Flow in Porous Media.....	11
2.6 Factors Affecting Foam Flow in Porous Media	16
2.6.1 Foam Texture	16
2.6.2 Foam Quality.....	17
2.6.3 Permeability of Porous Medium.....	17
2.6.4 Fluid Saturations	17
2.6.5 Trapped Gas Saturation.....	18
2.6.6 Gas Velocity	18
2.6.7 Presence of Oil.....	19
2.6.8 Temperature.....	20
2.6.9 Surfactant Concentration	20
2.7 Modeling Foam Flow in Porous Media.....	21
2.7.1 Population Balance.....	21

Chapter 3: Objectives.....	26
Chapter 4: Experimental Apparatus and Procedure	27
4.1 Experimental Apparatus.....	27
4.1.1 Physical Model.....	27
4.1.2 Materials and Fluids.....	27
4.1.3 Injection System.....	31
4.1.4 Production System.....	32
4.1.5 Data Acquisition System	32
4.2 Model Preparation.....	34
4.2.1 Packing Procedure.....	34
4.2.2 Saturation Process.....	36
4.3 Experimental Procedure.....	36
4.4 Sample Analysis.....	37
Chapter 5: Discussion of Results.....	40
5.1 Presentation of Results.....	40
5.2 Base Case Experiment for Water Runs	44
5.3 Type of Surfactant.....	44
5.3.1 Witcolate-1247H Surfactant.....	49
5.3.2 Witcolate-1276 Surfactant.....	56
5.3.3 Dowfax-8390 Surfactant	56
5.3.4 Overall Evaluation of the Surfactants Tested.....	63
5.4 Slug Injection Runs	71
5.4.1 Typical Slug Injection Run.....	71
5.4.2 Surfactant Slug Injection Experiments for Water Saturated Sand Packs.....	77
5.4.2.1 Surfactant Slug Injection Experiments for Water Saturated Sand Packs Displaced By a Gas Flowing at 8 cc/min.....	77

5.4.2.2 Overall Evaluation of Surfactant Slug Injection Experiments for Water Saturated Sand Packs Displaced By a Gas Flowing at 8 cc/min	89
5.4.2.3 Surfactant Slug Injection Experiments for Water Saturated Sand Packs Displaced By a Gas Flowing at 1.75 cc/min.....	97
5.4.2.4 Overall Evaluation of Surfactant Slug Injection Experiments for Water Saturated Sand Packs Displaced By a Gas Flowing at 1.75 cc/min	102
5.4.3 Surfactant Slug Injection Experiments for Sand Packs Involving Residual Oil.....	102
5.4.3.1 Base Case for Oil Runs.....	105
5.4.3.2 Surfactant Slug Injection Experiments for Sand Packs Water Saturated at Residual Oil Displaced By a Gas Flowing at 8 cc/min	105
5.4.3.3 Overall Evaluation of Surfactant Slug Injection Experiments for Sand Packs Water Saturated at Residual Oil Displaced By a Gas Flowing at 8 cc/min	117
5.4.3.4 Surfactant Slug Injection Experiments for Sand Packs Water Saturated at Residual Oil Displaced By a Gas Flowing at 1.75 cc/min	123
5.5 Injection Strategy	132
5.6 Foam Flow Mechanisms	139
5.7 Reproducibility of Results.....	151
Chapter 6: Conclusions	158
Chapter 7: Recommendations	159
References.....	160
Appendix A: Tabulated Experimental Results	167
Appendix B: Data For the Surfactants Used	180

List of Tables

Table 5.1:	Summary of Experimental Runs Conducted in This Research.....	42
Table 5.2:	Experimental Data for Run 25, Water Base Case.....	45
Table 5.3:	Summary of Runs Performed to Test and Compare Three Surfactants	48
Table 5.4:	Experimental Data for Run 1 Using Witcolate-1247H in a Slug of 10% PV.	50
Table 5.5:	Experimental Data for Run 3 Using Witcolate-1247H.....	52
Table 5.6:	Experimental Data for Run 12 Using Witcolate-1247H in a Slug of 10% PV.	54
Table 5.7:	Experimental Data for Run 8 Using Witcolate-1276 in a Slug of 10% PV.	57
Table 5.8:	Experimental Data for Run 9 Using 1% Witcolate-1276 in a Slug of 10% PV.	59
Table 5.9:	Experimental Data for Run 10 Using Witcolate-1276	61
Table 5.10:	Experimental Data for Run 5 Using Dowfax-8390 in a Slug of 10% PV.....	64
Table 5.11:	Experimental Data for Run 6 Using Dowfax-8390 in a Slug of 10% PV.....	66
Table 5.12:	Experimental Data for Run 7 Using Dowfax-8390 in a Slug of 10% PV.....	68
Table 5.13:	Summary of Overall Evaluation of Runs Performed to Test and Compare Three Surfactants.	70
Table 5.14:	Experimental Data for Run 38 Using 10% Dowfax-8390 in a Slug of 20% PV.....	73
Table 5.15:	Experimental Data for Run 19 Using 10% Dowfax-8390 in a Slug of 20% PV.....	78
Table 5.16:	Experimental Data for Run 20 Using 10% Dowfax-8390 in a Slug of 5% PV.....	168
Table 5.17:	Experimental Data for Run 22 Using 10% Dowfax-8390 in a Slug of 25% PV.....	169
Table 5.18:	Experimental Data for Run 23 Using 10% Dowfax-8390 in a Slug of 2.5% PV.....	170

Table 5.19:	Experimental Data for Run 24 Using 10% Dowfax-8390 in a Slug of 10% PV.....	171
Table 5.20:	Summary of Analysis of Runs 19 to 25, Slug Injection Experiments Where Water was Displaced By Nitrogen at a Flow Rate of 8 cc/min.	92
Table 5.21:	Experimental Data for Run 37 Using 10% Dowfax-8390 in a Slug of 2.5% PV.....	98
Table 5.22:	Experimental Data for Run 40 Using 10% Dowfax-8390 in a Slug of 10% PV.....	172
Table 5.23:	Experimental Data for Run 28, Oil Base Case, Nitrogen Displacing Water at Residual Oil Saturation.....	106
Table 5.24:	Experimental Data for Run 26 Using 10% Dowfax-8390 and a Slug of 20% PV, Run Conducted in Presence of Oil.	109
Table 5.25:	Experimental Data for Run 27 Using 10% Dowfax-8390 and a Slug of 5% PV Run Conducted in Presence of Oil.....	173
Table 5.26:	Experimental Data for Run 29 Using 10% Dowfax-8390 in a Slug of 10% PV, Run Conducted in Presence of Oil.	174
Table 5.27:	Experimental Data for Run 30 Using 10% Dowfax-8390 in a Slug of 2.5% PV, Run Conducted in Presence of Oil.	175
Table 5.28:	Experimental Data for Run 31 Using 10% Dowfax-8390 in a Slug of 25% PV, Run Conducted in Presence of Oil.	176
Table 5.29:	Experimental Data for Run 32 Using 10% Dowfax-8390 in a Slug of 2.5% PV, Run Conducted in Presence of Oil.	177
Table 5.30:	Experimental Data for Run 33 Using 10% Dowfax-8390 in a Slug of 10% PV, Run Conducted in Presence of Oil.	178
Table 5.31:	Experimental Data for Run 36 Using 10% Dowfax-8390 and a Slug of 20% PV, Run Conducted in Presence of Oil.	179
Table 5.32:	Experimental Data for Run 35 ,Using 10% Dowfax-8390 in a 20% PV Slug, Nitrogen Displacing Oil.	132
Table 5.33:	Experimental Data for Run 15, Nitrogen-Surfactant Co-injection.....	136
Table 5.34:	Experimental Data for Run 34, 10% Dowfax-8390, Nitrogen Surfactant Co-injection.	140
Table 5.35:	Experimental Data for Run 21 Using 10% Dowfax-8390 in a Slug of 10% PV.....	152

Table 5.36:	Experimental Data for Run 33-R Using 10% Dowfax-8390 in a Slug of 10% PV, Run Conducted in Presence of Oil.	153
Table 5.37:	Experimental Data for Run 41, Repeat of Run 6	154

List of Figures

Figure 4.1:	Schematic View of the Experimental Setup	28
Figure 4.2:	Cross-Sectional View of the Physical Model	29
Figure 4.3:	Schematic Overview of the Transducers Layout.....	30
Figure 4.4:	Schematic Representation of the Production System.....	33
Figure 4.5:	Calibration Curve of Concentration Versus Absorbance for Dowfax-8390 Surfactant Determined by Spectronic-21 Spectrophotometer.....	39
Figure 5.1:	Flow Chart of the Experimental Runs Performed in This Research	41
Figure 5.2:	Run 25, Base Case: Production Data Versus Time and Totalizer Reading Versus Time for Nitrogen Displacing Water.	46
Figure 5.3:	Run 25, Water Base: Pressure Profile of Nitrogen Displacing Surfactant-Free Water at a Gas Flow Rate of 8 cc/min.	47
Figure 5.4:	Run 1: Cumulative Production Versus Time and Pressure Profile for a Slug of 10% (PV) Having 1% Witcolate-1247H Surfactant Concentration.....	51
Figure 5.5:	Run 3: Cumulative Production Versus Time and Pressure Profile for a Slug of 10% (PV) Having 10% Witcolate-1247H Surfactant Concentration.....	53
Figure 5.6:	Run 12: Cumulative Production Versus Time and Pressure Profile for a Slug of 10% (PV) Having 1% Witcolate-1247H Surfactant Concentration.....	55
Figure 5.7:	Run 8: Cumulative Production Versus Time and Pressure Profile for a Slug of 10% (PV) Having a 10% Witcolate-1276 Surfactant Concentration.....	58
Figure 5.8:	Run 9: Cumulative Production Versus Time and Pressure Profile for a Slug of 10% (PV) Having 10% Witcolate-1276 Surfactant Concentration, Conducted in Presence of Oil.....	60
Figure 5.9:	Run 10: Cumulative Production Versus Time and Pressure Profile for a Slug of 10% (PV) Having 10% Witcolate-1276 Surfactant Concentration.....	62
Figure 5.10:	Run 5: Cumulative Production Versus Time and Pressure Profile for a Slug of 10% (PV) Having 10% Dowfax-8390 Surfactant Concentration.....	65
Figure 5.11:	Run 6: Cumulative Production Versus Time and Pressure Profile for a Slug of 10% (PV) Having 10% Dowfax-8390 Surfactant Concentration.....	67

Figure 5.12:	Run 7: Cumulative Production Versus Time and Pressure Profile for a Slug of 10% (PV) Having 10% Dowfax-8390 Surfactant Concentration.	69
Figure 5.13:	Run 38: Pressure Profile Using 10% Surfactant Concentration in a Slug size of 20% PV Displaced by a Gas Flow Rate of 1.75 cc/min.	74
Figure 5.14:	Run 38: Cumulative Production Versus Time and Concentration Versus Time for a Slug of 20% (PV) Having a 10% Dowfax-8390 Surfactant Concentration.	76
Figure 5.15:	Run 19: Cumulative Production Versus Time and Concentration Versus Time for a Slug of 20% (PV) Having a 10% Dowfax-8390 Surfactant Concentration.	80
Figure 5.16:	Run 19: Pressure Profile, Using 10% Surfactant Concentration in a Slug Size of 20% PV displaced by a Gas Flow Rate of 8 cc/min.	81
Figure 5.17:	Run 20: Cumulative Production Versus Time and Concentration Versus Time for a Slug of 5% (PV) Having a 10% Dowfax-8390 Surfactant Concentration.	82
Figure 5.18:	Run 20: Pressure Profile Using 10% Surfactant concentration in a Slug size of 5% PV Displaced by a Gas Flow Rate of 8 cc/min.	83
Figure 5.19:	Run 22: Cumulative Production Versus Time and Concentration Versus Time for a Slug of 25% (PV) Having a 10% Dowfax-8390 Surfactant Concentration.	85
Figure 5.20:	Run 22: Pressure Profile Using 10% Surfactant concentration in a Slug size of 25% PV Displaced by a Gas Flow Rate of 8 cc/min.	86
Figure 5.21:	Run 23: Cumulative Production Versus Time and Concentration Versus Time for a Slug of 2.5% (PV) Having a 10% Dowfax-8390 Surfactant Concentration.	87
Figure 5.22:	Run 23: Pressure Profile Using 10% Surfactant concentration in a Slug size of 2.5% PV Displaced by a Gas Flow Rate of 8 cc/min.	88
Figure 5.23:	Run 24: Cumulative Production Versus Time and Concentration Versus Time for a Slug of 10% (PV) Having a 10% Dowfax-8390 Surfactant Concentration.	90
Figure 5.24:	Run 24: Pressure Profile Using 10% Surfactant concentration in a Slug size of 10% PV Displaced by a Gas Flow Rate of 8 cc/min.	91
Figure 5.25:	Runs: 19, 22, 23, 24 , and 25: Total Foam Mobility Versus Slug Size and Relative Total Mobility and MRF Versus Slug size.	93

Figure 5.26:	Comparison of Runs 19, 20, 22, 23 and 24, Cumulative Production (%PV) and Breakthrough Time Versus Slug Size, and Totalizer Reading Versus Slug Size.....	94
Figure 5.27:	Comparison of Runs 19, 20, 22, 23 and 24, Pressure Drop at Breakthrough and Steady State Pressure Versus Slug Size and Effluent Concentration Versus Slug Size.....	96
Figure 5.28:	Run 37: Cumulative Production Versus Time and Concentration Versus Time for a Slug of 2.5% (PV) Having a 10% Dowfax-8390 Surfactant Concentration.	99
Figure 5.29:	Run 37: Pressure Profile Using 10% Surfactant Concentration in a Slug size of 2.5% PV Displaced by a Gas Flow Rate of 1.75 cc/min.....	100
Figure 5.30:	Run 40: Cumulative Production Versus Time and Concentration Versus Time for a Slug of 10% (PV) Having a 10% Dowfax-8390 Surfactant Concentration.	101
Figure 5.31:	Run 40: Pressure Profile Using 10% Surfactant Concentration in a Slug Size of 10% PV Displaced by a Gas Flow Rate of 1.75 cc/min.....	103
Figure 5.32:	Comparison of Runs 37, 38, and 40, Cumulative Production (%PV) at Breakthrough Versus Slug Size, and Totalizer Reading at Breakthrough Versus Slug Size.	104
Figure 5.33:	Run 28: Cumulative Production Versus Time and Totalizer Reading Versus Time for Nitrogen Displacing Water in the Presence of Residual Oil, No Surfactant Used.....	107
Figure 5.34:	Run 28: Pressure Profile of Nitrogen Displacing Surfactant-Free Water in the Presence of Residual Oil Saturation.	108
Figure 5.35:	Run 26: Cumulative Production Versus Time and Concentration Versus Time for a Slug of 20% (PV) Having a 10% Dowfax-8390 Surfactant Concentration, in Presence of Oil.....	110
Figure 5.36:	Run 26: Pressure Profile, Using 10% Surfactant Concentration in a Slug Size of 20% PV Displaced by a Gas Flow Rate of 8 cc/min.	112
Figure 5.37:	Run 27: Cumulative Production Versus Time and Concentration Versus Time for a Slug of 5% (PV) Having a 10% Dowfax-8390 Surfactant Concentration, in Presence of Oil.....	113
Figure 5.38:	Run 27: Pressure Profile Using 10% Surfactant Concentration in a Slug size of 5% PV Displaced by a Gas Flow Rate of 8 cc/min.....	114
Figure 5.39:	Run 29: Cumulative Production Versus Time and Concentration Versus Time for a Slug of 10% (PV) Having a 10% Dowfax-8390 Surfactant Concentration, Conducted in Presence of Oil.	115

Figure 5.40:	Run 29: Pressure Profile Using 10% Surfactant Concentration in a Slug size of 10% PV Displaced by a Gas Flow Rate of 8 cc/min.	116
Figure 5.41:	Run 30: Cumulative Production Versus Time and Concentration Versus Time for a Slug of 2.5% (PV) Having a 10% Dowfax-8390 Surfactant Concentration, Conducted in Presence of Oil.	118
Figure 5.42:	Run 30: Pressure Profile Using 10% Surfactant Concentration in a Slug size of 2.5% PV Displaced by a Gas Flow Rate of 8 cc/min.	119
Figure 5.43:	Run 31: Cumulative Production Versus Time and Concentration Versus Time for a Slug of 25% (PV) Having a 10% Dowfax-8390 Surfactant Concentration.	120
Figure 5.44:	Run 31: Pressure Profile Using 10% Surfactant Concentration in a Slug size of 25% PV Displaced by a Gas Flow Rate of 8 cc/min.	121
Figure 5.45:	Comparison of Runs 26 to 31, Cumulative Production (%PV) and Breakthrough Time Versus Slug Size, and Totalizer Reading Versus Slug Size.	122
Figure 5.46:	Comparison Between 100% Water Saturated Runs 19 to 25 and Residual Oil Runs 26 to 31 Performed at the Same Gas Flow Rate of 8 cc/min.	124
Figure 5.47:	Run 32: Cumulative Production Versus Time and Concentration Versus Time for a Slug of 2.5% (PV) Having a 10% Dowfax-8390 Surfactant Concentration, Conducted in Presence of Oil.	125
Figure 5.48:	Run 32: Pressure Profile Using 10% Surfactant Concentration in a Slug size of 2.5% PV Displaced by a Gas Flow Rate of 1.75 cc/min in Presence of Oil.....	127
Figure 5.49:	Run 33: Cumulative Production Versus Time and Concentration Versus Time for a Slug of 10% (PV) Having a 10% Dowfax-8390 Surfactant Concentration, Conducted in Presence of Oil.	128
Figure 5.50:	Run 33: Pressure Profile Using 10% Surfactant Concentration in a Slug size of 10% PV Displaced by a Gas Flow Rate of 1.75 cc/min in Presence of Oil.....	129
Figure 5.51:	Run 36: Cumulative Production Versus Time and Concentration Versus Time for a Slug of 20% (PV) Having a 10% Dowfax-8390 Surfactant Concentration, Conducted in Presence of Oil.....	130
Figure 5.52:	Run 36: Pressure Profile Using 10% Surfactant Concentration in a Slug size of 20% PV Displaced by a Gas Flow Rate of 1.75 cc/min in Presence of Oil.....	131
Figure 5.53:	Run 35: Cumulative Production Versus Time and Totalizer Reading Versus Time for a Slug of 20% (PV) Having 10% Dowfax-8390 Surfactant Concentration in a Nitrogen Displacing Oil Process.....	134

Figure 5.54:	Run 35: Pressure Profile, Using 10% Surfactant Concentration, a Slug Size of 20% PV, and Gas Flow Rate of 8 cc/min in Gas-Oil Displacement.....	135
Figure 5.55:	Run 15: Cumulative Production Versus Time and Concentration Versus Time for Nitrogen Surfactant Co-injection.	137
Figure 5.56:	Run 15: Pressure Profile, for Nitrogen- Surfactant Co-injection.....	138
Figure 5.57:	Run 34: Cumulative Production Versus Time and Concentration Versus Time for Nitrogen Surfactant Co-injection at Surfactant to Nitrogen Ratio of a) 1: 4 cc/min and b) 1: 14 cc/min.....	141
Figure 5.58:	Run 34: Pressure Profile, Co-injection of Nitrogen and Surfactant at a Surfactant to Nitrogen Ratio of a) 1:4 cc/min and b) 1:14 cc/min.	142
Figure 5.59:	Run 39: Pressure Profile Due to Foam That Was Staying in Porous Media, Gas Flow Rates used were: 1.75, 2, and 2.5 cc/min.	144
Figure 5.60:	Run 39: Early Time of the Pressure Profile Due to Foam That Was Staying in Porous Media, Gas Flow Rate used was 1.75 cc/min.	146
Figure 5.61:	Run 19: Pressure Profile Before Gas Breakthrough Using 10% Surfactant Concentration in a Slug of 20% PV Displaced by a Gas flow Rate of 8 cc/min.	147
Figure 5.62:	Run 37: Pressure Profile Before Gas Breakthrough Using 10% Surfactant Concentration in a Slug of 2.5% PV Displaced by a Gas flow Rate of 1.75 cc/min.	148
Figure 5.63:	Run 38: Pressure Profile Before Gas Breakthrough Using 10% Surfactant Concentration in a Slug of 20% PV Displaced by a Gas Flow Rate of 1.75 cc/min.	149
Figure 5.64:	Run 40: Pressure Profile Before Gas Breakthrough Using 10% Surfactant Concentration in a Slug of 10% PV Displaced by a Gas flow Rate of 1.75 cc/min.	150
Figure 5.65:	Run 21, Repeat of Run 24: Pressure Profile Using 10% Surfactant Concentration in a Slug of 10% PV Displaced by a Gas flow Rate of 8 cc/min.....	155
Figure 5.66:	Run 33-R, Repeat of Run 33: Pressure Profile Using 10% Surfactant Concentration in a Slug of 10% PV Displaced by a Gas flow Rate of 8 cc/min.	156
Figure 5.67:	Run 41, Repeat of Run 6: Pressure Profile Using 10% Surfactant Concentration in a Slug of 10% PV Displaced by a Gas flow Rate of 8 cc/min.....	157

Nomenclature

a	Constant
A	Cross sectional area, m^2
A_H	Hamaker constant
b	Constant
C_s	Molar concentration of surfactant in the aqueous phase
h	Film Thickness, m
K, K_1, K_{-1}	Constants
k	Absolute permeability of porous medium, m^2 or darcy
k_{rf}	Relative permeability to flowing foam, fraction
k_{rg}	Relative permeability to gas, fraction
k_{rw}	Relative permeability to water, fraction
L_{pt}	Distance over which pressure drop is measured, m
n	Index
n	Foam texture, number of foam bubbles/unit volume
P	Pressure, Pa or psi
P_g	Gas phase pressure, Pa or psi
Q_s	Source/sink terms, moles/volume/time
S_o	Oil saturation, fraction
S_w	Water saturation, fraction
S_w^*	Water saturation corresponding to the capillary pressure, fraction
t	Time, s
u	Darcy velocity, (q/A)
v	Velocity
X_t	Fraction of Trapped Foam

Subscript:

c	Coalescence
f	Flowing
g	Vapour phase
g	generation
o	Oleic phase
t	Trapped
w	Liquid phase

Greek Symbol:

α	constant of proportionality
β	Trapping parameter
ϵ	Constant
μ	Viscosity, mPa.s
Π	Disjoining pressure, Pa
ρ	Density, kg/m ³
ϕ	Porosity, fraction
Γ	Foam quality
λ	Mobility, m ² /Pa.s

nitrogen and various hydrocarbon gases. Foam can be generated in a porous medium. The conventional process of generating foams is a liquid stream and a gas stream at high velocity.

A problem associated with many secondary and tertiary recovery is the high mobility of the displacing phase relative to the displaced phase. This is particularly critical when low viscosity, low density drive fluids are used to displace higher viscosity, higher density fluids in a heterogeneous reservoir. Under these displacement conditions give rise to viscous fingering and gravity segregation. As a result, large sections of the reservoir may be bypassed; and this in turn reduces recovery efficiency.

Foam is used to reduce gravity override, which results from the large density contrast between the gas and liquid densities, to retard gas fingering that results from the large contrast in viscosities, and to block high permeability streaks, thereby obtaining better recovery. Foam is also used in treating production wells exhibiting high gas/oil ratios (GOR).

This study examines the possibility of using foam as a secondary recovery method to improve the gas-phase mobility, and as a result, improve the mobility ratio. It investigates the flow mechanism of foam in porous media by studying the movement of the foam front. The objective of this study is to understand the mechanism of foam in porous media and its effects on oil (and liquid) recovery.

2. Review of the Literature

2.1 Foam Applications in the Oilfield

The term foam is used to describe the state of aggregation of two phases, liquid and gas, which aggregate in such a way that they form a dispersion that consists of gas bubbles and a continuous liquid film⁽¹⁾.

Published field trials on the use of foam to improve recovery from oil reservoirs have been progressively showing success, despite the tendency of oil companies not to report successful projects. Castanier and Brigham⁽²⁾ reviewed sixteen published field tests in which foam was used. They reported that the majority of them were successful. They claim that companies choose not to report successful projects. Hanssen et al.⁽³⁾ reviewed thirty field projects in which foam was used. They classified fifteen projects as successes, six as failures and the remaining nine were inconclusive. In addition, they reported that several foam pilot projects were being considered for North Sea oil reservoirs.

Foam has been used to improve recovery from oil reservoirs through mobility control, diversion and GOR control. In mobility control, foam reduces the mobility of the gas by “thickening”⁽⁴⁾; that is, by transforming the mobile gas into foam flowing with a higher effective viscosity. Heller⁽⁵⁾ presented a discussion of the application of CO₂ foam as a mobility control agent for oilfields in which he detailed a process of design of a CO₂ foam flood.

In diversion/blocking, foam is ideally used as a treatment rather than a flooding agent. Foam is placed in the desired position and should stay in place for long times⁽³⁾.

The use of foam to reduce the GOR has shown some success. In the Prudhoe field, the injection of foam caused a significant GOR reduction which in turn increased oil production for a period of several weeks⁽⁶⁾.

Foam flow in porous media depends on many factors, though actual relationships between most variables are disputed by researchers. In the following sections a review of the findings of past and most recent research on foam is presented.

2.2 Foam Characterization

The criteria that are used to characterize a foam include: quality, texture and stability. These are discussed in more detail in the following sections.

2.2.1 Quality

Foam quality (Γ) is defined as the volume fraction of gas in the gas-liquid foam system. Foam can be described as having high, low, dry and wet quality. It is expressed by:

$$\Gamma = \frac{\text{gas volume}}{\text{total foam volume}} \quad (1)$$

Foam quality can be varied by changing the gas and liquid flow velocities. Foam quality represents the volume fraction of gas, which changes with pressure; therefore, foam quality is pressure dependent. Minssieux⁽⁷⁾ reported that the obtainable quality of foam ranges from 50 to 99 percent. Below a quality of 50 percent, foam mixtures appear as suspensions of bubbles in a liquid and can not be considered as a single phase. Khatib et al.⁽⁸⁾ have shown that at a constant gas flow rate, mobility decreases with increasing gas fractional flow for low quality foams and increases with gas fractional flow for high quality foam.

Duerksen⁽⁹⁾ investigated the effect of liquid volume fraction (LVF) on pressure drop. He concluded that for increasing LVF, pressure drop increases rapidly then levels off. Marsden and Khan⁽¹⁰⁾ reported that the effective permeability-apparent viscosity ratio decreases linearly with foam quality.

2.2.2 Texture

Foam texture or bubble size is an important parameter that affects the flow of foam in porous media. Texture is the number distribution of the volumes of the discrete gas cells that constitute the foam⁽¹¹⁾. The average cell volume or, equivalently, the radius of a sphere of equal volume, is but one measure of foam texture. In other words, texture is the uniformity and size of bubbles. Texture can be described as fine, coarse, homogeneous and non-homogeneous. Marsden et al.⁽¹²⁾ recognized that foam texture has a significant influence on foam mobility. They stated that, "it appears that bubbles size, rather than quality of foamer concentration, determines the mobility."

Although they could not control the size of the bubbles, Marsden et al.⁽¹²⁾ successfully measured the texture of the effluent.

Hirasaki and Lawson⁽¹³⁾ showed that texture is the major variable affecting the apparent viscosity of foams flowing through smooth glass capillaries of uniform diameter.

De Vries and Wit⁽¹⁴⁾ reported that changing the texture of a foam by changing the properties of the foam generator did not affect the results within experimental error. They concluded, from measurement of the pressure drop halfway along the length of the core, that the texture of the injected foam was changed by the porous medium to a value independent of the injected texture. However, Friedmann and Jensen⁽¹⁵⁾ observed that different foamers generate foams with different bubble size distributions. This, as a result, affected the foam propagation into the porous medium.

Ettinger and Radke⁽¹⁶⁾ observed that bubble size in the effluent is independent of the foam injection method.

2.2.3 Foam Stability and Resiliency

Stability and resiliency refer to the lifetime and resistance of foam to decay and collapse. Parameters affecting the stability of foam are liquid and surface viscosities, the Marangoni effect and the disjoining pressure.

Farouq Ali and Selby⁽¹⁷⁾ stated that stable foams cannot be formed from pure liquids and a surface active-agent has to be added to the liquid to lower the surface tension.

Raza⁽¹⁸⁾ reported that foam stability increased with increasing surfactant concentration until the critical micelle concentration (CMC) was reached. For concentrations higher than the CMC, the foam lost some of its stability and resiliency. In his study of CO₂-foam properties, Raza showed that foam stability was reduced at high temperatures, whereas high pressures affected the CO₂-foam stability favourably. Raza's findings were confirmed by other investigators^(19, 20, 21).

High liquid viscosity decreases the liquid drainage rate from the lamellae which, in turn, increases the stability. In liquids of high viscosity, the foam formation process is slow and so is the process of foam collapse⁽¹⁾. A high surface viscosity retards

drainage and surface deformation, and increases the life of the lamellae. Owete and Brigham⁽²²⁾ suggested increasing surface viscosity to increase the foam stability. High surface viscosity is known to reduce the rate of liquid film thinning; therefore, a high surface viscosity would increase lamellae stability.

The Marangoni effect is another factor influencing the stability of foam. It is the departure from equilibrium surface tension produced by dilational deformation of the interface to resist lamella deformation. The bulk material is carried through movements induced by surface tension effects. When a film is stretched, the surface area increases causing a reduction in the surfactant concentration at the local level. This results in a higher surface tension that tends to restore the thinned portion of the stretched region by liquid movement to the stretched region^(1, 23).

The disjoining pressure plays a major role in lamellae stability. It is defined by Derjaguin and Titiievskaja⁽²⁴⁾ as the pressure in excess of the external pressure that must be applied to the medium between the lamellae faces to maintain a given separation. The disjoining pressure may be regarded as a net of several attractive intermolecular forces. Jimenez and Radke⁽²⁵⁾ used the Derjaguin-Landau-Verwey-Overbeek (DLVO) theory of classical colloid science to investigate the effects of joining/disjoining pressure on foam structure, concentration and physical properties. They quantified the effect of disjoining pressure on foam in porous media. The driving force for liquid movement into and out of the lamellae was found to be $(P_C - \Pi)$, where P_C is the capillary pressure and Π is the disjoining pressure given by⁽²⁵⁾:

$$\Pi = -\frac{A_H}{8h^3} + \frac{2\pi q_l^2}{\epsilon} \text{csch}(\kappa h) \quad (2)$$

where A_H is the Hamaker constant, q_l is the lamellae surface charge density, h is the film thickness, κ is the inverse Debye length and ϵ is the permittivity constant. When P_C is greater than Π , the liquid movement is out of the lamellae; and when Π is greater than P_C , the liquid movement is into the lamellae. When P_C equals Π , the lamellae are in metastable equilibrium.

Minssieux⁽⁷⁾ described two mechanisms that affect foam stability. The first mechanism is the drainage and statistical rupture of films. When this mechanism is dominant, stability increases as quality increases. The second mechanism is the

coalescence of gas between adjacent bubbles of different sizes. When this mechanism is dominant, the foam stability increases as quality decreases.

Ross⁽²³⁾ analyzed the thermodynamic instability of foam by the use of Gibb's function for a one component system where surface energy is significant.

$$dG = VdP - SdT + \gamma dA \quad (3)$$

Here γ is the interfacial tension and A is the surface area per mole.

At constant pressure and temperature the interfacial tension is given by:

$$\gamma = \left[\frac{\partial G}{\partial A} \right]_{P,T} \quad (4)$$

Therefore,

$$\Delta G = [\gamma \Delta A]_{P,T} \quad (5)$$

A decrease in Gibb's free energy causes a decrease in bubble area. Therefore, a foam created from pure liquid is thermodynamically unstable. For thermodynamic stability, the equation requires additional terms of opposite sign so that the sign of the whole ΔG expression is changed. This can be accomplished by a surface-active agent.

2.3 Foam Rheology

In order to determine the apparent viscosity of foam, it is important to understand the rheological behaviour of foam. Earlier work on the rheology of foam was conducted by Penny and Blackman⁽²⁶⁾ who reported that fire-fighting foams had both a limiting shear stress and a tensile yield stress; and by Grove et al.⁽²⁷⁾ who investigated the effect of pressure and shear rate on the viscosity of fire-fighting foams. They reported that the apparent viscosity remained constant for the range of velocity used (2-19 ft/sec). On the other hand, increasing the pressure led to a decrease in viscosity. Sibree⁽²⁸⁾ reported that the apparent viscosity of foam decreased with increasing shear to a certain point at which it became constant. He also found that the foam has an apparent viscosity greater than its constituent phases.

David and Marsden⁽²⁹⁾ studied the rheological behaviour of foam by simultaneously injecting compressed air and an aqueous solution to generate foam into a short porous medium. The foam then flowed into a capillary tube viscometer having four interchangeable glass tubes of different radii. They found that the apparent viscosity, corrected for slippage and foam compressibility, was independent of foam quality and was dependent on the tube radius. They reported that the flowing foam behaved like a pseudoplastic fluid, but the static foam had a measurable gel strength which increased with quality.

Raza and Marsden⁽³⁰⁾ investigated the apparent viscosity of foam by the use of different diameter capillary tubes. They found that at a low flow rate the foam flowed as a Newtonian fluid, whereas at a higher flow rate it flowed as a pseudoplastic fluid. In their analysis of foam behaviour, they utilized the analytical method developed by Mooney⁽³¹⁾

$$S = K \left(\frac{d\bar{u}}{dr} \right)^n \quad (6)$$

Here S is the shear stress, $\left(\frac{d\bar{u}}{dr} \right)$ is the shear rate, K is the consistency index, \bar{u} is the average or bulk velocity and n is the flow behaviour index.

From the above relation, Mooney⁽³¹⁾ derived the following equation,

$$\frac{r_i \Delta P}{2L} = K \left(\frac{4\bar{u}}{r_i} \right)^n = K \left(\frac{4q}{\pi r_i^3} \right)^n \quad (7)$$

where ΔP is the pressure drop, L is the length, q is the volumetric flow rate and r_i is the inside tube radius.

From the analytical method proposed by Mooney⁽³¹⁾ and used by Raza and Marsden⁽³⁰⁾, both K and n can be found from a logarithmic plot of $(r_i \Delta P / 2L)$ versus $(4\bar{u}/r_i)$. The slope of the resultant line is indicative of the type of flow at the corresponding shear rates and shear stresses. The intercept of the tangents drawn at various shear rates and shear stresses gives the consistency index. For a Newtonian

fluid, n is unity (slope of unity) and is indicative of a parabolic velocity distribution, and the intercept gives K which corresponds to the consistency index of the fluid. A slope of less than unity indicates that the foam is behaving as a pseudoplastic fluid. Values of $n > 1$ are indicative of dilatant fluids. A slope of zero would indicate purely piston-like flow.

Hirasaki and Lawson⁽¹³⁾ developed a theory to predict the apparent viscosity of foam in smooth capillaries. To determine the apparent viscosity as a function of foam texture, quality, gas velocity, capillary radius and capillary length, Hirasaki and Lawson used the Hagen-Poiseuille law.

According to the Hirasaki and Lawson⁽¹³⁾ theoretical model, three major factors resist the flow of foam. The three constituents of foam viscosity are: the Newtonian viscosity of any liquid slugs between gas bubbles, the viscous resistance to the liquid between the foam bubbles and the capillary wall. This viscous resistance manifests itself as an interface deformation. The third constituent is a surface traction that results from a surface tension gradient.

Falls et al.⁽¹¹⁾ extended Hirasaki and Lawson's work by accounting for the radii of curvature of the foam lamellae being formed by the capillary pressure in the porous medium and pore constrictions. They accounted for the capillary pressure through an ordinary idealized capillary pressure function, whereas the pore constrictions was determined through an analysis of the pressure gradient required to mobilize stationary lamellae and a steady-state, dynamic mechanical energy balance. From their experimental data, Falls et al. calculated the mobility of gas in a foam of known average bubble size from the pressure drop using Darcy's law.

$$\lambda_{rg} = - \left(\frac{q_g}{A} \right) \left(\frac{L_{pt}}{k \Delta p} \right) \quad (8)$$

where q_g is the gas volumetric flow rate and A is the cross sectional area of the core. The parameter L_{pt} is the distance over which the pressure drop is measured, k is the absolute permeability and Δp is the pressure drop. The relative permeability to gas was taken as an ordinary function of saturation reduced by the fraction of gas that is flowing.

$$k_{rg}^{foam} = \left[k_{rg}(S_w) \right] \left(\frac{S_{gf}}{S_g} \right) \quad (9)$$

where S_{gf} is the flowing gas saturation and S_g is the gas saturation.

Accordingly, they calculated the apparent viscosity from the two above equations. For the controlled bubble-size case, Falls at al. estimated the moving gas saturation S_{gf} from the measured residence time of flowing gas. So the apparent viscosity is:

$$\mu_{g,app} = \left(-t / S_g L \phi \right) \left(\frac{k \Delta p}{L_{pt}} \right) \quad (10)$$

The derived apparent viscosity due to the contribution of the pore constriction is given by:

$$\frac{\mu_{con}}{\mu_w} = \begin{cases} \xi_1 n_l r_{cap} (3\mu_w v_g / \sigma)^{-1} & \text{for } n_l < n_{pc} \\ \xi_2 (3\mu_w v_g / \sigma)^{-1} & \text{for } n_l > n_{pc} \end{cases} \quad (11)$$

where μ_{con} is the constriction contribution to the foam apparent viscosity, μ_w is the water viscosity, ξ_1 and ξ_2 are weight parameters for the contribution of pore constrictions, n_l is the number of lamellae per unit length, r_{cap} is the capillary radius or equivalent capillary radius, v_g is gas-phase velocity and σ is the interfacial tension.

Falls at al.⁽¹¹⁾ reported that the total apparent viscosity is equal to the sum of their derived constriction contribution and the apparent viscosity derived by Hirasaki and Lawson⁽¹³⁾. According to their results, the theoretical and the experimental apparent viscosity were in a good agreement.

2.4 Mechanisms of Foam Generation in Porous Media

Many investigators agree on three main foam generation mechanisms^(19,22,32,33). They are: leave-behind, snap-off and lamellae division.

2.4.1 Leave-Behind Mechanism

Leave-behind occurs when gas displaces liquid from porous media; often the lamellae remain behind in the pore throats. This occurs when two gas channels invade two adjacent and communicating pores drying the liquid from the pores and leaving a lamella in between the two pores. These stationary lamellae remain at the pore throats where they were generated. The leave-behind process does not require that two gas fronts converge simultaneously on the same liquid-filled region. Rather a gas front arriving at a later time can converge on an existing gas-filled channel and squeeze down the lamellae as the capillary pressure increases.⁽³⁴⁾ The lamellae formed by the leave-behind mechanism block gas flow channels, thereby decreasing the relative permeability to the gas phase. The lamellae created by the leave-behind mechanism are generally oriented parallel to the local direction of flow and do not make the gas phase discontinuous.⁽³³⁾

The stationary lamellae, formed by the leave-behind mechanism, are subject to lamellae stability factors.⁽²²⁾ The lamellae can be mobilized, if the pressure differential is high enough and the lamellae do not rupture. Once a lamella is ruptured or mobilized from its generation site, liquid has to re-invade the two adjacent pores before a lamella can be regenerated by gas invasion. In glass bead pack experiments, Ransohoff and Radke⁽³³⁾ reported that foam generated solely by this mechanism gave approximately a five-fold reduction in the steady-state gas relative permeability. This mechanism does not make the gas phase discontinuous as mentioned earlier; for this reason it is not a very effective gas mobility reduction mechanism as compared with the snap-off mechanism.

2.4.2 Snap-off Mechanism

Snap-off is a very important mechanism for foam generation in porous media. The phenomena was first studied and explained by Roof⁽³⁵⁾ to understand the origin of residual oil. Snap-off occurs when a gas front advances through a pore throat initially filled with wetting phase. The gas front causes a decline in capillary pressure. This induces flow of liquid from around the bubble back into the constriction. When the capillary pressure decreases below a critical value, the liquid in the pore throat bridges and snaps off creating a gas bubble^(34,36). The snap-off mechanism is recognized as a mechanical process, for it occurs repeatedly during multiphase flow in porous media

regardless of the presence or absence of a foaming-surfactant⁽³⁶⁾. Ransohoff and Radke⁽³³⁾ reported that the snap-off mechanism is the primary mechanism responsible for the generation of strong foam. This mechanism is believed to be the dominant foam generation mechanism in porous media, occurring frequently at high gas velocities^(19,37,38). Unlike the leave-behind mechanism, snap-off produces a discontinuous- gas phase and reduces the gas mobility by several hundred fold^(16,39).

2.4.3 Lamella Division Mechanism

The third foam generation mechanism is the lamellae division phenomena. This mechanism is different from the first two in that it requires a pre-existing and a moving lamella, as well as a branching path. When a moving lamella encounters a branching path, it will divide into two or more lamellae. Chambers and Radke⁽³⁴⁾ observed in their experiments that foam bubbles that are smaller than the pore-body size do not divide when they encounter a branch point. The bubble flows undivided down one or the other of the paths. However, if the bubble size is larger than the pore-body and the foam lamella spans the pore space, division generally occurs. Ettinger and Radke⁽¹⁶⁾ measured the effluent bubble size in Berea sandstone and found that the foam coarsens with increasing gas flow rate. The rate of the lamella division process was greater at a higher gas flow rate.

2.5 Foam Flow in Porous Media

The mechanism of foam flow in porous media has been investigated by many researchers, yet there is no consensus on the mechanism of foam flow. Foams are gas-liquid suspensions that exhibit viscous behaviour in porous media⁽¹⁰⁾. Several researchers have proposed mechanisms or observed flow patterns pertinent to the viscous behaviour of foams in porous media. Fried⁽⁴⁰⁾ proposed that foam moves through porous media as a body. Holm⁽⁴¹⁾ proposed that gas flows as a discontinuous phase separated by liquid lamellae and that the lamellae break and reform as gas passes through the pore channels.

Islam and Farouq Ali⁽⁴²⁾ reviewed experimental foam flow mechanisms and concluded that there are five major mechanisms of foam flow that have been recognized. Foam may flow in a porous medium with changing quality; four phases may be present. Foam may flow as a combination of liquid and gas in a foam body and the liquid flows in fixed channels. Another possible mechanism is that the gas flows as

a discontinuous phase by the breaking and reforming of films and that the liquid flows as free phase. A large portion of gas is trapped in the porous medium and a small fraction flows as free gas, following Darcy's law. Finally foam may flow as a single body; the rate of gas flow is the same as the rate of liquid flow.

In another work on foam, Islam et al.⁽⁴³⁾ reviewed the existent theories of foam flow in porous media. They also conducted foam experiments. They presented experimental evidence that four different phases flow simultaneously. They found that the oil recovery performance with foam depended on the surfactant concentration, injection pressure and quality of the foam generated.

Bernard and Holm⁽⁴⁴⁾ and Bernard et al.⁽⁴⁵⁾ pursued pioneering studies quantifying gas and liquid permeabilities in the presence of foam. They used both co-injection of surfactant solution and nitrogen and alternating slugs of each. For consolidated cores with absolute permeabilities ranging from 0.1 to 0.25 μm^2 , they found several-hundred-fold permeability reductions to gas. For a sand pack with an absolute permeability of 3.89 μm^2 , the gas permeability was reduced to less than 10^{-3} μm^2 in the presence of foam. At this early stage of foam research, Bernard et al.⁽⁴⁵⁾ made two important experimental observations. They varied the aqueous-phase flow rates, and measured the aqueous saturations and the overall pressure drops. The first observation is that water relative permeabilities calculated with Darcy's law were unaffected by foam. When compared under identical flow-rate conditions, steady-state water saturations were different between foam and surfactant-free, two-phase flow cases, but the aqueous-phase relative permeability versus water saturation relation was unchanged. This observation has been confirmed numerous times by other researchers^(14,15,46,47).

The second observation is that, after foam flooding cores, Bernard et al.⁽⁴⁵⁾ flushed the one with water or brine to estimate the trapped-gas saturation. They assumed that water or brine filled the pore space through which the gas flowed, but that it did not substantially alter the fraction of gas trapped. Their trapped saturation ranged from 10 to 70% depending on the surfactant type and the presence of oil in the porous medium during foam flooding. The trapped gas saturation was found to be lower for systems containing both water and oil than for systems containing water only.

Bernard et al.⁽⁴⁵⁾ conducted their saturation measurements after a waterflood; as a consequence they do not represent the dynamic or the steady-state foam flooding saturation. Friedmann et al.⁽³⁷⁾ and Radke and Gillis⁽⁴⁸⁾ conducted gas-phase tracer experiments in which they measured the trapped gas saturation of foams at steady-state. These experiments have revealed that the trapped gas saturation for nitrogen foams at steady-state in Berea sandstones ranged from about 80% to nearly 100% over a variety of flow rates.

Friedmann et al.⁽³⁷⁾ used a krypton tracer for a range of frontal advance rates between 25 and 130 m/day. They measured the fraction of gas trapped as a function of gas phase velocity at a constant fractional flow. They found little change in the fraction of gas trapped even though they varied the gas velocity by over two orders of magnitude. Radke and Gillis⁽⁴⁸⁾ used sulfur hexafluoride and methane tracers simultaneously in their attempt to correct for partitioning of the tracer into the trapped gas fraction. The total flow rate ranged from 0.5 to 4 m/day. They also reported no consistent trend of trapped gas fraction with liquid or gas velocity.

Flumerfelt and Prieditis⁽⁴⁹⁾ performed similar experiments; they injected gas into a 7 μm^2 beadpack. They first generated foam under conditions of simultaneous injection of gas and surfactant solution at a variety of gas rates and at fixed liquid rates. After reaching steady state, the liquid flow was discontinued and the foam was allowed to decay until continuous gas was produced. They showed that the permeability of the core to gas at the first appearance of effluent continuous gas was two orders of magnitude less than the foam-free case. This permeability was independent of gas and initial liquid flow rates. They concluded that the number of channels available for gas flow was 100 times less in the presence of foam than in the no foam case.

Fried⁽⁴⁰⁾ was another of the early researchers who conducted foam experiments. He reported that foam causes a rapid reduction in gas phase relative permeability, resulting in a delayed gas breakthrough. Gas relative permeability was found to be a multivalued function of surfactant concentration. He observed that the presence of surfactant increased the residual gas saturation. He showed that the flow resistance to foam increases with increasing surfactant concentration. He also observed that weak foam flowed with continuous breaking and reforming of lamella.

Marsden and Khan⁽¹⁰⁾ reported that foam components flow simultaneously through the channels of the porous medium. Their experimental results showed a decrease in foam mobility with increasing quality. They also observed an increase in the apparent viscosity of foam with increasing surfactant concentration. Holm⁽⁴¹⁾ disagreed with this observation. He visually and experimentally investigated the mechanism of gas and liquid flow through porous media in the presence of foam. He reported that foam is unlikely to flow in porous media as a body, and that the gas and liquid separated during the foam films breaking and reforming process in the porous medium. As a result, he reported foam was unlikely to flow as a body. He observed that the mobility of foam increased with an increase in quality. He concluded that gas could not flow as a continuous phase. This observation differs from that of Marsden and Khan⁽¹⁰⁾ mentioned earlier. The reason given by Holm for this difference is that different experimental techniques were used. He argued that Marsden and Khan used a very small pressure drop across the core. This small pressure drop led to very little expansion of foam bubble thus enhancing the stability of some small bubbles that created less resistance to flow. Because low quality foam contains more of these small bubbles, a wetter foam gave a higher mobility.

Raza⁽¹⁸⁾ found in his laboratory study that foam can be propagated in a reservoir rock at pressures ranging from atmospheric to 1000 psig (6895 kPa). He stated that flow behaviour of foam in porous media could not be correctly described in terms of the high apparent viscosity of foam alone, nor could the relative permeability relationships apply as the fluids are associative. He reported that foam restricted the flow of all the fluids in porous media, but mostly the flow of gas. As the foam decays, the liquid phase flow becomes less restricted. For hydrocarbon flow, foam temporarily restricted it.

Minssieux⁽⁷⁾ observed, for a fixed pressure differential across the core, a continual decrease in foam rate until gas flow completely ceased. He concluded that a minimum ΔP across the core was necessary to overcome the elastic limit of films impeded by pore constrictions. He noticed, as did Holm⁽⁵⁰⁾, that foam was constantly regenerated by breaking and reforming gas bubbles in the porous medium instead of being one phase. He reported that foam flow could not be treated as an equivalent of gas flow because foam appeared as the wetting phase in relation to oil. He suggested the same relative permeability curves could be used for both water and foam.

Heller et al.⁽⁵¹⁾ conducted CO₂ foam experiments at high pressure and temperature. They stated that the mobility of foam was changing with flow rate, and increased at higher velocity. They also found that the mobility of foam decreased with increasing surfactant concentration, and increasing the quality resulted in only a small decrease in mobility.

Wang⁽⁵²⁾ investigated the displacement mechanism of CO₂ foam. The results showed that an increase in pressure led to a better foam stability, whereas an increase in temperature destabilized the foam.

Khatib et al.⁽⁸⁾ introduced the term “limiting capillary pressure” in relation to foam in porous media. It is the maximum capillary pressure that can be attained by simply increasing the fraction of gas flow. They observed that if the gas fractional flow was increased after the limiting capillary pressure had been attained, coalescence coarsened foam texture, while the liquid saturation remained constant and relative gas mobility became proportional to the ratio of gas to liquid fractional flow. They reported that the limiting capillary pressure varied with the surfactant type, gas velocity and absolute permeability. They observed that at low gas fractional flows, the relative gas mobility was nearly constant, whereas for higher gas fractional flow the relative gas mobility increased rapidly. They attributed this increase to a limiting capillary pressure value and that coalescence caused the foam to coarsen. They reported a relationship between gas mobility and permeability in which gas mobility decreased rapidly as the permeability increased up to 12 mD. This was followed by a region in which the gas mobility remained insensitive to absolute permeability. For higher permeability the gas mobility increased rapidly.

Huh and Handy⁽⁴⁷⁾ compared steady and unsteady-state relative permeabilities of gas and foaming solution in Berea sandstones with relative permeabilities obtained in the absence of foaming agent. They observed that the permeability reduction factor for the gas phase was largely a function of lamellae stability. They reported significant differences between the steady-state and unsteady-state permeabilities. Unsteady-state experiments showed insignificant change of relative permeability to gas over a wide range of saturations and exhibited no blocking effect. For steady-state flow experiments, the simultaneous flow of liquid and gas could be stabilized only above a minimal gas saturation in the range of 35 to 40%, due to the formation of a large number of foam lamellae by the continuous supply of foaming solution. The pressure

gradient increased with increasing distance from the inlet end of the core, indicating that the higher gas fraction results in a greater blocking effect.

2.6 Factors Affecting Foam Flow in Porous Media

Many factors affect foam flow in porous media. Researchers have investigated a variety of parameters that affect foam. In the next sections a review of some of the parameters that affect foam flow in porous media is presented.

2.6.1 Foam Texture

Foam texture or bubble size is an important parameter that affects the mobility of foam in porous media. The relationship between bubble size and pore size affects the mechanism of foam propagation. Published data show that foam pregeneration does not affect foam flow^(14,16), but affects foam propagation⁽¹⁵⁾.

De Vries and Wit⁽¹⁴⁾ reported that varying the texture of the injected foam by varying the properties of the foam generator did not influence the results within experimental error. They monitored the pressure halfway along the length of a short core. Therefore, they concluded that the texture of the injected foam is changed by the porous medium to a value independent of the injected texture in a short distance.

However, Friedmann and Jensen⁽¹⁵⁾ observed that different prefoamers generate foams with different bubble size distributions. As a result, this affects foam penetration into the porous medium.

Ettinger and Radke⁽¹⁶⁾ observed that bubble sizes at the effluent end of a core are independent of the injection method; that is, whether a prefoamer was used or not. Hirasaki and Lawson⁽¹³⁾ showed in smooth capillaries that the gas apparent viscosity is proportional to the inverse second power of the bubble radius in the bulk-foam region and proportional to the inverse third power of the bubble radius in the individual-lamella region. Falls et al.⁽¹¹⁾ showed a similar dependence on foam texture in beadpacks.

2.6.2 Foam Quality

Foam quality is defined as the volume fraction of gas in the gas-surfactant foam system. Foam quality can be changed by varying the gas and liquid flow velocities. Therefore, a study of the effect of the individual velocities would be sufficient. Khatib et al.⁽⁸⁾ have shown that at constant gas flow rate, mobility decreases with increasing gas fractional flow for low quality foam and increases with gas fractional flow for high quality foams.

Marsden and Khan⁽¹⁰⁾ found that mobility decreases linearly with increasing foam quality. Heller et al.⁽⁵¹⁾ and others^(13,40) found that apparent viscosity increased with increasing quality. Foam quality also affects its propagation rate in porous media. High quality foams were found to propagate better than wet foams⁽¹⁵⁾.

2.6.3 Permeability of Porous Medium

Bernard and Holm⁽⁴⁴⁾ found that greater mobility reduction is achieved in higher permeability porous media. They suggested that foam would selectively plug high permeable channels. Friedmann and Jensen⁽¹⁵⁾ found that foam propagates faster in high permeability rocks. Owete and Brigham⁽²²⁾ concluded that mobility reduction factors decreased to a constant value with absolute permeability.

MacDonald⁽⁵³⁾ conducted foam experiments and found that there was an optimal surfactant concentration. This optimal concentration varied with the absolute permeability. She found also that the mobility of the gas phase in the presence of foam increased with increasing absolute permeability. This observation is in contrast to the idea that foam would preferentially block high permeability channels.

2.6.4 Fluid Saturations

Data available in the literature^(7,16,37,39,41) show that, after reaching steady state with foam injection into cores, liquid saturations are about 30- 40%. These saturations are independent of the flow rates and foam quality.

De Vries and Wit⁽¹⁴⁾ conducted foam experiments at high foam qualities (more than 95%) and high gas velocities. They reported that liquid saturations were reduced

to about 18%. Radke and Gillis⁽⁴⁸⁾ obtained liquid saturations of about 20% with only gas flowing.

2.6.5 Trapped Gas Saturation

Foam reduces gas mobility by immobilizing a fraction of the gas. Bernard and Holm⁽⁴⁴⁾ determined that up to 70% of the gas is trapped in the presence of foam. Chen et al.⁽⁵⁴⁾ reported that an increase in surfactant concentration causes higher gas trapping due to an increase in film stability.

Stationary foam does not contribute to the flow of gas and it increases the resistance of the flowing gas by reducing the cross sectional area for flow. Falls et al.⁽¹¹⁾ estimated the relative-permeability component of the gas mobility to be equal to the product of the gas relative permeability in the absence of foam and the fraction of the gas phase that is flowing.

Friedmann et al.⁽³⁷⁾ performed tracer studies in Berea cores. The tracer breakthrough was monitored by a gas chromatograph. They determined that the trapped gas saturation was about 85% under steady state conditions of foam flow.

Results by Radke and Gillis⁽⁴⁸⁾ indicate a trapped gas saturation of 70 -99% under a weak foam flow regime.

2.6.6 Gas Velocity

Khatib et al.⁽⁸⁾ demonstrated that increasing gas fractional flow and gas velocity tends to destabilize foam and thereby increase the mobility. Falls et al.⁽¹¹⁾ showed that the dependence on velocity for sand packs where pore constrictions are included ranged from the inverse first power at low shear rates, to the inverse two-thirds power with small bubbles and high shear rates. Friedmann et al.⁽³⁷⁾ measured a critical gas velocity, at constant liquid volume fraction, above which bubbles generate in Berea cores. This critical gas velocity (V_c) is given as

$$V_c = 1.52 (LVF)^{-1.54} \quad (12)$$

where LVF is the liquid volume fraction.

The effect of gas velocity on bubble size distribution has been studied. Ettinger and Radke⁽¹⁶⁾ and Friedmann and Jensen⁽¹⁵⁾ reported that smaller bubbles were produced at higher gas velocities. Dilgren and Owens⁽⁵⁵⁾ conducted experiments at constant volume and constant mass injection modes. They found no significant effect of the mode of gas injection on the response of foam drive experiments.

Experimental results obtained by De Vries and Wit⁽¹⁴⁾ indicate that at a fixed liquid velocity, increasing the gas velocity causes the pressure gradient first to increase, reach a maximum value, and then decrease. With low quality foam, increasing the gas velocity would increase the pressure gradient, whereas the opposite is true for high quality foams.

Chou⁽⁵⁶⁾ investigated experimentally the formation of N₂ and CO₂ foams in Berea sandstones. He found that foam was readily formed by co-injecting gas and surfactant solution whenever the core was presaturated with surfactant, regardless of the flow rate or pressure gradient.

2.6.7 Presence of Oil

The available literature shows that foam can reduce gas mobility in porous media, but is sensitive to the presence and saturation level of residual oil. Kuhlman⁽⁵⁷⁾ conducted microvisual experiments for CO₂ foams and crude oil and observed foam destruction due to the spreading of oil over foam.

Manlowe and Radke⁽⁵⁸⁾ used microvisual experiments to study foams made from steam-foamers with air in the presence of pure alkane oils and observed foam destruction caused by pseudoemulsion film thinning and rupture.

Hudgins and Chung⁽⁵⁹⁾ found the presence of crude oil was very detrimental to foaming in long sand-packed slim tubes, but under certain conditions of low oil saturation foam was generated.

Schramm et al.⁽⁶⁰⁾ conducted foam floods in sandstone cores and found a range of sensitivities to residual crude oil saturation from oil-tolerant foams to oil-sensitive foams. Isaacs et al.⁽⁶¹⁾ conducted a number of steam-foam floods in sand packs saturated with heavy crude oil and, also, found that foam effectiveness depended on

residual oil saturation. In their experiments, foams were effective at saturations below about 10% and were not effective at oil saturations above about 15%.

2.6.8 Temperature

Maini and Ma⁽²⁰⁾ found that as the temperature increased foam decayed faster and liquid drained more rapidly. Results presented by Wang⁽⁵²⁾ showed that the quality and the stability of foam decreased with an increase in temperature. Robin⁽⁶²⁾ found that the stability of foam was reduced at higher temperatures. In another study by McPhee⁽⁶³⁾ opposite results were observed.

Duerksen⁽⁹⁾ observed lower pressure drops across a foam generator with increasing temperature. In a foam flow system in a Boise core, after shutting down the flow, the pressure decay was monitored with time. The pressure in high temperature systems decayed faster than in the low temperature ones.

2.6.9 Surfactant Concentration

Traces of surfactant are capable of stabilizing foam lamellae⁽⁶⁴⁾. As the surfactant concentration is increased, molecules aggregate into larger oriented groups called micelles. A further increase in surfactant concentration beyond the point where the micelles form does not increase the concentration of single molecules in solution. This point is called the critical micelle concentration (CMC).

Increasing surfactant concentration improves the stability of foam by retarding the rate of drainage of liquid from the lamellae. Studies done by several researchers^(21,54,65) indicate that concentrations above the CMC do not improve foam stability any further. Raza⁽¹⁸⁾ studied the effect of surfactant concentration on foam stability and quality. He found that the foam quality increased with increasing surfactant concentration, up to the CMC and further increases in concentration had no effect on the quality. However, Huh and Handy⁽⁴⁷⁾ found that the concentration for maximum stability of foams was higher than the CMC. They stated that micelle formation enhanced lamellae stability. In another study, Huh et al.⁽⁶⁶⁾ conducted experiments in which the surfactant concentration used was higher than the CMC. They explained that the formation of micelles above the CMC accelerated the movement

of surface active molecules to the interface, when the lamellae experienced stretching or thinning.

2.7 Modeling Foam Flow in Porous Media

A variety of methods have been proposed for modeling foam flow and displacement in porous media^(67,68,69). Most of these methods account for the fact, first observed by Bernard and Holm.⁽⁴⁴⁾, that foam does not affect the relation between water mobility and water saturation (S_w).

$$k_{rw}^f = k_{rw}^o(S_w) \quad (13)$$

where k_{rw}^f is the relative permeability to water in the presence of foam, and k_{rw}^o is the relative permeability function that applies in the absence of foam. Since foam directly affects only gas mobility, predicting foam mobility is a matter of predicting gas mobility in the presence of foam. There are four broad approaches for modeling foam mobility in the literature. First, there are empirical expressions for gas mobility as a function of flow rates, surfactant concentration and other factors^(42,57,70,71,72). These empirical models are computationally simple, but they lack generality. The second approach in foam modeling is applying so-called fractional flow theories^(67,69,73). This method may be unsuitable for modeling of foam flooding because fractional flow theory is approximate when applied to compressible phases⁽⁶⁷⁾. Its application requires excessive extrapolation from available data to fit model parameters⁽⁶⁷⁾. The third approach is using percolation models^(38,74). These models, while allowing replication of pore-level mechanisms, have the disadvantage of requiring large amounts of computation time and provide results on a prohibitively small grid⁽³⁶⁾. Due to their disadvantages, it seems unlikely that percolation models can be useful in transient displacements that demand tracking of saturation, surfactant concentration, and foam on a laboratory scale let alone on a field scale.⁽³⁶⁾

2.7.1 Population Balance

The population method for modeling foam flow^(16,32,37,75,76) was originally proposed because it incorporates foam into reservoir simulators in a manner that is similar to the writing of mass and energy equations in porous media. The population balance model comprises two components⁽⁶⁷⁾. The first component is a non-Newtonian description of gas mobility at a fixed foam texture. Further, the gas

mobility is divided into relative permeability and viscosity. The relative permeability accounts for the reduction in mobility that results from the trapping of a substantial fraction of gas phase. The viscosity accounts for all other effects of foam on gas mobility.

The second component in the population balance method is the population balance itself⁽⁶⁷⁾. It is a conservation equation quantifying the relation between foam mobility and texture and all the mechanisms of creation and destruction of the liquid films or lamellae that separate and define gas bubbles⁽⁶⁸⁾. The next section treats the population balance in detail.

First the mass balance equations for the gaseous and the aqueous phases are written in a standard reservoir simulator in one-dimensional form as follows:⁽³⁶⁾

for the nonwetting phase

$$\frac{\partial[\phi\rho_g S_g]}{\partial t} + \frac{\partial[\rho_g u_g]}{\partial x} = q_g, \quad (14)$$

for the wetting phase

$$\frac{\partial[\phi\rho_w S_w]}{\partial t} + \frac{\partial[\rho_w u_w]}{\partial x} = q_w \quad (15)$$

where t and x denote time and axial location respectively. The subscripts g and w denote the non-wetting (gas) and wetting (liquid) phases, respectively. The parameter ρ is the density, ϕ is the porosity of the porous medium, S is the saturation, u is the Darcy velocity and q is the source/sink term.

and for surfactant

$$\frac{\partial[\phi C_s S_w + \Gamma]}{\partial t} + \frac{\partial[C_s u_w]}{\partial x} = Q_s \quad (16)$$

where C_s is the molar concentration of surfactant in the aqueous phase. The parameter Γ is the amount of surfactant adsorption on the rock surfaces in moles per void volume, and Q_s is the source/sink term in units of moles/volume/time.

Next, the conservation equation relating the mobility of foam as a function of texture is written in the following form:⁽³⁶⁾

$$\frac{\partial[\phi(S_f n_f + S_t n_t)]}{\partial t} + \frac{\partial[u_f n_f]}{\partial x} = \phi S_g (r_g - r_c) + Q_b \quad (17)$$

where the subscripts f and t denote the flowing and trapped foam, respectively. The parameters n_f and n_t are the foam texture or bubble number density (number of foam bubbles per unit volume) of flowing and stationary gas, respectively. The parameter Q_b is the source/sink term for foam bubbles in units of number per unit volume per unit time. The total gas saturation is given by $S_g = 1 - S_w = S_f - S_t$. The first term of the time derivative shows the rate at which flowing foam texture becomes finer or coarser per unit rock volume while the second term is the net rate at which foam bubbles trap. The second term on the right hand side represents the convection of foam bubbles. The terms r_g and r_c represent the generation and coalescence, respectively.

The generation and the coalescence terms are found from kinetic considerations and are given as follow⁽³⁶⁾:

the generation term

$$r_g = k_1 v_f^a v_w^b \quad (18)$$

where k_1 is the generation rate constant which reflects the number of foam germination sites. The term $v_f = u_f / \phi S_f$ is the local interstitial velocity of the flowing foam; and $v_w = u_w / \phi S_w$ is the interstitial liquid velocity; a and b are power indices. Kovscek et al.⁽³⁶⁾ used $a=1/3$ and $b=1$. The coalescence is given as:

$$r_c = k_{-1}(S_w) v_f n_f \quad (19)$$

where the $k_{-1}(S_w)$ is a coalescence rate constant which varies strongly with the local value of S_w . Kovscek et al.⁽³⁶⁾ defined $k_{-1}(S_w)$ as:

$$k_{-1}(S_w) = k_{-1}^o \frac{(1 - S_w)}{(S_w - S_w^*)} \quad (20)$$

where S_w^* is the saturation corresponding to the limiting capillary pressure and k_{-1}^o denotes a reference or scaling value.

Equations describing the flow-rate relationships for foam and wetting liquid phase are outlined next. For the flowing foam, the structure of Darcy's law is retained in its used form,⁽³⁶⁾

$$u_f = \frac{k k_{rf}}{\mu_f} \left(-\frac{\partial p_g}{\partial x} \right) \quad (21)$$

where k is the absolute permeability, k_{rf} is the relative permeability to the flowing foam, and μ_f is the effective foam viscosity. On the basis of the work done by Hirasaki and Lawson,⁽¹³⁾ and Bretherton⁽⁷⁷⁾, Kavscek et al. adapted the following expression for μ_f :

$$\mu_f = \mu_g + \frac{\alpha n_f}{v_f^c} \quad (22)$$

where α is a constant of proportionality dependent primarily on the surfactant system and c is an exponent given theoretically as $1/3$ (11,13) or empirically as 0.29 (37,77).

A Stone-type model for the relative permeability of the flowing foam (non-wetting phase) was used by Kavscek et al. of the following form:

$$k_{rf} = k_{rg}^o S_{fd}^g \quad (23)$$

where

$$S_{fd} = X_f(1 - S_{wd}) \quad (23a)$$

and

$$S_{wd} = \frac{(S_w - S_{wc})}{(1 - S_{wc})} \quad (23b)$$

The term $X_f = \frac{S_f}{S_g}$ is the fraction of the foam phase that is flowing. The parameter S_{wc} is the connate aqueous phase saturation and g is the Corey exponent for gas flow. The subscript d indicates that the aqueous phase saturation is normalized over the saturation range where two-phase flow occurs. The term $k_{rf} (=k_{rg})$ is obtained from relative permeability measurements for continuum gas-liquid flow in the porous medium.

The relative permeability for the wetting phase is unaffected by the presence of foam; and it is given by:

$$k_{rw} = k_{rw}^o S_{wd}^f \quad (24)$$

where f is the Corey exponent for liquid flow. The term k_{rw} is obtained in the same manner as k_{rg}

The relative permeability of the trapped foam is zero. To complete the flow model, a relation describing the fraction of foam trapped, X_t , is written as:

$$X_t = X_{t,max} \left(\frac{\beta n_t}{1 + \beta n_t} \right) \quad (25)$$

where $X_{t,max}$ is the maximum fraction of the trapped foam, and β is a trapping parameter. n_t is trapped texture.

The above twelve equations are solved simultaneously by assuming a local equilibrium⁽³⁷⁾. In their simulations, Kovscek et al.⁽³⁶⁾ set n_t equal to n_f . Further, they assumed that the aqueous surfactant phase is incompressible and nonvolatile; the gas (N₂) in the foam phase is insoluble and obeys the ideal gas law. They simulated only the case of steady coinjection of surfactant solution and gas into a one-dimensional core initially filled with surfactant solution. Their experimental and simulated results showed close agreement. Moreover, they stated that their simulation prediction that foam moves in a piston-like fashion through a linear porous medium presaturated with surfactant solution was verified experimentally.

In this study, the effectiveness of surfactants to lower the residual oil saturation will be investigated. The effect of foam quality on foam flow behaviour and residual oil saturation will be examined. Temperature effects on foam flow should be investigated to shed some light on the contradicting results obtained by different researchers. Foam flow mechanism is another area where researchers differ and it should be investigated further. A comprehensive foam research should be undertaken to eliminate many of the contradicting results. It is the aim of this study to clarify some of foam flow problems such as foam flow mechanism, and contribute to the efforts of other researchers to have a better understanding of foam flow in porous media.

3. Objectives

This study investigates the flow mechanism of foam in porous media by examining the pressure along the sand pack. The primary objective of this research is to understand the behaviour of the foam in the porous medium and its effects on recovery. The main objectives of this study are summarized as follows:

1. (a) Examine the possibility of lowering the residual oil saturation after water flooding by use of foaming surfactants.
1. (b) Investigate the effects of foam quality on foam flow and on residual oil saturations.
2. Test and compare different types of foaming surfactants, and determine if a foam forms in a porous medium or not.
3. Investigate the effects of gas flow rate on foam flow.
4. Determine the optimum slug size that would produce the maximum favourable effects on the displacement process.
5. Design and install a data acquisition system to facilitate the recording of experimental data.
6. Investigate the injection method of foam flooding that would give the best results.

4. Experimental Apparatus and Procedure

4.1 Experimental Apparatus

The apparatus used in this study consisted of the following main components: stainless steel coreholder, fluid injection system, gas injection system, production system and data acquisition system. Figure 4.1 shows a schematic diagram of the experimental apparatus.

4.1.1 Physical Model

The physical model used in this work consisted of a stainless steel cylindrical coreholder, 61 cm (24 in) in length by 4.95 cm (1.95 in) in diameter, as shown in Figure 4.2. Two flanges were fitted on each end of the coreholder. A sintered screen was fitted into the inside wall of the cap flanges to act as a distributor for the fluids injected. Three transducer ports were drilled through the wall of the cylinder at an equal distance of 15.25 cm (6 in) from each other, along the length of the coreholder. The transducers helped to sense the foam front and detect foam zone propagation. Four transducers were fitted along the whole length of the core to detect and measure the frontal pressure of the moving foam. The transducers were connected in a way that facilitated easy calibration as illustrated in Figure 4.3. The tubing at the injection end of the coreholder was designed to allow the injection of more than one fluid at the same time.

4.1.2 Materials and Fluids

The materials used to pack the coreholder were Ottawa sand with a US mesh size of 70-140 and distilled water. The sand pack porosity obtained ranged from 35.4 to 36.6 percent and the absolute permeability ranged from 11.25×10^{-12} to 12.8×10^{-12} m² (11.4 to 13.0 darcies).

The surfactants were supplied at no cost by two companies, Witco Corporation* and Dow Chemical Canada INC.** on the condition that the surfactants were to be used only for the purpose of research and not to be analyzed.

* Witco Corporation, Oleochemicals/Surfactants Group
3200 Brookfield St, Houston, TX, 77045.

** Dow Chemical Canada INC.
Sarnia, ONT, Canada, N7T 7K7

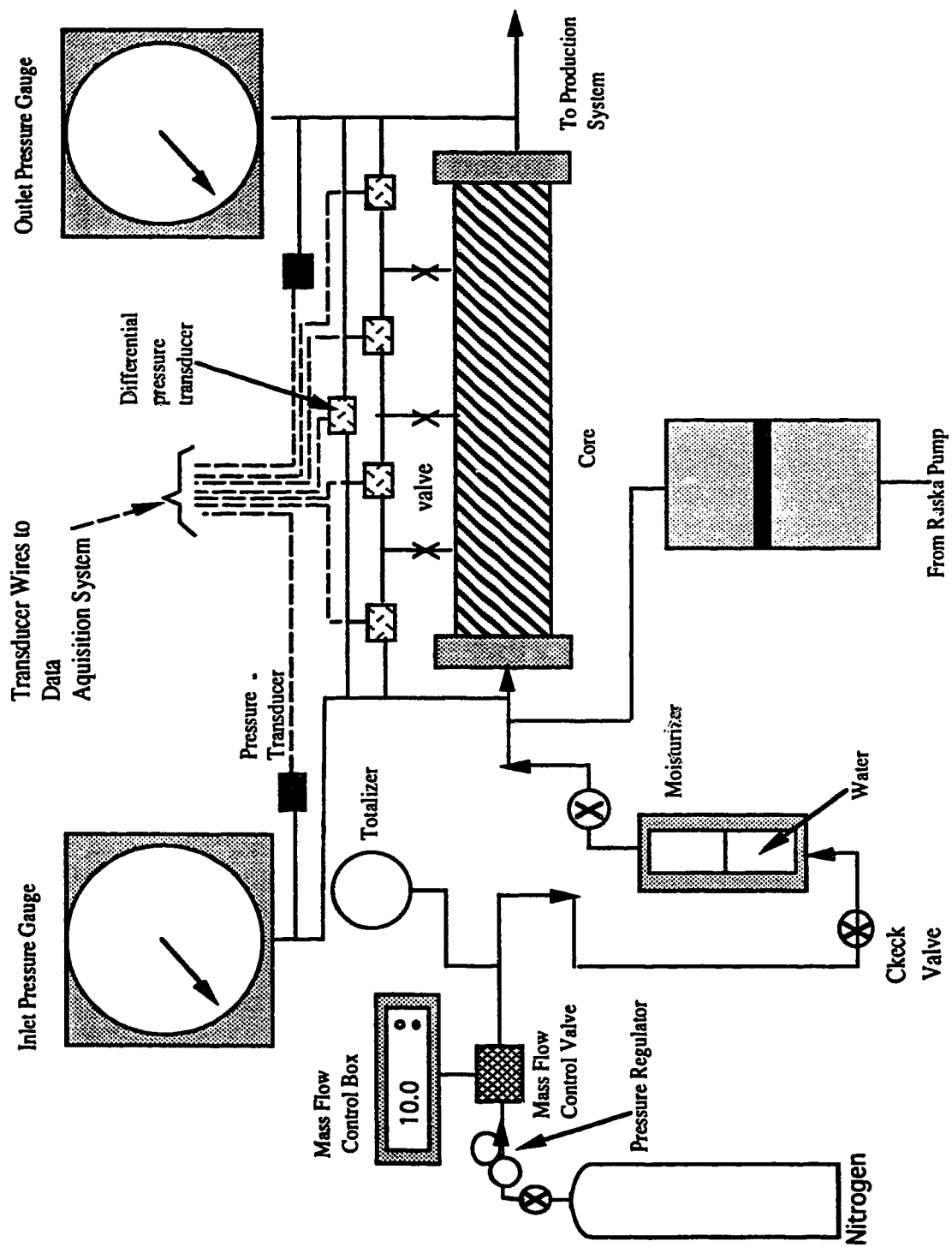


Figure 4.1: Schematic Overview of the Experimental Setup.

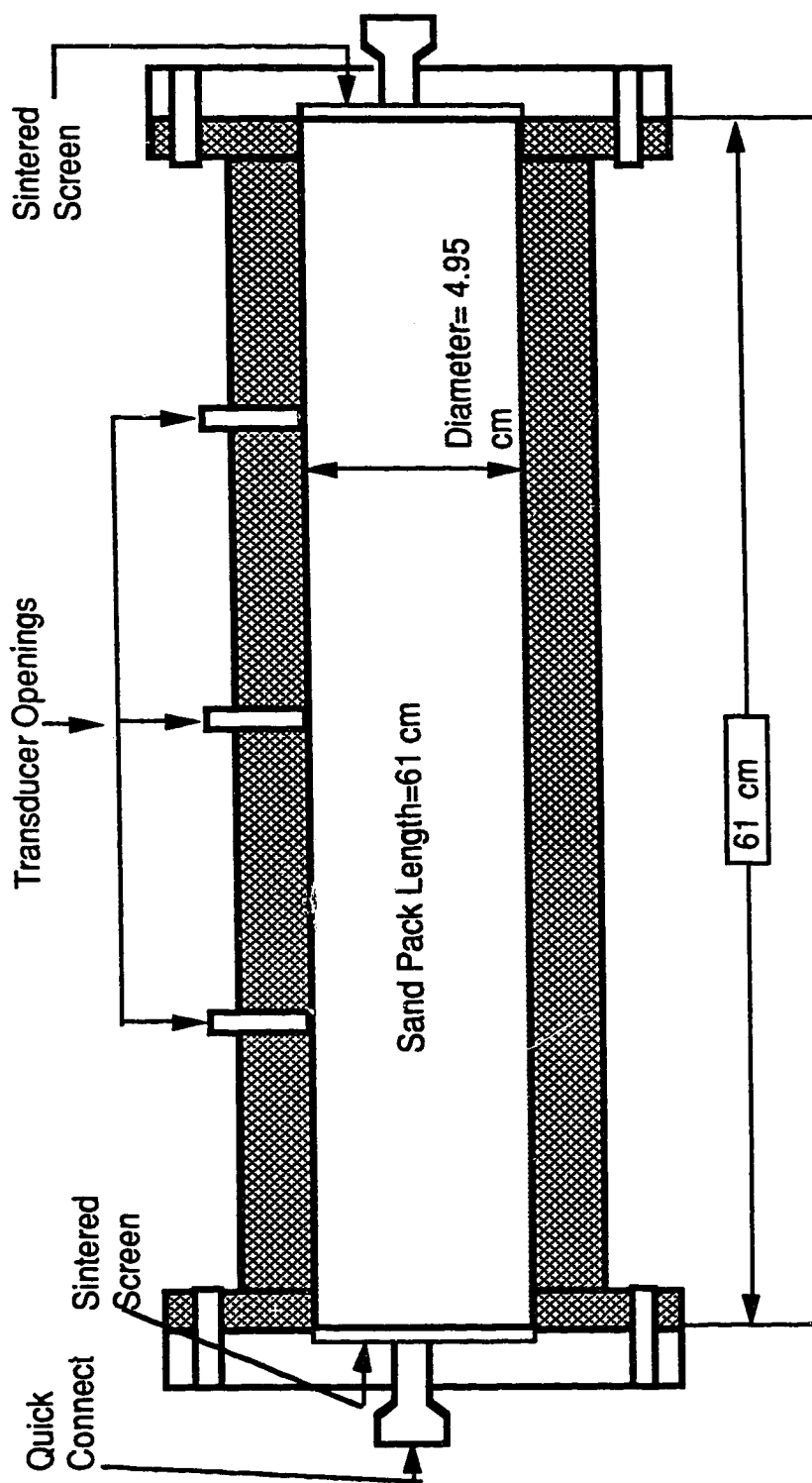


Figure 4.2: Cross-Sectional View of the Physical Model

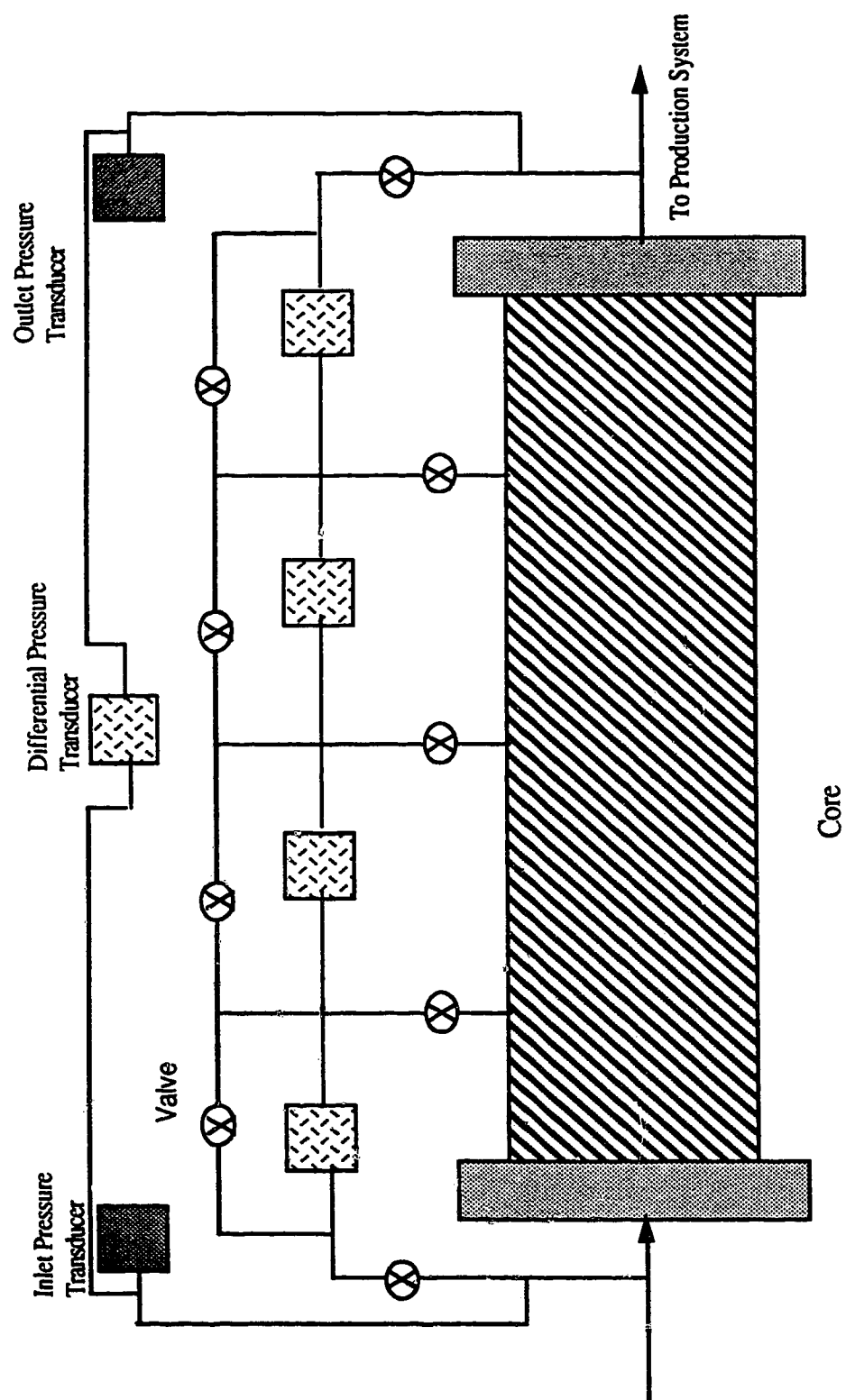


Figure 4.3 Schematic Overview of the Transducer Layout

Three types of surfactants were used to investigate their effect on oil recovery performance, and the effect of oil on foam stability. Dowfax-8390 is sodium sulfate solution surfactant having a specific gravity range of 1.03- 1.13. This surfactant is completely soluble in water. In bottle-shaking tests, Dowfax-8390 gave slightly better results. So, it was used in the majority of experiments. Witcolate-1247H and Witcolate-1276 had specific gravities of 1.06 and 1.01, respectively. Both are also water-soluble. Witcolate-1247H was used in Runs 1, 3 and 12; and Witcolate-1276 was used in Runs 8, 9 and 10. Among six surfactants tested, the three surfactants were chosen based on preliminary bottle-shaking tests by hand in which a small amount of surfactant was mixed with oil and water. The oil used in this study was a refined oil with a viscosity of 50 cp.

4.1.3 Injection System

The injection system consisted of a Ruska pump to inject surfactants, two Milroyal constant rate pumps, and a gas injection system. The Ruska pump was used to inject surfactants. The Ruska pump had a storage for pump oil of 500 cc, which translates to a capacity of 500 cc for continuous pumping. The pump also had two 1000 cc cylinders attached at the end which quadrupled the capacity to 2000 cc, but an interruption period to re-circulate the oil into the pump oil storage could affect the course of the experiments in the case where a fluid volume of more than 500 cc was to be injected. The two Milroyal constant rate pumps were used in the saturation process; one to inject oil and the other to inject water.

Nitrogen was injected and controlled by a pressure regulator and mass flow controller (MFC). The pressure regulator was set so that the mass flow controller was working within the specified range of pressure drop of 10- 40 psig (68.9- 275.8 kPa) across the MFC. The mass flow controller was a Matheson model 8270. This MFC was specifically designed to measure the mass flow rate of nitrogen. The maximum flow rate was 100 sccm (standard cubic centimetre per minute); with an accuracy of +/- 1% full scale and a maximum operation pressure of 150 psig (1034 kPa). The MFC is controlled by a mass flow control box (MFCB). The Box incorporated all the circuitry to operate the mass flow equipment unit. The MFCB controlled the operations of setting the desired flow rate and monitoring the set flow rate. A Matheson totalizer model 8122B was attached to the MFC. It measured the total gas injected in millilitres.

4.1.4 Production System

The collection system consisted of two visual Jergoson cells attached to the outlet end of the coreholder. The two cells were used alternatively. The effluent coming from the coreholder entered the Jergoson cell from the bottom. At the base of both cells a separate valve allowed the emptying of the effluent to atmospheric conditions. These cells were rated for a maximum pressure of 1000 psi (68950 kPa) at 100° F and 585 psi (4033 kPa) at 600° F. A back pressure regulator was attached at the top of the cells. This pressure regulator was used to set the production pressure. A pressure line was connected from a nitrogen cylinder to the back pressure regulator and then into the Jergoson cells. The produced gas was released to the atmosphere as this gas could not be separated from the gas coming from the nitrogen cylinder used for back pressure control. So as a consequence of this, the produced gas could not be measured, but the injected gas was measured by the totalizer. At the beginning of this research, a few experiments were performed under back pressure. Unfortunately, these experiments had to be discarded due problems with the back pressure regulator and rust in the production lines. Consequently, all other runs were performed while venting gas to the atmosphere. Another problem associated with the production system was that gas breakthrough could not be determined accurately. Thus, the line connecting the core to the sample collector was changed to a transparent plastic to facilitate a more accurate determination of the gas breakthrough point. The production system is shown in Figure 4.4.

4.1.5 Data Acquisition System

The data acquisition system used had two parts: hardware and software systems. The hardware consisted of seven Validyne transducers and a Validyne UPC601-L sensor interface card. The card came with its own sensor excitation and carrier demodulation, which meant that no external signal conditioning was required. The card could accommodate a maximum of sixteen single-ended or 8 differential input channels. Out of the seven transducers, five Validyne variable reluctance differential pressure transducers were used to measure the pressure drop across the core. The other two transducers were Validyne gauge (or single-ended) pressure transducers that were utilized, one to measure injection pressure and the other to record the production pressure. Although two pressure gauges existed within the apparatus setup, the two

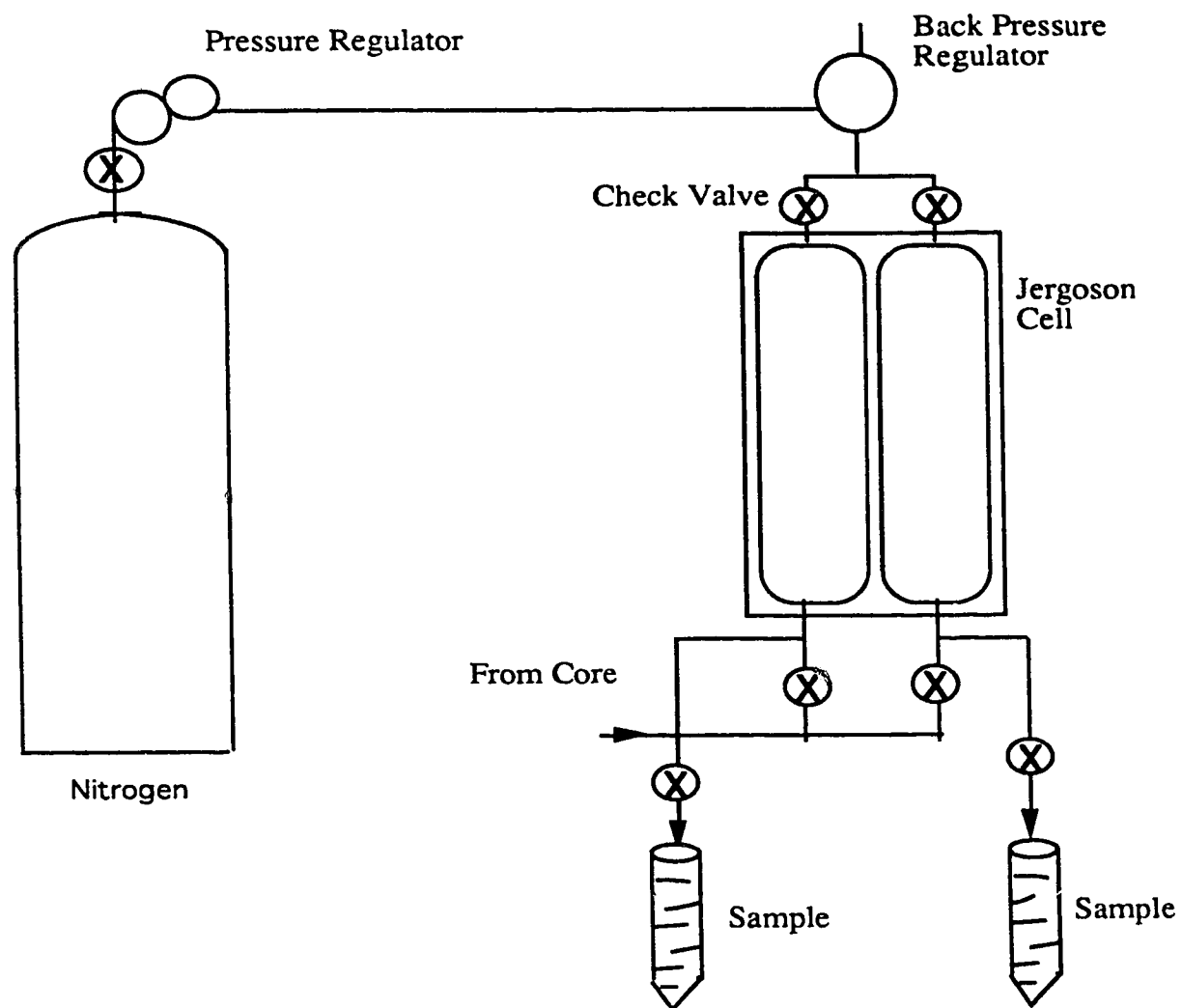


Figure 4.4 : Schematic Representation of the Production System

pressure transducers were used to provide a continuous recording of the injection and the production pressures.

The software side of the data acquisition was Easy Sense, a menu-driven data acquisition program that supports real-time graphs and logging of data to disk files. All set-up parameters were available through pull-down window selections. An ASCII file was generated which could be imported into spreadsheet software for analysis.

4.2 Model Preparation

The first step in preparing the model was making sure that all parts of the apparatus were clean and working properly. Then the coreholder was isolated from the transducer connections, and the injection and production systems. The coreholder was placed vertically in preparation for packing. Then the model was evacuated with a vacuum pump, and was saturated with water. After saturation, the model was placed horizontally and connected to the injection and production systems, and to the transducers. At this stage, the absolute permeability was measured. Then the model was put back in a vertical position to be saturated with oil. After the oil saturation was complete, a slug of surfactant was injected (in case of a slug experiment). In the case of continuous injection experiments, the start of the experiment commenced at the start of the injection of nitrogen and surfactant. In the next paragraphs a detailed explanation of each of the model preparation stages is given.

4.2.1 Packing Procedure

The dry packing method was used in all experiments in this study. The packing process started with the coreholder mounted vertically, with the injection end pointing upwards and the production end pointing downwards. A mechanical vibrator was strapped onto the core. Then a transparent extension was attached to the inlet end. This extension acted to extend the core length, and as a result maintained a more consistent packing throughout the core and insured that the sand pack level flushed with the top of the end flange. The sand was loaded into the coreholder while vibrating. The core was vibrated for 5 hours. The top-extension was removed and an end flange was installed. Then the model was subjected to a vacuum of 1 (6.89 kPa) for three hours. After drawing the vacuum, distilled water was allowed to imbibe into the sandpack core from the bottom end. At this stage, the core was 100% water saturated.

The amount of imbibed water was then taken to be the pore volume of the sand pack. Porosity was then determined by dividing the pore volume by the bulk volume.

Next, the coreholder was put in a horizontal position for absolute permeability measurement. The core initially was 100 % water saturated, and the pressure inside the sandpack was atmospheric. Distilled water was injected at different pressure differentials from the inlet end and produced at the outlet end of the core. When the pressure stabilized, the flow rate and the pressure differential were recorded. Then a different pressure differential was set, left to stabilize, and the corresponding flow rate was recorded. This was repeated five times; to get enough data to draw a straight line.

Darcy's law for linear flow was used to calculate the absolute permeability for each experiment.

$$q = k \left(\frac{A \Delta p}{\mu L} \right)$$

Given that

$L = 0.610$ m (Length of the sand pack)

$\mu = 0.001$ Pa.s (Water viscosity at 24°C and 101.325 kPa)

$A = 0.001924$ m² (Cross-sectional area of the sand pack)

q = Water flow rate in m³/s

Δp = Pressure difference in Pa

k = Absolute permeability in m²

then

$$q = k(3.1541\Delta p)$$

A plot of q versus $(3.1541\Delta p)$ gives a straight line with a slope equal to k (m²) and which passes through the origin. The five points of pressure and their corresponding flow rates were used to construct this line, then a least squares fit was used to estimate k . The absolute permeability measurement was done for every experimental run in this study.

4.2.2 Saturation Process

After the absolute permeability was measured, the transducers were bled-off and checked for calibration. If the transducers needed calibration, they were re-calibrated and prepared for the experimental run. Then the transducers were isolated from the core by shutting off the valves connecting them to the core. For the runs conducted at residual oil saturation, the core was subjected to a sequence of floods. Initially the core was 100 per cent water saturated.

The model was positioned vertically when the oil vessel and saturation lines were air-free and full of oil, the pump was turned on and oil circulated for several minutes to purge any gas trapped in the system. Then the saturation line was connected to the saturation face at the top of the sand pack, and water was drained from the bottom of the sand pack at atmospheric pressure. The core was flooded with 1000 cc of oil. Since the specific gravity of oil was less than that of water, the oil saturation process took place from the top down. This orientation of oil flooding was chosen to achieve a uniform and stable displacement.

After oil saturation was completed, the core holder was flipped upside-down. Distilled water was injected into the core holder from the bottom up toward the outlet end. The core was flooded with an equivalent of 5 pore volumes of distilled water. The residual oil saturation and the initial water saturation were determined by a material balance.

4.3 Experimental Procedure

To conduct an experiment, a surfactant solution of appropriate concentration was prepared. The concentration of the surfactant solution was prepared by mixing distilled water with the desired amount of surfactant. The volume of surfactant used was measured by a very fine graded syringe. The surfactant solution was stirred and then poured into the Ruska pump cylinder. In slug experiments, the surfactant solution of the appropriate slug was injected using the Ruska pump at a rate of 1 cc per minute. After the slug was injected, the Ruska pump was turned off. Meanwhile the mass flow controller was set to the desired flow rate. Then nitrogen injection started, and at the same time the totalizer, the timer and the data acquisition were turned on.

In co-injection (nitrogen and surfactant solution) experiments, the Ruska pump and the mass flow controller were started at the same time. The nitrogen line was equipped with a check valve to prevent any flow of liquid from entering the nitrogen line.

The effluent was collected continuously throughout the experiment. First, the effluent was accumulated in the Jergeson cell until the 50 ml mark. Then the sample was drained into a sample container. The corresponding pressure, time, and the totalizer readings were recorded. The refractive index or the spectrophotometer reading of the sample was determined. This is explained in the next section.

4.4 Sample Analysis

Upon the completion of an experiment, the pressure data were retrieved from the data acquisition system to Microsoft Excel, and plotted. The produced fluids were analyzed from the recorded data. The production data were entered manually into a spreadsheet and then plotted. To determine the concentration of the surfactant in the effluent, the absorbance was measured. A Bausch and Lomb Spectronic-21 spectrophotometer was used to measure the surfactant concentration in the effluent.

A plot of absorbance versus concentration was generated and found to be a straight line. This plot was used to analyze the effluent and determine the surfactant concentration.

The spectrophotometer was used to determine the surfactant concentration. The Spectronic 21 measures the surfactant concentration based on the fundamental law of absorption which is that the rate of decrease in radiant power with the length of the light path b , or with the concentration of the absorbing material c , will follow the mathematical expression:

$$T = 10^{-A} = 10^{-abc}$$

where A is the absorbance and a is the absorptivity. From the above relation, Beer's law is written as:

$$A = abc$$

A plot of A versus c yields a straight line passing through the origin and having a slope of ab . A surfactant sample was scanned over the wavelength range to determine the

location of a characteristic peak. A plot of absorbance versus concentration was generated. The plot was used to determine the surfactant concentration in the effluent. This plot is included as Figure 4.5.

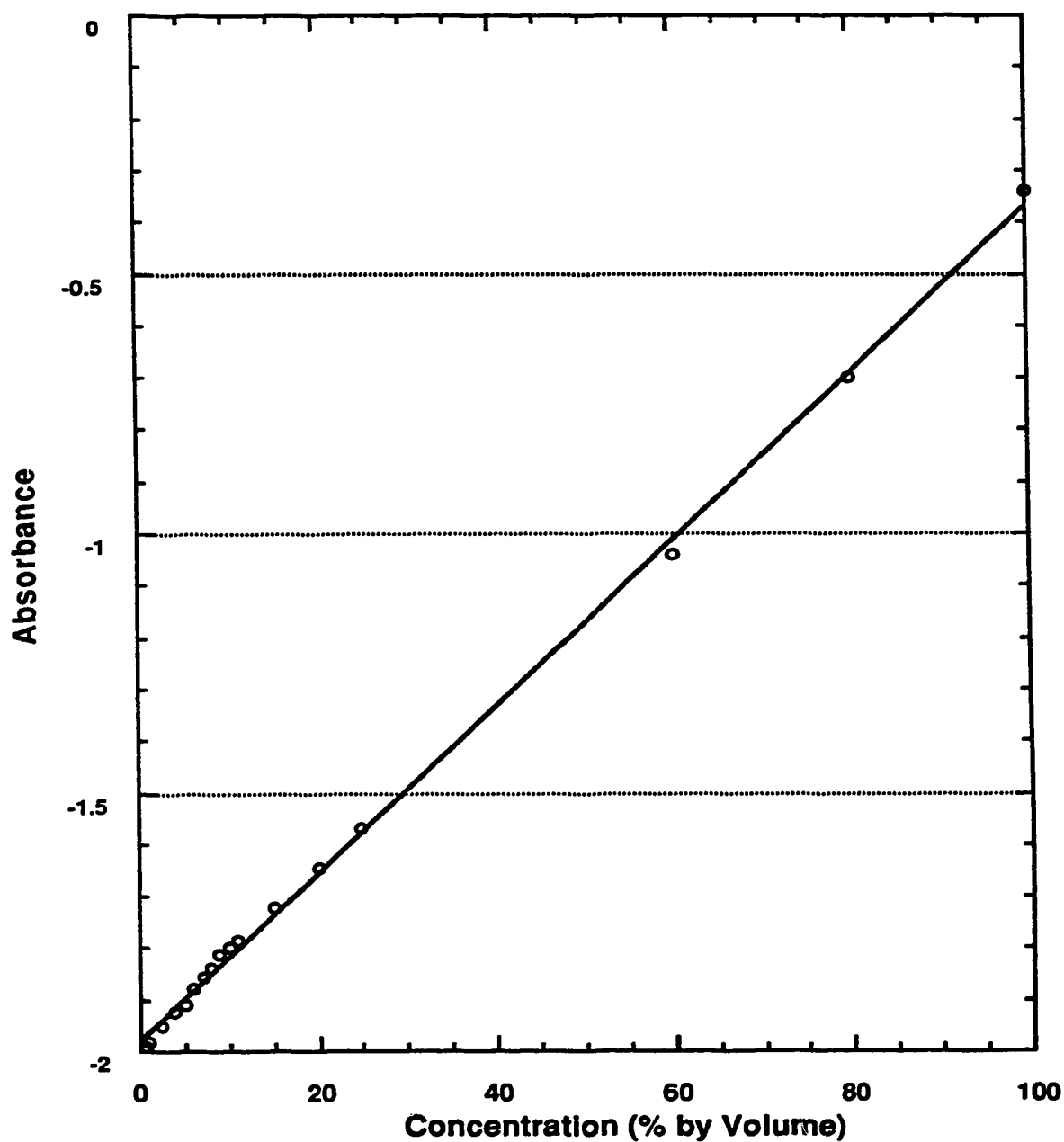


Figure 4.5: Calibration Curve of Absorbance Versus Concentration for Dowfax 8390 Surfactant Determined by Spectronic-21 Spectrophotometer.

5. Discussion of Results

This chapter presents the results of the experimental work conducted on flow of foam in porous media. Figure 5.1 shows a summary of the different experiments performed in this research. Table 5.1 gives a listing of runs and the initial properties of the pertinent sand packs, such as porosity, fluid saturation, and absolute permeability.

This research was aimed at investigating some of the important parameters that affect foam flow in porous media. Effort was directed toward studying parameters individually while keeping other parameters constant within experimental limitations. The foam was generated in situ in Ottawa sand packs at room temperature by injecting nitrogen into sand packs that contained some surfactant solution. In the following sections, the experiments conducted in this research are examined individually and in categories to visualize the effect of the changing variables on the mechanism of foam flow.

5.1 Presentation of Results

Forty-one experiments were carried out to investigate the flow of foam in porous media. Eight of the forty-one experiments were discarded due to mechanical failures during the experiments. In all experiments, foam was formed in situ by injecting nitrogen into the sand pack. The following parameters were investigated: type of surfactant, slug size, surfactant concentration and gas velocity with and without the oil present. The experimental results are discussed for each run by analyzing the production data and the pressure profiles along the sand pack length. The results of each run were compared with a base case experiment to examine the effect of the changing variable on the foam performance and on recovery.

For all experiments, comparison and analysis of the experimental results were done at gas breakthrough. Gas breakthrough was determined visually as the production line was transparent and gas bubbles were easily seen as they exit the core. Several types of experimental runs were conducted. In the first series of runs, three surfactants were tested and compared. The second series of experiments were conducted to examine the effect of the slug size on foam performance.

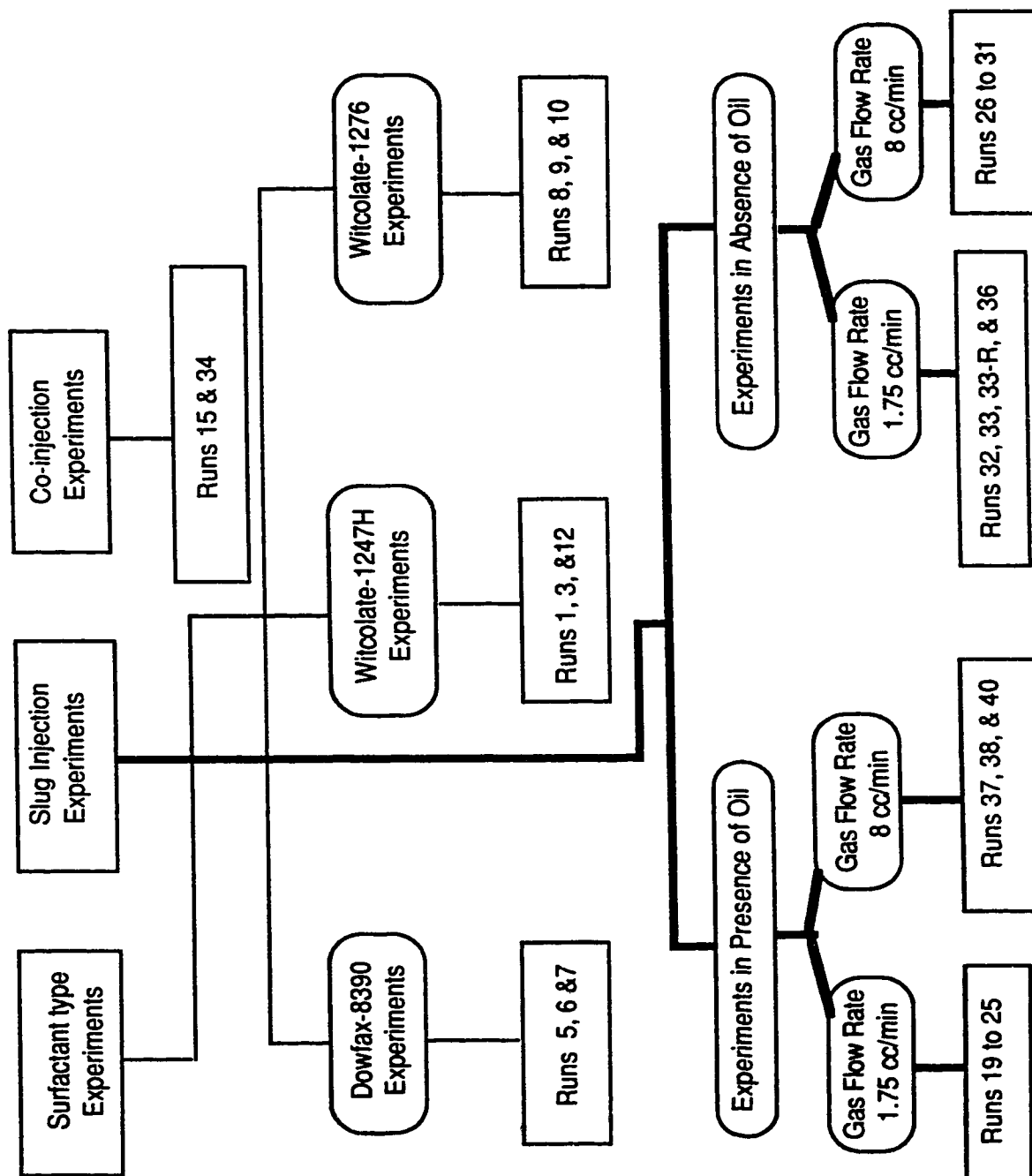


Figure 5.1: Flow Chart of the Experimental Runs Performed in This Research

Summary of Experimental Runs Conducted in this Study

Run No.	Surfactant Name	Surfactant Concentration (%)	Absolute Permeability (darcies)	Sor (%)	Sw (%)	ϕ (%)	Gas Flow Rate (cc/min)	Quality* or Slug Size
1	Witcolate 1247H	1	12.6	38	62	38	5	Slug (10% PV)
3	Witcolate 1247H	1	13	none	100	35	5	Slug (10% PV)
5	Dowfax 8390	1	11.8	30.6	69.4	35	5	Slug (10% PV)
6	Dowfax 8390	1	11.7	30.6	69.4	35	8	Slug (10% PV)
7	Dowfax 8390	20	13	none	100	35	5	Slug (10% PV)
8	Witcolate 1276	1	11.8	none	64.4	35.6	5	Slug (10% PV)
9	Witcolate 1276	1	11.5	43	57	35	5	Slug (10% PV)
10	Witcolate 1276	1	12.6	35	65	35	8	Slug (10% PV)
12	Witcolate 1247H	1	12.6	33	67	34.9	8	Slug (10% PV)
15	Dowfax 8390	10	12.9	28.6	71.4	34.7	1 surf, 10 gas	91%
19	Dowfax 8390	10	12.8	none	100	36	8	Slug (20% PV)
20	Dowfax 8390	10	12.3	none	100	35.7	8	Slug (5% PV)
21	Dowfax 8390	10	12.5	none	100	35.7	8	Slug (10% PV)
22	Dowfax 8390	10	12.5	none	100	34.1	8	Slug (25% PV)

Table 5.1: Summary of Experiments Conducted in the Research

* Quality is given only for continuous injection Runs.

Table 5.1- Continued

23	Dowfax 8390	10	12.5	none	100	35.7	8	Slug (2.5% PV)
24	Dowfax 8390	10	12.1	none	100	35.4	8	Slug (10% PV)
25	Dowfax 8390	none	12.3	none	100	35.5	8	none
26	Dowfax 8390	10	12.5	29.3	70.7	35.7	8	Slug (20% PV)
27	Dowfax 8390	10	12.4	29	71	35.6	8	Slug (5% PV)
28	Dowfax 8390	10	12.4	28.5	71.5	37	8	none
29	Dowfax 8390	10	12.3	30.1	69.9	35.7	8	Slug (10% PV.)
30	Dowfax 8390	10	12.4	28.7	71.3	36	8	Slug (2.5% PV.)
31	Dowfax 8390	10	12.4	28.9	71.1	35.4	8	Slug (25% PV.)
32	Dowfax 8390	10	12.5	28.4	71.6	36.2	1.75	Slug (2.5% PV.)
33	Dowfax 8390	10	12.2	29.8	70.2	35.4	1.75	Slug (10% PV.)
33-R	Dowfax 8390	10	12.3	28.9		35.7	1.75	Slug (10% PV.)
34	Dowfax 8390	10	12.3	28.9	71.1	35.4	1 Surf, 4 gas	80%
35	Dowfax 8390	10	12.2	92.1**	7.9	35.4	8	Slug (20% PV.)
36	Dowfax 8390	10	12.4	31.3	68.7	35.4	1.75	Slug (20% PV.)
37	Dowfax 8390	10	12.4	0	100	35.4	1.75	Slug (2.5% PV.)
38	Dowfax 8390	10	12.2	0	100	35.7	1.75	Slug (20% PV.)
39	Dowfax 8390	10	11.8	Foam	Foam	35.7	1.75	none
40	Dowfax 8390	10	11.4	0	100	35.7	1.75	Slug (10% PV.)
41	Dowfax 8390	1	11.9	31	69	35.8	8	Slug (10% p.v.)

** Initial oil saturation

In the next series of runs, gas flow rate was the variable, and its effects on recovery and the pressure response are discussed. The following sections discuss in detail the objective of each run.

Some clarification of the terminology used in the discussion is given. The word "sand pack" and "core" are used interchangeably. As explained previously, the core was divided into four sections (see Figure 4.3). The transducers across the core are named as follows: $\Delta P1$ and $\Delta P2$ measure the pressure gradient across the first and second sections of the core, respectively, while $\Delta P3$ and $\Delta P4$ record the differential pressure across the third and fourth sections of the core, respectively. Transducer $\Delta P5$ measures the differential pressure across the entire length of the sand pack.

5.2 Base Case Experiment for Water Runs

Run 25 was conducted as a base case run. The objective of this experiment was to serve as a base case for comparing the effect of changing a particular variable in other runs. Run 25 was performed using no surfactant. The sand pack was 100% water saturated. Nitrogen was injected into the sand pack. Table 5.2 presents the production data for this base case run. This data was used to draw Figure 5.2. The Gas breakthrough time was 13.5 minutes. The cumulative percentage pore volume produced at gas breakthrough was 23.3%.

Figure 5.3 shows the pressure history for Run 25. The pressure at the start of the experiment was atmospheric and then nitrogen injection started. The effluent exited the production end of the core at atmospheric pressure. As can be seen from the plot, the pressure reached a maximum value of 1.55 psi (10.7 kPa), then it declined rapidly to about 0.8 psi (5.5 kPa). The expected trend was that all the curves would stabilize at the same differential pressure provided that no saturation gradient exists.

5.3 Type of Surfactant

In this series of experiments, three surfactants: Dowfax-8390, Witcolate-1247H and Witcolate-1276 were tested and compared. Nine experiments were run to compare the above three surfactants. Table 5.3 summarizes the nine experiments. Since the purpose of the nine experiments was to compare the performance of the three surfactants, only the differential pressure along the whole length of core was recorded.

Experimental Data for Run 25, Base Case Run

Pore Volume (cc):	420	Surfactant Name:	none
Porosity (%):	35.8	Surfactant Concentration (%):	0
Absolute Perm. (darcies):	12.3	Slug size (% PV):	0
Oil Saturation:	0	Gas Flow Rate (cc/min):	8
Totalizer Reading at B.T. (cc):	115	Gas Breakthrough Time (min)	14.47
		Cum. Recovery at B.T. (% PV):	23.3

Sample Number	Time (sec)	Sample Volume (cc)	Cumulative Volume (cc)	Totalizer Reading (cc)
1	0	0	0	0
2	485	45	45	67
3	811	45	90	108
4	868	8	98	115
5	1716	60	158	231
6	5866	30	188	784
7	15670	6	194	2091

Table 5.2 : Experimental Data for Run 25, Water Base Case

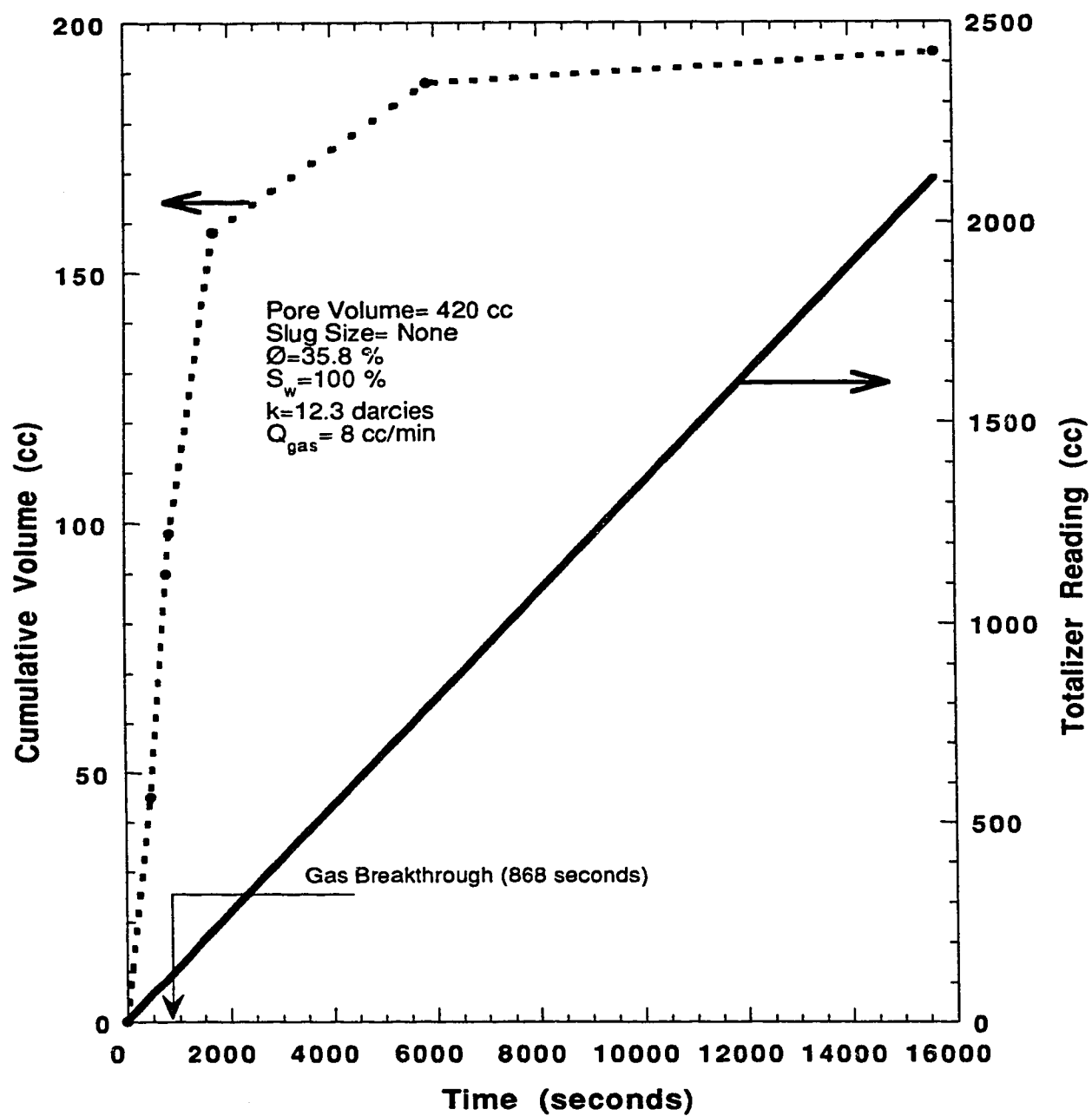


Figure 5.2- Run 25, Base Case: Production Data Versus Time and Totalizer Reading Versus Time for Nitrogen Displacing Water.

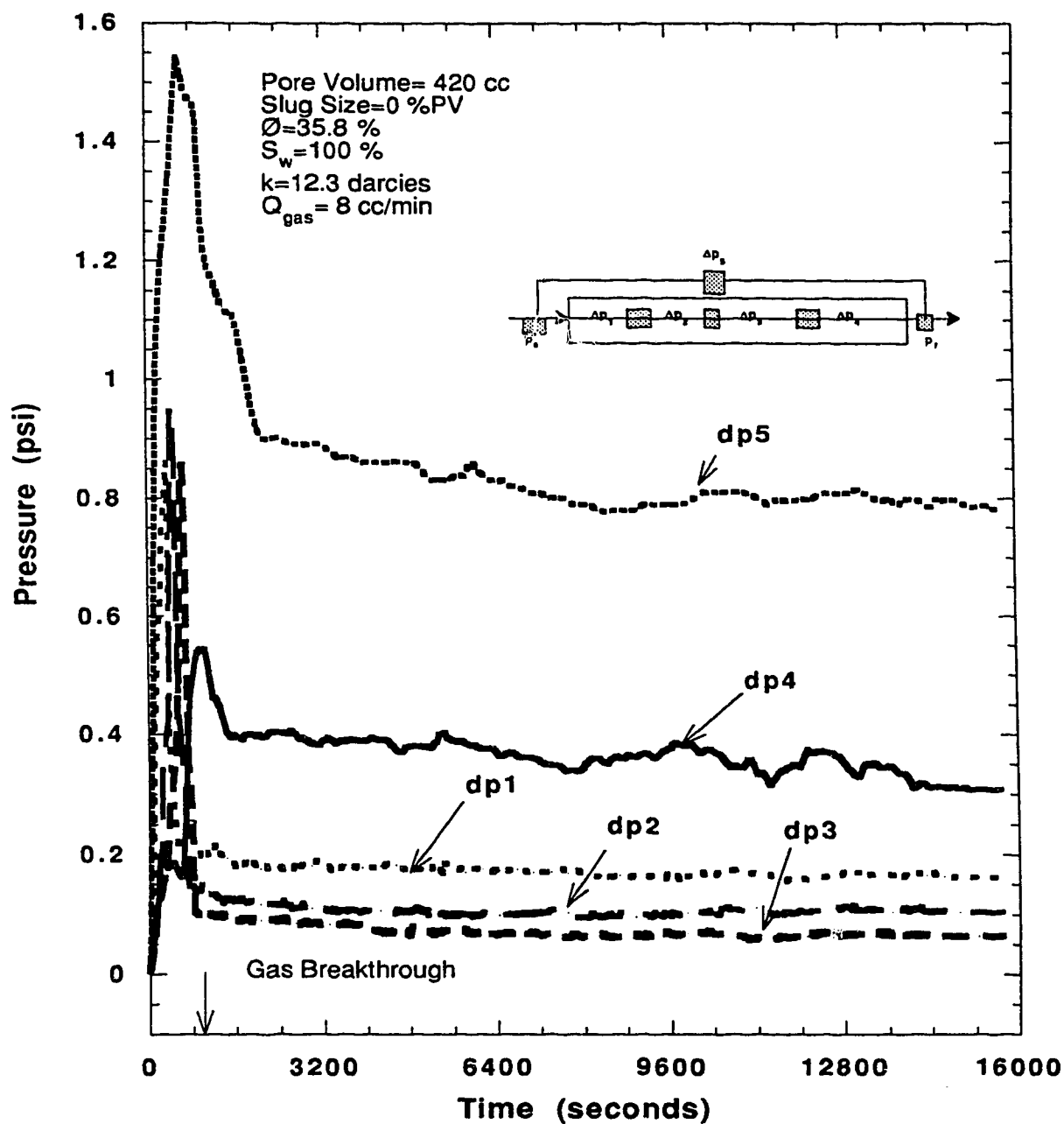


Figure 5.3- Run 25, Water Base: Pressure Profile of Nitrogen Displacing Surfactant-Free Water at a Gas Flow Rate of 8 cc/min.

Surfactant Name →	Witcolate-1247H	Witcolate-1276	Dowfax-8390
Variables	Runs		
Slug Size= 10 (%PV) Surf. Concentration= 1% Gas Flow Rate= 5cc/min Presence of Oil= Yes	Run 1	Run 9	Run 5
Slug Size= 10 (%PV) Surf. Concentration= 1% Gas Flow Rate= 8cc/min Presence of Oil= Yes	Run 12	Run 10	Run 6
Slug Size= 10 (%PV) Surf. Concentration= 1% Gas Flow Rate= 5cc/min Presence of Oil= No	Run 3	Run 8	Run 7

Table 5.3 : Summary of Runs Performed to Test and Compare Three Surfactants.

The following sections detail each of the experiments done to test the aforementioned surfactants and then the results are compared with each other.

5.3.1 Witcolate-1247H Surfactant

Runs 1, 3 and 12 were performed using Witcolate-1247H surfactant. Run 1 was performed in a sand pack having a residual oil saturation of 31.4%. A slug of 10% pore volume (PV) was used. The slug had a surfactant concentration of 1% by volume. After injection of the slug, nitrogen was injected. Table 5.4 gives the production data for Run 1. The cumulative volume produced versus time and the pressure profile for Run 1 are drawn in Figure 5.4. Gas breakthrough occurred 21.47 minutes into the experiment. The cumulative volume produced at breakthrough was 15.5% PV. The pressure curve shows that the differential pressure increased, reached a maximum at the gas breakthrough and then declined.

Run 3 is similar to Run 1 except that Run 3 was performed in a 100% water saturated sand pack. The purpose of excluding oil was to test the surfactant tolerance to the presence of oil. Table 5.5 shows the experimental and production data used to draw Figure 5.5 which graphically illustrates the production history of Run 3. The gas breakthrough time was 79.2 minutes. This time is much higher than that for the base case where no surfactant was used. The delay in gas breakthrough time provides evidence that foam was formed and that foam acted to retard the gas phase flow. The total recovery at breakthrough was 75.1% PV. This is much higher than that for the base case where the recovery was 23.3%.

Compared to Run 1, the differential pressure for Run 3 was higher and stabilized shortly after breakthrough. This means that oil had an adverse effect on Witcolate-1247H surfactant. To find more about the effect of the oil on this surfactant, another experiment (Run 12) was undertaken.

Run 12 was performed in a sand pack having 30% residual oil saturation. The slug size and surfactant concentration were the same as in the previous two experiments. A gas flow rate of 8 cc/min was used. The idea here is that the higher gas flow rate would create stronger foam. The purpose of this run was to investigate the cause of the low differential pressure obtained in Run 1. The experimental data are listed in Table 5.6. Figure 5.6 shows the pressure and the production histories for Run 12. The total produced volume at breakthrough which came 13.35 minutes from start

Experimental Data for Run 1

Pore Volume (cc):	420	Surfactant Name:	Witcolate-1247H
Porosity (%):	35.8	Surfactant Concentration (%):	1
Absolute Perm. (darcies):	12.7	Slug size (% PV):	10
Oil Saturation (%):	31.4	Gas Flow Rate (cc/min):	5
Totalizer Reading at B.T. (cc):	107	Gas Breakthrough Time (min):	21.47
		Cum. Recovery at B.T. (%PV):	15.48

Sample No.	Time (sec)	Sample Volume (cc)	Cumulative Volume (cc)	Pressure Drop (psi)	Totalizer Reading (cc)
1	0	0	0	0	0
2	610	30	30	0.678	50
3	1288	35	65	1.43	107
4	2877	34	99	1.23	240
5	6637	34	133	0.95	555
6	11837	20	153	0.85	985

Table 5.4 : Experimental Data for Run 1 Using Witcolate-1247H in a Slug of 10% PV.

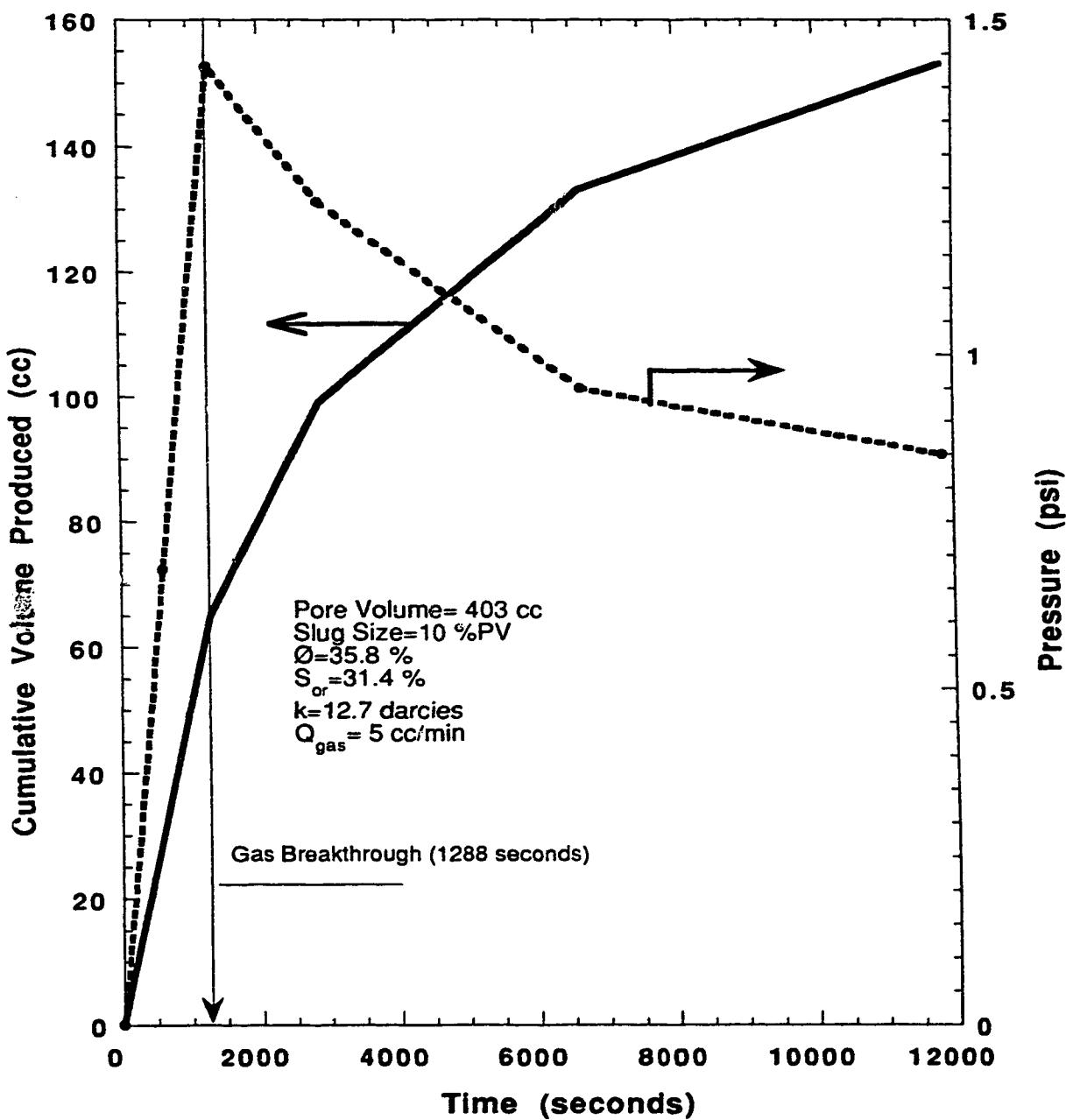


Figure 5.4- Run 1: Cumulative Production Versus Time and Pressure Profile for a Slug of 10% (PV) Having 1% Witcolate-1247H Surfactant Concentration.

Experimental Data for Run 3

Pore Volume (cc):	425	Surfactant Name:	Witcolate-1247H
Porosity (%):	36.2	Surfactant Concentration (%):	1
Absolute Perm. (darcies):	13	Slug size (% PV):	10
Oil Saturation:	0	Gas Flow Rate (cc/min):	5
Totalizer Reading at B.T. (cc):	452	Gas Breakthrough Time (min):	90.52
		Cum. Recovery at B.T. (%PV):	75.1

Sample No.	Time (sec)	Sample Volume (cc)	Cumulative Volume (cc)	Pressure Drop (psi)	Totalizer Reading (cc)
1	0	0	0	0	0
2	695	47	47	0.838	58
3	1148	28	75	0.987	96
4	1658	34	109	1.402	138
5	2336	31	140	1.61	195
6	3078	36	176	2.115	257
7	3839	40	216	2.491	320
8	4379	35	251	2.92	365
9	4939	36	287	3.58	412
10	5431	32	319	3.55	452
11	6631	30	349	3.649	553
12	12031	20	369	3.65	1003

Table 5.5 : Experimental Data for Run 3 Using Witcolate-1247H

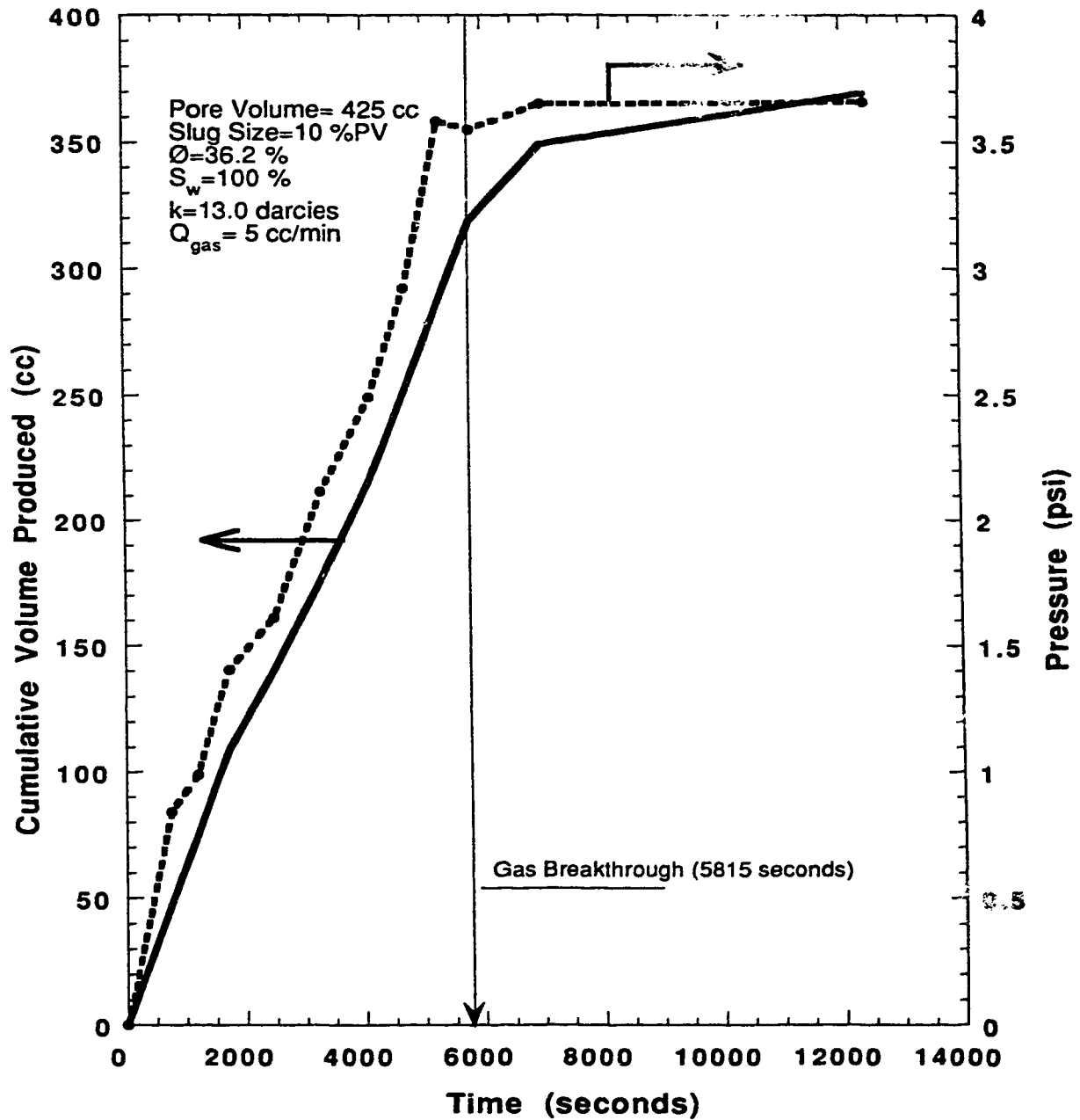


Figure 5.5- Run 3: Cumulative Production Versus Time and Pressure Profile for a Slug of 1% (PV) Having 10% Witcolate-1247H Surfactant Concentration.

Experimental Data for Run 12

Pore Volume (cc):	422	Surfactant Name:	Witcolate-1247H
Porosity (%):	35.9	Surfactant Concentration (%):	1
Absolute Perm. (darcies):	12.6	Slug size (% PV):	10
Oil Saturation (%):	30	Gas Flow Rate (cc/min):	8
Totalizer Reading at B.T. (cc):	107	Gas Breakthrough Time (min):	13.35
		Cum. Recovery at B.T. (% PV):	16.35

Sample No.	Time (sec)	Sample Volume (cc)	Cumulative Volume (cc)	Pressure Drop (psi)	Totalizer Reading (cc)
1	0	0	0	0	0
2	348	35	35	0.76	46
3	801	34	69	1.45	107
4	4461	60	129	1.1	595
5	8141	38	167	0.86	1085
6	12681	52	212	0.8	1691

Table 5.6 : Experimental Data for Run 12 Using Witcolate-1247H in a Slug of 10% PV.

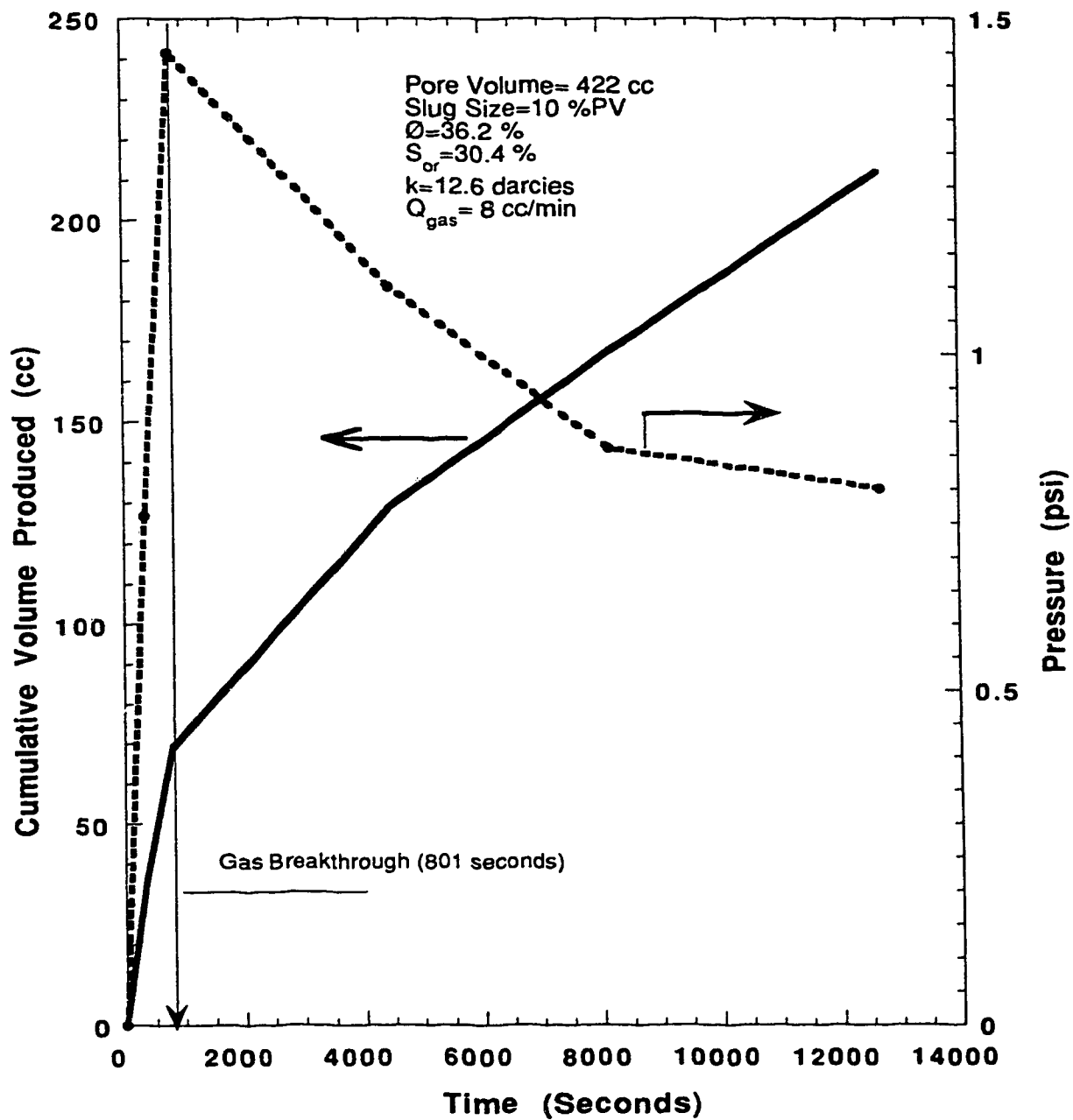


Figure 5.6- Run 12: Cumulative Production Versus Time and Pressure Profile for a Slug of 10% (PV) Having 1% Witcolate-1247H Surfactant Concentration.

of nitrogen injection was 69 cc, an equivalent of 16.35% PV. The pressure gradient was almost the same as that of Run 1. This means that oil had a deleterious effect on Witcolate-1247H, and that the gas channeled through.

5.3.2 Witcolate-1276 Surfactant

Witcolate-1276 was the second surfactant to be tested. The three experiments conducted with Witcolate-1247H were repeated using Witcolate-1276. Runs 8, 9 and 10 were carried out using this surfactant.

Run 8 was conducted in a 100% water saturated sand pack. The gas flow rate for this run was 5 cc/min. The experimental data is listed in Table 5.7 and is drawn in Figure 5.7. From the graph, the cumulative volume produced versus time curve shows a gentle slope until gas breakthrough. This is indicative of an efficient displacement. The breakthrough time was 85.13 minutes at which time a cumulative volume of 78.14% was produced.

To test the effectiveness of this surfactant in the presence of oil, Run 9 was performed in a sand pack having 30.4% residual saturation. The data for this run is tabulated in Table 5.8. Figure 5.8 presents the production and the pressure data. From Figure 5.8, the pressure gradient increased until gas breakthrough, then it continued to decline until the end of the experiment. The total produced water at breakthrough was 14.59% PV. No oil was produced. This run gave results similar to those for Run 1. This means that Witcolate-1276 surfactant was not effective in the presence of oil.

To confirm that the low differential pressure was caused by the deleterious effect of oil on the surfactant and not the gas flow rate, Run 10 was performed at 8 cc/min. The data for Run 10 is given in Table 5.9. The pressure and the production are drawn against time in Figure 5.9. The experimental results were very similar to those for Run 9. At breakthrough, the cumulative volume produced was 16.47% PV for Run 10 and 14.59% PV for Run 9. In Run 10, the produced volume at breakthrough was higher because a more stable foam was formed than in Run 9.

5.3.3 Dowfax-8390 Surfactant

The third surfactant and the last one to be tested was Dowfax-8390. Three experiments, Run 5, 6 and 7, were conducted with and without the presence of oil.

Experimental Data for Run 8

Pore Volume (cc):	430	Surfactant Name:	Witcolate-1276
Porosity (%):	36.6	Surfactant Concentration (%):	1
Absolute Perm. (darcies):	11.8	Slug size (% PV):	10
Oil Saturation:	0	Gas Flow Rate (cc/min):	5
Totalizer Reading at B.T. (cc):	425	Gas Breakthrough Time (min):	85.13
		Cum. Recovery at B.T. (%PV):	78.14

Sample No.	Time (sec)	Sample Volume (cc)	Cumulative Volume (cc)	Pressure Drop (psi)	Totalizer Reading (cc)
1	0	0	0	0	0
2	921	58	58	1.097	76
3	2246	78	136	1.814	186
4	3002	54	190	2.409	250
5	3998	66	256	2.838	333
6	4655	45	301	3.085	390
7	5108	35	336	3.19	425
8	12908	38	374	3.285	1075

Table 5.7 : Experimental Data for Run 8 Using Witcolate-1276 in a Slug of 10% PV.

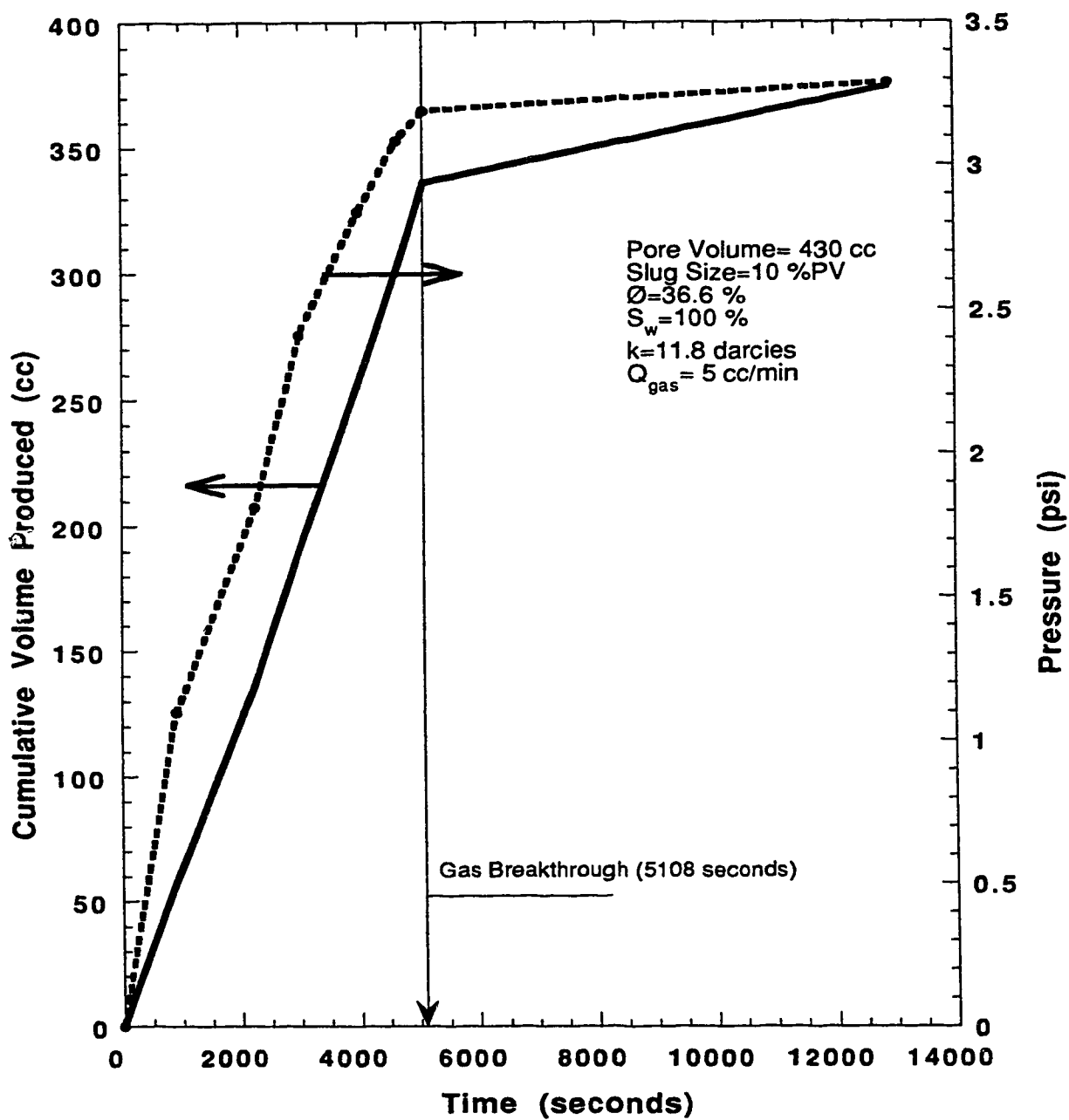


Figure 5.7- Run 8: Cumulative Production Versus Time and Pressure Profile for a Slug of 1% (PV) Having a 10% Witcolate-1276 Surfactant Concentration.

Experimental Data for Run 9

Pore Volume (cc):	425	Surfactant Name:	Witcolate-1276
Porosity (%):	36.2	Surfactant Concentration (%):	1
Absolute Perm. (darcies):	11.9	Slug size (% PV):	10
Oil Saturation (%):	30.4	Gas Flow Rate (cc/min):	5
Totalizer Reading at B.T. (cc):	112	Gas Breakthrough Time (min):	22.43
		Cum. Recovery at B.T. (%PV):	14.59

Sample No.	Time (sec)	Sample Volume (cc)	Cumulative Volume (cc)	Pressure Drop (psi)	Totalizer Reading (cc)
1	0	0	0	0	0
2	593	38	38	0.832	49
3	1346	24	62	1.52	112
4	3043	45	107	1.23	254
5	6723	34	141	0.95	560
6	12323	20	161	0.89	1027

Table 5.8 : Experimental Data for Run 9 Using 1% Witcolate-1276 in a Slug of 10% PV.

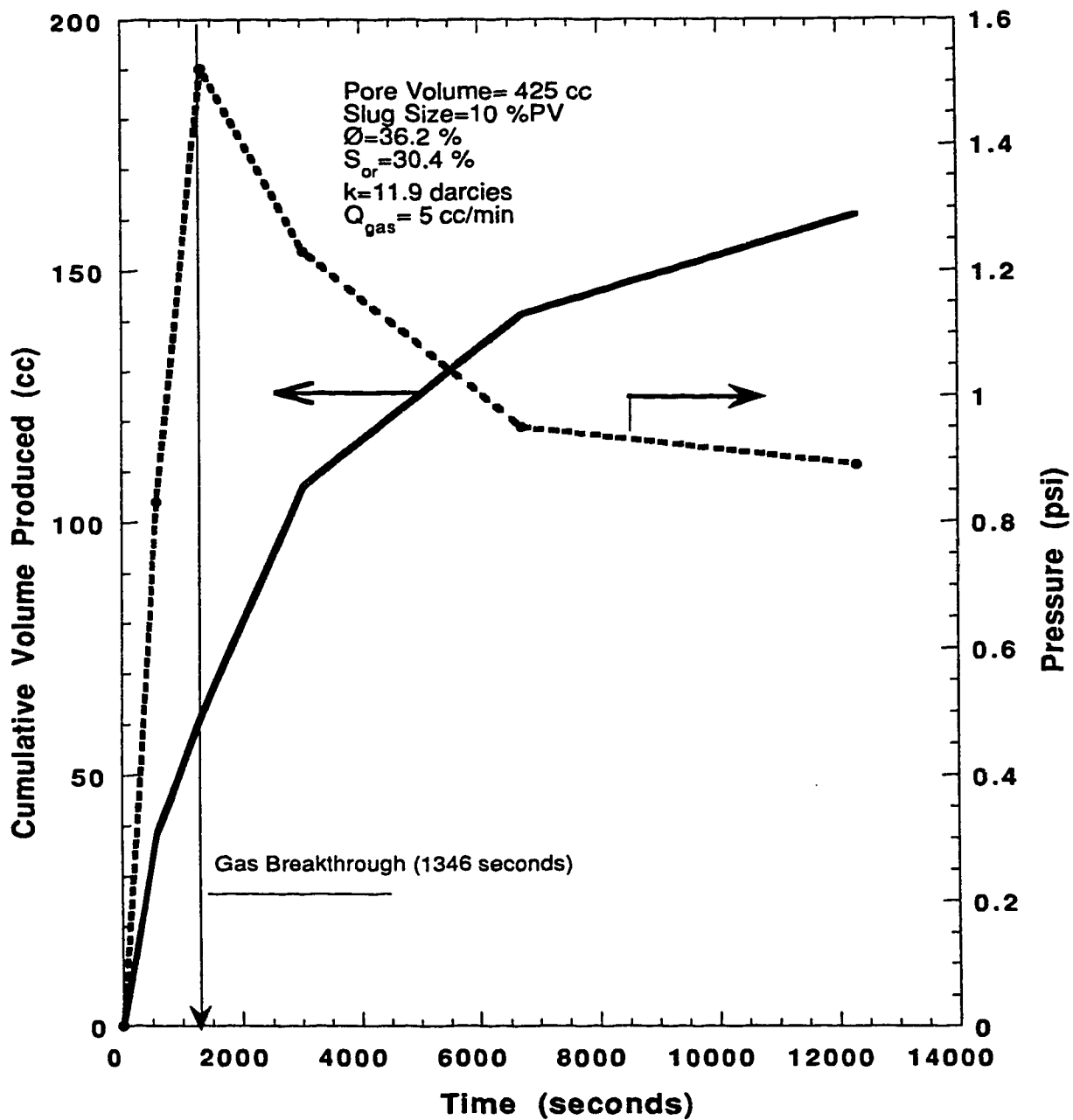


Figure 5.8- Run 9: Cumulative Production Versus Time and Pressure Profile for a Slug of 1% (PV) Having 10% Witcolate-1276 Surfactant Concentration, Conducted in Presence of Oil.

Experimental Data for Run 10

Pore Volume (cc):	425	Surfactant Name:	Witcolate-1376
Porosity (%):	36.2	Surfactant Concentration (%):	1
Absolute Perm. (darcies):	12.6	Slug size (% PV):	10
Oil Saturation:	31	Gas Flow Rate (cc/min):	8
Totalizer Reading at B.T. (cc):	129	Gas Breakthrough Time (min):	16.12
		Cum. Recovery at B.T. (%PV):	16.47

Sample No.	Time (sec)	Sample Volume (cc)	Cumulative Volume (cc)	Pressure Drop (psi)	Totalizer Reading (cc)
1	0	0	0	0	0
2	520	35	35	0.76	69
3	967	35	70	1.68	129
4	1527	34	104	1.2	204
5	3377	30	134	0.95	450
6	12277	45	179	0.82	1637

Table 5.9 : Experimental Data for Run 10 Using Witcolate-1276

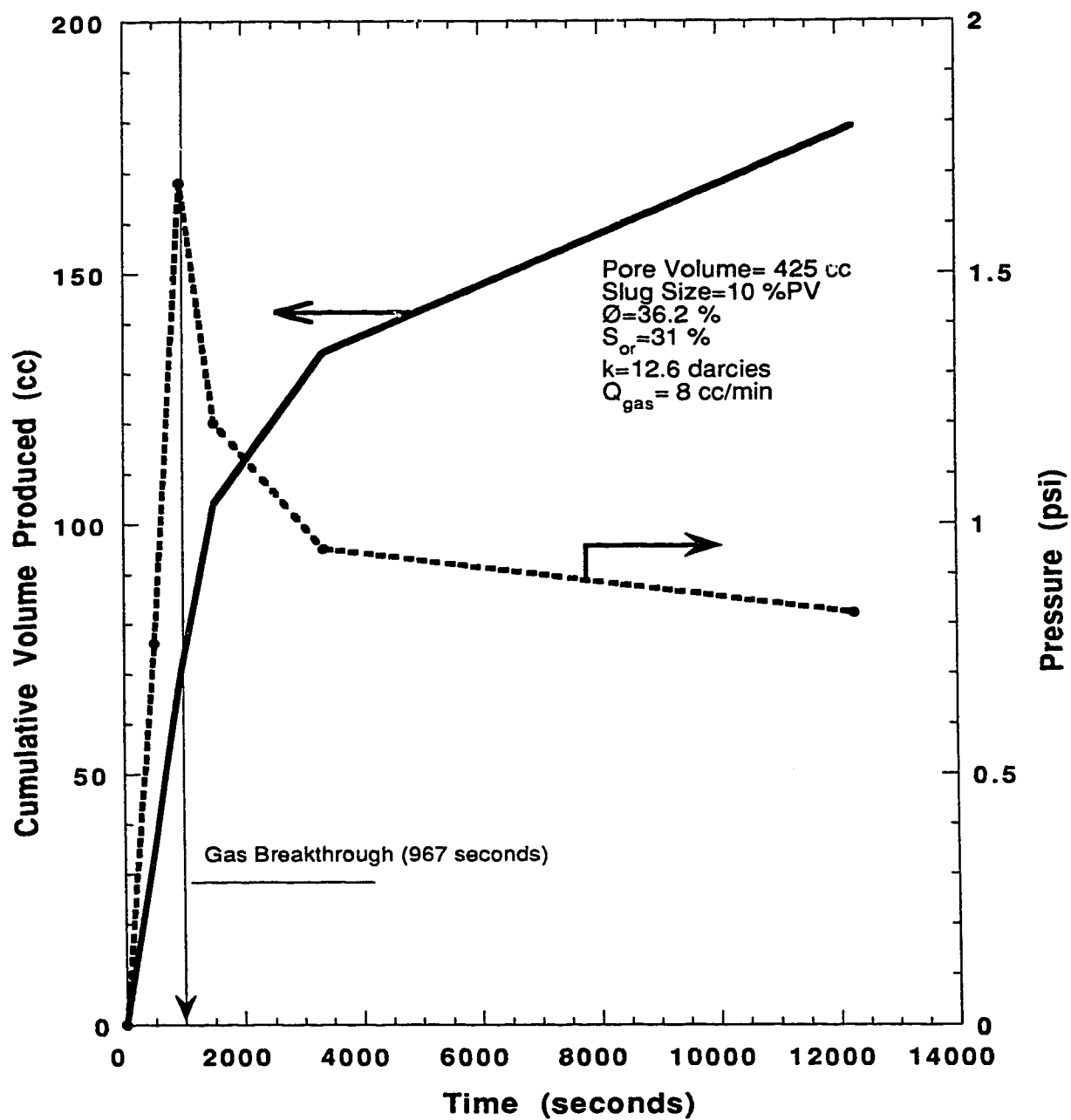


Figure 5.9- Run 10: Cumulative Production Versus Time and Pressure Profile for a Slug of 1% (PV) Having 10% Witcolate-1276 Surfactant Concentration.

Two different gas flow rates were used, 5 cc/min and 8 cc/min, and a slug size of 10% PV was used in all three runs.

Table 5.10 lists the experimental data for Run 5 which was carried out in a 11.8 darcy sand pack having a residual oil saturation of 30.5%. A gas flow rate of 5 cc/min was used. The measured pressure and production are drawn against time in Figure 5.10. Compared to the Runs 1 and 9, done with the other two surfactants (see table 5.3), Run 5 gave a higher recovery of 17.41% PV at breakthrough. The pressure versus time curve in Figure 5.10 did not fall immediately after breakthrough, but it continued to rise reaching 1.85 psi (12.8 kPa) then started to fall.

Run 6 was carried out to investigate the effect of gas flow rate on the foamability of Dowfax-8390 and to investigate further the effect of oil on the surfactant. Table 5.11 provides the production data for this run. A gas flow rate of 8 cc/min was used. The recorded pressure and production versus time are plotted in Figure 5.11. The cumulative volume produced at breakthrough was 14.25%. From the graph, the pressure profile was unexpectedly very different from that for Run 5. This indicates the unpredictable nature of foam in the presence of oil in porous media; this is in reference to the tested surfactant and the oil used in this study. Run 6 was repeated to confirm the results, and will be discussed later in Section 5.7, Reproducibility of Results.

Run 7 was done in a 100% water-saturated core. The purpose was to compare Dowfax-8390 with the other two surfactants tested. A gas flow rate of 5 cc/min was used. Table 5.12 presents the experimental data for Run 8. The tabulated data are drawn in Figure 5.12. Breakthrough occurred after the injection of 455 cc of gas as measured by the totalizer. At this point, the cumulative water produced was 78.25% PV. The differential pressure, as can be seen from the graph, stabilized after gas breakthrough at 4.25 psi (29.3 kPa).

5.3.4 Overall Evaluation of the Surfactants Tested

Table 5.13 provides a summary of the evaluation of the runs performed with the above three surfactants. The results for the three surfactants were very similar. All three surfactants were detrimentally affected by the refined oil used in this study. In order to choose one surfactant out of the three tested, the cumulative volume produced and the differential pressure were compared for the runs. Comparing Runs 3, 7 and 8

Experimental Data for Run 5

Pore Volume (cc):	425	Surfactant Name:	Dowfax-8390
Porosity (%):	36.2	Surfactant Concentration (%):	1
Absolute Perm. (darcies):	11.8	Slug size (% PV):	10
Oil Saturation (%):	30.5	Gas Flow Rate (cc/min):	5
Totalizer Reading at B.T. (cc):	120	Gas Breakthrough Time (min):	23.8
		Cum. Recovery at B.T. (%PV):	17.41

Sample No.	Time (sec)	Sample Volume (cc)	Cumulative Volume (cc)	Pressure Drop (psi)	Totalizer Reading (cc)
1	0	0	0	0	0
2	556	36	36	0.843	46
3	1428	38	74	1.76	120
4	2746	35	109	1.85	230
5	4211	35	144	1.35	350
6	6911	30	174	1	575
7	12311	20	194	0.95	1026

Table 5.10 : Experimental Data for Run 5 Using Dowfax-8390 in a Slug of 10% PV.

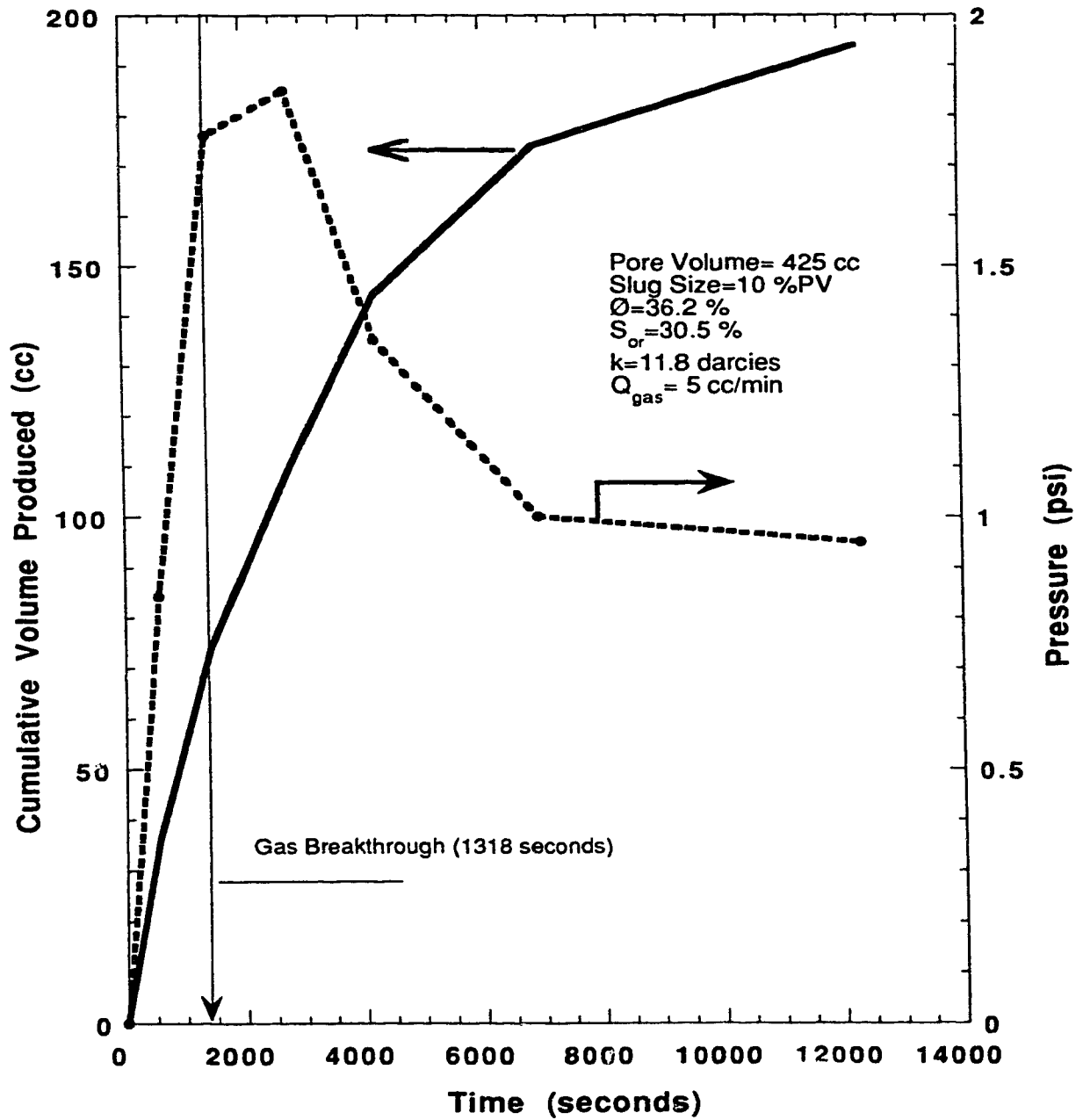


Figure 5.10- Run 5: Cumulative Production Versus Time and Pressure Profile for a Slug of 1% (PV) Having 10% Dowfax-8390 Surfactant Concentration.

Experimental Data for Run 6

Pore Volume (cc):	425	Surfactant Name:	Dowfax-8390
Porosity (%):	36.2	Surfactant Concentration (%):	1
Absolute Perm. (darcies):	11.9	Slug size (% PV):	10
Oil Saturation:	31	Gas Flow Rate (cc/min):	8
Totalizer Reading at B.T. (cc):	75	Gas Breakthrough Time (min):	9.53
		Cum. Recovery at B.T. (%PV):	14.59

Sample No.	Time (sec)	Sample Volume (cc)	Cumulative Volume (cc)	Pressure Drop (psi)	Totalizer Reading (cc)
1	0	0	0	0	0
2	327	32	32	1.215	44
3	572	30	62	1.843	75
4	1307	36	98	1.113	175
5	3592	30	128	0.852	480
6	22842	45	173	0.85	3046

Table 5.11 : Experimental Data for Run 6 Using Dowfax-8390 in a Slug of 10% PV.

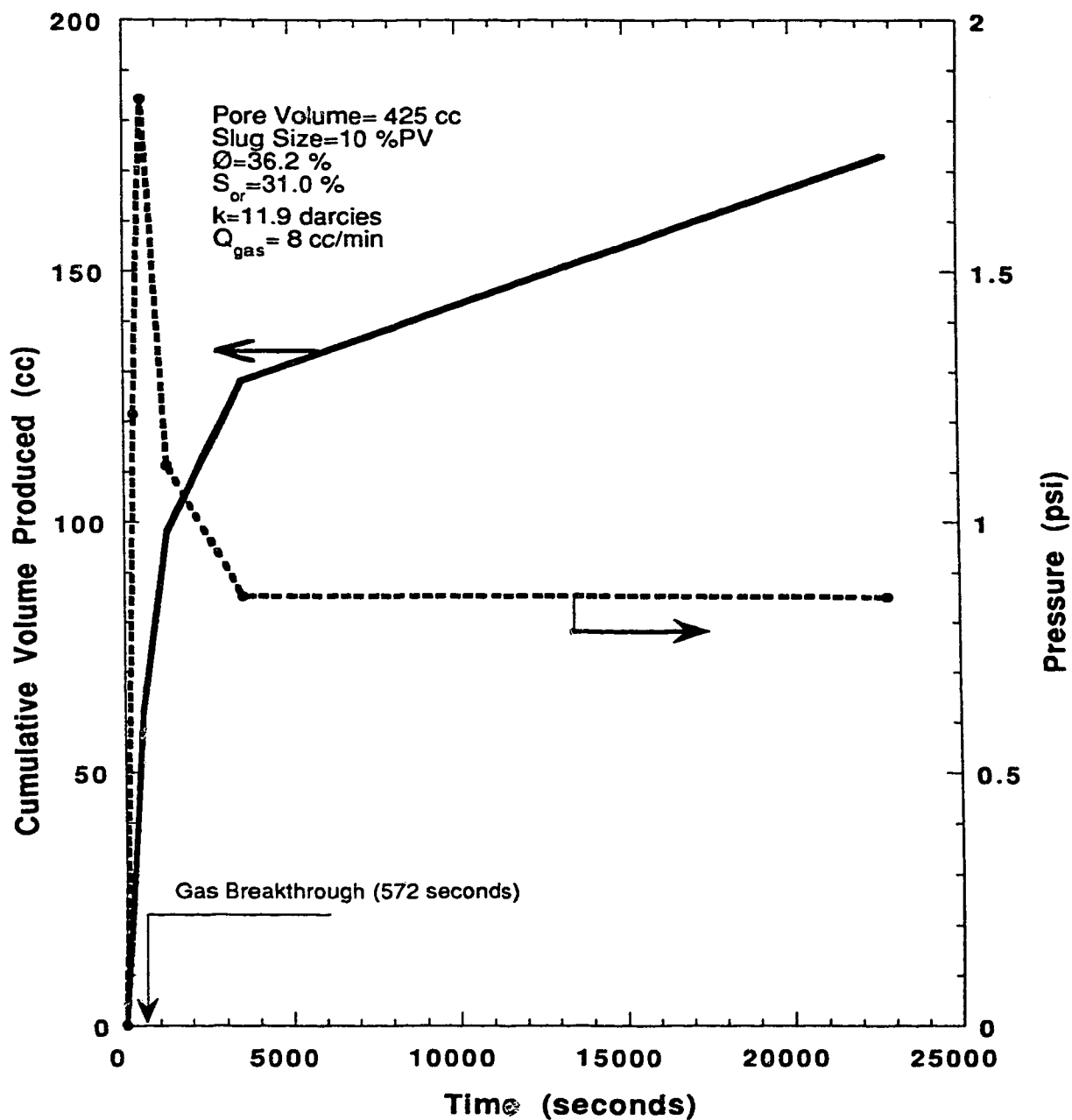


Figure 5.11- Run 6: Cumulative Production Versus Time and Pressure Profile for a Slug of 1% (PV) Having 10% Dowfax-8390 Surfactant Concentration.

Pore Volume (cc):	423	
Porosity (%) :	36	
Absolute Perm. (darcies):	13	
Oil Saturation:	0	
Totalizer Reading at B.T. (cc)	455	
Surfactant Name:		Dowfax-8390
Surfactant Concentration (%) :		1
Slug size (% PV):		10
Gas Flow Rate (cc/min):		5
Gas Breakthrough Time (min):		90.7
Cum. Recovery at B.T. (%PV):		78.25

Table 5.12 : Experimental Data for Run 7 Using Dowfax-8390 in a Slug of 10% PV.

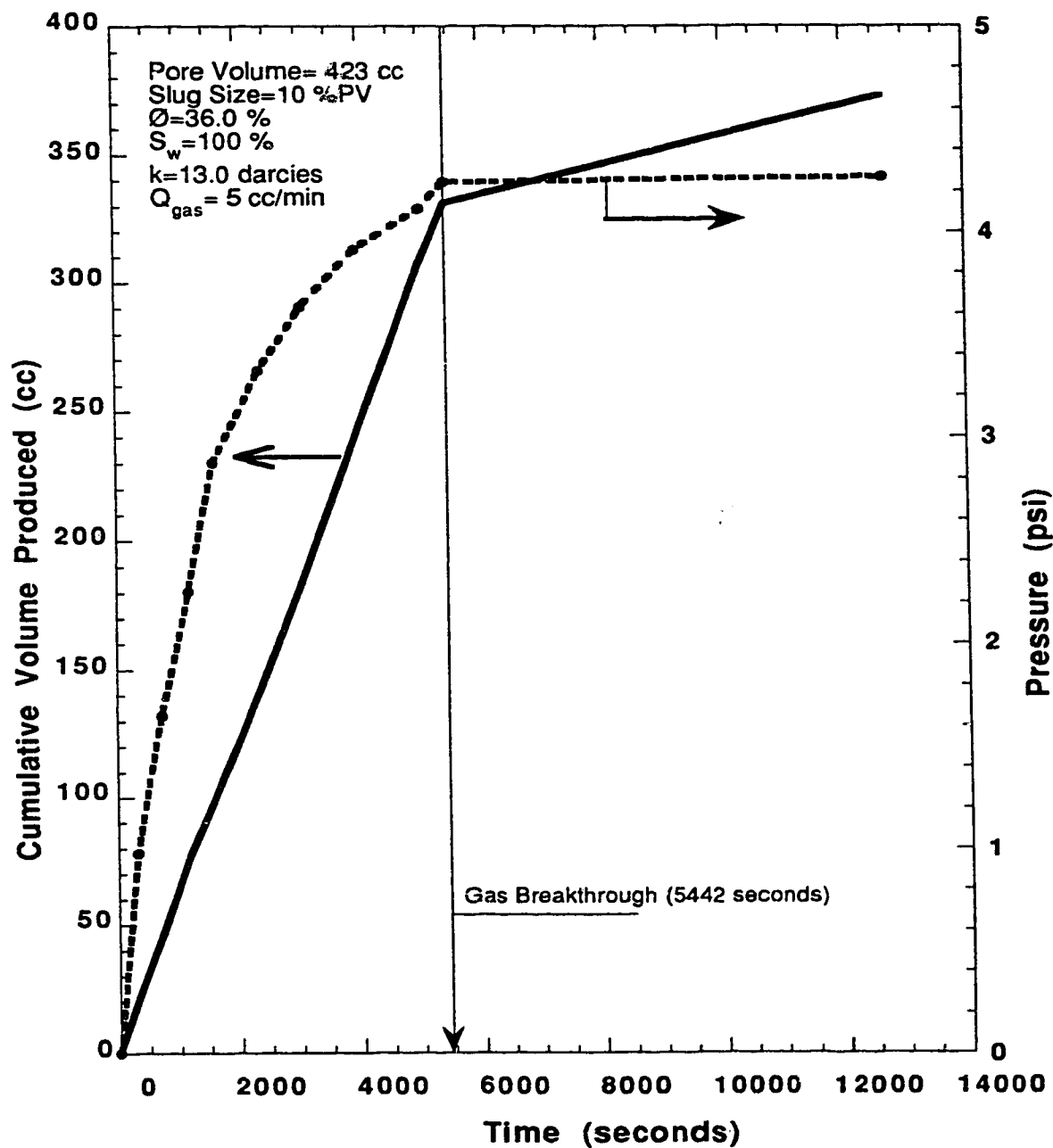


Figure 5.12- Run 7: Cumulative Production Versus Time and Pressure Profile for a Slug of 1% (PV) Having 1% Dowfax-8390 Surfactant Concentration.

Surfactant Name -->	Witcolate-1247H	Witcolate-1276	Dowfax-8390
Variables	Runs		
Slug Size= 10 (%PV)	Run 1	Run 9	Run 5
Surf. Concentration= 1%	B.T. Time= 21(min)	B.T. Time= 22.43 (min)	B.T. Time= 23.8 (min)
Gas Flow Rate= 5cc/min	Rec. @ B.T.= 15.48(%PV)	Rec. @ B.T.= 14.59(%PV)	Rec. @ B.T.=17.41 (%PV)
Presence of Oil= Yes	Tot. Read @ B.T.= 107(cc)	Tot. Read @ B.T.= 112(cc)	Tot. Read @ B.T.=120 (cc)
Slug Size= 10 (%PV)	Run 12	Run 10	Run 6
Surf. Concentration= 1%	B.T. Time= 13.35 (min)	B.T. Time= 16.12 (min)	B.T. Time= 9.53 (min)
Gas Flow Rate= 8cc/min	Rec. @ B.T.= 16.35 (%PV)	Rec. @ B.T.= 16.47(%PV)	Rec. @ B.T.=14.59 (%PV)
Presence of Oil= Yes	Tot. Read @ B.T.= 107(cc)	Tot. Read @ B.T.=129 (cc)	Tot. Read @ B.T.= 75 (cc)
Slug Size= 10 (%PV)	Run 3	Run 8	Run 7
Surf. Concentration= 1%	B.T. Time= 90.52 (min)	B.T. Time= 85.13 (min)	B.T. Time= 90.7 (min)
Gas Flow Rate= 5cc/min	Rec. @ B.T.= 75.1 (%PV)	Rec. @ B.T.=78.18 (%PV)	Rec. @ B.T.=78.72 (%PV)
Presence of Oil= No	Tot. Read @ B.T.= 452 (cc)	Tot. Read @ B.T.= 425 (cc)	Tot. Read @ B.T.= 455 (cc)

Table 5.13 : Summary of Overall Evaluation of Runs Performed to Test and Compare Three Surfactants.

Note:

B.T. = Gas Breakthrough

Rec. = Cumulative Produced Volume

Tot. Read= Totalizer Reading

reveals that Run 7 showed the highest differential pressure, 4.25 psi (29.3 kPa), and slightly higher cumulative volume produced, 78.72% PV, at breakthrough than Run 8 which gave 78.18% PV. So Dowfax was chosen to be used in the rest of the runs.

5.4 Slug Injection Runs

In this set of experiments, nitrogen was injected continuously into the sand pack after the injection of the surfactant slug. The effluent, from the core, was then collected and tested for surfactant concentration using the Spectronic-21 spectrophotometer. Surfactant-slug injections were conducted in Runs 19 to 24, 26-27 and 36-40. The objective of these runs was to examine the effect of slug size in the presence and absence of oil on the total mobility and the gas phase mobility. The mechanism of foam flow is examined.

The slug injection runs were subdivided into two groups according to the principal variable investigated. In the first set of runs, 19 to 24, the sand pack was initially 100% water-saturated. A slug of surfactant was then injected. The purpose of these experiments was to investigate the flow of foam in the absence of oil and to determine the optimum slug size for the condition of no oil. These runs also will form a basis for comparison for the flow of foam experiments in the presence of oil.

The second series of runs were conducted in the presence of a residual oil saturation, S_{or} . These experiments are Runs 26 to 31 that were previously listed in Table 5.1. The purpose of these runs was to investigate the foam flow regime when a residual oil saturation is present. Furthermore, it was intended to find the optimum slug size which would give maximum recovery.

5.4.1 Typical Slug Injection Run

The objective of the set of experiments was to investigate the foam flow mechanism as well as the effect of foam on gas phase mobility as the slug size is changed. Run 25 was the base case, gas displacing water with no surfactant present, for all the foam experiments conducted in this research. Besides Run 25, Run 28 was also a base case for experiments conducted in the presence of residual oil. Run 28 was conducted at residual oil saturation where water was displaced by nitrogen without the use of a surfactant. Discussion of Run 28 will be given later. For Run 25, water was

displaced by nitrogen and did not involve any surfactant. The Data for Run 25 were previously given in Table 5.2 and plotted in Figure 5.2.

To provide a clear understanding of the experimental results and the pertinent calculations, Run 38 will be examined and discussed as an example in detail. The data for this run is given in Table 5.14. The table lists the sand pack initial conditions such as porosity, absolute permeability and saturations, along with the surfactant concentration, slug size and gas flow rate. The gas breakthrough time and cumulative produced volume at breakthrough are also listed in the table. The second column represents the time from the commencement of gas injection until the collection of the sample. The third and fourth columns show the sample volumes and the cumulative volume produced, respectively. The totalizer reading, the amount of gas injected, is given in the fifth column. The last column shows the surfactant concentration as determined by either the refractometer or by the Spectronic-21 spectrophotometer.

The totalizer reads at atmospheric conditions of pressure and temperature, here taken as 14.7 psi (101.4 kPa) and 20° C. The surfactant concentration for Run 38 was 10% of Dowfax-8390. The experiment was carried out in a sand pack having a permeability of 12.2 darcies, a measured porosity of 35.8% and a water saturation of 100%. Nitrogen injection was regulated by the mass flow controller and read at one atmosphere and room temperature (20° C). Therefore, whenever the pressure needs to be used in any calculation, it has to be corrected by using the ideal gas law at constant temperature.

$$P_1 V_1 = P_2 V_2$$

Here the subscript 1 represents the atmospheric conditions and 2 represents the conditions in question.

The pressure used in the calculation is the steady state differential pressure (ΔP_{ss}) which is determined from the pressure history of the experiment. Figure 5.13 shows the pressure history of Run 38. It is clear from the graph that the differential pressure stabilized at about 3.45 psi (23.8 kPa). The differential pressure stabilized some time after gas breakthrough.

The steady-state differential pressure is used to calculate the total foam mobility using the equation:

Experimental Data for Run 38

Pore Volume (cc):	420	Surfactant Name:	Dowfax-8390
Porosity (%):	35.8	Surfactant Concentration (%):	10
Absolute Perm. (darcies):	12.2	Slug size (% PV):	20
Oil Saturation:	0	Gas Flow Rate (cc/min):	1.75
Totalizer Reading at B.T. (cc):	451	Gas Breakthrough Time (min)	257.3
		Cumulative Recovery at B.T. (% PV):	83.81

Sample Number	Time (sec)	Sample Volume (cc)	Cumulative Volume (cc)	Totalizer Reading (cc)	Concentration (% Vol)
1	0	0	0	0	0
2	1669	34	34	49	0
3	2958	32	66	87	0
4	4216	30	96	123	0
5	5841	37	133	171	0
6	7115	30	163	209	0.99
7	8386	30	193	246	1.13
8	9695	30	223	284	1.42
9	10988	30	253	322	1.42
10	12324	30	283	361	1.72
11	13690	30	313	402	3.55
12	15071	30	343	442	25.91
13	15438	9	352	451	63.91
14	28049	29	381	820	60.18

Table 5.14 : Experimental Data for Run 38 Using 10% Dowfax-8390 in a Slug of 20% PV.

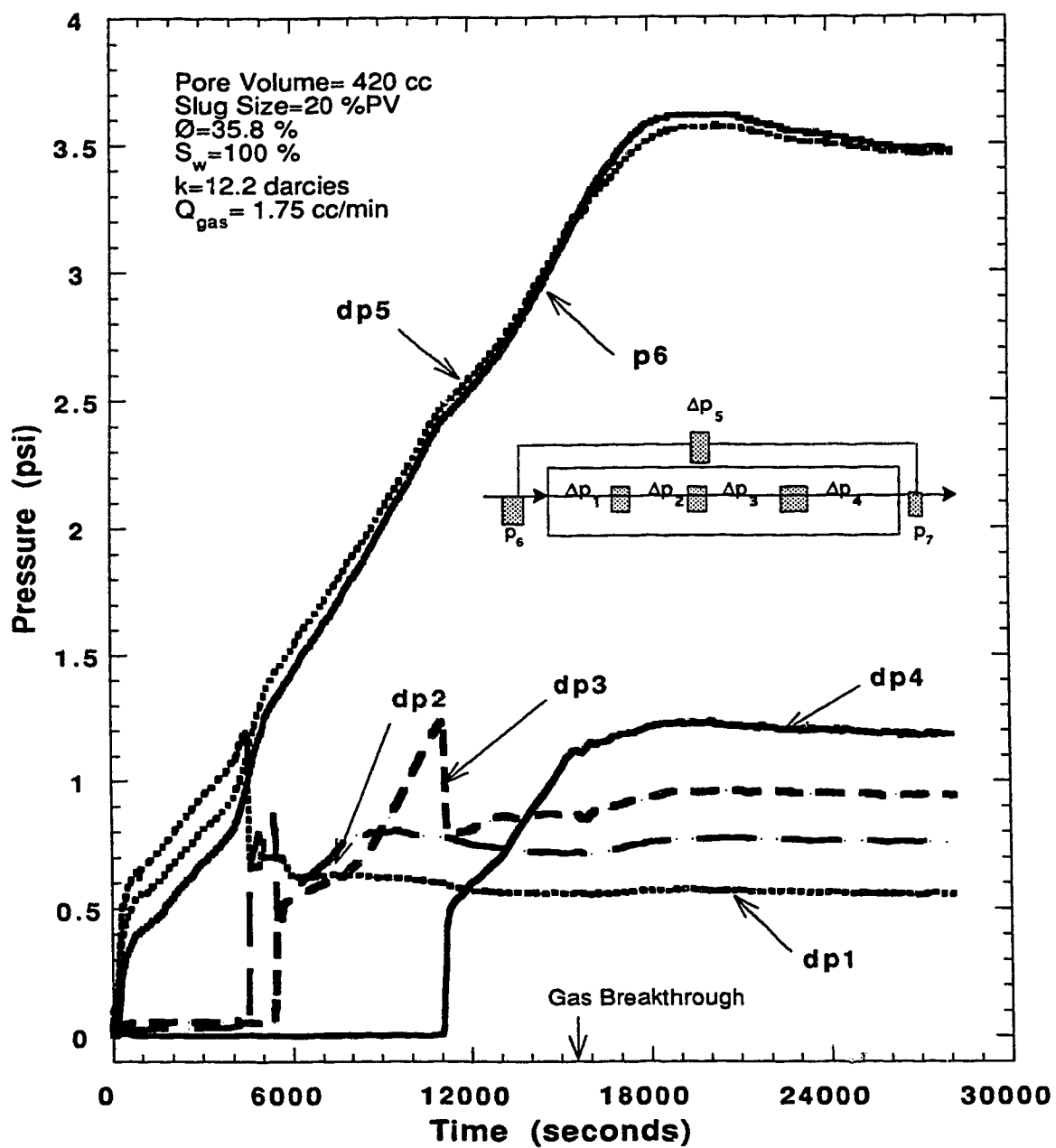


Figure 5.13- Run 38: Pressure Profile Using 10% Surfactant Concentration in a Slug size of 20% PV Displaced by a Gas Flow Rate of 1.75 cc/min.

$$\lambda_T = \left(\frac{k_g}{\mu_g} + \frac{k_w}{\mu_w} \right) = \frac{L q_T}{A \Delta P}$$

Using the appropriate conversion factors, the above equation is multiplied by (0.2449) to give the total mobility in darcies/ cp.

$$\lambda_T = (0.2449) \frac{L q_T}{A \Delta P},$$

where q_T is the total flow rate in cc/min and L is the core length in cm. The term A is the cross-sectional area in cm^2 and ΔP is the stabilized differential pressure in psi. For Run 38, the flow rate was 1.75 cc/min. The total mobility for Run 38 is 0.394 darcies/cp. The total mobility is a useful measure to assess the reduction in mobility provided by the surfactant. Compared with the base case Run 25, the total mobility of Run 38 is much reduced due to the generation of foam in the sand pack. Another measure for comparison of different foam runs with water base runs is the relative total mobility. It is found by dividing the total foam mobility by the absolute permeability. The relative total mobility for Run 38 is 0.032 cp^{-1} .

Heller⁽⁷⁸⁾ compared runs by the mobility reduction factor (MRF) defined as:

$$\text{MRF} = \frac{\lambda_1}{\lambda_2},$$

where λ_1 is the total mobility of foam and λ_2 is the total mobility of the surfactant-free water base case. Both mobilities are determined at the same flow velocities. The MRF can represent the pressure drop attributed to the presence of foam in the case where λ_1 and λ_2 are determined at the same gas fraction and flow velocity. If foam is not generated, the MRF would be unity. If foam is generated, the MRF values quantify the effect of the presence of foam. For Run 38, the MRF is 0.051.

The production data of Run 38 were previously given in Table 5.14 and are presented in Figure 5.14. The graph shows the cumulative production versus time and the surfactant concentration of the effluent versus time as well. The cumulative produced volume at gas breakthrough was 83.81% (PV). The gas breakthrough time was 257.3 minutes. The concentration curve shows a maximum value of 64 percent

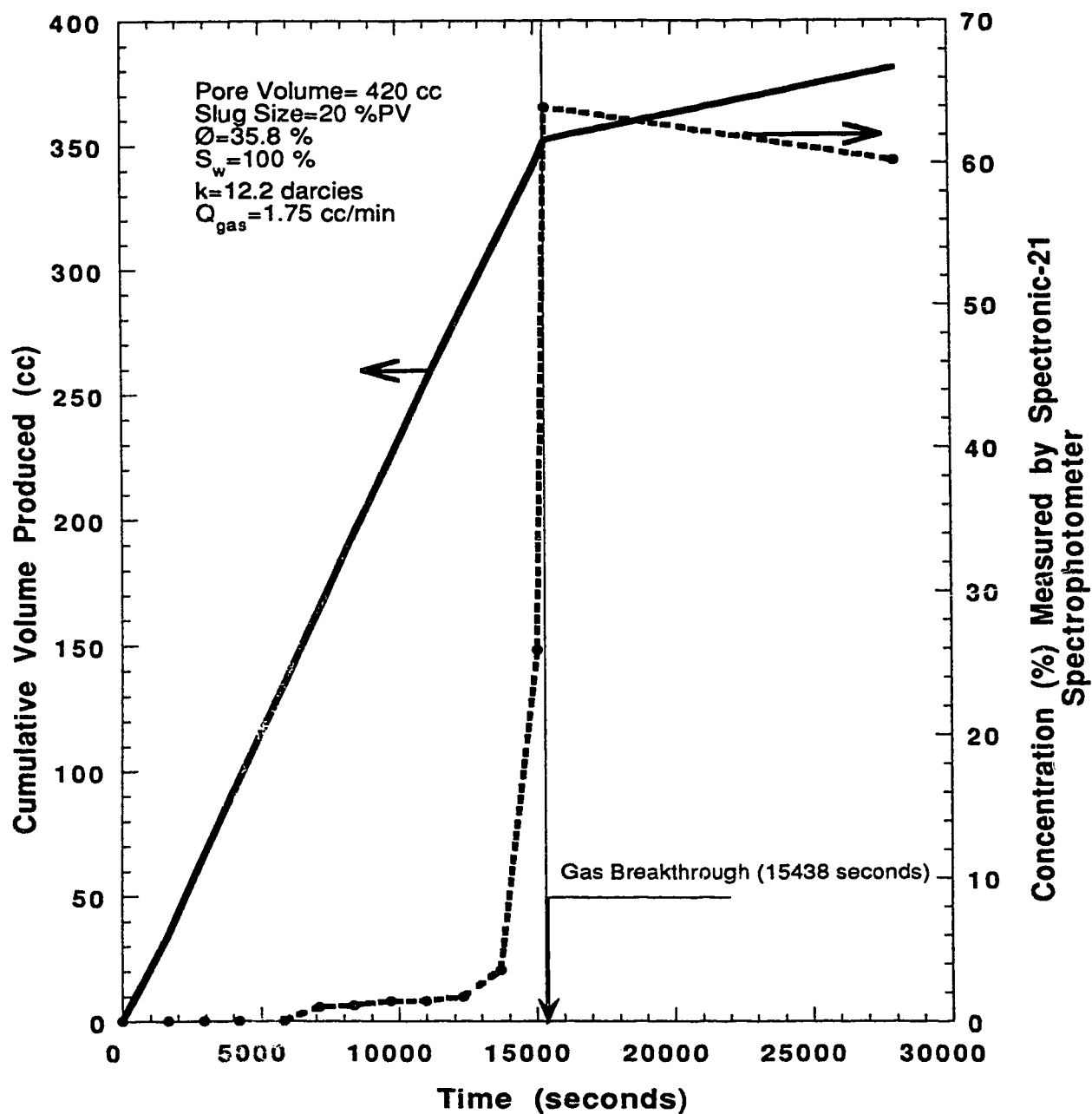


Figure 5.14- Run 38: Cumulative Production Versus Time and Concentration Versus Time for a Slug of 20% (PV) Having a 10% Dowfax-8390 Surfactant Concentration.

(by volume) of the surfactant slug injected. The maximum value of concentration was reached at gas breakthrough. This means that some of the surfactant slug was produced. It is noted that foam was not observed at the effluent end of the core, but the change of color of the effluent from a clear to a yellowish color was evidence of the production of some of the slug.

The cumulative produced volume curve shows a straight line which indicates piston-like displacement. This is supported by the pressure versus time plot, Figure 5.13. In the pressure plot, the transducers $\Delta P1$, $\Delta P2$, $\Delta P3$ and $\Delta P4$ were gradually increasing as the foam front was moving from the injection side towards the production side. The transducers recorded a maximum pressure at the end of the segment; that is, when the foam front reached the second port of the individual transducer, the pressure dropped sharply. In the same graph, beside the overall pressure drop as measured by the $\Delta P5$ transducer, the injection pressure, $P6$, is plotted to show that the calibration of the transducers were within a reasonable error of 0.15 psi (1.0 kPa).

5.4.2 Surfactant Slug Injection Experiments for Water-Saturated Sand Packs

Two sets of experiments were conducted in which a slug of surfactant was injected into a 100% water-saturated sand pack. The first set of runs was performed at a gas flow rate of 8 cc/min, and the other set was carried out at 1.75 cc/min. The purpose of these runs was to investigate the effect of gas flow rate on the optimum slug size. Surfactant slugs ranging from 2.5 to 25% PV were used, with a Dowfax-8390 surfactant concentration of 10% (by vol.).

5.4.2.1 Surfactant Slug Injection Experiments for Water-Saturated Sand Packs Displaced By a Gas Flowing at 8 cc/min

The first set of experiments was conducted with a gas flow rate of 8 cc/min. These were Runs 19 to 24. In all the experiments, immediately after the start of gas injection into the sand pack, the pressure across the sand pack as measured by $\Delta P5$ increased continuously until it reached a maximum value.

Table 5.15 gives the experimental data for Run 19. This run started with the injection of a 20% PV slug having 10% (by volume) Dowfax-8390 surfactant concentration into the sand pack. Then the injection of nitrogen was commenced. The

Experimental Data for Run 19

Pore Volume (cc):	420	Surfactant Name:	Dowfax-8390
Porosity (%):	36.2	Surfactant Concentration (%):	10
Absolute Perm. (darcies):	12.8	Slug size (% PV):	20
Oil Saturation:	0	Gas Flow Rate (cc/min):	8
Totalizer Reading at B.T. (cc):	416	Gas Breakthrough Time (min)	52
		Cum. Recovery at B.T. (% PV):	84.45

Sample Number	Time (sec)	Sample Volume (cc)	Cumulative Volume (cc)	Totalizer Reading (cc)	Concentration (Vol%)
1	0	0	0	0	0
2	432	45	45	60	0
3	847	51	96	113	0
4	1297	52	148	173	0
5	1839	56	204	245	0.55
6	2262	55	259	302	1.11
7	2792	53	312	373	1.39
8	3121	47	359	416	39.24
9	4815	20	379	641	61.63
10	14004	15	394	1868	80.26

Table 5.15 : Experimental Data for Run 19 Using 10% Dowfax-8390 in a Slug of 20% PV.

cumulative production versus time and concentration versus time are drawn in Figure 5.15. The cumulative produced volume curve showed almost a straight line until gas breakthrough. Gas breakthrough occurred after 52 minutes from the start of the gas injection. The percentage pore volume produced at gas breakthrough was 84.45%. The gas breakthrough and the cumulative produced volume at breakthrough were much higher than those for the water base case (Run 25) of 14.47 minutes and 23.3% PV.

The surfactant concentration at breakthrough was about 1.4%. The significance of this will be discussed later when all the runs are compared.

The pressure history for Run 19 is shown in Figure 5.16. As can be seen from the plot, the pressure in the first segment of the core started to increase and as the foam moved farther into the core, the pressure in the second segment began to rise. At this moment, the pressure in the first segment dropped then stabilized at around 1 psi (6.9 kPa). The process happened in the second half of the core. The differential pressure stabilized at about 6.6 psi (45.5 kPa) as can be seen from the graph. This is higher than that for the water base case and Run 38.

From this differential pressure, the total mobility for Run 19 is 0.941 darcies/cp. Dividing the total foam mobility by the absolute permeability of 12.8 gives, for the relative total mobility for Run 19, 0.074 cp^{-1} . A comparison of runs done at a different gas flow rate will be given later. Runs 20 to 24 are discussed next.

Data for Runs 20, and 22 to 24, are given in Tables 5.16, 5.17, 5.18 and 5.19 of Appendix A. In Run 20, a surfactant slug of 5% PV was used. Figure 5.17 gives the production history and the effluent surfactant concentration for Run 20. Gas breakthrough came after an elapsed time of 28.97 minutes from the start of nitrogen injection. The cumulative produced volume at gas breakthrough was 52.6% PV. The surfactant concentration in the effluent at breakthrough was zero. This means that the gas was able to penetrate the slug without forming a strong enough foam to have a better displacement efficiency. This is supported by the pressure history of this run which is presented as Figure 5.18. From the plot, it can be seen that the pressure in the last segment of the core ΔP_4 increased. This increase was not sustained as there was not enough surfactant or foam reaching the last one fourth of the length of the core segment. As a result, the pressure dropped, after a short time, to a lower stabilized pressure.

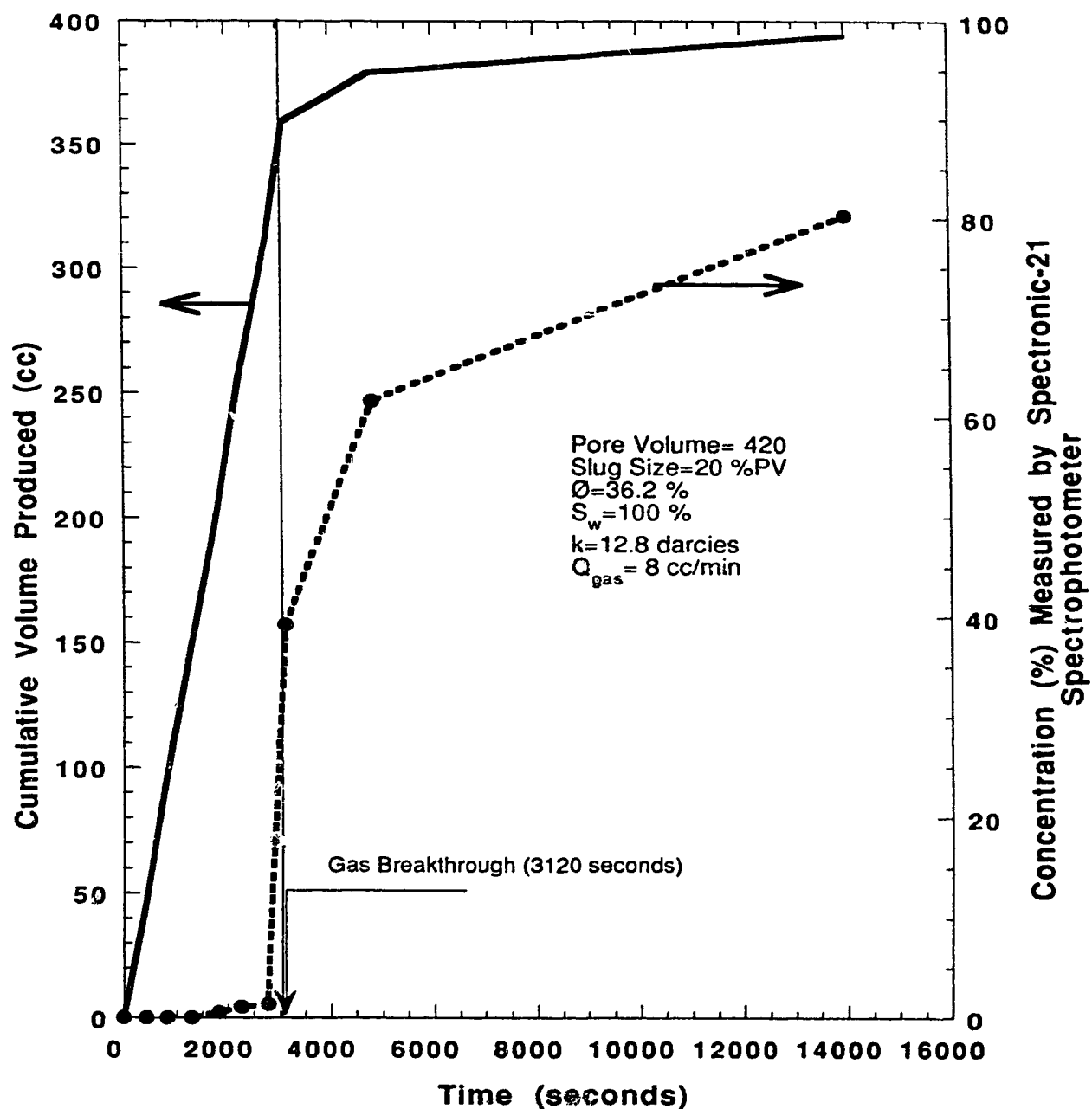


Figure 5.15- Run 19: Cumulative Production Versus Time and Concentration Versus Time for a Slug of 20% (PV) Having a 10% Dowfax-8390 Surfactant Concentration.

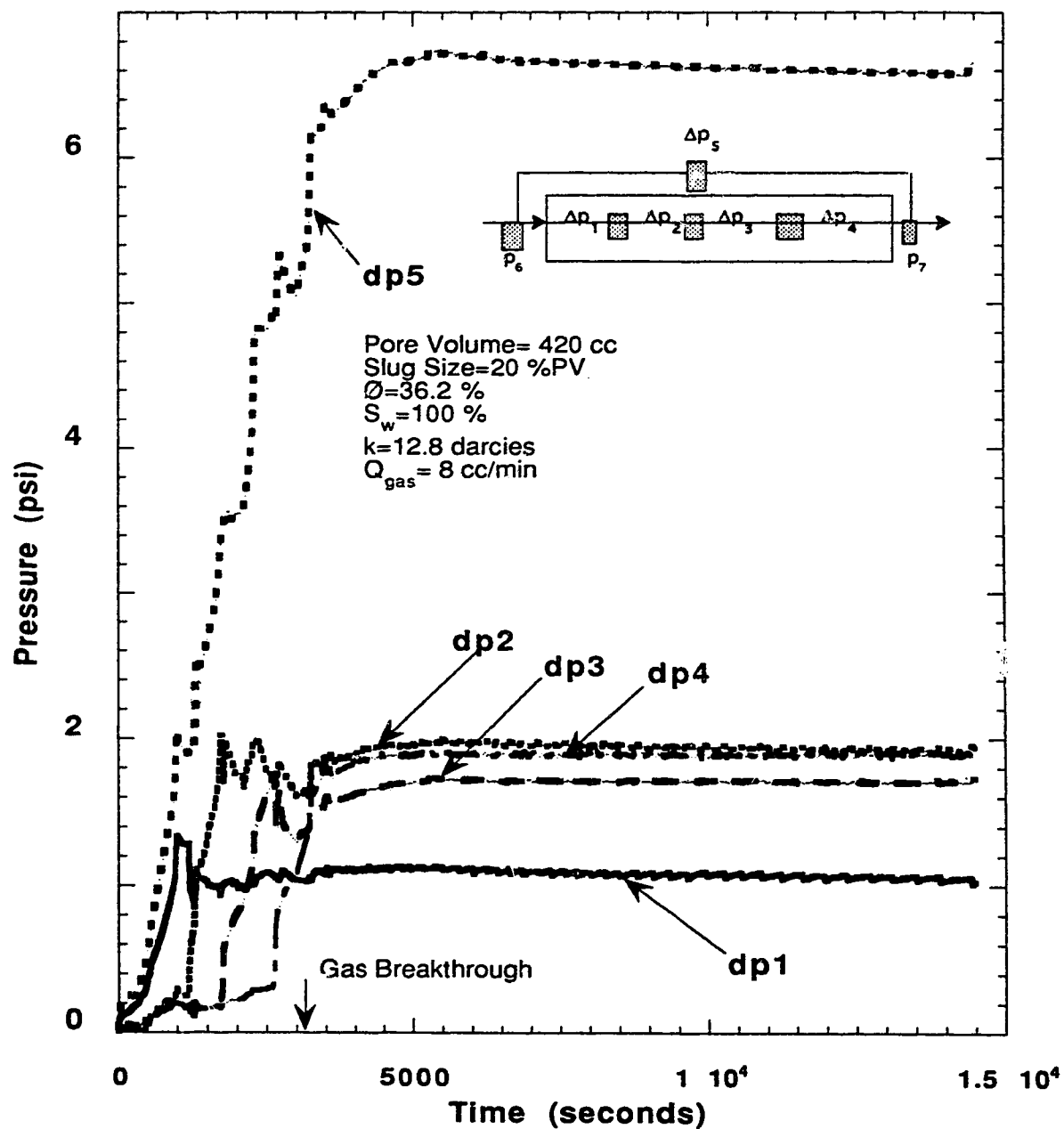


Figure 5.16 - Run 19: Pressure Profile, Using 10% Surfactant Concentration in a Slug Size of 20% PV displaced by a Gas Flow Rate of 8 cc/min.

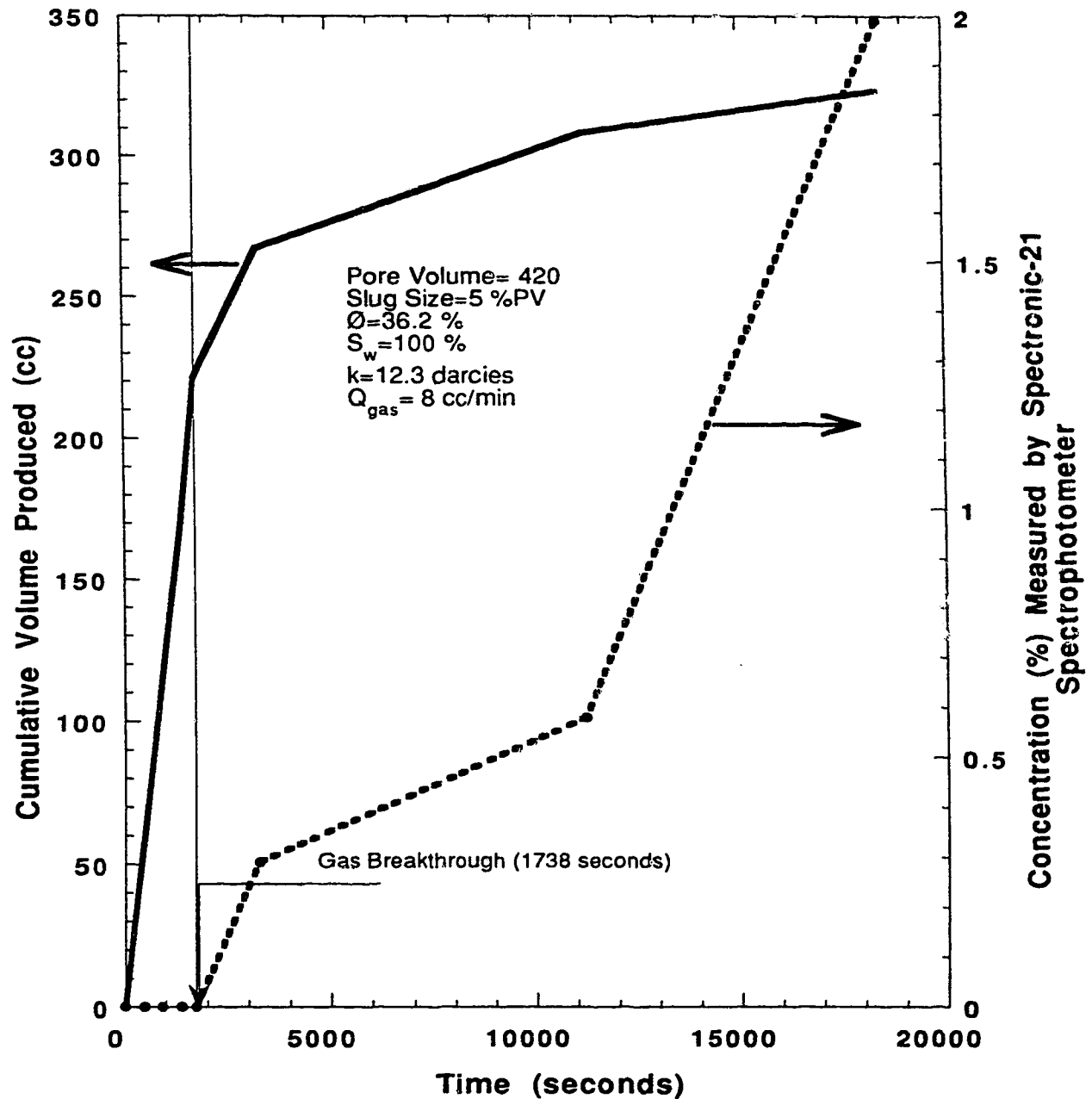


Figure 5.17- Run 20: Cumulative Production Versus Time and Concentration Versus Time for a Slug of 5% (PV) Having a 10% Dowfax-8390 Surfactant Concentration.

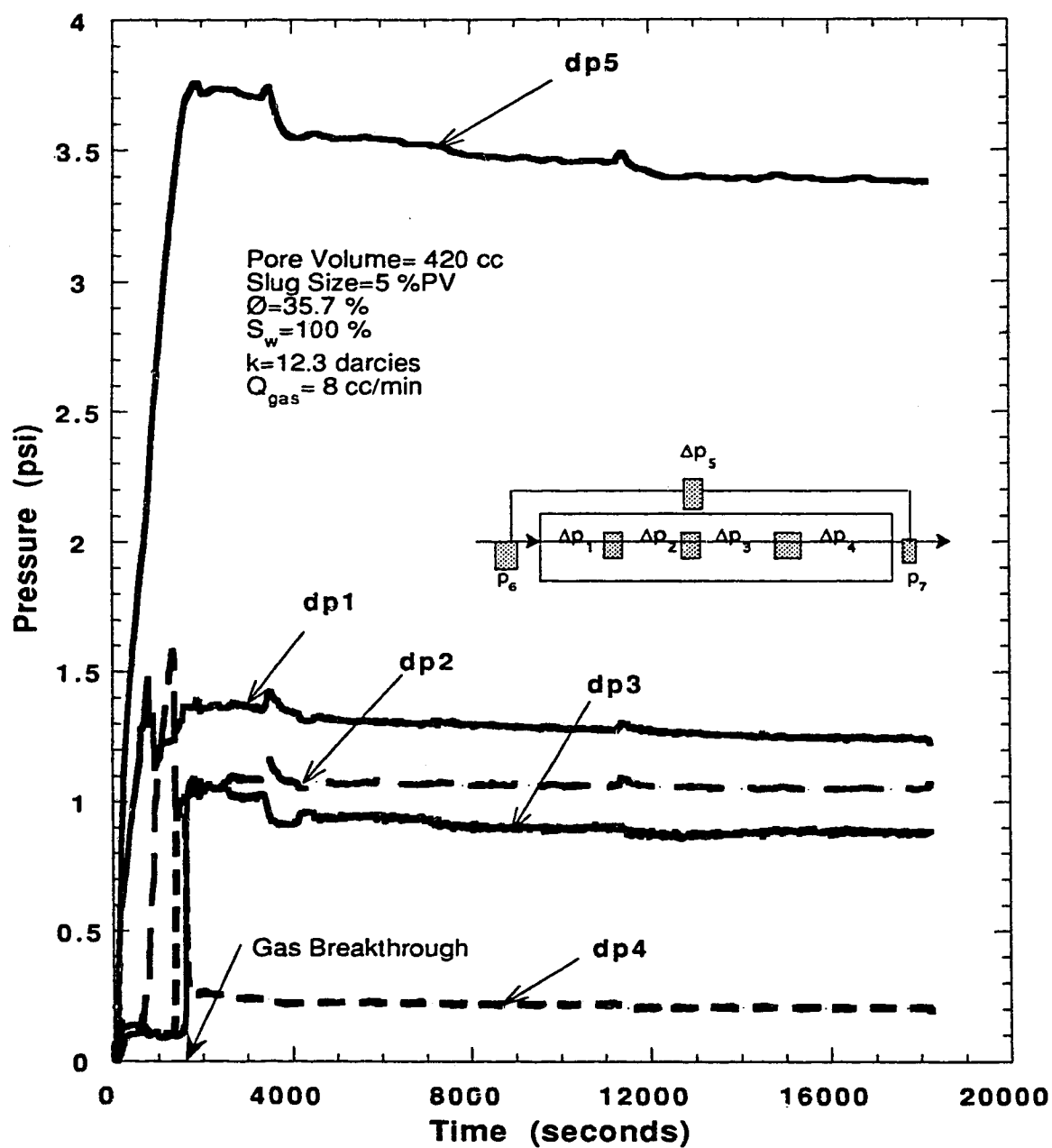


Figure 5.18- Run 20: Pressure Profile Using 10% Surfactant concentration in a Slug size of 5% PV Displaced by a Gas Flow Rate of 8cc/min.

The total mobility for Run 20 was 1.827 darcies/cp. This is lower as compared to the water base case, Run 25, with a total mobility of 7.667 darcies/cp. The relative total mobility was 0.149 cp^{-1} . The MRF for Run 20 was 0.294.

Run 22 was performed in a 12.5 darcy sand pack using a 25% PV surfactant slug with 10 percent Dowfax-8390. The concentration of the effluent shown in Figure 5.19 at gas breakthrough was higher than in runs done with lower slug sizes. The gas breakthrough time was 54.32 minutes. At this point, the cumulative produced volume was 352 cc.

The differential pressure profile stabilized at 7.5 psi (51.7 kPa) as can be seen from Figure 5.20. This stabilized pressure is higher than that for Runs 19, 22, 23 and 24, in which smaller slugs were used.

From the steady state stabilized differential pressure, the total mobility was 0.828 darcies/cp. This gave a relative total mobility of 0.066 cp^{-1} . This is the lowest total and relative total mobility for this set of runs.

In Run 23 a 2.5% PV slug was injected into a sand pack having a permeability of 12.3 darcies. The production data is given in Appendix A, Table 5.18, and is plotted in Figure 5.21. From the graph, the concentration profile shows that some of the surfactant slug was produced after breakthrough, but in a very small amount. The slope of the cumulative volume produced curve was constant until gas breakthrough. The gas breakthrough time was 19.62 minutes and the total fluid produced at this point was 147 cc. This is higher than the water base case of 98 cc.

The pressure history of Run 23 is presented in Figure 5.22. The general response of the individual transducers somewhat resembles that for the water base run, Run 25, but the steady state pressure gradient is higher for Run 23 than that of Run 25.

From Figure 5.22, the steady-state pressure gradient stabilized at 1.4 psi (9.7 kPa). From this gradient, total foam mobility was calculated to be 4.436 darcies/cp. Dividing the total mobility by the absolute permeability of 12.3 darcies gives a relative total mobility of 0.361 cp^{-1} .

The last experiment to be analyzed in this set of runs is Run 24. This run was carried out in a 12.3 darcy sand pack. A slug of 10% was used with a Dowfax-8390

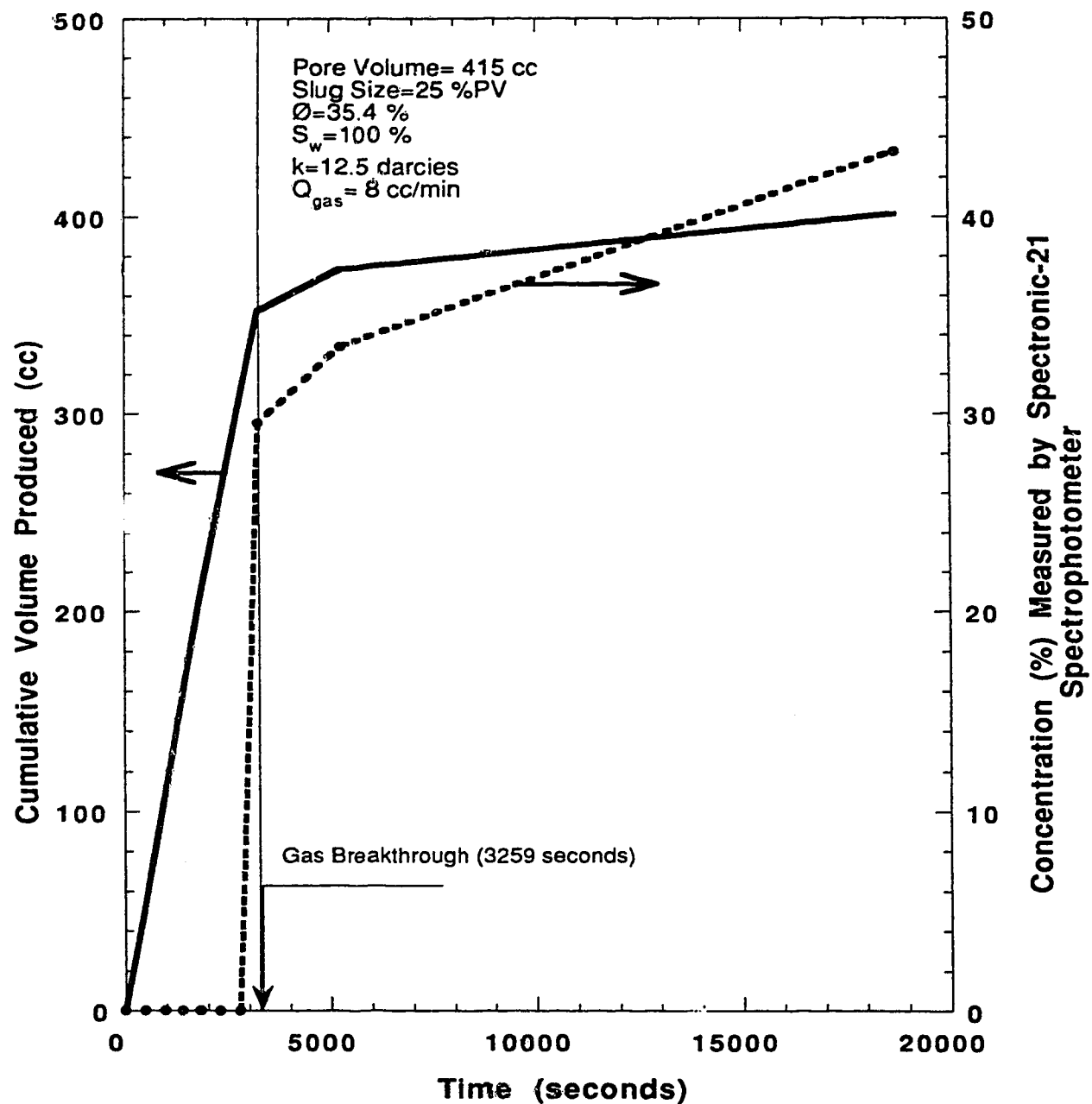


Figure 5.19- Run 22: Cumulative Production Versus Time and Concentration Versus Time for a Slug of 25% (PV) Having a 10% Dowfax-8390 Surfactant Concentration.

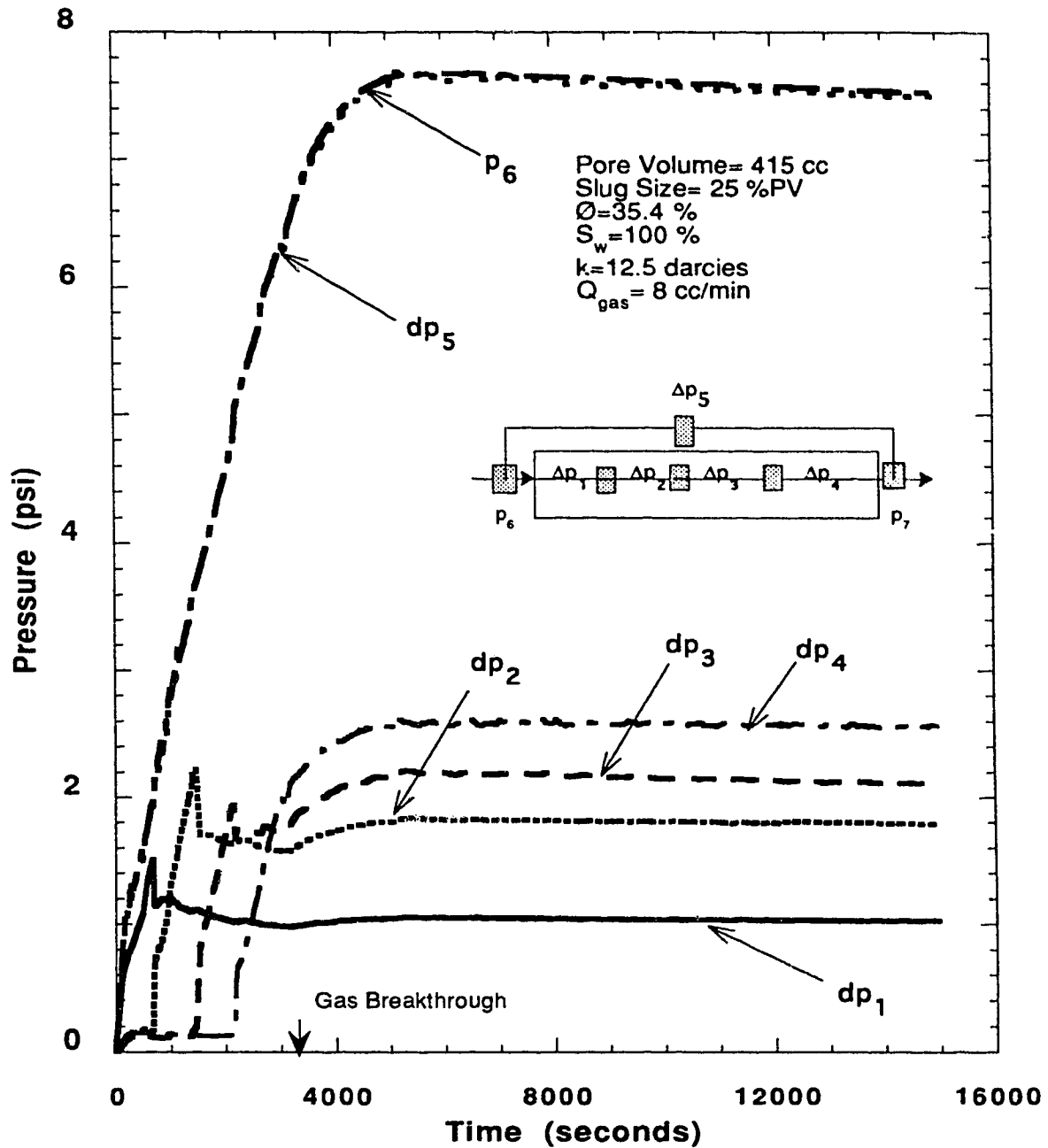


Figure 5.20- Run 22: Pressure Profile Using 10% Surfactant concentration in a Slug size of 25% PV Displaced by a Gas Flow Rate of 8cc/min.

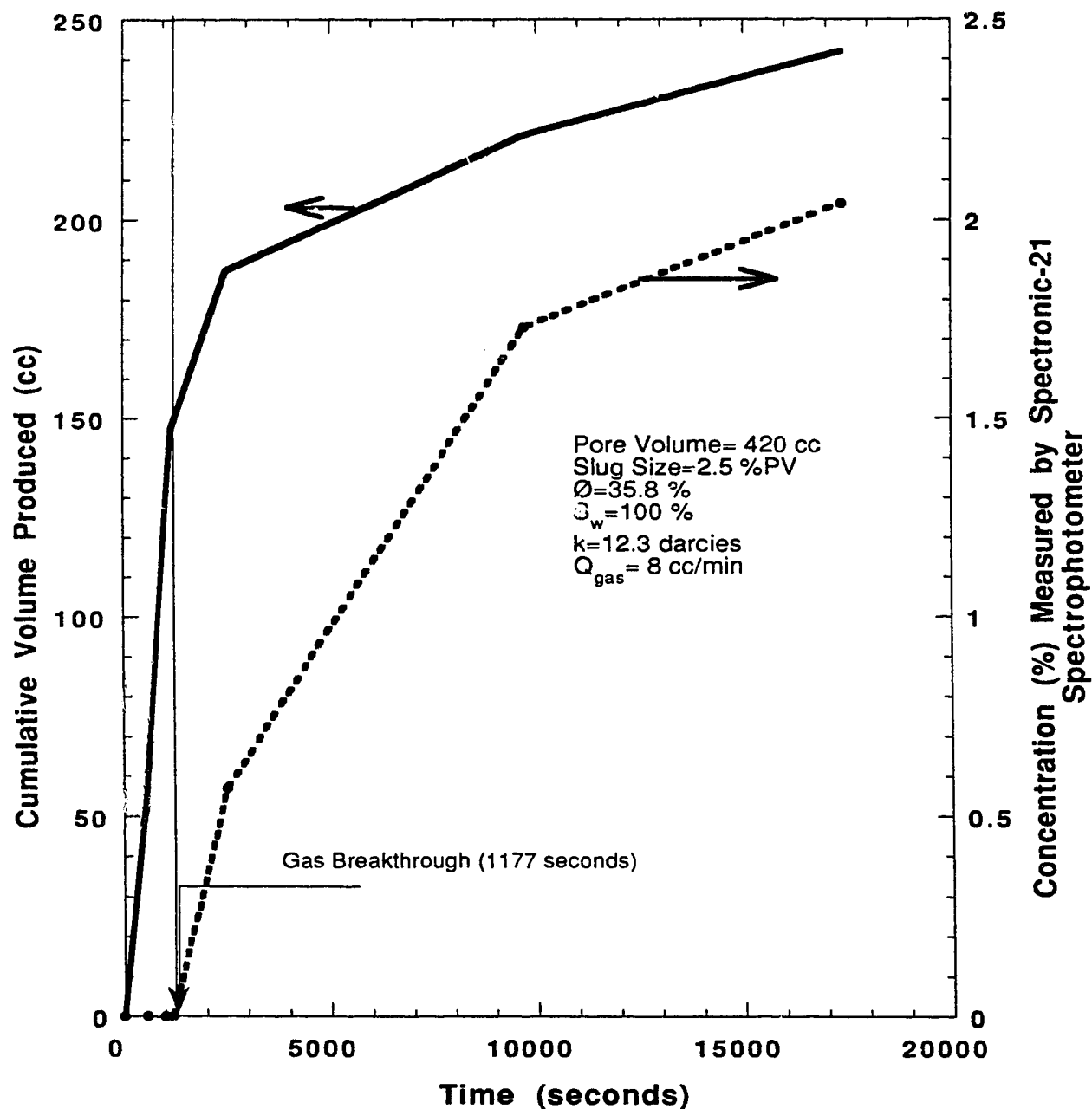


Figure 5.21- Run 23: Cumulative Production Versus Time and Concentration Versus Time for a Slug of 2.5% (PV) Having a 10% Dowfax-8390 Surfactant Concentration.

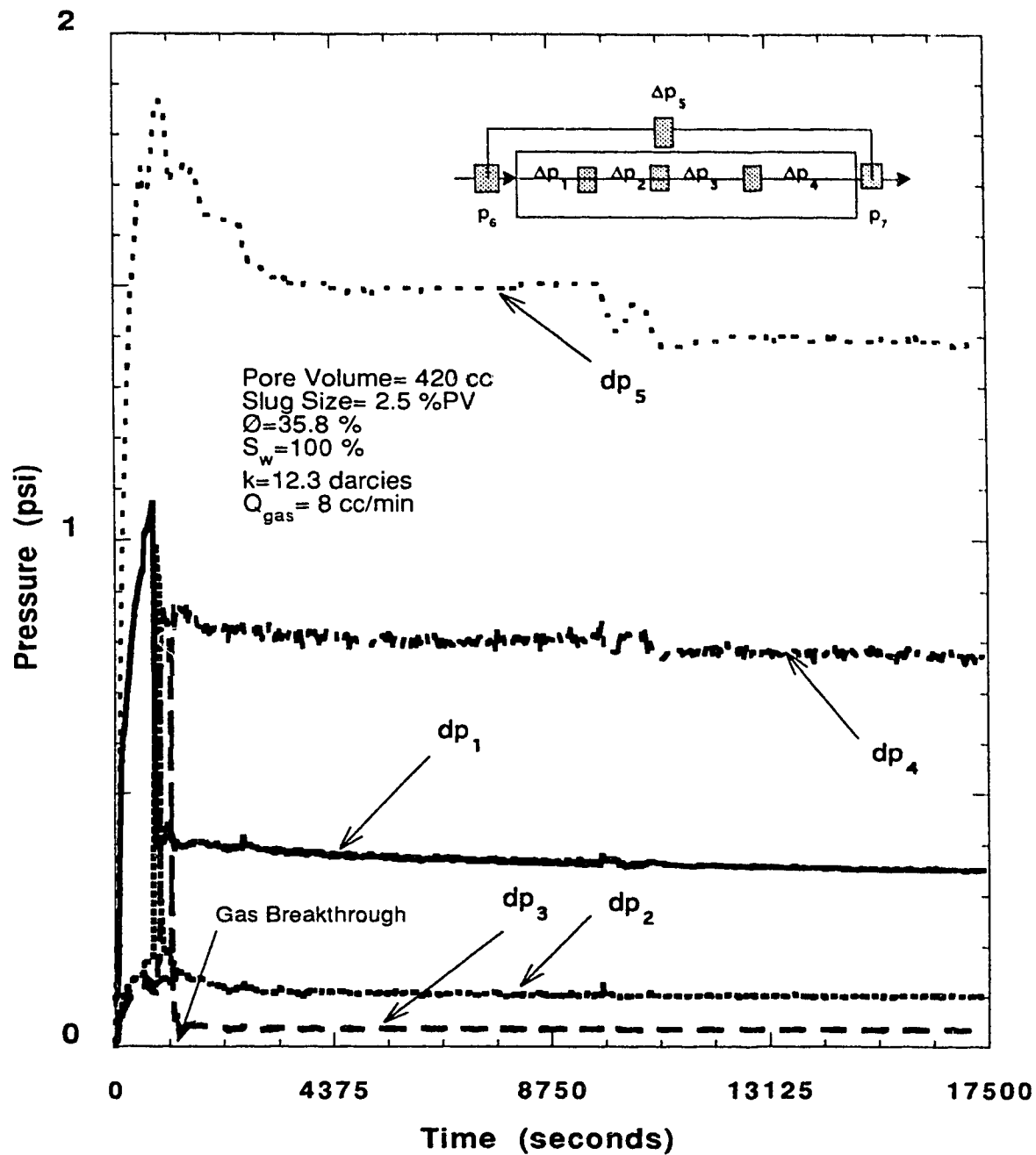


Figure 5.22- Run 23: Pressure Profile Using 10% Surfactant concentration in a Slug size of 2.5% PV Displaced by a Gas Flow Rate of 8cc/min.

concentration of 10%. The production history and the pressure profile for Run 24 are given in Figure 5.23 and 5.24, respectively.

The gas breakthrough time was 49.3 minutes which is less than the runs with 20 and 25% PV slug. The cumulative volume produced was 77.3% PV. This is also less than the recovery from the 20 and 25% slug experiments, Runs 19 and 22.

The steady state differential pressure, as can be seen from Figure 5.24, stabilized at 5.2 psi (35.9 kPa). The total foam mobility as determined from the steady state pressure gradient was 1.109 darcies/cp and the relative total mobility was 0.092 cp⁻¹.

5.4.2.2 Overall Evaluation of Surfactant Slug Injection Experiments for Water-Saturated Sand Packs Displaced By a Gas Flowing at 8 cc/min

Runs 19 to 24 were performed at the same gas flow rate of 8 cc/min and surfactant concentration, and the only changing variable was the slug size. The resulting frontal advance rates as estimated from the pressure versus time plots for Runs 19, 20, 22, 23 and 24, were 17.6, 31.4, 18.3, 54 and 21.6 m/day, respectively. The frontal advance rate increased with decreasing slug size. Table 5.20 summarizes the analysis of the effect of the slug size on the flow of foam and its propagation in 100% water-saturated sand packs.

Table 5.20 lists in the last three rows the total and the relative foam mobility and the mobility reduction factor (MRF). They are plotted against the slug size in Figure 5.25. The 2.5% slug had the highest MRF of 0.579 hence a poor displacement efficiency. As the slug size increased from 2.5 to 20%, the total foam mobility and MRF decreased. Even though the 25% slug size run had total foam mobility and MRF slightly lower than those for the 20% slug run, Run 19 was the optimal slug size. This means that the 20% slug size was the best that foam could do to displace water with minimal amount of surfactant. This point will be further explained in the discussion that follows.

Figure 5.26 presents the cumulative recovery, breakthrough time and totalizer readings versus slug size. As the slug size was increased from 2.5 to 20% PV, the recovery at breakthrough increased from 35 to 84.45% PV. However, it remained essentially constant, 84.84% PV, when a slug of 25% PV was used. This means that

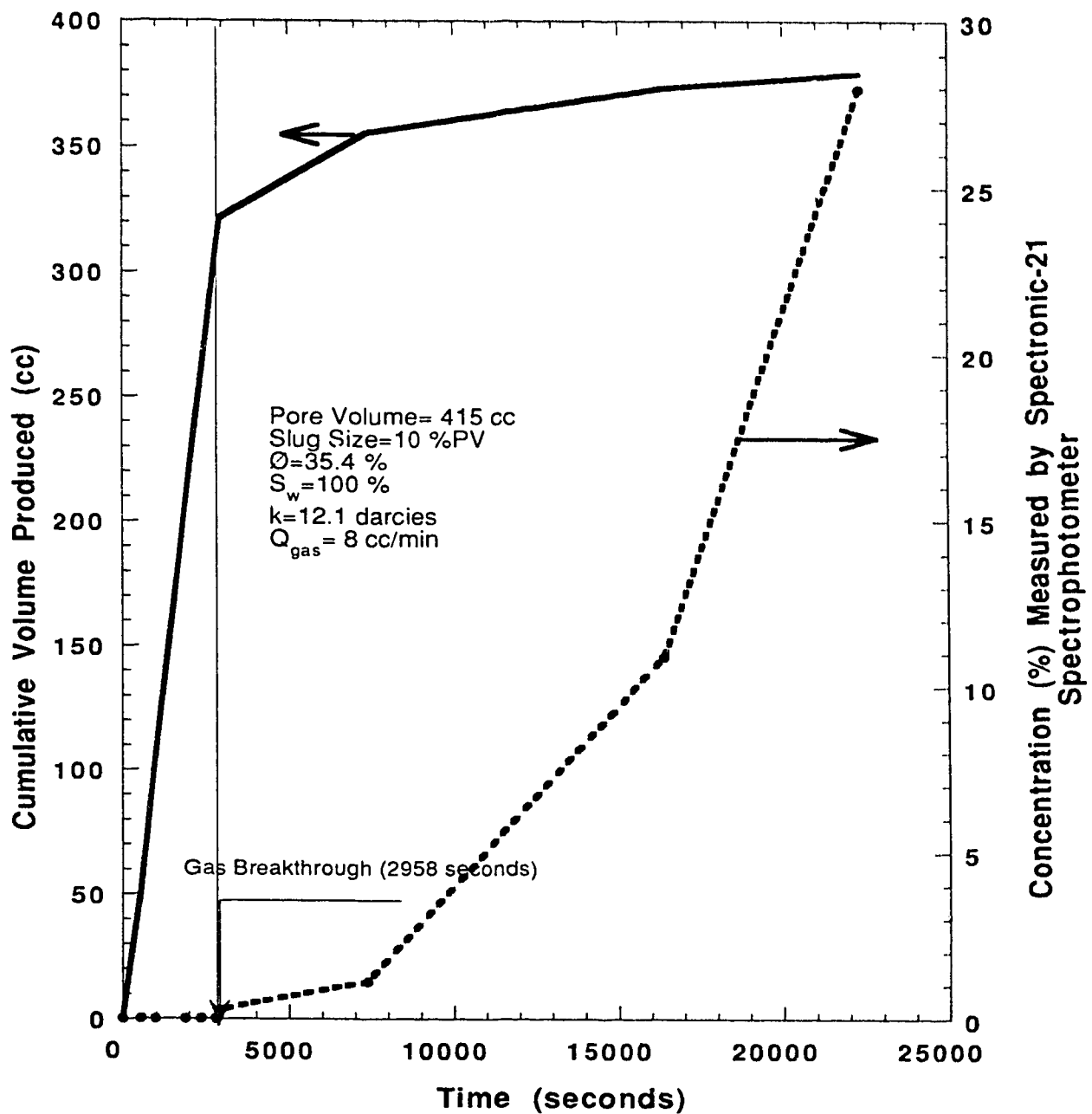


Figure 5.23- Run 24: Cumulative Production Versus Time and Concentration Versus Time for a Slug of 10% (PV) Having a 10% Dowfax-8390 Surfactant Concentration.

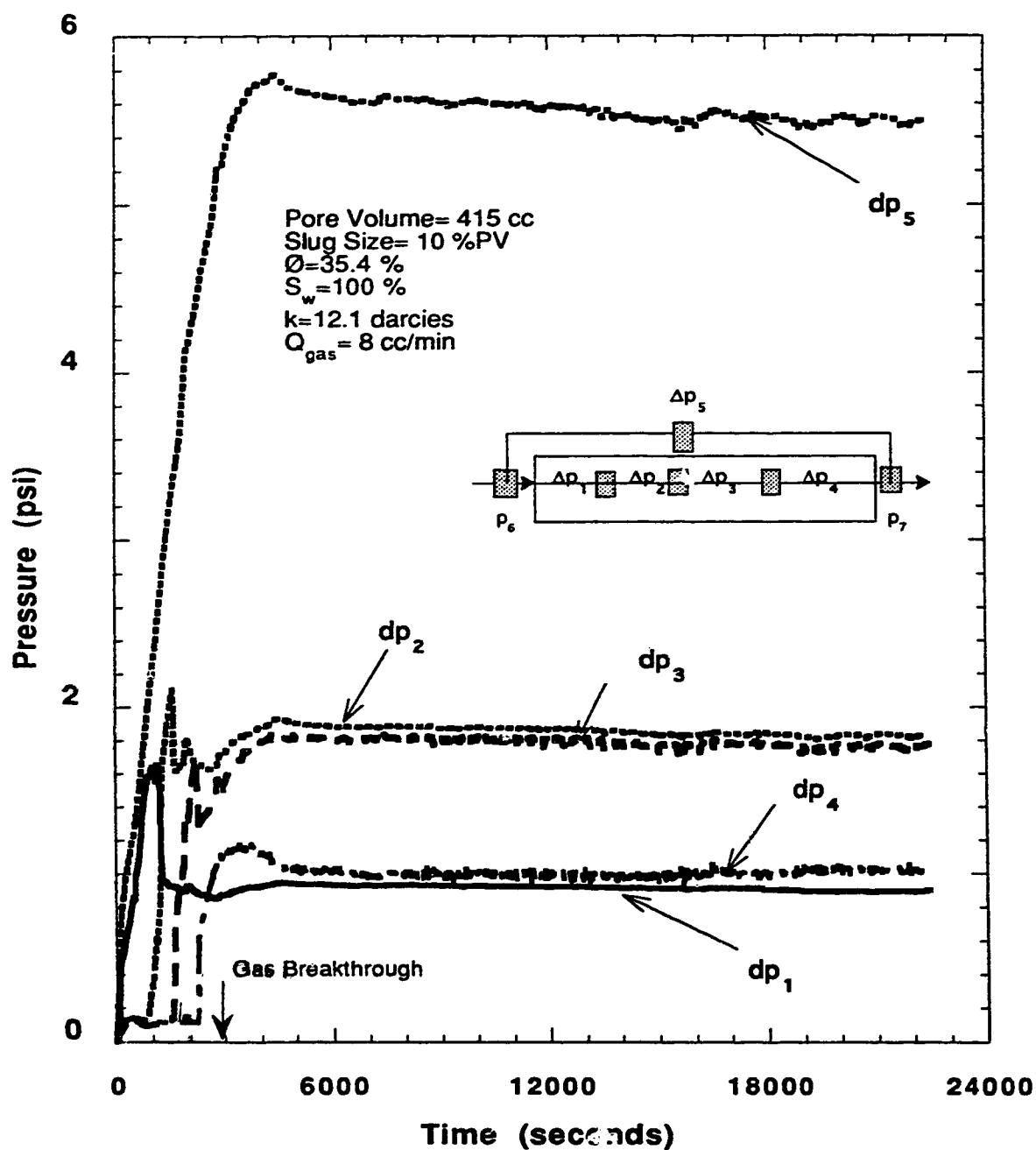


Figure 5.24- Run 24: Pressure Profile Using 10% Surfactant concentration in a Slug size of 10% PV Displaced by a Gas Flow Rate of 8cc/min.

Run No. ==>	19	20	21	22	23	24	25
Slug Size (%PV)	20	5	10	25	2.5	10	0
Gas Breakthrough (minutes)	52	28.97	50.15	54.32	19.62	49.3	14.47
Recovery at B.T. (%PV)	84.45	52.6	79.3	84.84	35	77.3	23.3
Totalizer Reading at B.T. (cc)	416	232	400	435	160	395	115
Concentration at B.T. (% Vol)	1.39	0	0.57	29.53	0	0.27	0
Pressure at B.T. (psi)	5.246	3.722	4.4	6.544	1.661	5.17	1.503
Steady State Pressure (psi)	6.6	3.4	4.8	7.5	1.4	5.6	1
Total Mobility (darcies/cp)	0.941	1.827	1.194	0.828	4.436	1.109	7.667
Relative Total Mobility (1/cp)	0.074	0.149	0.095	0.066	0.361	0.092	1
MFF	0.123	0.238	0.156	0.108	0.579	0.145	1

Table 5. 26. Summary of Analysis of Runs 19 to 25, Slug Injection Experiments
Where Water was Displaced By Nitrogen at a Flow Rate of 8 cc/min.

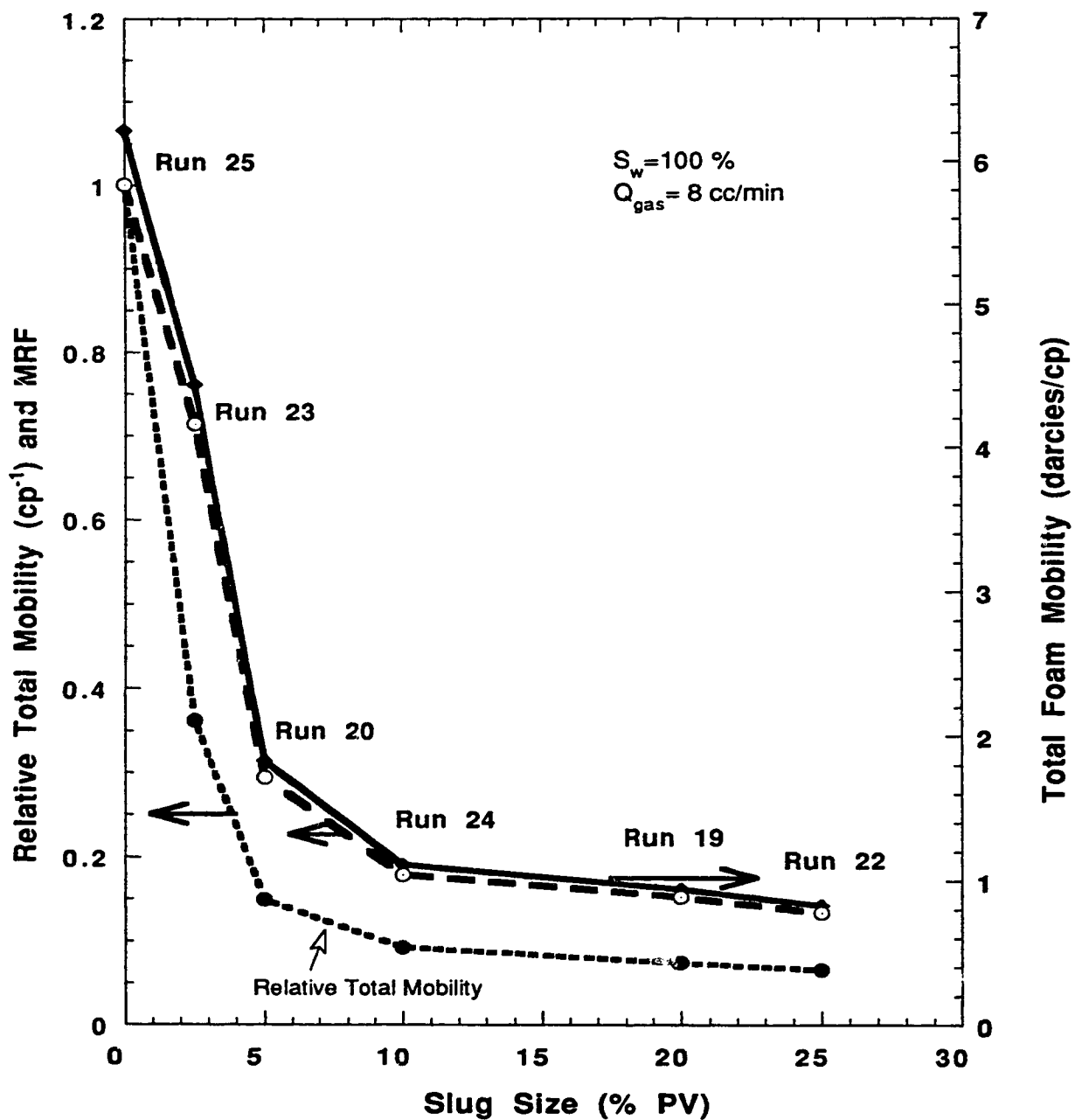


Figure 5.25- Runs 19, 20, 22, 23, 24 and 25: Total Foam Mobility Versus Slug Size and Relative Total Mobility and MRF Versus Slug size.

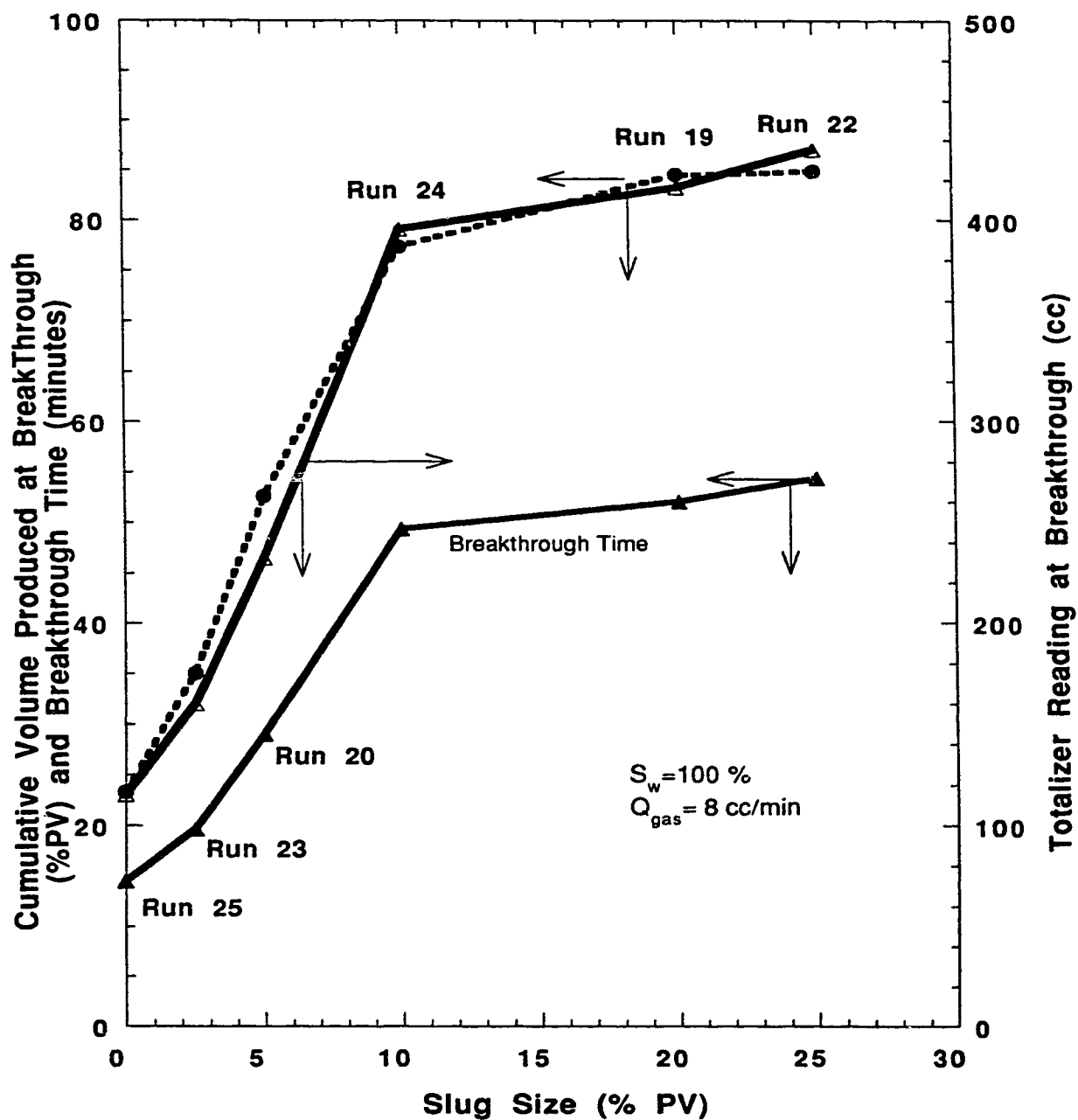


Figure 5.26: Comparison of Runs 19, 20, 22, 23, 24 and 25: Cumulative Production (%PV) and Breakthrough Time Versus Slug Size and Totalizer Reading Versus Slug Size.

the optimal slug size is 20% PV. It is the smallest slug size that gives the highest recovery at breakthrough. The graph also shows the totalizer readings at breakthrough. It has the same behaviour as the cumulative recovery; that is, it increased as the slug size was changed from 2.5 to 20% PV. However, it rose slightly when a slug of 25% PV was used. The gas breakthrough time is also plotted in Figure 5.26. It shows the expected trend.

One striking observation on the trend of the three curves on Figure 5.26 is that all three curves change slope at a slug size of 10%, Run 24. Below a 10% slug size, the displacement seems inefficient as compared to 20 and 25% PV slug runs. Examining the effluent concentration at breakthrough reveals that little or very minimal surfactant was produced when slug sizes of less than 20% were used as shown in Figure 5.27. This again proves that the 20% slug was the smallest slug size that produced a pore-volume-full of foam; hence, it gave the best recovery at breakthrough. Moreover, the surfactant produced at breakthrough in the 25% slug was high, 29.53% (by vol.).

Pressures at breakthrough as well as the steady state pressure are drawn in Figure 5.27. In conducted with slug sizes of 10% PV and greater, the steady state pressures were higher than pressures at breakthrough. Surprisingly, the pressures at breakthrough in Runs 19 and 24 were almost the same, 5.25 and 5.17 psi (36.2 and 35.6 kPa), respectively. But looking back at the pressure profiles of both Runs 19 and 24 in Figures 5.16 and 5.24, one can see that in Run 24 the pressure in the last section of the core, as measured by ΔP_4 transducer, stabilized at a lower pressure gradient than that of the same section in Run 19. This indicates that, in Run 24, the foam did not propagate with the same lamellae density to the end of the core. Here the foam texture is referred to as "Lamellae density" which does not have the notion of the uniformity of bubble size distribution, but it gives the idea of the number of foam bubbles per unit volume (see Section 2.7.1, Population Balance). In other words, the higher the number of bubbles or lamellae the higher the resistance to gas flow, and the higher the pressure.

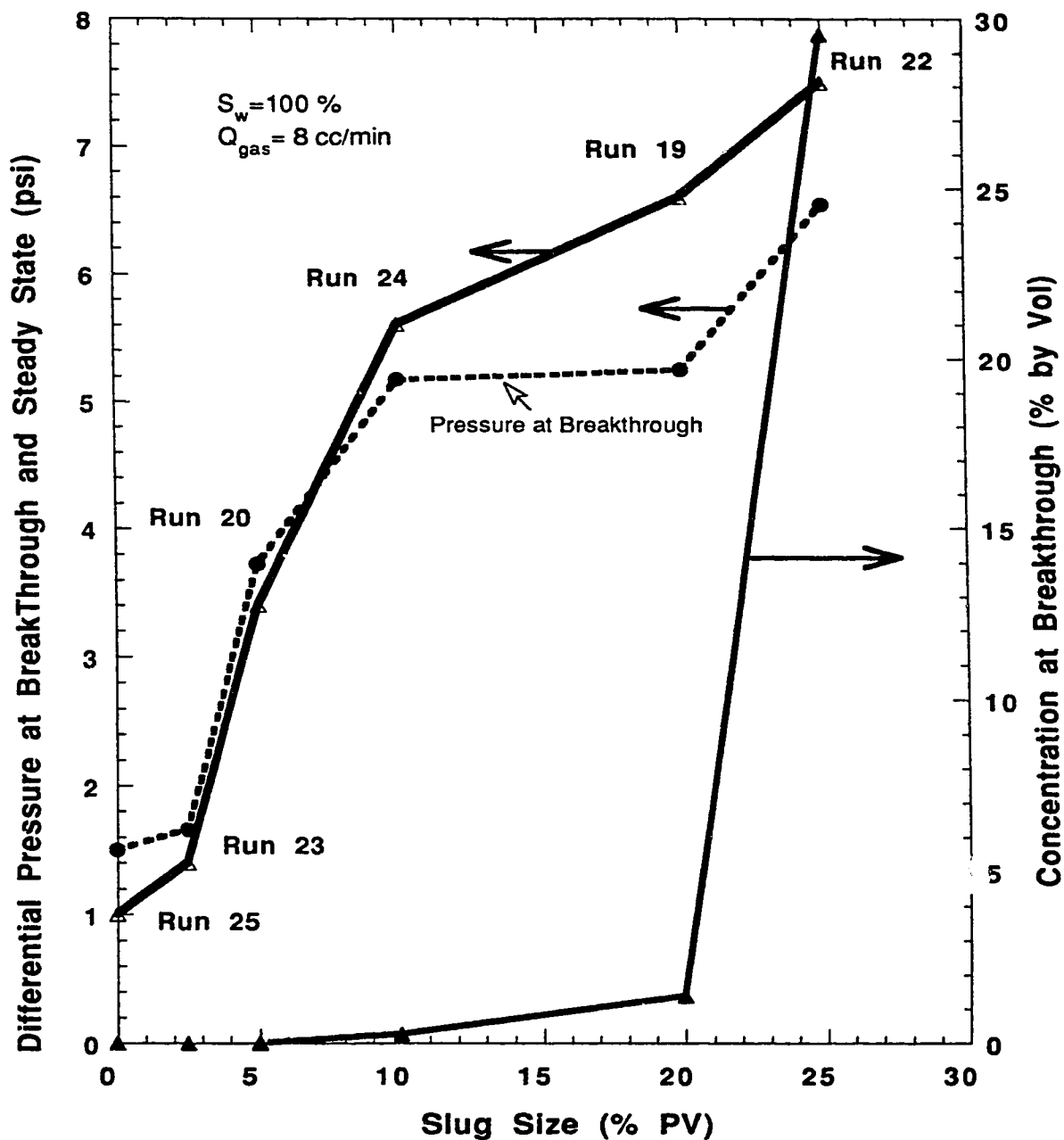


Figure 5.27 : Comparison of Runs 19, 20, 22, 23, 24 and 25 Pressure Drop at Breakthrough and Steady State Pressure Versus Slug Size and Effluent Concentration Versus Slug Size.

5.4.2.3 Surfactant Slug Injection Experiments for Water-Saturated Sand Packs Displaced By a Gas Flowing at 1.75 cc/min

Runs 37, 38 and 40 were conducted with slug sizes of 2.5, 10 and 20% PV, respectively, to determine the effect of gas flow rate on the slug size and on recovery. As with previous runs, Runs 37, 38 and 40 began with the injection of the surfactant slug of 10% Dowfax-8390. The slug was then followed by nitrogen injection; this was the actual start of the experiment. Many of the findings of the previous set of experiments were verified by these three runs as will be seen in the following discussion.

Run 37 was performed in a 12.4 darcy sand pack saturated with 100% water. Table 5.21 gives the production data for Run 37 which is plotted in Figure 5.28. The plot shows the cumulative produced volume versus time curve has a much smaller slope than that of the same slug size, Run 23. This is due to the gas flow rate. After an elapsed time of 130.1 minutes, the cumulative recovery at breakthrough was 36.9% PV. This is almost the same as that of Run 23, which was 35.0% PV.

Figure 5.29 presents the pressure profile for Run 37. The overall differential pressure and the pressure gradient in the first section of the core started to rise immediately upon nitrogen injection, which indicated foam formation. It rose slowly, reaching a peak of one psi (6.9 kPa), then dropped sharply and stabilized at 0.4 psi (2.8 kPa). At this point, as the foam was still formed, the pressure in the second section increased and reached a maximum of one psi, then eventually dropped and stabilized. The pressure gradient of the end section of the core, as it can be seen from the dp4 curve, did not show any response. This means that the foam did not propagate beyond the middle section of the core. This point is also supported by the response of ΔP_3 transducer which rose to about 0.8 psi (5.5 kPa) and never dropped.

Run 38 was already analyzed in Section 5.4.1 (Typical Slug Injection Run.) The cumulative produced volume at breakthrough was 83.81% PV. This is almost the same as that of Run 19, the same slug size of 20% PV was used, which was 84.45% PV.

Run 40 was conducted with a slug of 10% PV in a 11.4 darcy and a porosity of 35.8% sand pack. The production data is given in Appendix A as Table 5.22 and is shown in Figure 5.30. The total produced fluids at breakthrough was 78.57% PV

Experimental Data for Run 37

Pore Volume (cc):	420	Surfactant Name:	Dowfax-8390
Porosity (%):	35.8	Surfactant Concentration (%):	10
Absolute Perm. (darcies):	12.4	Slug size (% PV):	2.5
Oil Saturation:	0	Gas Flow Rate (cc/min):	1.75
Totalizer Reading at B.T. (cc):	229	Gas Breakthrough Time (min)	130.1
		Cumulative Recovery at B.T. (%)	36.9

Sample Number	Time (sec)	Sample Volume (cc)	Cumulative Volume (cc)	Totalizer Reading (cc)	Concentration (Vol%)
1	0	0	0	0	0
2	1663	30	30	49	0
3	3167	31	61	93	0
4	4634	30	91	136	0
5	6251	30	121	183	0.28
6	7642	30	151	223	0.55
7	7806	4	155	229	0.55
8	14883	35	190	435	0.84
9	23834	25	215	696	1.12

Table 5.21 : Experimental Data for Run 37 Using 10% Dowfax-8390 in a Slug of 2.5% PV.

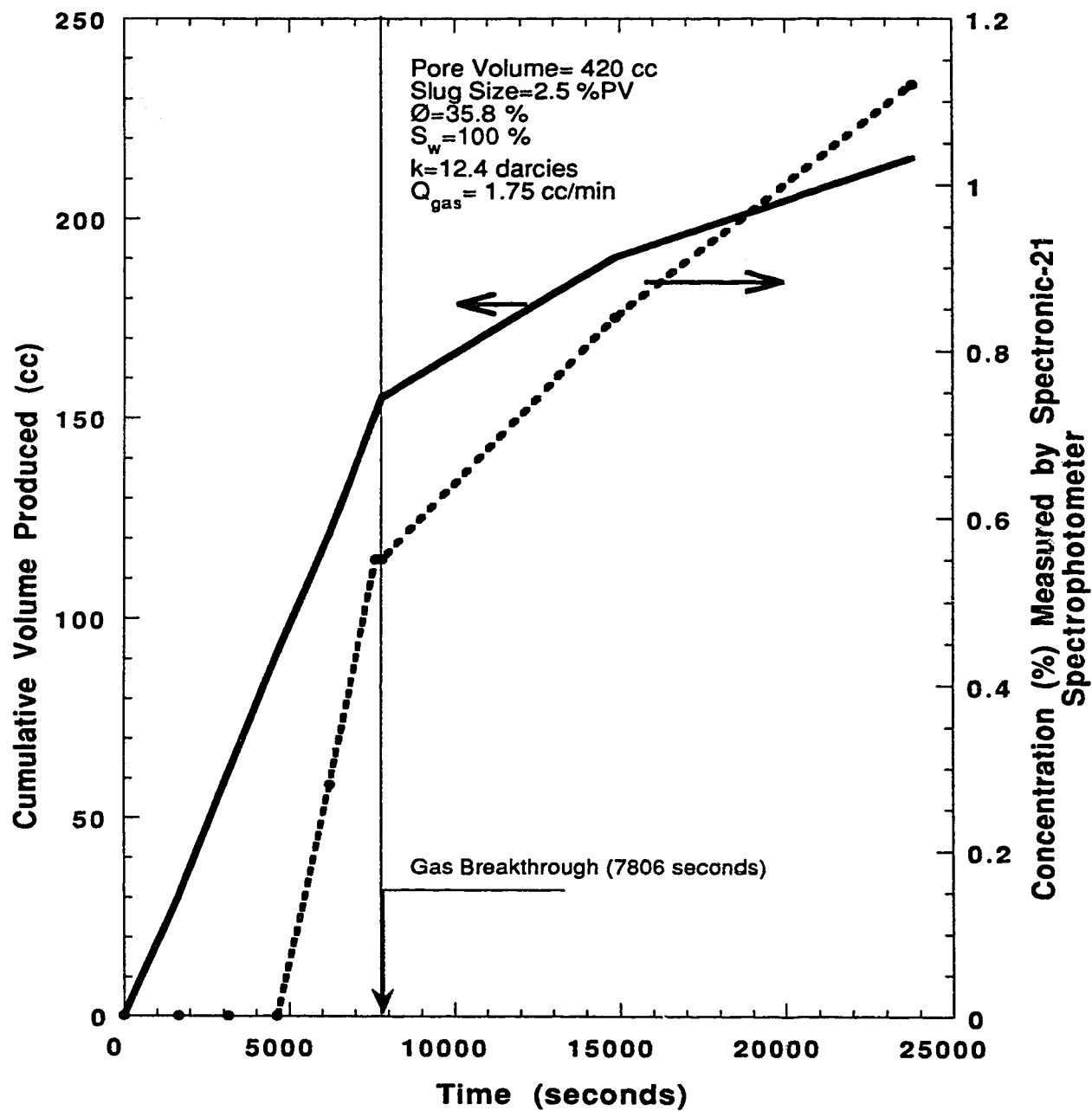


Figure 5.28- Run 37: Cumulative Production Versus Time and Concentration Versus Time for a Slug of 2.5% (PV) Having a 10% Dowfax-8390 Surfactant Concentration.

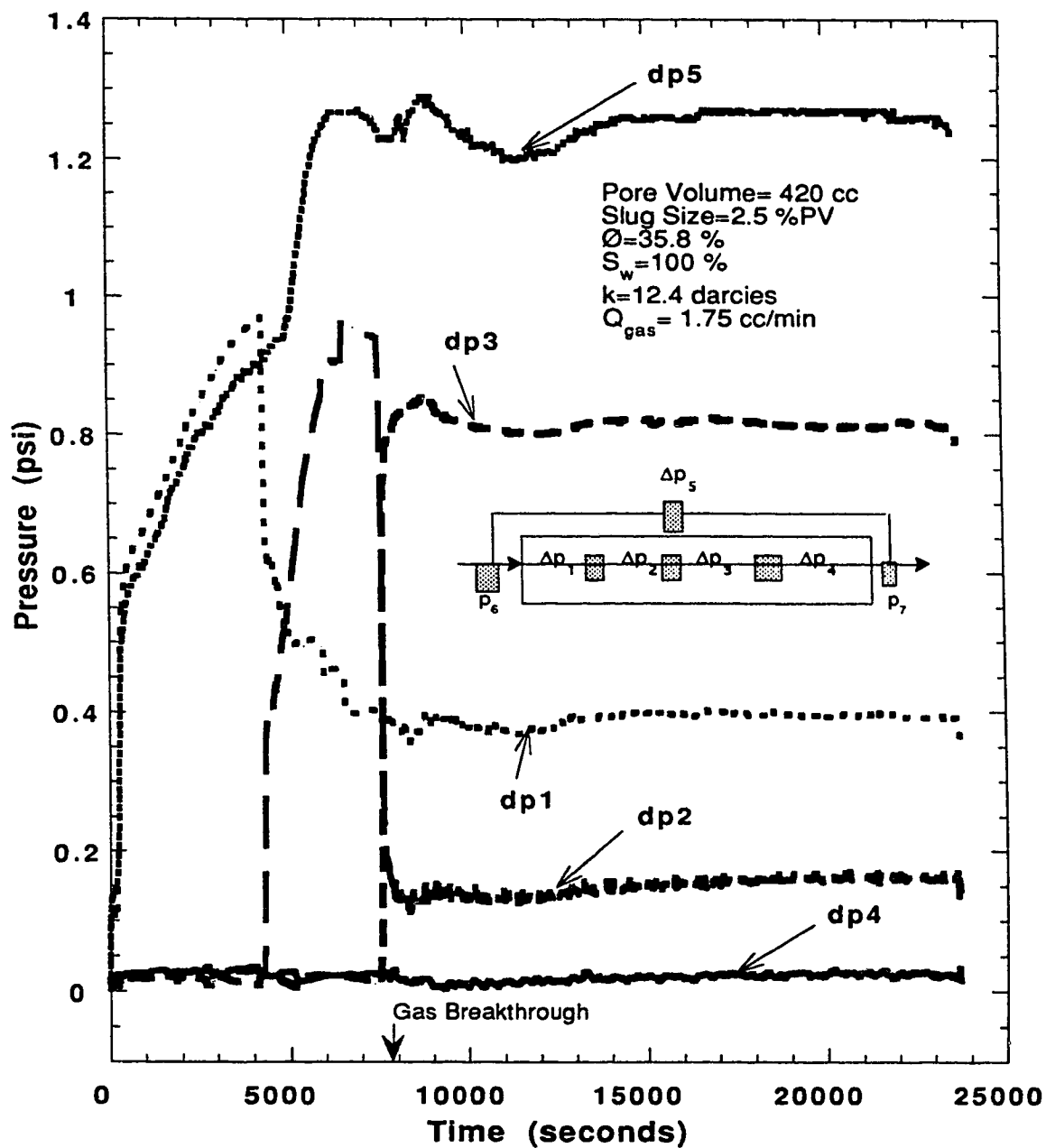


Figure 5.29- Run 37: Pressure Profile Using 10% Surfactant concentration in a Slug size of 2.5% PV Displaced by a Gas Flow Rate of 1.75 cc/min.

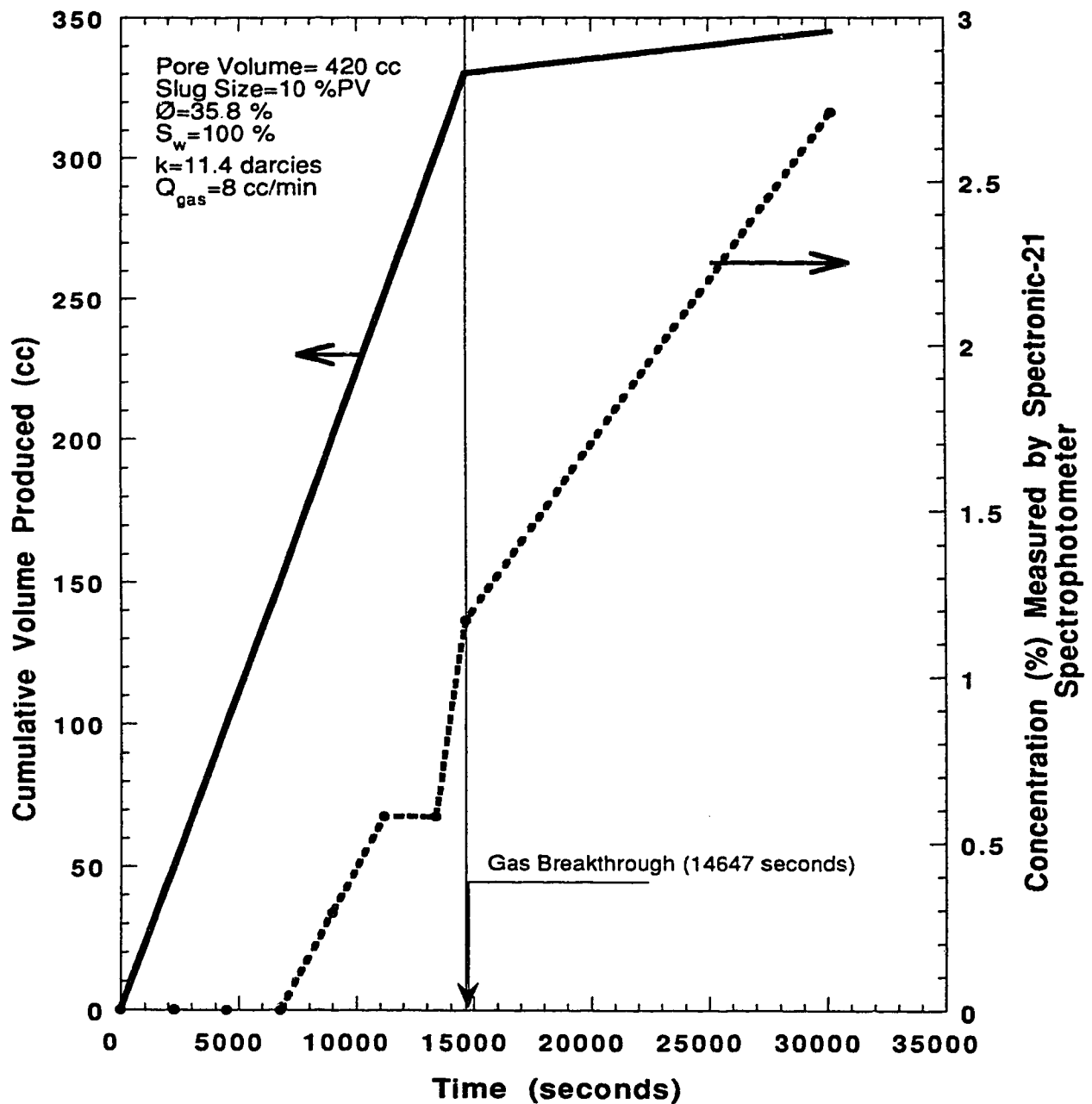


Figure 5.30- Run 40: Cumulative Production Versus Time and Concentration Versus Time for a Slug of 10% (PV) Having a 10% Dowfax-8390 Surfactant Concentration.

which is about the same as that of Run 24, 77.3 % PV, in which the same slug size was used.

The pressure history for this experiment is presented in Figure 5.31. By analyzing the response of all transducers, it appears that all of them manifested the expected trend except transducer ΔP_4 which kept rising until gas breakthrough, then decreased sharply to a stabilized lower differential pressure of 0.09 psi (0.6 kPa). The differential pressure across the core as measured by ΔP_5 rose continuously until gas breakthrough at which point it decreased, then stabilized at a differential pressure of 1.7 psi (11.7 kPa). The total foam mobility was 0.8 darcies/cp.

5.4.2.4 Overall Evaluation of Surfactant Slug Injection Experiments for Water-Saturated Sand Packs Displaced By a Gas Flowing at 1.75 cc/min

Figure 5.32 shows the cumulative production at breakthrough versus the slug size and totalizer reading both at gas breakthrough. The cumulative fluid produced at breakthrough curve shows the same trend as that of the slug-size runs when a gas flow rate of 8 cc/min was used, Figure 5.26. This indicates that the cumulative percentage pore volume produced at breakthrough was not affected by changing the gas flow rate from 8 to 1.75 cc/min.

The difference between the two sets of experiments is in the pressure response as discussed earlier. In the experiments run at a gas flow rate of 8 cc/min, the steady state differential pressures were higher than the ones run at a gas flow rate of 1.75 cc/min. This is due to the lamellae density where it was higher for higher gas flow rate. The frontal advance rates as estimated from the pressure versus time plots for Runs 37, 38 and 40 were 3.5, 6.6 and 5.5 m/day, respectively.

5.4.3 Surfactant Slug Injection Experiments for Sand Packs Involving Residual Oil

The next set of experiments was designed to examine the ability of foam to reduce the residual oil saturation, and to investigate the foam flow mechanism. These experiments were a repeat of the 100% water-saturated experiments, but, this time, they were conducted at residual oil saturation. The purpose of these experiments was to

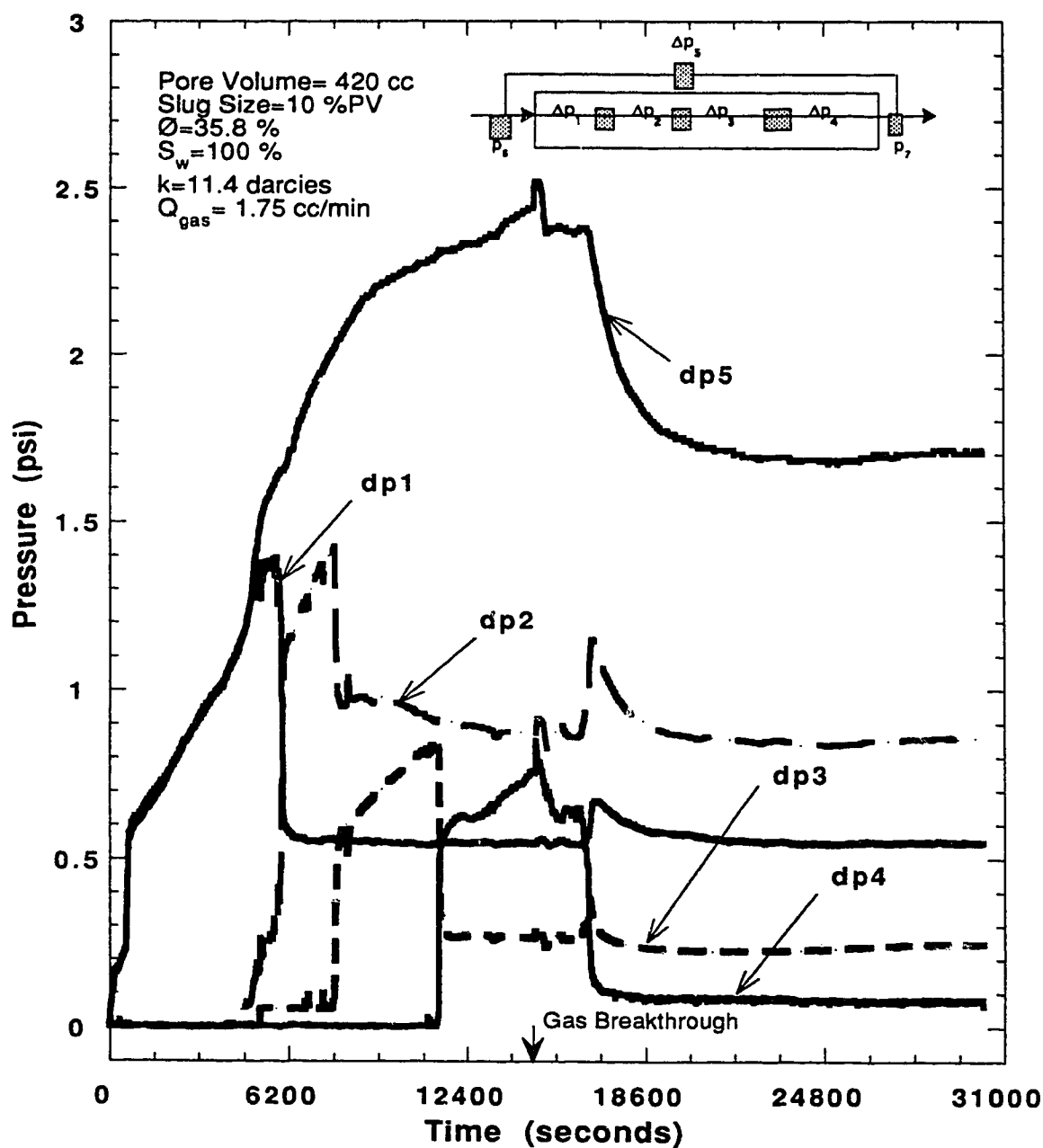


Figure 5.31- Run 40: Pressure Profile Using 10% Surfactant Concentration in a Slug Size of 10% PV Displaced by a Gas Flow Rate of 1.75 cc/min.

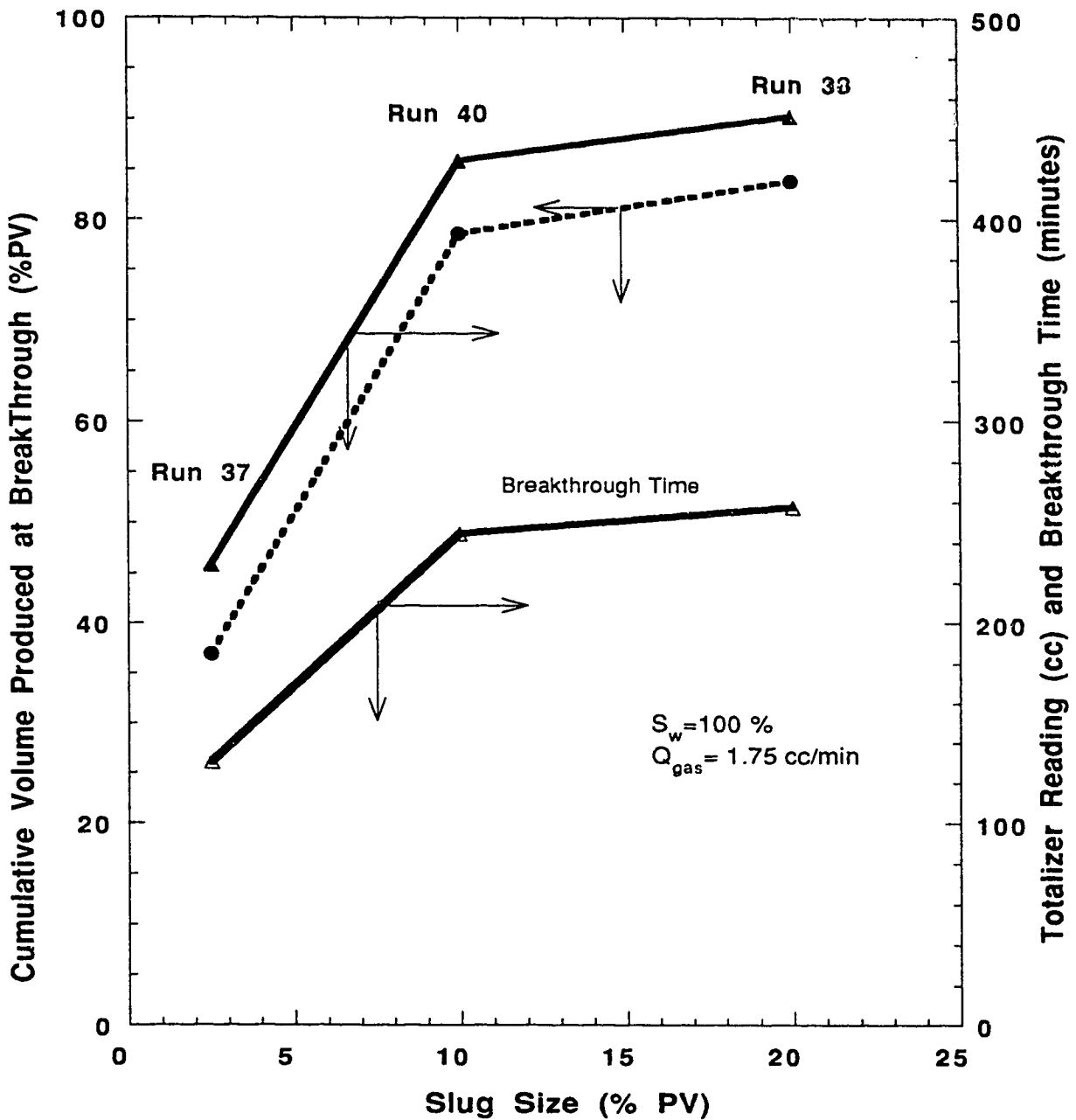


Figure 5.32: Comparison of Runs 37, 38, and 40, Cumulative Production (%PV) at Breakthrough Versus Slug Size, and Totalizer Reading at Breakthrough Versus Slug Size.

determine if the foam flow mechanism would be the same as in water-saturated sand packs.

After saturating the core with water to determine the pore volume and to run the permeability test, as discussed in Chapter 3 (Experimental Setup and Procedure) the core was re-saturated with oil. This oil was then displaced with water until no or negligible oil was produced. At this point the core was ready for the slug injection and the start of the experiment.

In the first set of experiments, Runs 26 to 31 were conducted using slug sizes ranging from 2.5 to 25% PV. Gas flow rates of 8 cc/min were used. Runs 32, 33 and 36 were carried out using surfactant slugs of 2.5, 10 and 20% PV, and displaced by gas flowing at a rate of 1.75 cc/min. In all the runs a Dowfax-8390 surfactant concentration of 10% was used.

5.4.3.1 Base Case for Oil Runs

Run 28 was the base case for the experiments performed at residual oil saturation. This run was conducted without surfactant. Nitrogen displaced water at residual oil saturation. The data for this run is given in Table 5.23 and is drawn in Figure 5.33. Gas breakthrough came after 10.87 minutes from the start of nitrogen injection. At this point, the total produced volume of fluid was 16.3% PV. This was less than the water base case, Run 25. No oil production was observed in this run.

The pressure history for this run is shown in Figure 5.34. The differential pressure rose the moment nitrogen injection was started. It reached a maximum value of 1.6 psi (11.0 kPa), then dropped sharply and stabilized at 0.8 psi (5.5 kPa). From the stabilized differential pressure, the mobility was determined to be 7.763 darcies/cp. In the sections to follow, when referred to the base case, it means Run 28, unless explicitly mentioned otherwise.

5.4.3.2 Surfactant Slug Injection Experiments for Sand Packs Water-saturated at Residual Oil Displaced By a Gas Flowing at 8 cc/min

Run 26 was performed in a 12.5 darcy sand pack using a 10% concentration of Dowfax-8390. Table 5.24 lists the production history for this run. Figure 5.35 shows the cumulative production and concentration plotted against time. The gas

Experimental Data for Run 28, Oil Base Case

Pore Volume (cc):	430	Surfactant Name:	none
Porosity (%):	36.6	Surfactant Concentration (%):	0
Absolute Perm. (darcies):	12.4	Slug size (% PV):	0
Oil Saturation:	28.5	Gas Flow Rate (cc/min):	8
Totalizer Reading at B.T. (cc):	87	Gas Breakthrough Time (min)	10.87
		Cumulative Recovery at B.T. (% PV):	16.28

Sample Number	Time (sec)	Sample Volume (cc)	Cumulative Volume (cc)	Totalizer Reading (cc)
1	0	0	0	0
2	556	53	53	74
3	652	17	70	87
4	1726	45	115	231
5	5917	30	145	790
6	15813	6	151	2110

Table 5.23 : Experimental Data for Run 28, Oil Base Case, Nitrogen Displacing Water at Residual Oil Saturation.

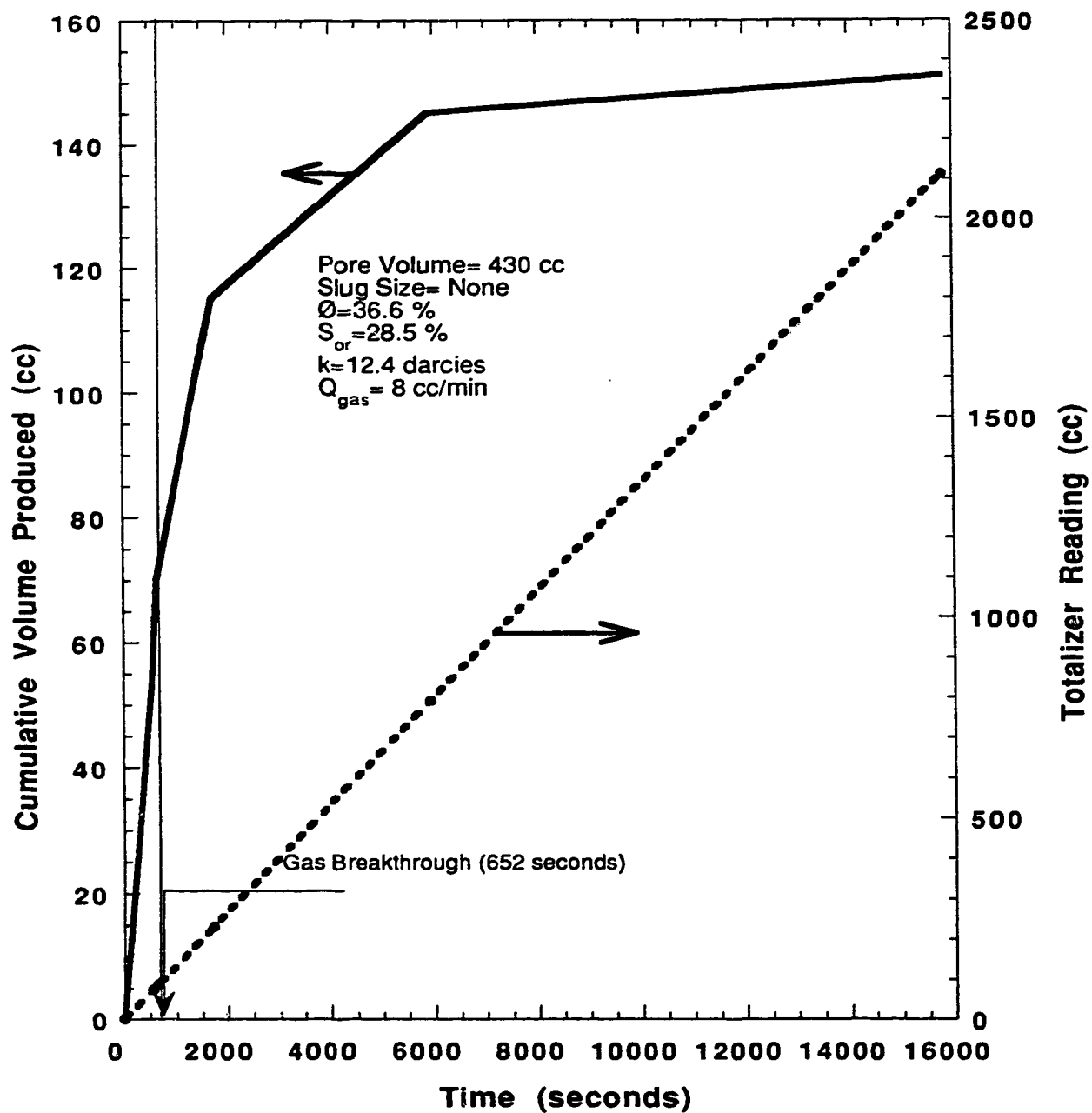


Figure 5.33- Run 28: Cumulative Production Versus Time and Totalizer Reading Versus Time for Nitrogen Displacing Water in the Presence of Residual Oil, No Surfactant Used.

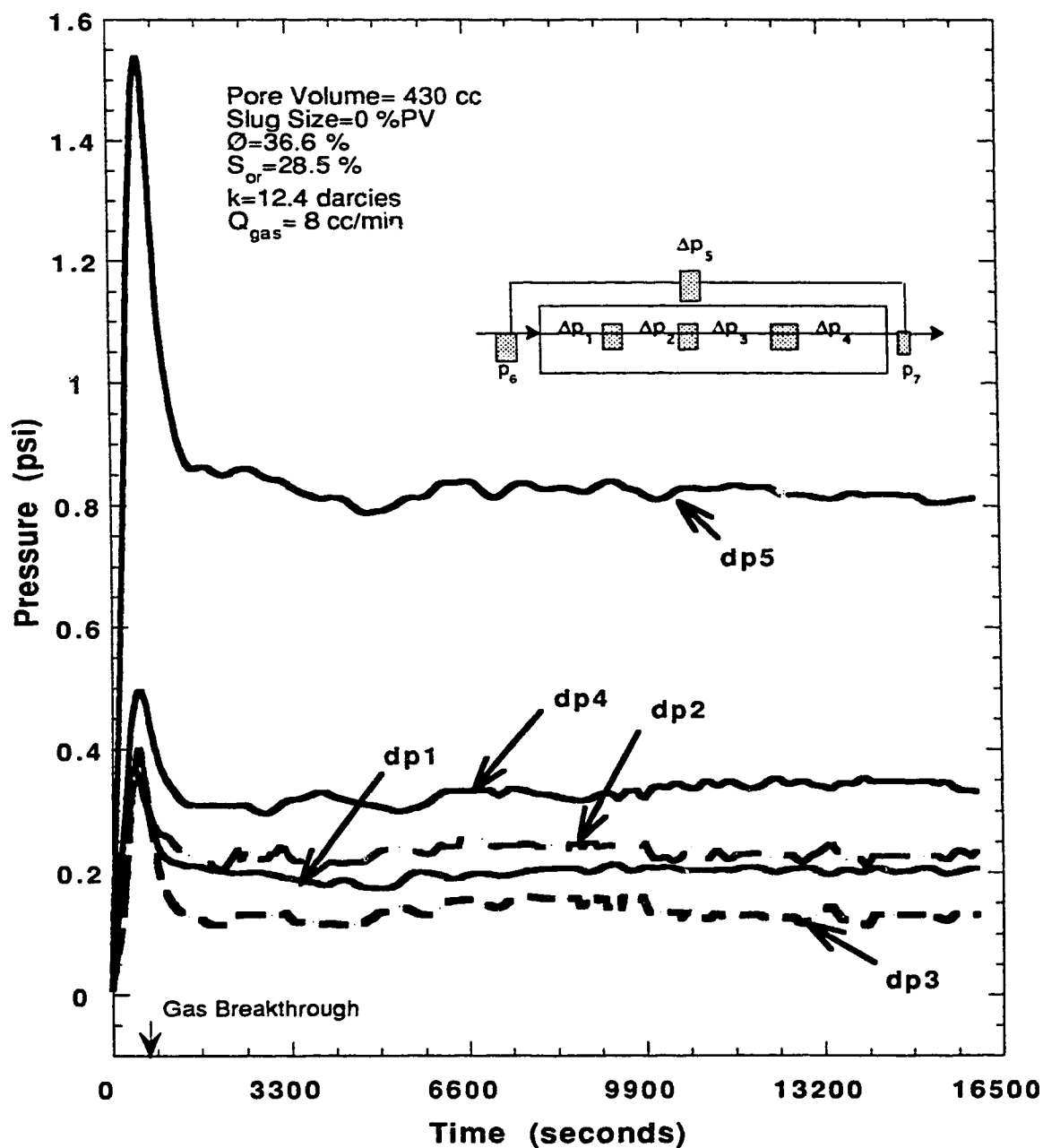


Figure 5.34- Run 28: Pressure Profile of Nitrogen Displacing Surfactant-Free Water in the Presence of Residual Oil Saturation.

Experimental Data for Run 26

Pore Volume (cc):	420	Surfactant Name:	Dowfax-8390
Porosity (%):	35.4	Surfactant Concentration (%):	10
Absolute Perm. (darcies):	12.5	Slug size (% PV):	20
Oil Saturation:	29.3	Gas Flow Rate (cc/min):	8
Totalizer Reading at B.T. (cc):	114	Gas Breakthrough Time (min)	14.4
		Cumulative Recovery at B.T. (% PV):	23.6

Sample Number	Time (sec)	Sample Volume (cc)	Cumulative Volume (cc)	Totalizer Reading (cc)	Concentration (Vol%)
1	0	0	0	0	0
2	541	50	50	70	0
3	864	49	99	114	0
4	1939	43	142	259	0.28
5	10144	47	189	1354	1.12
6	15616	17	206	2085	1.41

Table 5.24 : Experimental Data for Run 26 Using 10% Dowfax-8390 in a Slug of 20% PV, Run Conducted in Presence of Oil.

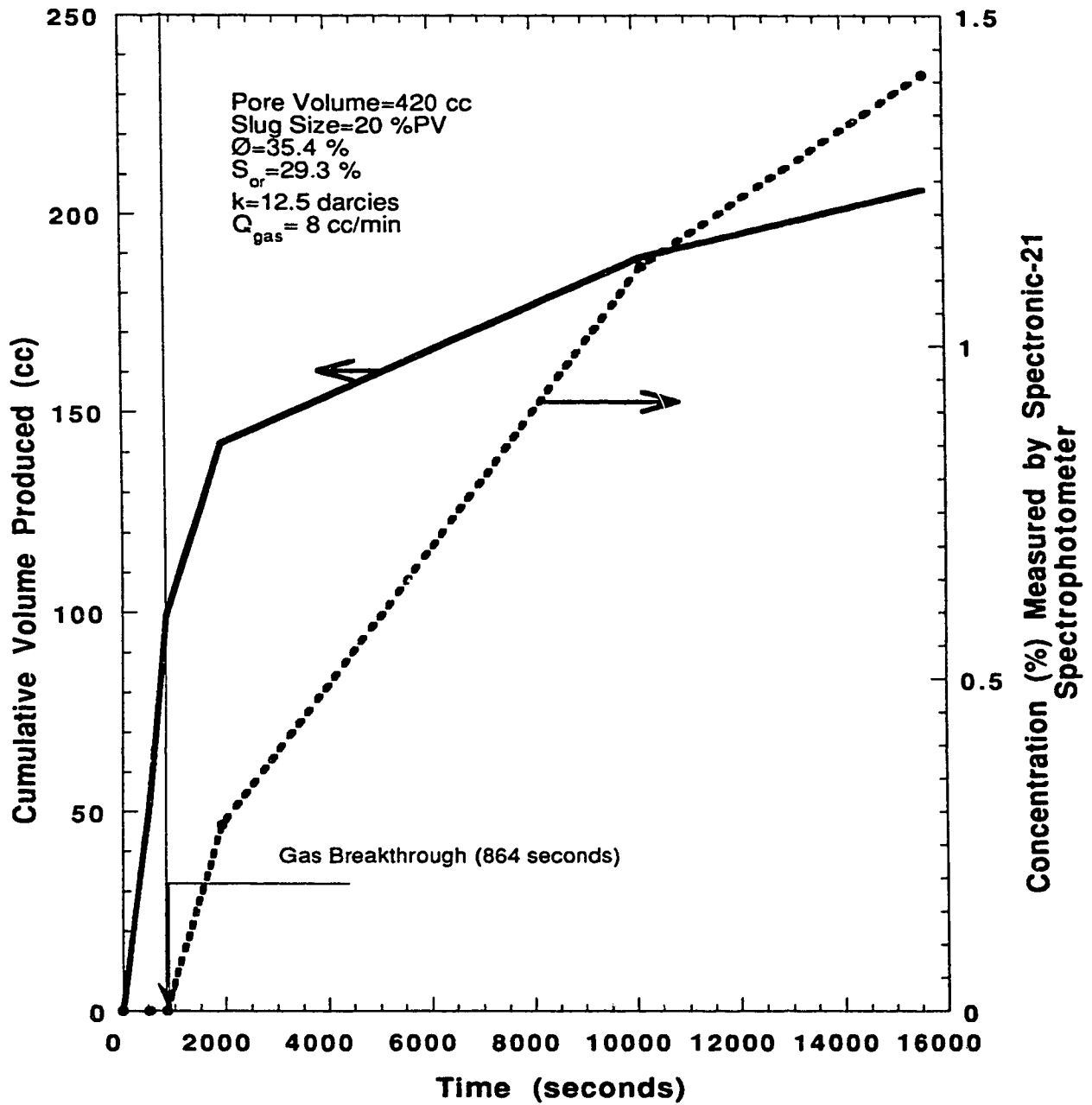


Figure 5.35- Run 26: Cumulative Production Versus Time and Concentration Versus Time for a Slug of 20% (PV) Having a 10% Dowfax-8390 Surfactant Concentration, in the Presence of Oil.

breakthrough came after 14.4 minutes from the start of nitrogen injection. The cumulative volume produced at breakthrough was 23.6% PV. This is higher than that of the base case, but not by much. About 10 cc of oil was produced. This reduced the initial residual oil saturation from 29.3 to 21.2%. It can be seen from Figure 5.35 that the cumulative volume produced curve clearly has a different shape from that for Runs 19 and 38 which utilized the same slug size but without the complication of oil. This is due to the inefficient displacement which was caused by the effect of oil on the surfactant. Oil spreading over the foam lamellae weakened the foam and caused the foam to collapse.

Figure 5.36 gives the recorded pressure for Run 26. The differential pressure, after rising, did not stabilize anywhere near the maximum pressure reached, 2.7 psi (18.6 kPa); instead, it dropped to 1.35 psi (9.3 kPa) at the end of the experiment. This indicates the detrimental effect of the oil on the surfactant.

Run 27 was performed in a sand pack having 28.6% residual oil saturation and using a slug of 5% PV. The production data of Run 27 is given in Appendix A as Table 5.25. The production data is drawn in Figure 5.37. The cumulative percentage pore volume produced at breakthrough, 13.42 minutes, was 21.67. Less than 6 cc of oil was produced in this run, possibly because there was not enough pressure gradient to mobilize the residual oil.

The pressure profile for this experiment is presented in Figure 5.38. Noteworthy in the plot is the pressure response in the second and the third sections of the core as measured by ΔP_2 and ΔP_3 . The response shows that foam was breaking and reforming. This is supported by the observations of Fried⁽⁴⁰⁾ and Holm⁽⁴¹⁾.

Run 29 was conducted under conditions similar to those for Run 27, only the slug size was changed to 10% PV. The residual oil saturation was 30.1%. The data for this run are given in Appendix A as Table 5.26, and drawn in Figure 5.39. After 13.97 minutes of production, the produced cumulative volume of fluid was 22.6% PV. Out of the total produced fluid, 8 cc of oil was produced. This means that the residual oil saturation was reduced from 30.1 to 28.2% which is not a significant reduction.

Figure 5.40 gives the pressure history for this run. The same response as that of Run 27 was observed again as it can be seen from the graph. This supports the idea that foam in presence of oil is breaking and reforming.

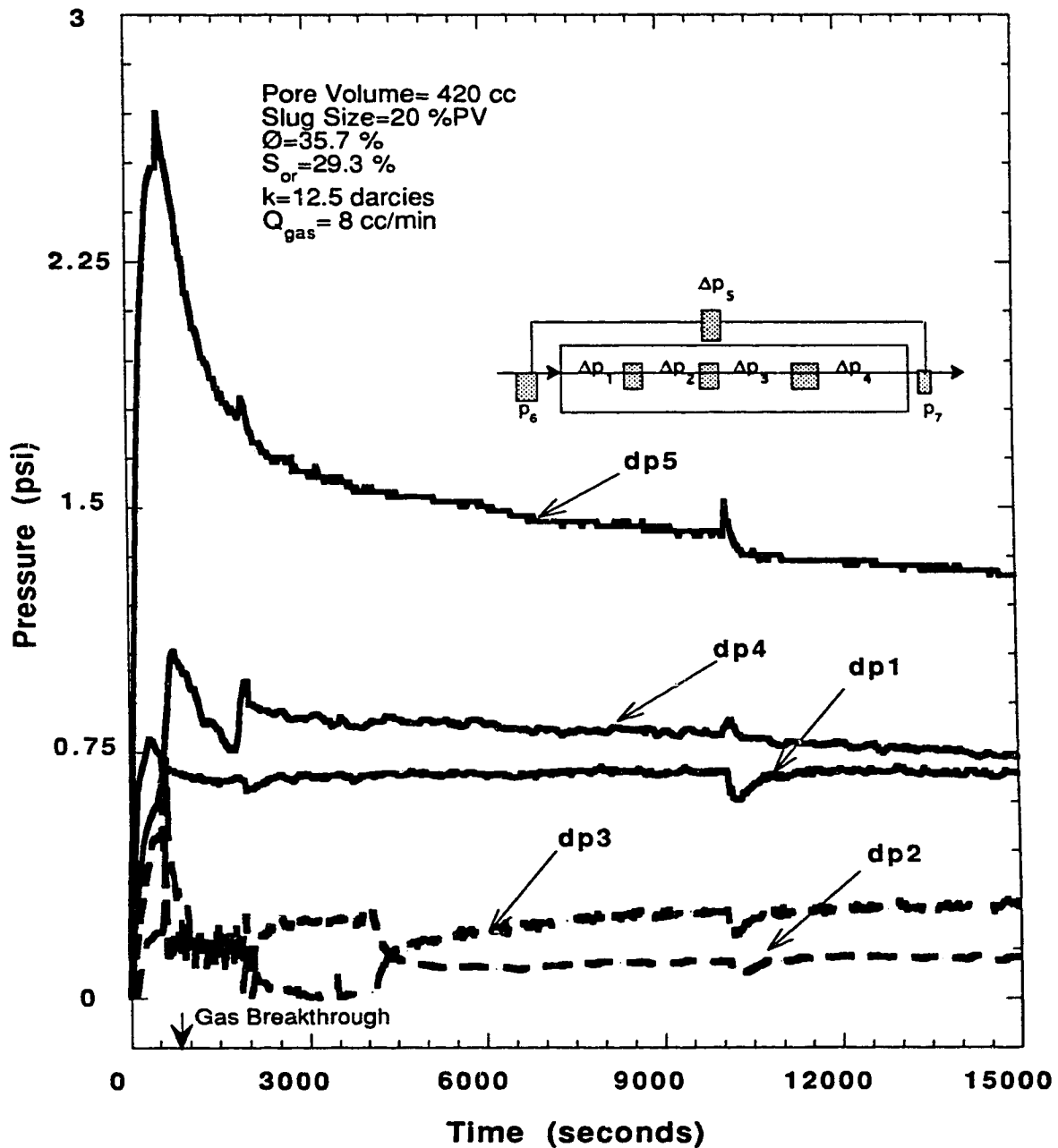


Figure 5.36- Run 26: Pressure Profile, Using 10% Surfactant Concentration in a Slug Size of 20% PV Displaced by a Gas Flow Rate of 8 cc/min.

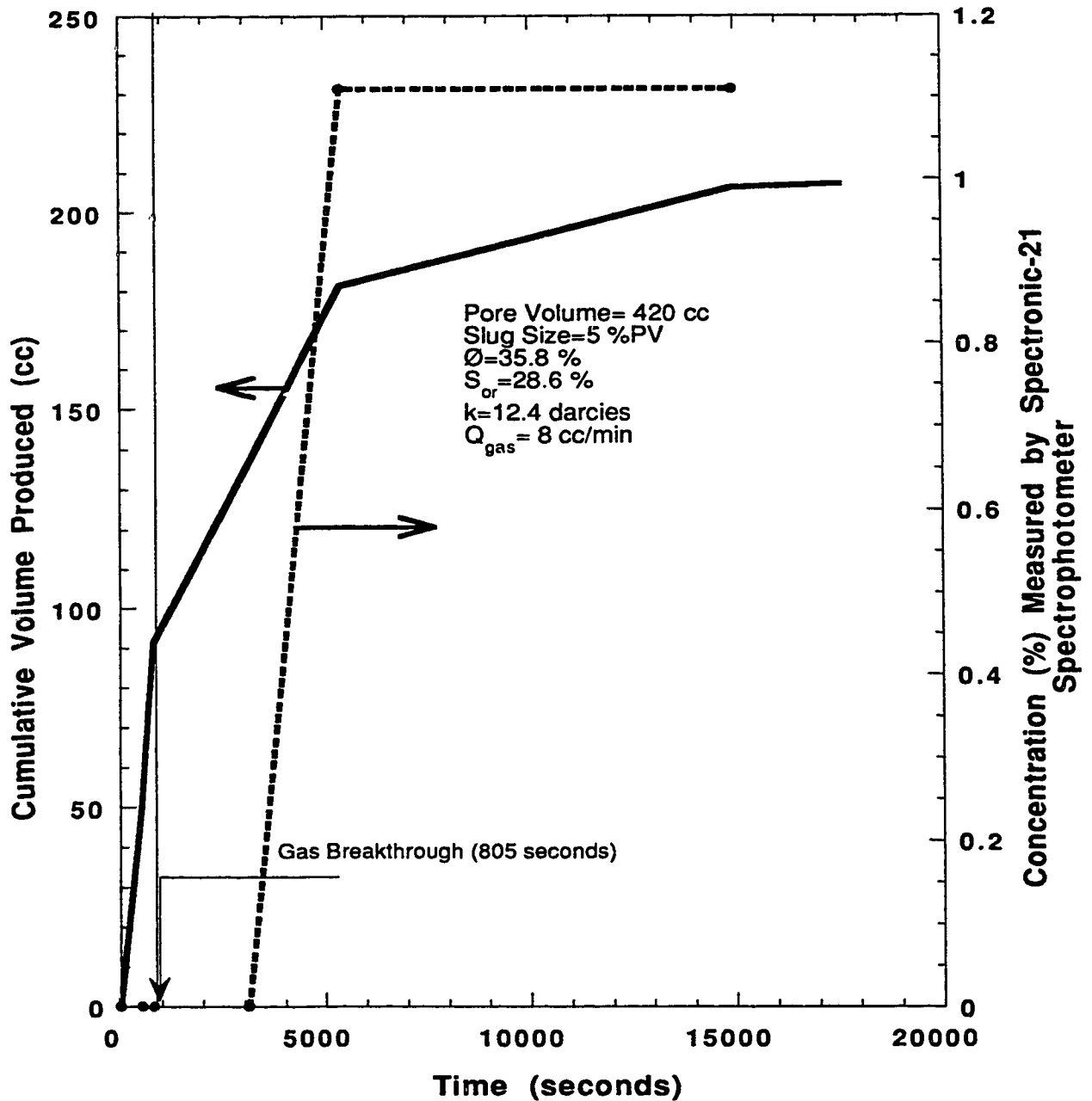


Figure 5.37- Run 27: Cumulative Production Versus Time and Concentration Versus Time for a Slug of 5% (PV) Having a 10% Dowfax-8390 Surfactant Concentration, in the Presence of Oil.

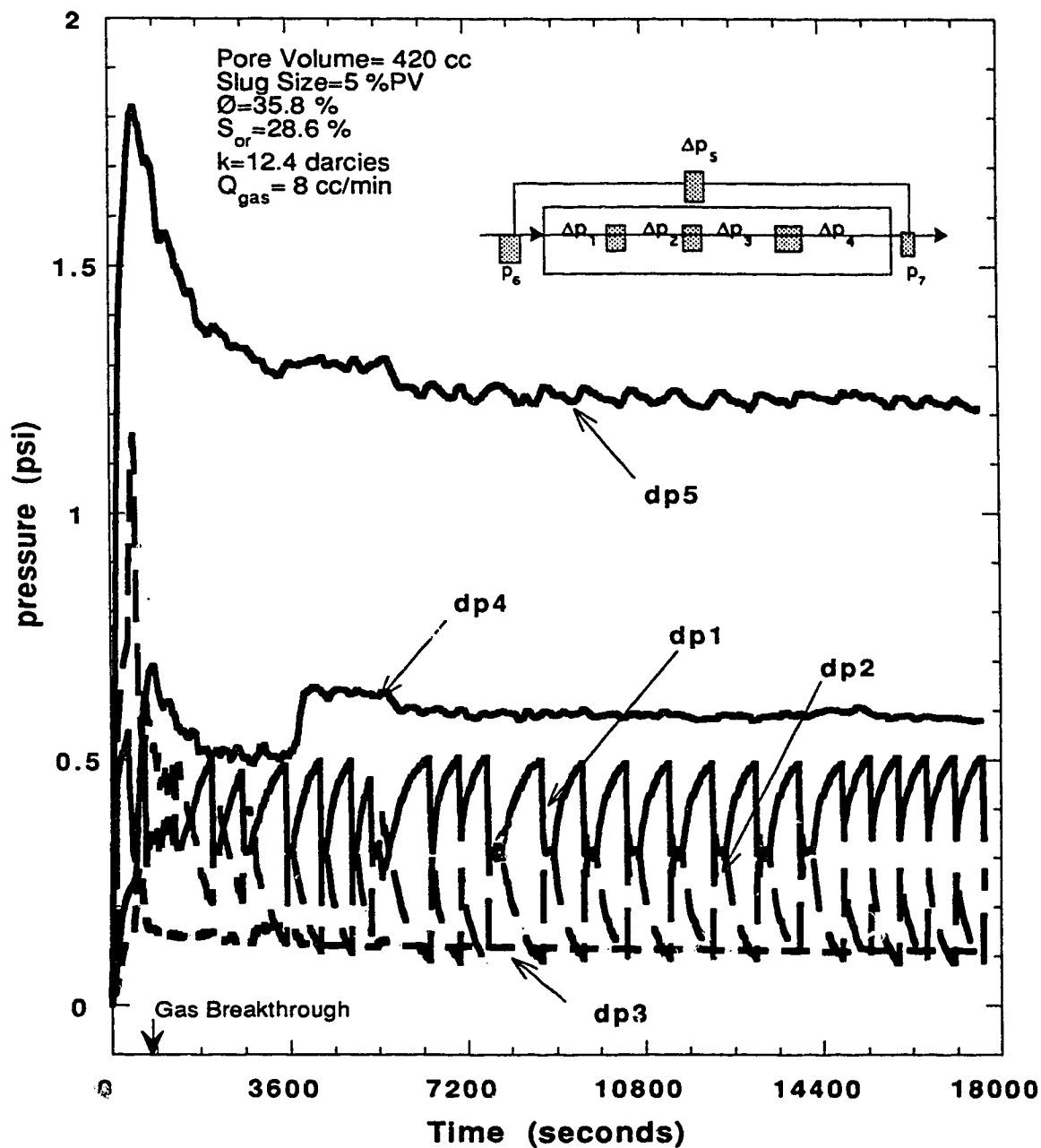


Figure 5.38- Run 27: Pressure Profile Using 10% Surfactant Concentration in a Slug size of 5% PV Displaced by a Gas Flow Rate of 8 cc/min.

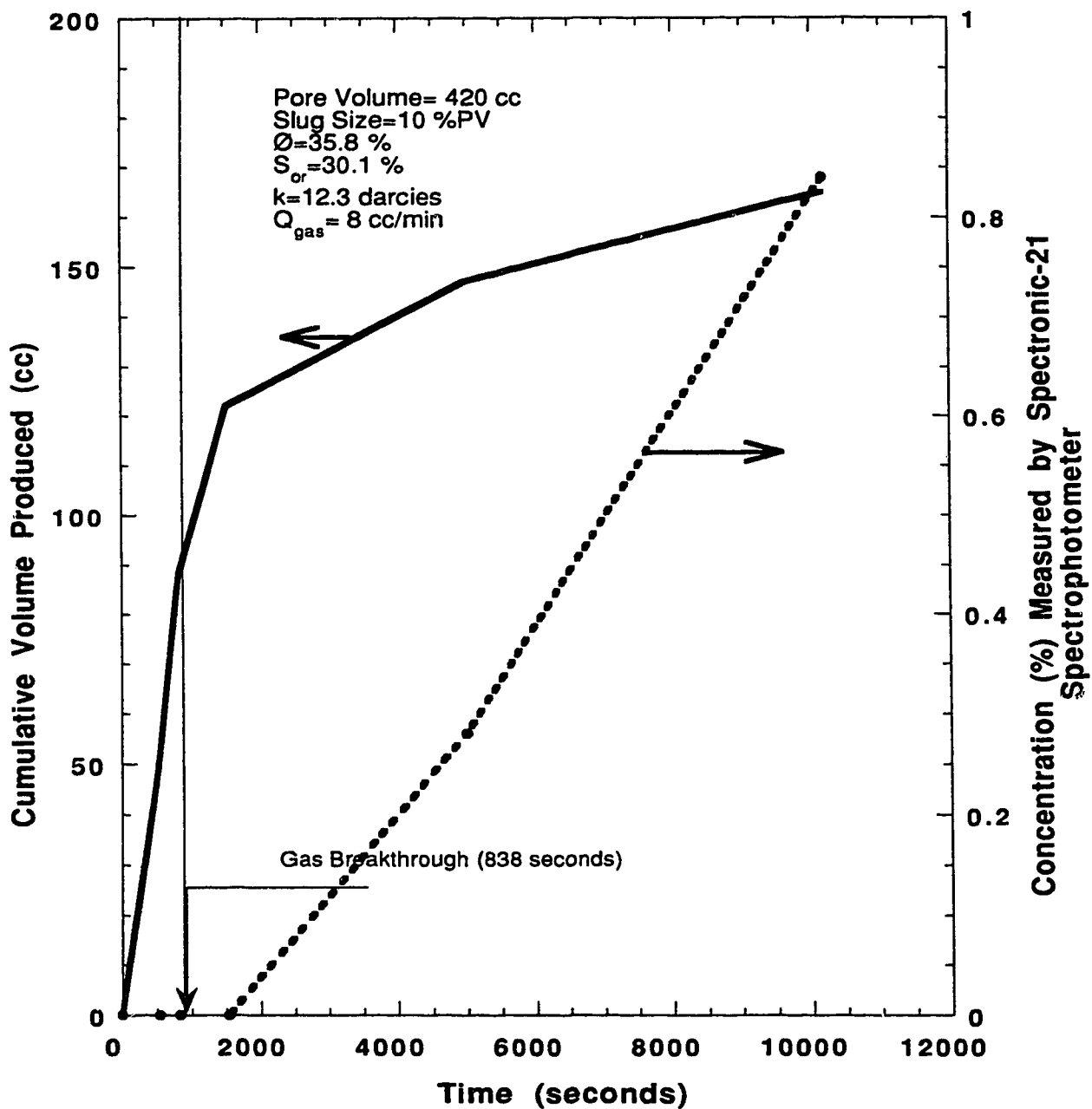


Figure 5.39- Run 29: Cumulative Production Versus Time and Concentration Versus Time for a Slug of 10% (PV) Having a 10% Dowfax-8390 Surfactant Concentration, Conducted in the Presence of Oil.

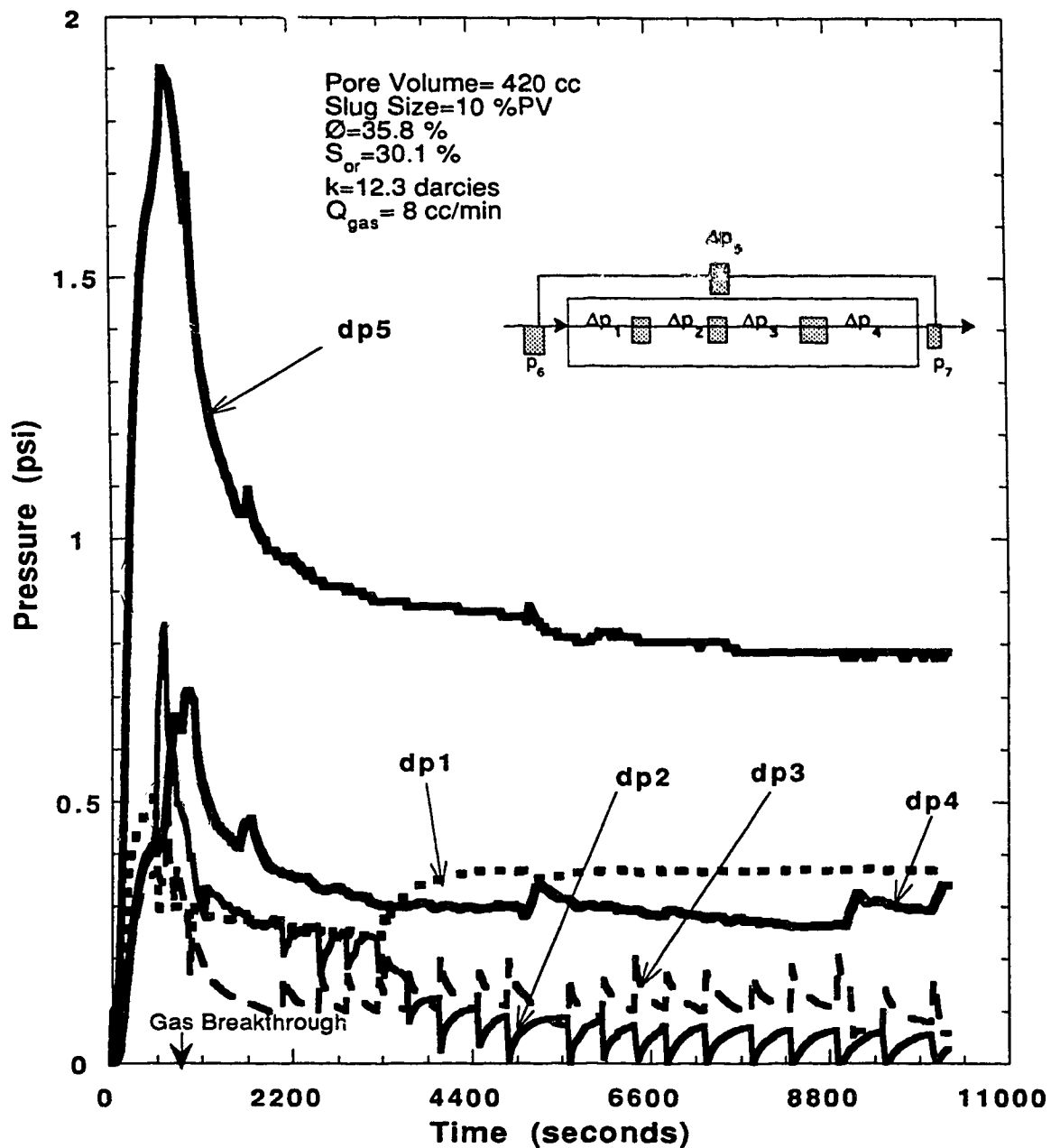


Figure 5.40- Run 29: Pressure Profile Using 10% Surfactant Concentration in a Slug size of 10% PV Displaced by a Gas Flow Rate of 8cc/min.

Run 30 was carried out in a sand pack having a permeability of 12.4 darcies, and an oil saturation of 28.7%. A slug size of 2.5% was used. The production data is given in Appendix A, Table 5.27. The cumulative volume produced and the concentration profile are drawn in Figure 5.41. At breakthrough, 10.72 minutes from the start of the experiment, the total produced liquid was 82 cc.

The pressure history recorded for Run 30 is shown in Figure 5.42. Again the plot displays the same response as that of Runs 27 and 29. This further supports the hypothesis that the foam was breaking and reforming. Also it is noted that breaking and reforming occurred in the middle sections of the sand pack.

Run 31 was the last experiment to be carried out in the presence of oil using a gas flow rate of 8 cc/min. A slug of 25% PV was used. The production data are given in Appendix A, Table 5.28, and are drawn in Figure 5.43. The breakthrough time was 10.63 minutes at which time 80 cc of fluid was produced. From the graph, one can see that, even though a large slug size was used, the effluent concentration was not as high as in Run 22, in which the same slug size was used in a 100% water-saturated core. This can be explained by examining the pressure profile. Figure 5.44 gives the pressure history for this run. The differential pressure across the core initially increased, reached a maximum of 2.2 psi (15.2 kPa), then continued to decrease gradually. As the foam propagated farther into the sand pack, it contacted more oil. The repeated contacts weakened the foam further. Therefore, the overall differential pressure never increased enough to mobilize the residual oil saturation. As a result, the displacement efficiency was very poor leaving most of the surfactant slug behind.

The pressure response of the foam breaking and reforming was also observed in Run 31 as can be seen from the pressure gradient recorded by ΔP_2 and ΔP_3 transducers in second and third sections of the core.

5.4.3.3 Overall Evaluation of Surfactant Slug Injection Experiments for Sand Packs Water-Saturated at Residual Oil Displaced By a Gas Flowing at 8 cc/min

Figure 5.45 shows the slug size versus cumulative volume produced and totalizer readings at breakthrough. The graph of the cumulative volume produced at breakthrough shows an increasing trend up to a slug of 20% PV, then it decreased.

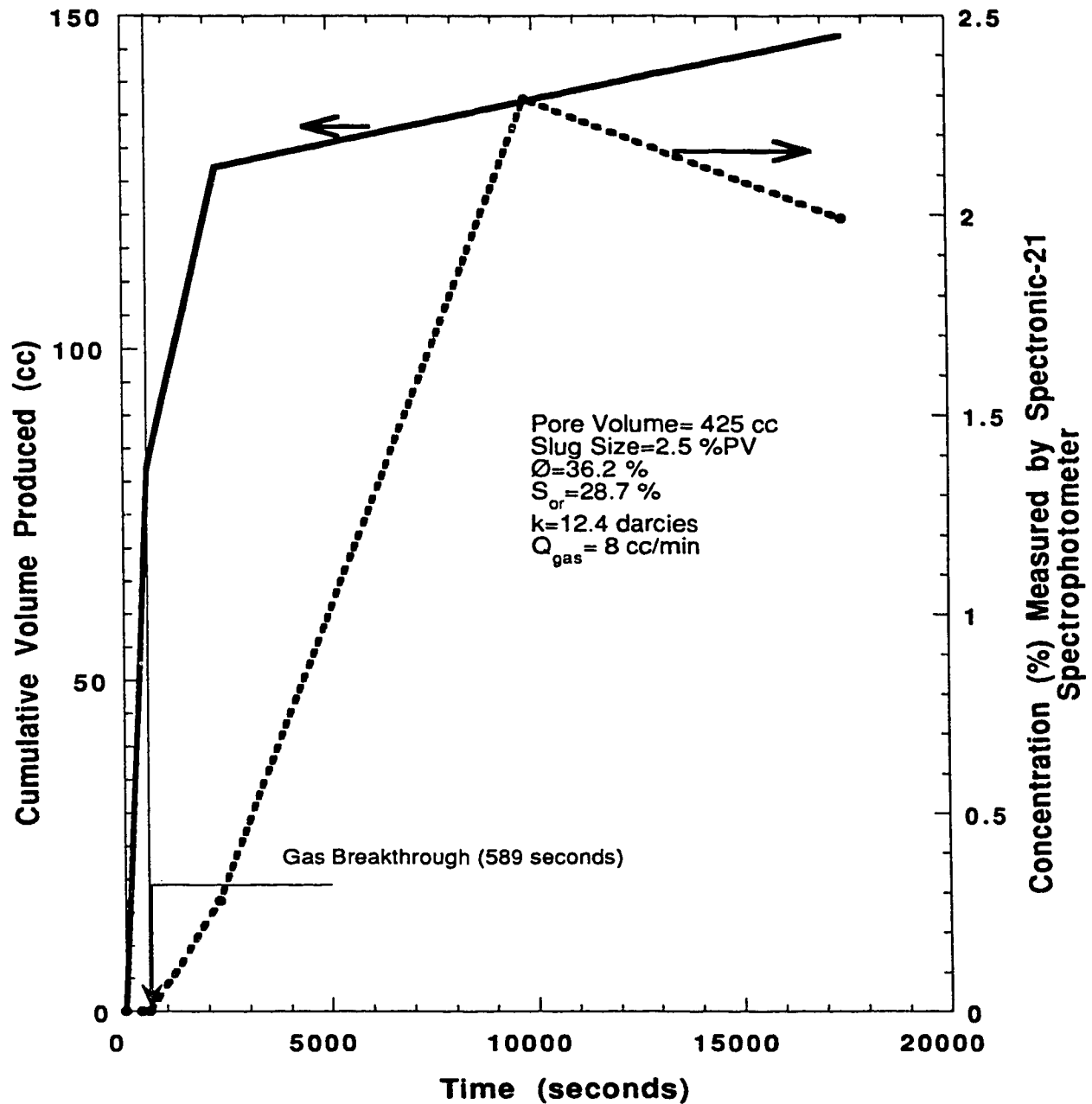


Figure 5.41- Run 30: Cumulative Production Versus Time and Concentration Versus Time for a Slug of 2.5% (PV) Having a 10% Dowfax-8390 Surfactant Concentration, Conducted in the Presence of Oil.

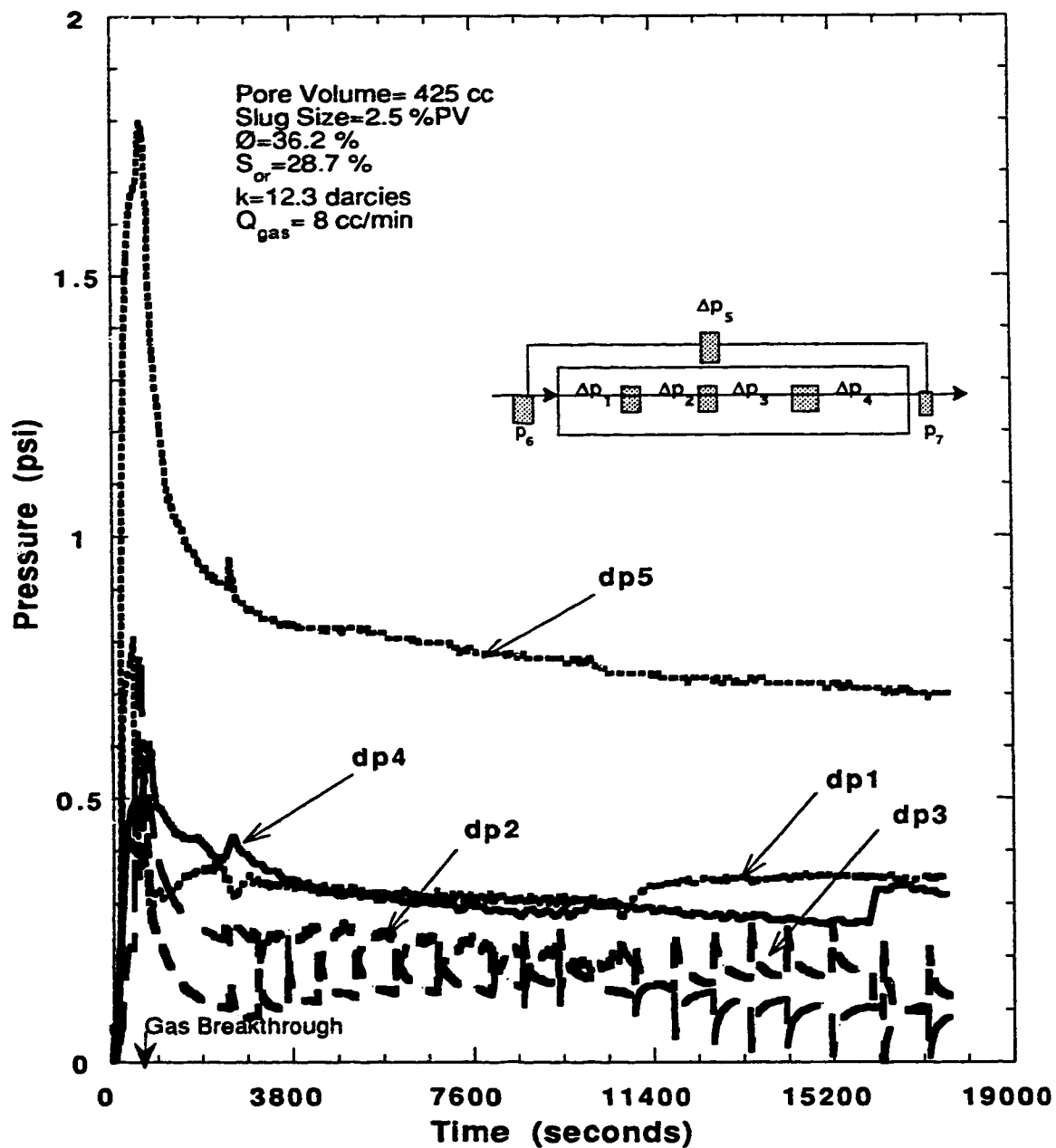


Figure 5.42- Run 30: Pressure Profile Using 10% Surfactant Concentration in a Slug size of 2.5% PV Displaced by a Gas Flow Rate of 8 cc/min.

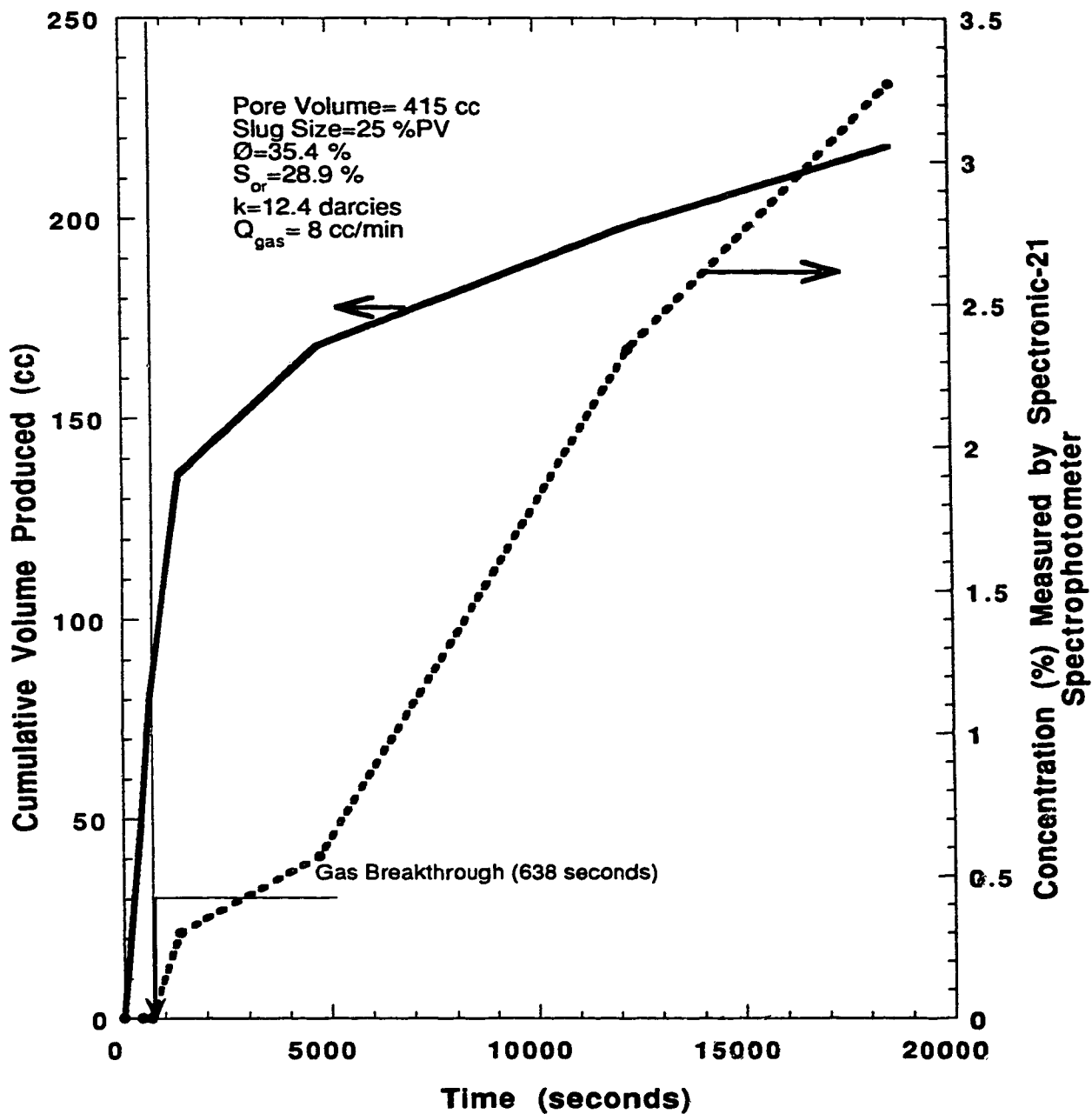


Figure 5.43- Run 31: Cumulative Production Versus Time and Concentration Versus Time for a Slug of 25% (PV) Having a 10% Dowfax-8390 Surfactant Concentration.

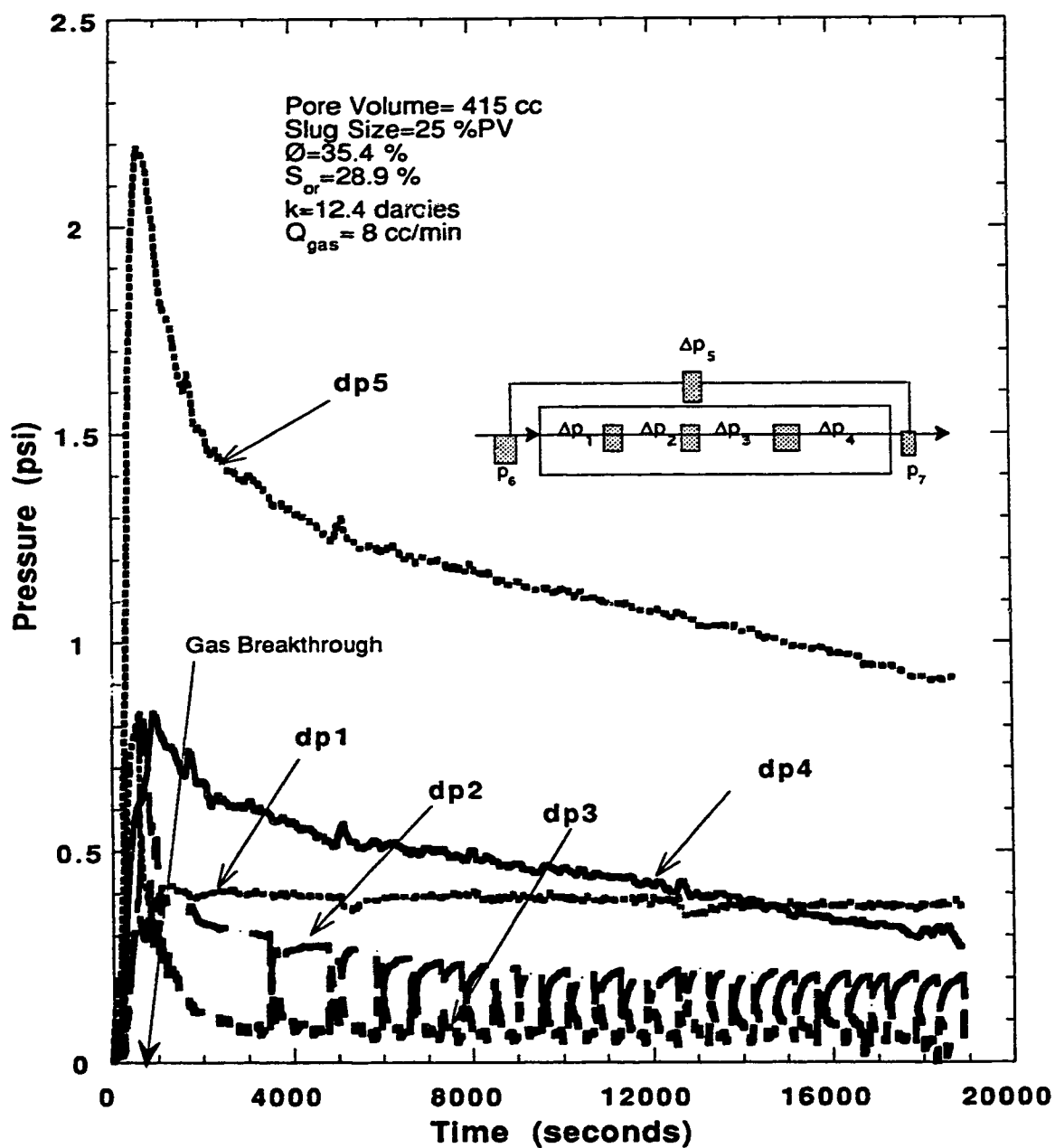


Figure 5.44- Run 31: Pressure Profile Using 10% Surfactant Concentration in a Slug size of 25% PV Displaced by a Gas Flow Rate of 8 cc/min.

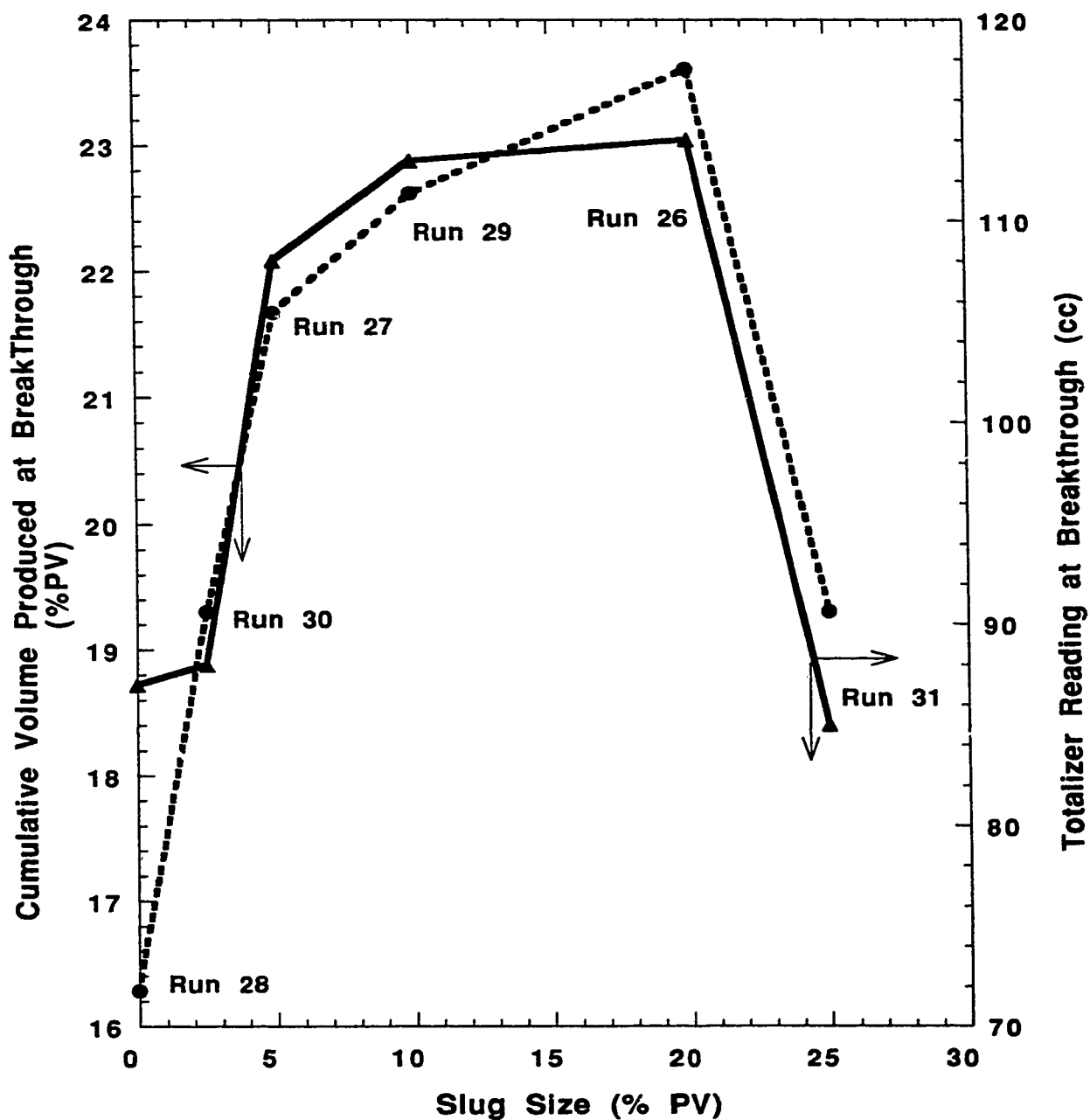


Figure 5.45: Comparison of Runs 26 to 31, Cumulative Production (%PV) and Breakthrough Time Versus Slug Size, and Totalizer Reading Versus Slug Size.

The totalizer reading and cumulative gas injected, curves are plotted to give an idea of the amount of nitrogen injected to produce the corresponding samples of liquids.

The analysis of Runs 26 to 31 revealed that the cumulative volume produced at breakthrough was much lower than the recoveries obtained with the same slug sizes when there was no oil present in the core. This was due to the effect of the oil on the surfactant. The pressure differentials as recorded for the present runs gave a much lower stabilized pressure gradient and in some cases did not stabilize. Unlike the 100% water-saturated sand packs, where the stabilized pressure increased with increasing slug size, the pressure did not show any trend as the slug size was changed in these runs. Also the cumulative production at breakthrough was very low for Runs 26 to 31 as compared to Runs 19 to 24 which had the same slug sizes. Figure 5.46 compares the cumulative volume at breakthrough for the slug size experiments in the case of 100% and at residual oil water saturated sand packs. The difference between the two curves is due to the detrimental effect of oil on the surfactant which retarded the formation of foam by the spreading of oil over the lamellae. Interestingly, bottle-shaking tests by hand produced foam in the presence of oil, using the same slug concentration of 10% (Vol.) with ambient air as the gas. The produced foam persisted for over two weeks.

5.4.3.4 Surfactant Slug Injection Experiments for Sand Packs Water-Saturated at Residual Oil Displaced By a Gas Flowing at 1.75 cc/min

To investigate the effect of the gas flow rate on the recovery three runs, Runs 32, 33 and 36, were conducted at a gas flow rate of 1.75 cc/min using surfactant slug sizes of 2.5, 10 and 20% PV, respectively. In all three runs, the sand pack was initially saturated with water, then oil displaced the water to a connate water saturation. Then the oil was displaced by water to a residual oil saturation of approximately 30% of the pore volume. The data of the three runs are given in Appendix A as Tables 5.29, 5.30, and 5.31. The three runs are analyzed in following section.

Run 32 was carried out in a 12.5 darcy sand pack having a residual oil saturation of 28.4%. A slug of 2.5% PV was injected prior to nitrogen injection. Figure 5.47 gives the production history and the concentration profile versus time. Breakthrough occurred after 57.92 minutes, at which time 88 cc, corresponding to

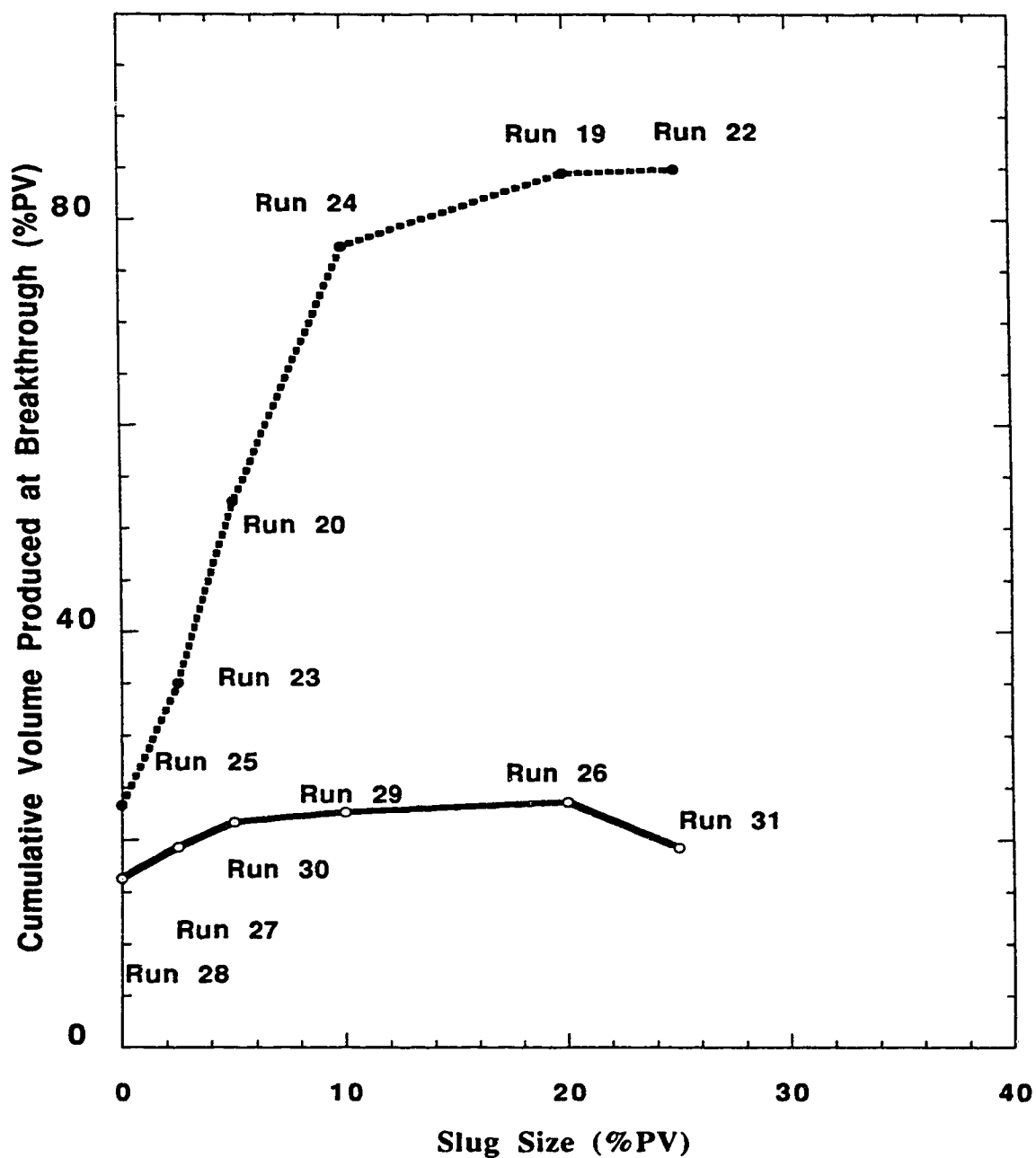


Figure 5.46 : Comparison Between 100% Water Saturated Runs 19 to 25 and Residual Oil Runs 26 to 31 Performed at the Same Gas Flow Rate of 8 cc/min.

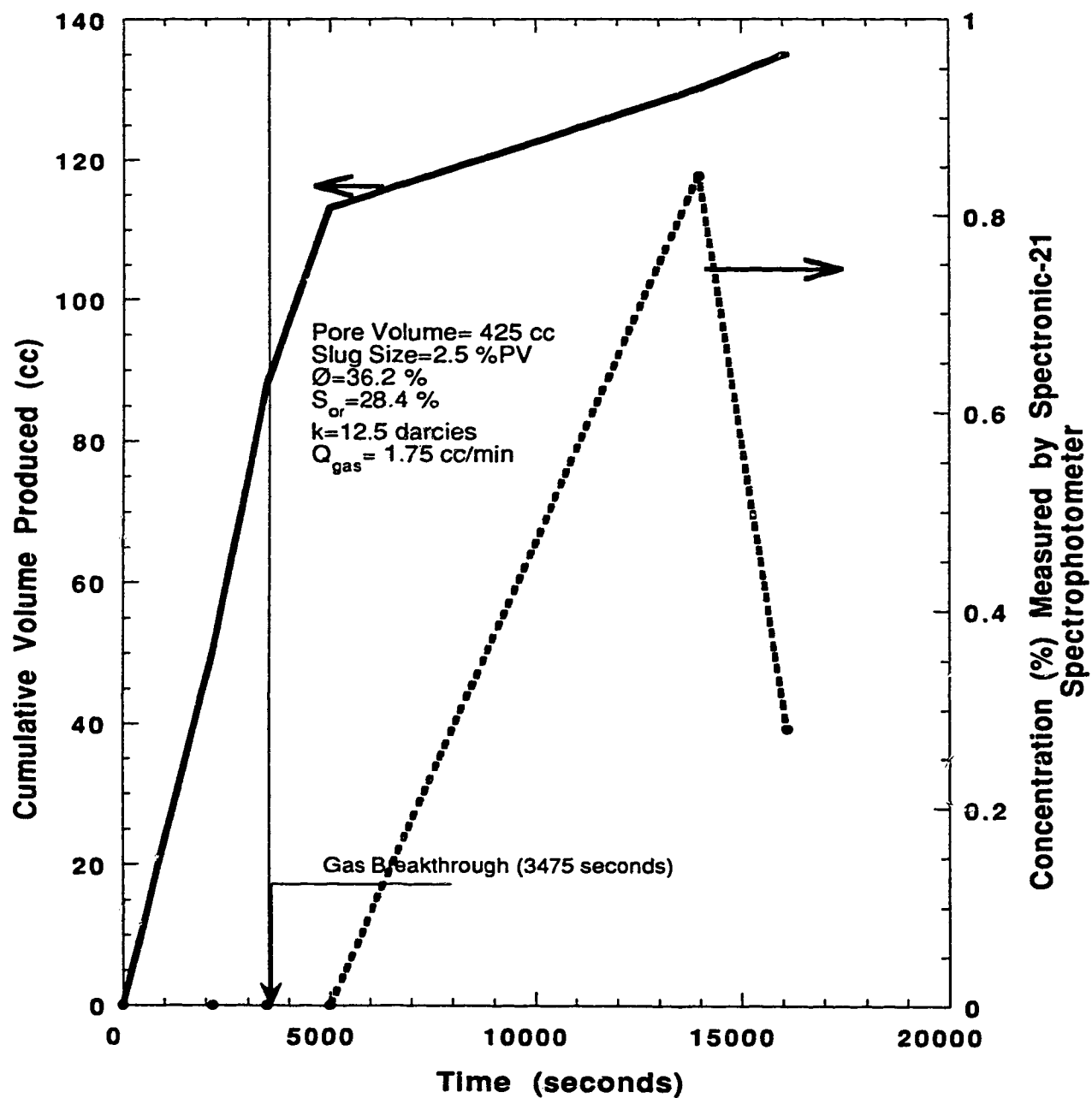


Figure 5.47- Run 32: Cumulative Production Versus Time and Concentration Versus Time for a Slug of 2.5% (PV) Having a 10% Dowfax-8390 Surfactant Concentration, Conducted in the Presence of Oil.

20.7% PV, of fluid were produced. Comparing the production at breakthrough, this run and Run 30, for the same slug size, had almost the same cumulative volume produced. No concentration was measured at breakthrough. The pressure history for this run is presented in Figure 5.48 which exhibits the same trend of foam breaking and forming as seen from the response of the dp2 and dp3 curves. So the foam flow mechanism of breaking and reforming in the presence of oil does exist at a low gas velocity, 1.75 cc/min, as well as at a higher gas velocity, 8 cc/min.

The production data for Run 33 is given in Appendix A, Table 5.30. The production history and the pressure profile are drawn in Figures 5.49 and 5.50, respectively. Breakthrough occurred 63 minutes from the start of the experiment. At this point, 21.69% PV was produced. Little oil was produced -less than 8 cc. The pressure profile did not exhibit the response seen in other experiments in the presence of oil. This foam was not strong enough to reduce gas mobility. Breakthrough occurred 3780 seconds into the experiment.

Run 36 was the last run done at a gas flow rate of 1.75 cc/min. In this run a slug of 20% PV was used. The production data for Run 36 are given in Appendix A, Table 5.31. This data was used to draw Figure 5.51 which shows the cumulative volume produced versus time and the effluent concentration versus time. The percentage pore volume produced at breakthrough which occurred after an elapsed time of 54.12 minutes was 21.21. The pressure profile for this run is given in Figure 5.52. From the graph, the dp5 curve, the differential pressure across the sand pack, does not attain a high pressure gradient. This suggests that a very weak foam, if any, was formed. It seems that a very weak foam was generated because gas breakthrough coincided with the peak of the ΔP_4 transducer. This was followed by gas expansion which led to the breaking of the weak foam lamellae, as can be seen from the dp4 curve. Meanwhile, the pressure gradient in the first section, the dp1 curve, was increasing which means that foam regeneration was taking place, but very slowly. In the second section, the dp2 curve, the differential pressure was decreasing which means that no foam existed and that the gas was flowing in fixed channels with no resistance. About halfway into the experiment, one can see from the dp3 and dp4 curves that foam was generated and broken.

To further investigate the effect of the oil used on Dowfax-8390, Run 35 was performed at irreducible water saturation and an initial oil saturation of 92.1%. Run 35

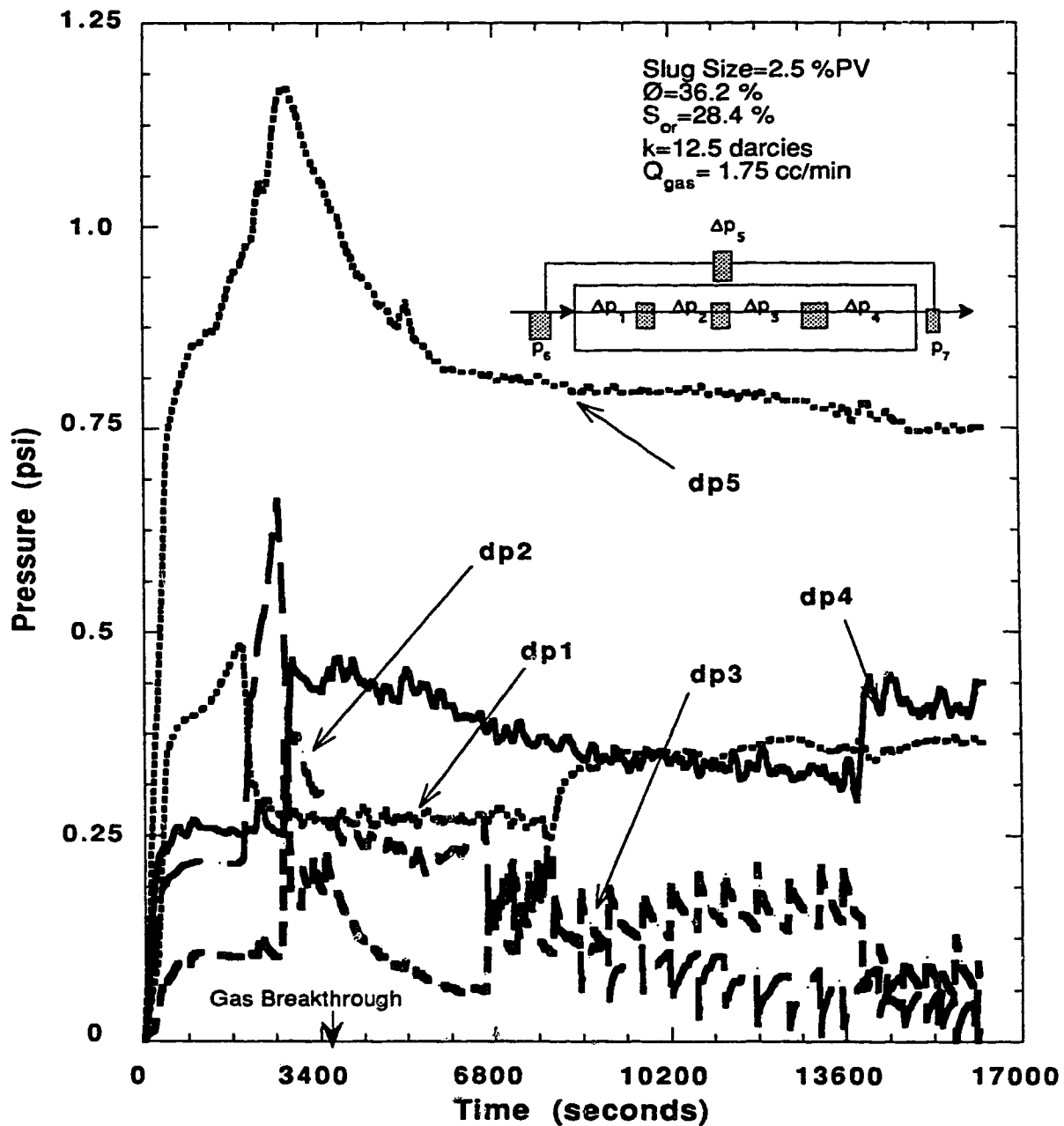


Figure 5.48- Run 32: Pressure Profile Using 10% Surfactant Concentration in a Slug size of 2.5% PV Displaced by a Gas Flow Rate of 1.75 cc/min in the Presence of Oil.

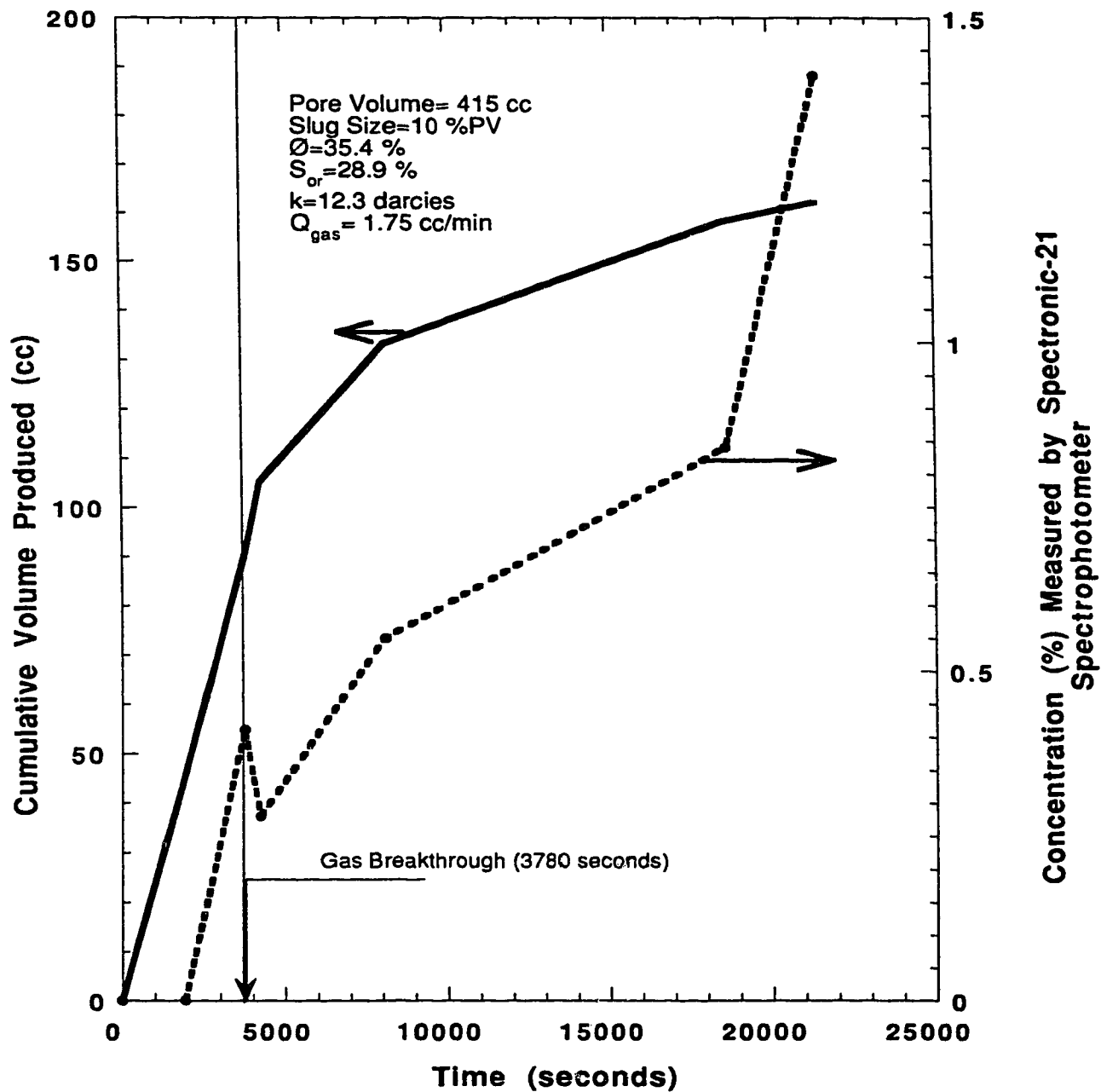


Figure 5.49- Run 33: Cumulative Production Versus Time and Concentration Versus Time for a Slug of 10% (PV) Having a 10% Dowfax-8390 Surfactant Concentration, Conducted in the Presence of Oil.

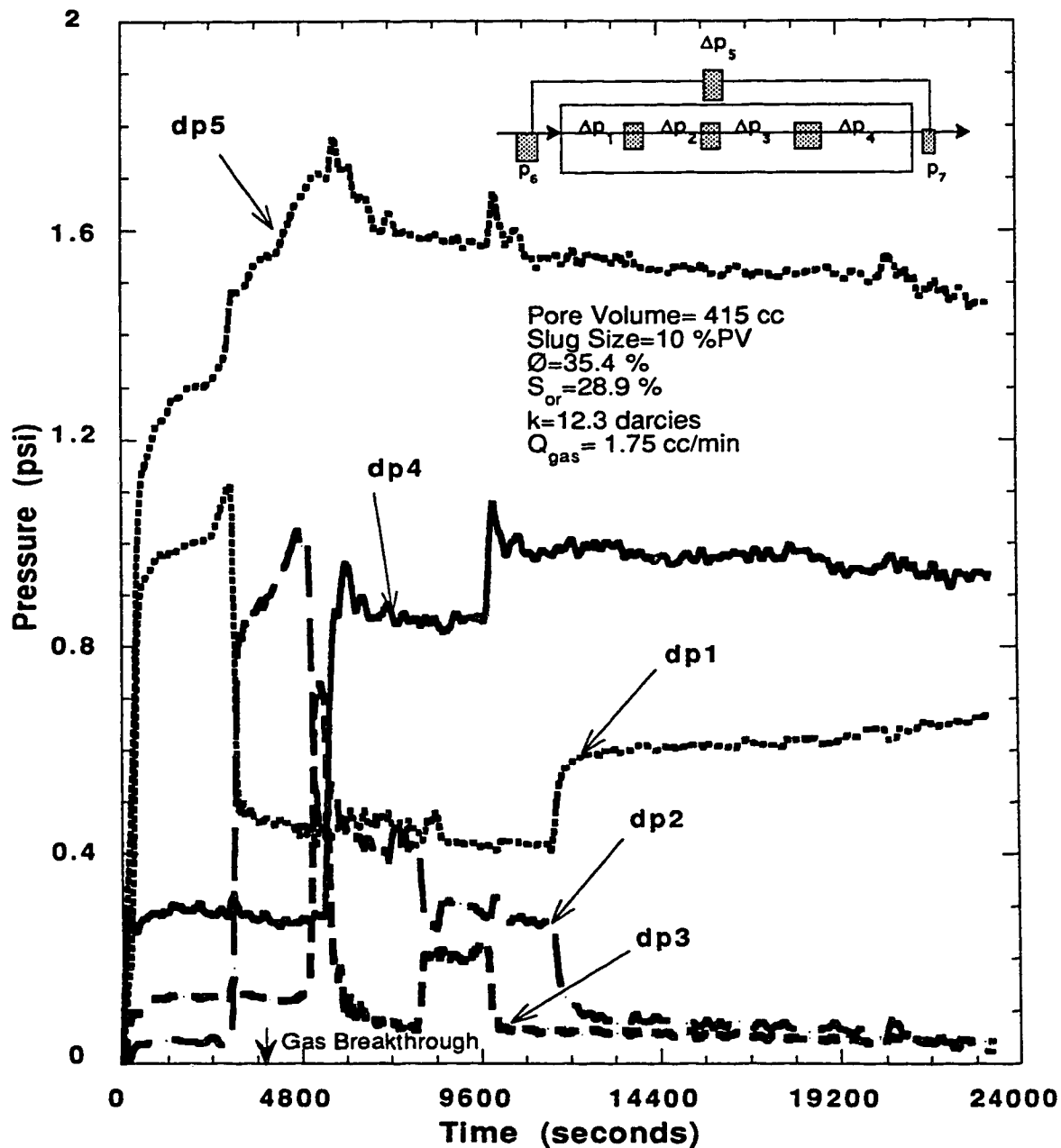


Figure 5.50- Run 33: Pressure Profile Using 10% Surfactant Concentration in a Slug size of 10% PV Displaced by a Gas Flow Rate of 1.75 cc/min in Presence of Oil.

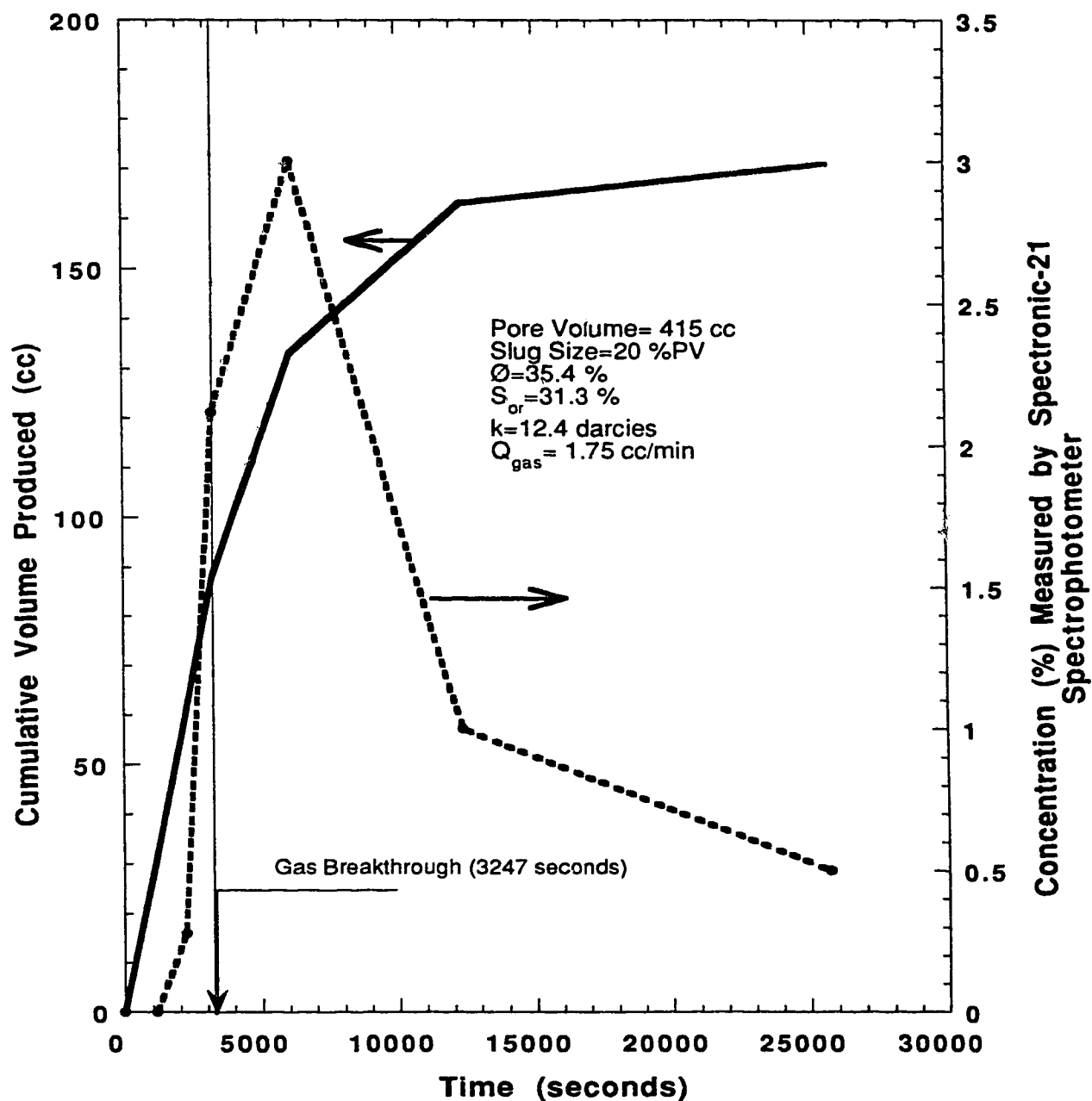


Figure 5.51- Run 36: Cumulative Production Versus Time and Concentration Versus Time for a Slug of 20% (PV) Having a 10% Dowfax-8390 Surfactant Concentration, Conducted in the Presence of Oil.

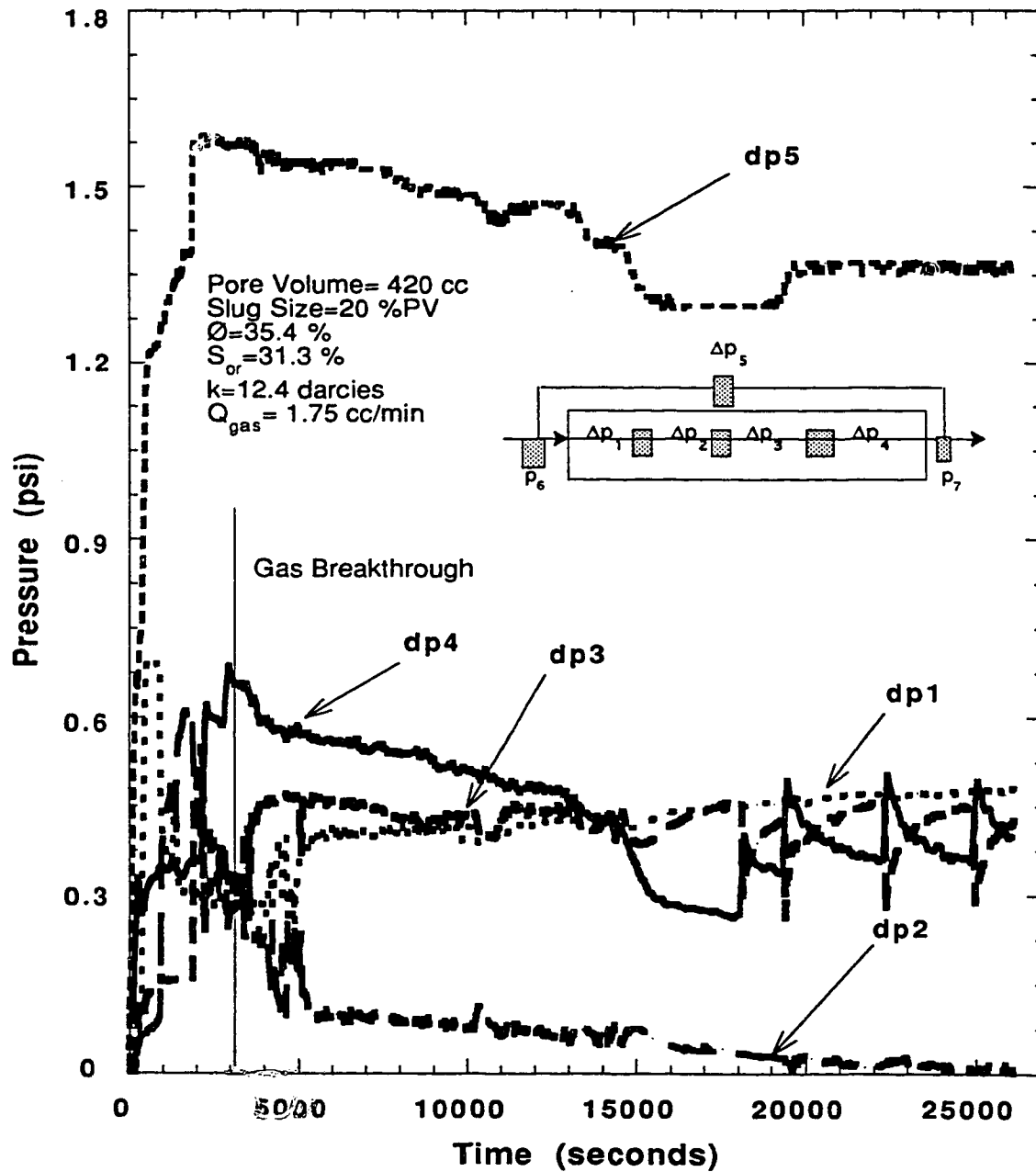


Figure 5.52- Run 36: Pressure Profile Using 10% Surfactant Concentration in a Slug size of 20% PV Displaced by a Gas Flow Rate of 1.75 cc/min in the Presence of Oil.

data are tabulated in Table 5.32. Figure 5.53 shows the cumulative production plotted against time. Gas breakthrough occurred 11.75 minutes from the beginning of the run. A pore volume percentage of 4.82 of oil was produced. The pressure profile is shown in Figure 5.54. The differential pressure increased to a maximum value of 10 psi (68.9 kPa), then shortly after breakthrough it fell sharply and continued to fall. The high rise in differential pressure was caused by foam formation at the injection side of the core. The collapse of foam may be attributed to the spreading of oil over the foam⁽⁵⁷⁾.

5.5 Injection Strategy

The results of slug injection experiments conducted in the presence of oil did not reduce the residual oil saturation due to the adverse effect of oil on the surfactant used. Next, nitrogen- surfactant co-injection runs were performed to determine whether a continuous supply of surfactant would remedy the effect of the oil and lower the residual oil saturation. Runs 15 and 34 were performed by co-injecting nitrogen and a solution of 10% Dowfax-8390 surfactant.

In Run 15, a slug of 5% PV was injected prior to the start of nitrogen and surfactant co-injection. The ratio of the injected liquid to nitrogen was 1:10 cc/min. This ratio gives a foam quality of 90%.

Run 15 experimental data is given in Table 5.33. The production data and the pressure profile are shown in Figures 5.55 and 5.56, respectively. In Figure 5.55, the corrected cumulative volume produced was increasing which meant that steady state was not reached. This is also seen in the pressure history, where the differential pressure was increasing. Despite the fact that the run did not reach steady state at the time of termination, the results were satisfactory. After 15.22 minutes, the breakthrough time, the corrected cumulative volume was 20.43% PV. A total of 15 cc of oil was produced. So the residual oil saturation was reduced from 28.6 to 25.03%.

One interesting remark to make, looking at the pressure profile in Figure 5.56, is that the foam did not show the pattern of breaking and reforming as it did in the slug runs in the presence of oil.

The second run performed by co-injection was Run 34. A slug of 5% PV was injected. Then surfactant solution and nitrogen were co-injected at a ratio of 1:4 cc/min. The foam quality at this ratio and an average pressure of 1.35 psi (9.3 kPa) was 78.6

Experimental Data For Run 35

Pore Volume (cc):	415	Surfactant Name:	Dowfax-8390
Porosity (%):	35.4	Surfactant Concentration (%):	10
Absolute Perm. (darcies):	12.3	Slug size (% PV):	20
Oil Saturation:	92.1	Gas Flow Rate (cc/min):	8
Totalizer Reading at B.T. (cc):	95	Gas Breakthrough Time (min)	11.75
		Cumulative Recovery at B.T. (% PV):	4.82

Sample Number	Time (sec)	Sample Volume (cc)	Cumulative Volume (cc)	Totalizer Reading (cc)
1	0	0	0	0
2	705	20	20	95
3	2162	39	59	286
4	6516	25	84	869
5	13203	16	100	1758
6	16519	10	110	2200

Table 5.32 : Experimental Data for Run 35, Using 10% Dowfax-8390 in a 20% PV Slug, Nitrogen Displacing Oil.

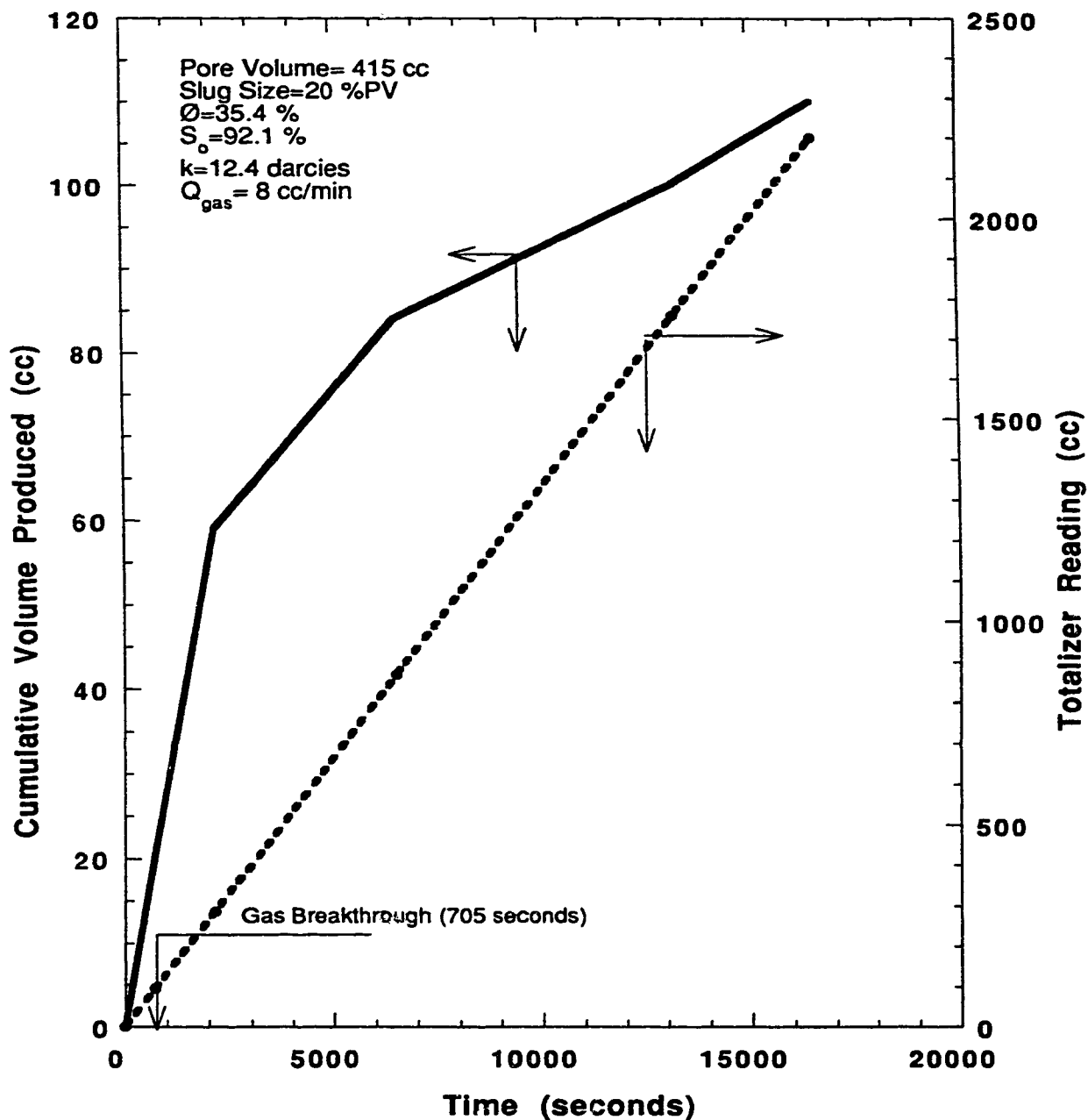


Figure 5.53- Run 35: Cumulative Production Versus Time and Totalizer Reading Versus Time for a Slug of 20% (PV) Having 10% Dowfax-8390 Surfactant Concentration in a Nitrogen Displacing Oil Process.

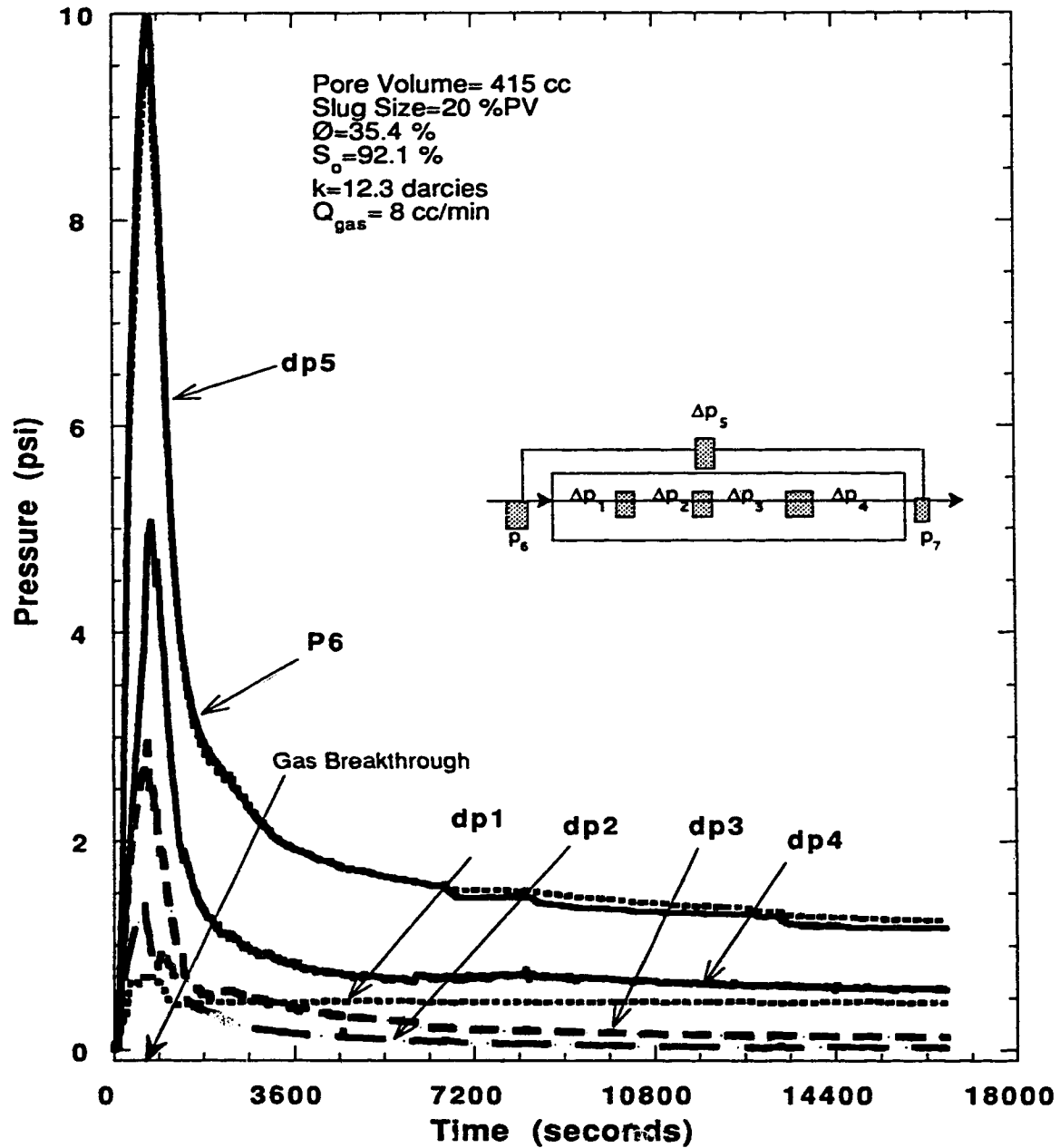


Figure 5.54- Run 35: Pressure Profile, Using 10% Surfactant Concentration, a Slug Size of 20% PV, and a Gas Flow Rate of 8 cc/min in Gas-Oil Displacement.

Experimental Data For Run 15

Pore Volume (cc):	420	Surfactant Name:	Dowfax-8390
Porosity (%)	35.8	Surfactant Concentration (%):	10
Absolute Perm. (darcies):	12.9	Slug size (% PV):	5
Oil Saturation:	28.6	Gas & Surfactant Flow Rate (cc/min):	10, 1
Totalizer Reading at B.T. (cc):	154	Gas Breakthrough Time (min)	15.22
		Cumulative Recovery at B.T. (% PV):	20.43

Sample Number	Time (sec)	Sample Volume (cc)	Cumulative Volume (cc)	Corrected Cumulative Volume (cc)	Totalizer Reading (cc)
1	0	0	0	0.0	0
2	700	64	64	52.3	119
3	913	27	91	85.8	154
4	2023	36	127	103.3	340
5	4263	43	170	109.0	710
6	6446	45	215	117.6	1075
7	10016	66	281	124.1	1670

Table 5.33 : Experimental Data for Run 15, Nitrogen-Surfactant Co-injection.

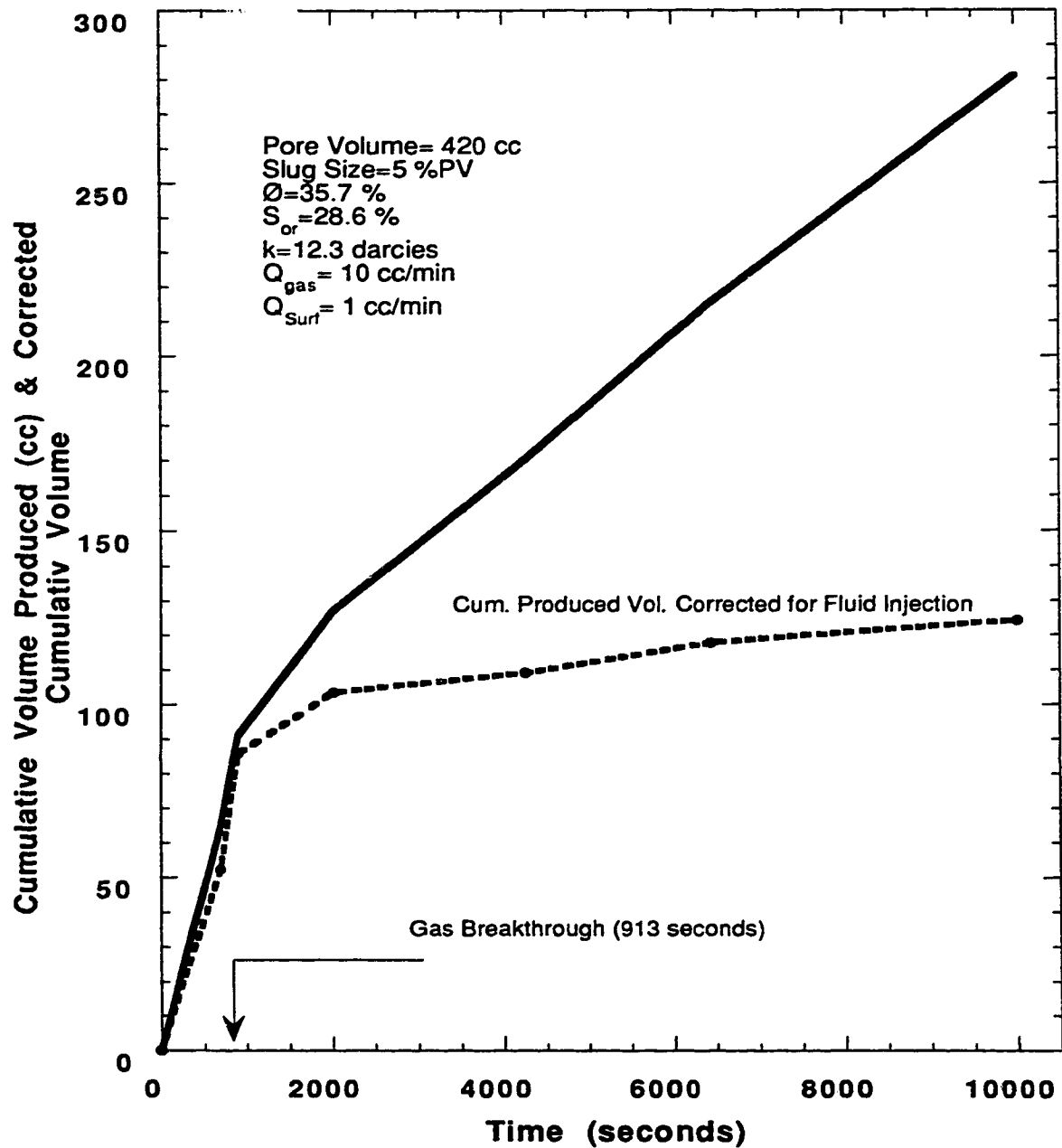


Figure 5.55- Run15: Cumulative Production Versus Time and Concentration Versus Time for Nitrogen Surfactant Co-injection.

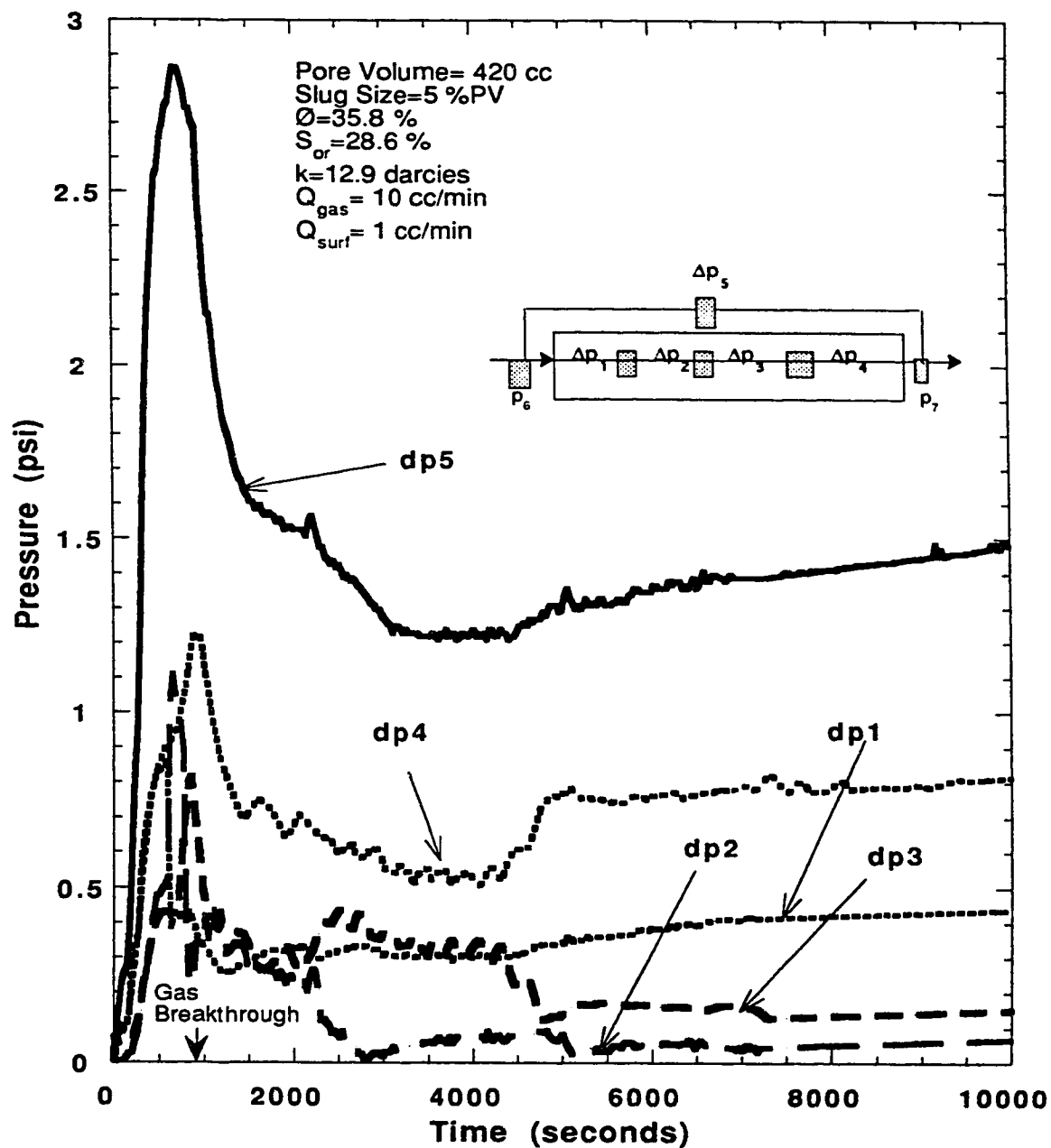


Figure 5.56- Run 15: Pressure Profile, for Nitrogen- Surfactant Co-injection.

%. Later into the experiment this ratio was changed to 1:14 cc/min, giving a quality of 92.5%, to find out if the residual oil would be decreased further.

Table 5.34 gives the experimental data for Run 34. The cumulative volume produced and the corrected cumulative volume produced along with the effluent concentration are drawn in Figure 5.57. Breakthrough occurred after an elapsed time of 22.17 minutes from the start of the experiment. At breakthrough, a corrected cumulative volume of 20.44% PV was produced. After six-and-a-half hours into the experiment, at which time steady state was reached, the foam quality was 92.5%. Before changing the foam quality, 13 cc of oil was produced; this is equivalent to 3.13% reduction in the initial residual oil saturation. Although the increase in foam quality resulted in a higher differential pressure, as can be seen in the pressure profile in Figure 5.58, it did not produce any additional oil. It is obvious from the corrected cumulative volume produced curve that there was some additional liquid produced due to the change in foam quality. The concentration curve was steadily increasing until the moment when the gas flow rate was changed. Then it fell as more of the surfactant was foamed with the extra gas entering the sand pack.

5.6 Foam Flow Mechanisms

The experiments reported in this study provide insight into the mechanisms of foam flow in porous media. The behaviour of foam in porous media is a function of lamellae density. Two foam flow mechanisms have been identified: one when oil is present, foam was breaking and reforming, and one when oil is absent, foam was propagating as a front.

Dowfax-8390 was used in the oil displacement experiments aimed at studying foam flow. In slug injection as well as continuous injection, Dowfax-8390 did not reduce the S_{Or} significantly due to the detrimental effect of oil. Residual oil displacement can be accomplished by increasing the capillary number which is defined by the ratio of the viscous to capillary forces, $\frac{k \Delta P}{L \sigma}$. To reduce the residual oil saturations using foaming surfactants, the capillary number should be increased by decreasing the mobility of the gas and by reducing the interfacial tension between the aqueous and the oil phases. In this study, Dowfax-8390 did not provide any of the elements needed to lower significantly the residual oil saturations.

Experimental Data For Run 34

Pore Volume (cc):	415	Surfactant Name:	Dowfax-8390
Porosity (%):	35.4	Surfactant Concentration (%):	10
Absolute Perm. (darcies):	12.2	Slug size (% PV):	5 & Co-injection
Oil Saturation:	28.9	Gas & Surfactant Flow Rate (cc/min):	4 & 1
Totalizer Reading at B.T. (cc):	89	Gas Beakthrough Time (min)	22.17
		Cumulative Recovery at B.T. (% PV):	20.44

Sample Number	Time (sec)	Sample Volume (cc)	Cumulative Volume (cc)	Corrected Cum. Volume (cc)	Totalizer Reading (cc)	Concentration (Vol%)
1	0	0	0	0	0	0
2	783	57	57	43.95	53	0
3	1330	50	107	84.83	89	0
4	2639	45	152	108.02	175	0.27
5	5731	45	197	101.48	384	0.55
6	7262	35	232	110.97	485	2.86
7	13106	91	323	104.57	875	16.29
8	23752	180	503	107.13	1583	30.36
9	27141	78	581	128.65	6333*	19.46
10	31620	84	665	138.00	7380*	18.91

Table 5.34 : Experimental Data for Run 34, 10% Dowfax-8390, Nitrogen Surfactant Co-injection.

* The gas flow rate was changed to 14 cc/min

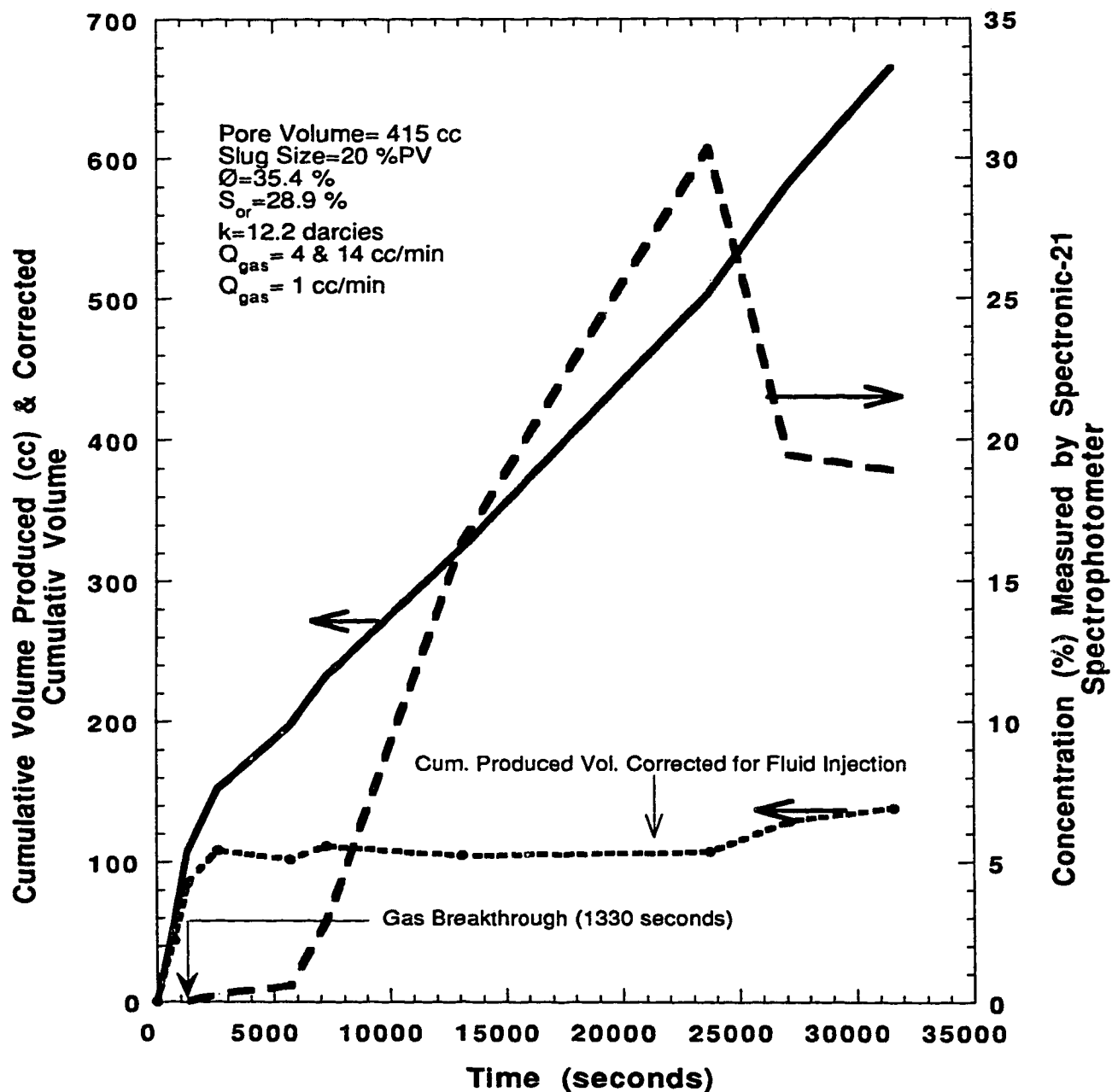


Figure 5.57- Run 34: Cumulative Production Versus Time and Concentration Versus Time for Nitrogen Surfactant Co-injection at Surfactant to Nitrogen Ratio of a) 1: 4 cc/min and b) 1: 14 cc/min.

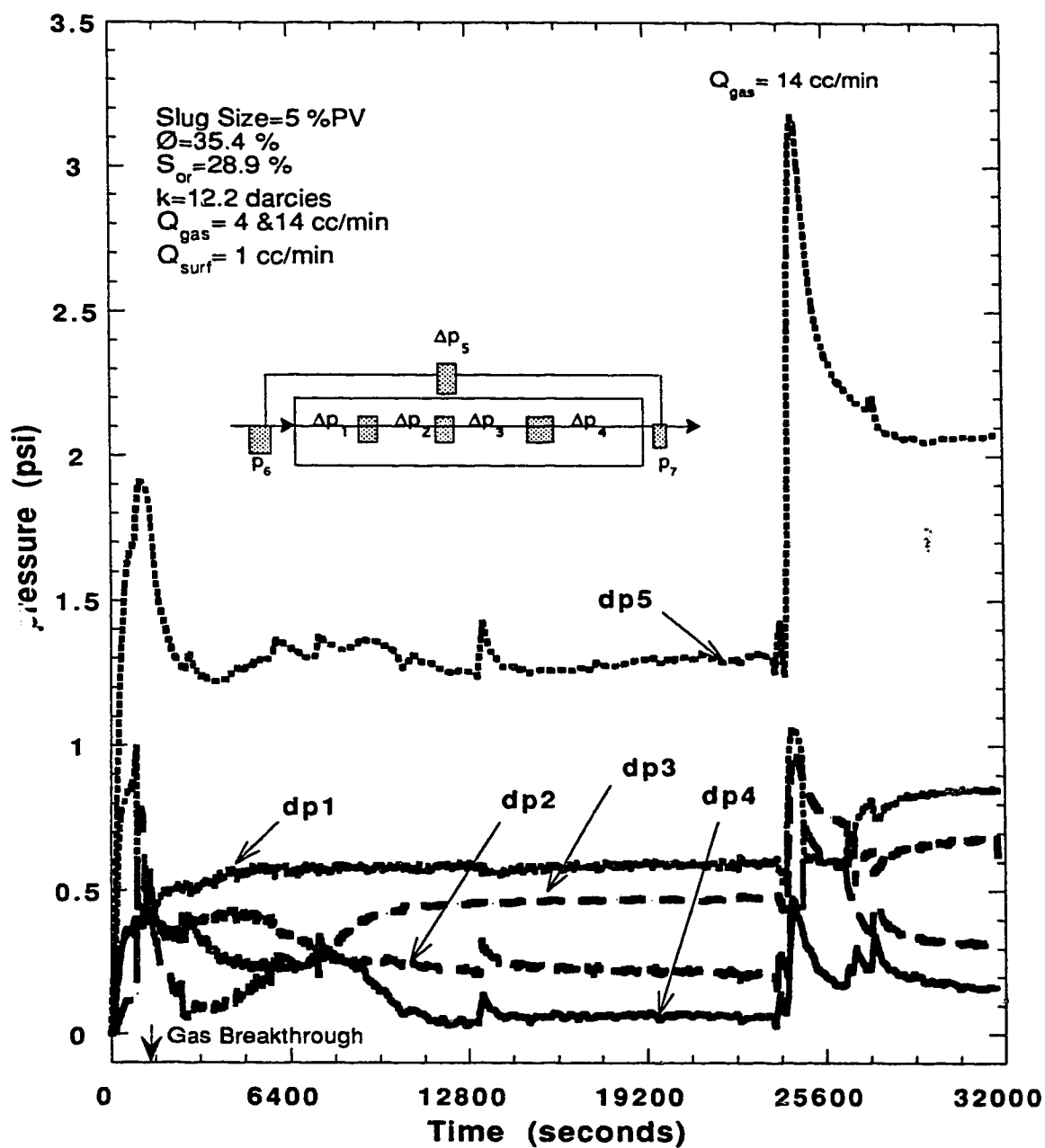


Figure 5.58- Run 34: Pressure Profile, Co-injection of Nitrogen and Surfactant at a Surfactant to Nitrogen Ratio of a) 1:4 cc/min and b) 1:14 cc/min.

Looking at the foam flow mechanism in the presence of oil, first consider the pore level distribution of the three phases. Oil occupies the larger pores in the form of blobs. With three phases present, water is usually the wetting phase and the gas is the non-wetting phase. However, when oil is present in the core, oil is wetting with respect to gas and non-wetting with respect to water. Therefore, oil spreads between the gas and water and forms a thin film. When the gas invades pores filled with the water-surfactant solution and oil, lamellae formation is retarded by the presence of oil and the lamellae cannot span the whole pore. If a lamella does span the pore space, oil soon spreads over it and causes it to collapse. This explains the lower pressure gradients obtained in the experiments conducted in the presence of oil as compared to those in the absence of oil.

Oil was produced in these experiments, even though the amount was small, mainly at the beginning of the foam flood. Run 34, where the change in foam quality led to an increase in the cumulative produced water, but not oil. The change did not produce high enough pressure gradient to lower further the residual oil, as explained previously. Therefore, the oil used in this study has a detrimental effect on foaming with Dowfax-8390.

The foam mechanism identified in the experiments performed in the presence of oil is that the foam is breaking and reforming. This can be seen in the differential pressure response of Runs 27, 29, 30, 31, 32 and 36. These pressure profiles were given previously in Figures 5.38, 5.40, 5.42, 5.44, 5.48 and 5.52, respectively.

The responses of the experiments performed in the absence of oil indicates frontal propagation of foam rather than in situ foam mobilization. In this case the foam stays in the porous medium as can be seen from the pressure response of Run 39, Figure 5.59 that there was no frontal foam propagation and that the pressure increased gradually throughout the entire core. This run was conducted after leaving the core for eight days after the termination of Run 38. After Run 38 was completed, the pressure in the core was allowed to deplete to atmospheric pressure. Then the core was shut off by closing the inlet and outlet valves to prevent evaporation. The core was left for eight days. After eight days, nitrogen injection was initiated and the pressure differential was recorded. Injection started with a gas flow rate of 1.75 cc/min, the same flow rate as used in Run 38. The differential pressure rose to 1.95 psi (13.4 kPa), and stabilized at this level. This was less than the stabilized pressure obtained in Run 38; this implied

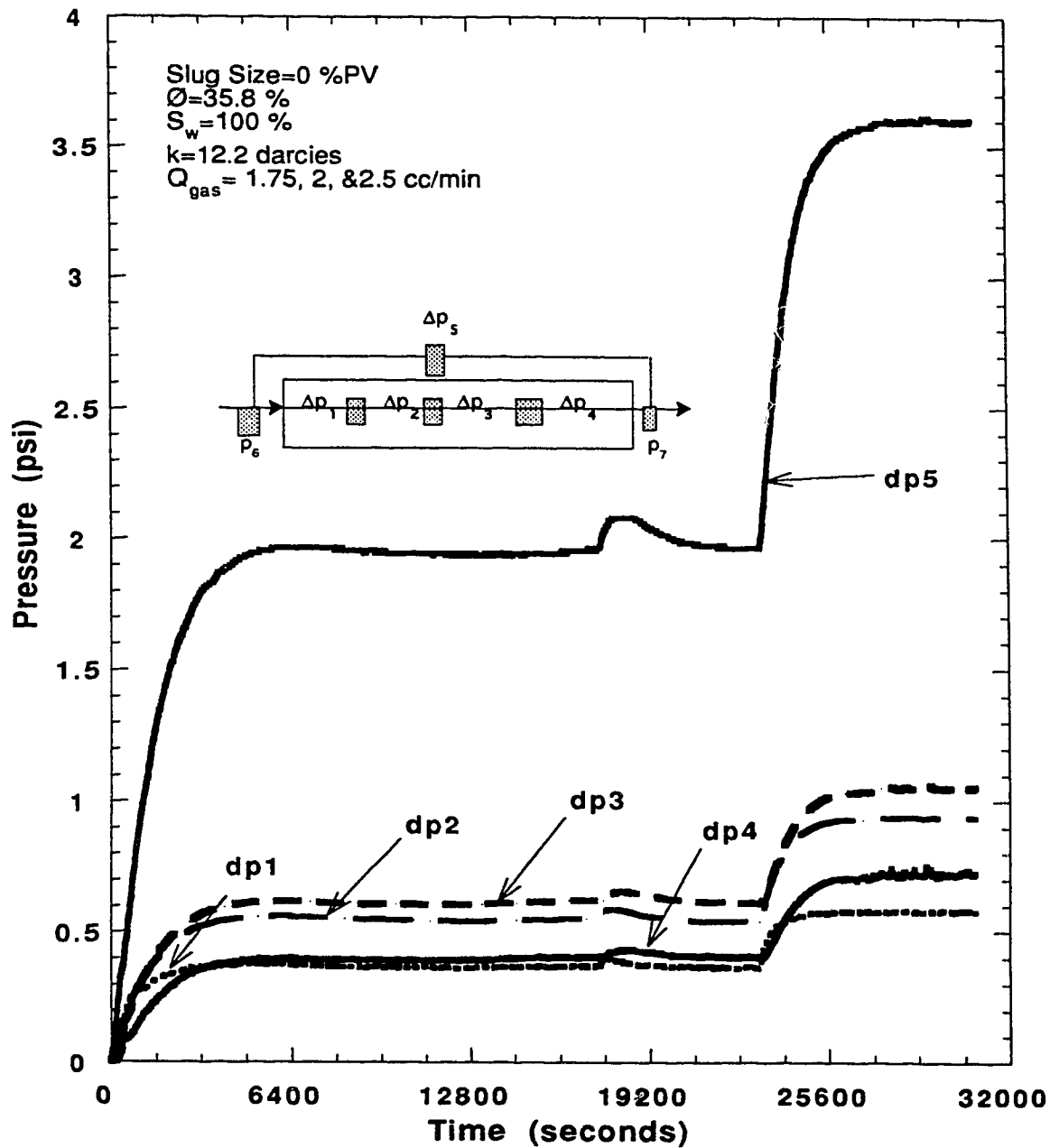


Figure 5.59- Run 39: Pressure Profile Due to Foam That Was Staying in the Porous Medium, Gas Flow Rates used were: 1.75, 2, and 2.5 cc/min.

that the foam was weaker than when originally formed. To find out if the transducers were not off calibration, the gas flow rate was changed twice as can be seen from Figure 5.59 to 2 and 2.5 cc/min. The total differential pressure across the length of the core was equal to the sum of the four individual transducers which meant that the transducers were not off calibration.

When the flow rate was changed, the differential pressure increased indicating an increase in the lamellae density. The pressure gradient rose to 3.6 psi (24.8 kPa) due to the change in gas flow rate. There was no frontal propagation seen from the pressure response in this run. Sharp decrease in the pressure gradients of the different sections of the core was not observed in Run 39. This suggested that the foam occupied the entire sand pack.

Examining the early time response of Run 39 which is shown in Figure 5.60 revealed that no frontal movement was detected. This supports the idea that foam stayed in the porous medium and was occupying the whole sand pack.

In contrast with the above, the early time responses of Runs 19, 37, 38, and 40, in which slug sizes of 20, 2.5, 20, and 10% PV were used, respectively, are examined. Figures 5.61, 5.62, 5.63 and 5.64 represent the early time of Runs 19, 37, 38 and 40, respectively.

These figures clearly demonstrate the frontal propagation of foam. Moreover, the pressure responses of Runs 19 and 38, given earlier in Figures 5.16 and 5.13, verify that foam filled the entire sand pack as the pressure gradients across the four sections of the core rose then stabilized before gas breakthrough.

It is clear from Figure 5.29 that in Run 37 foam did not fill the whole sand pack prior to gas breakthrough. Likewise, the pressure response in Run 40, at the effluent end section of the core, as shown in the dp4 curve in Figure 5.31, suggests that gas breakthrough occurred before the foam front reached the outlet end of the core. Because not enough foam reached the effluent section of the core, the expanding gas caused the lamellae ahead of the front to collapse and the pressure gradient to fall. However, this expanding gas caused the density of the foam lamellae to increase in the other three sections of the core, as can be seen from the rise in the pressure gradients in those sections.

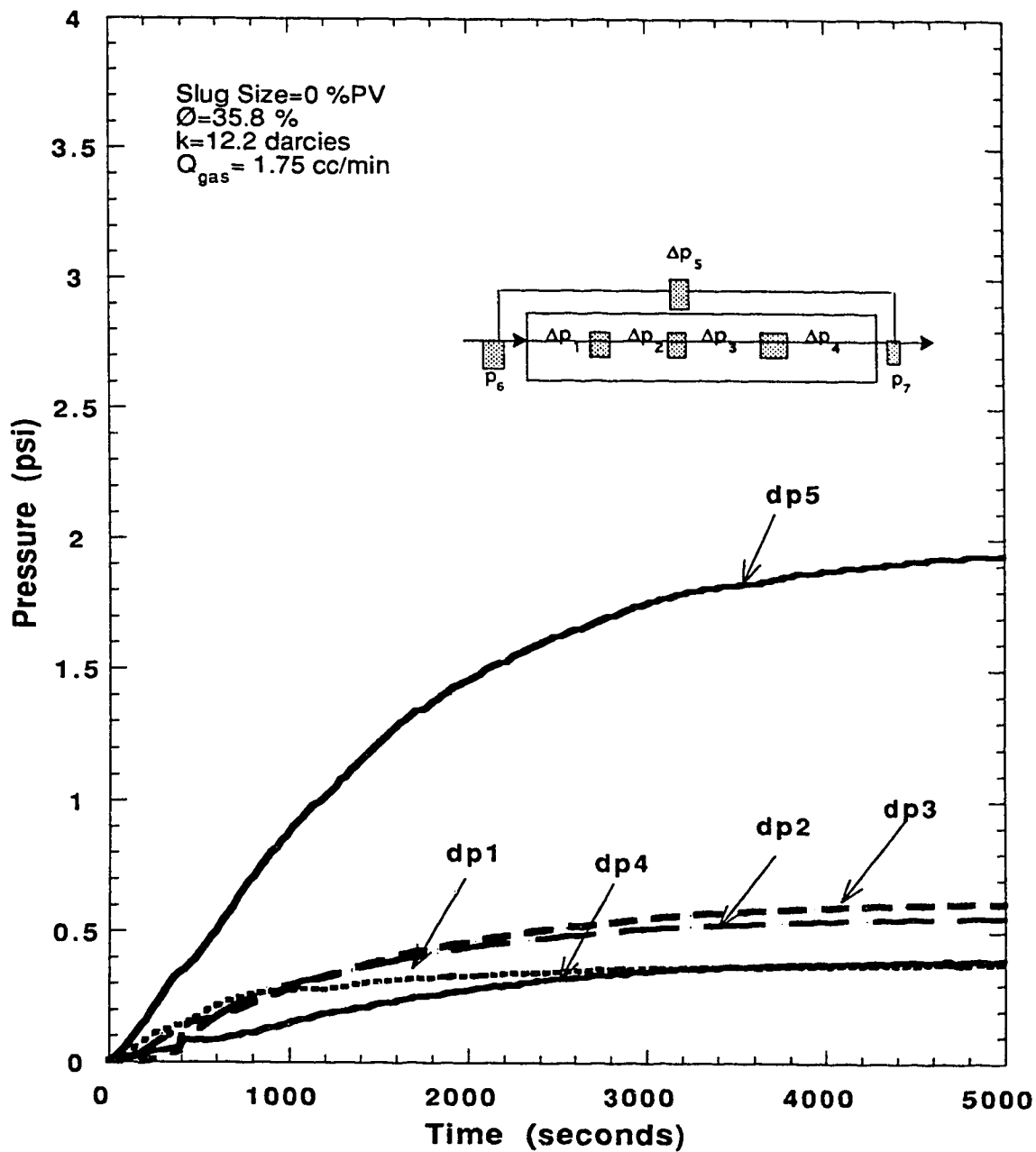


Figure 5.60- Run 39: Early Time of the Pressure Profiles Due to Foam That Was Staying in the Porcus Medium, Gas Flow Rate used was 1.75 cc/min.

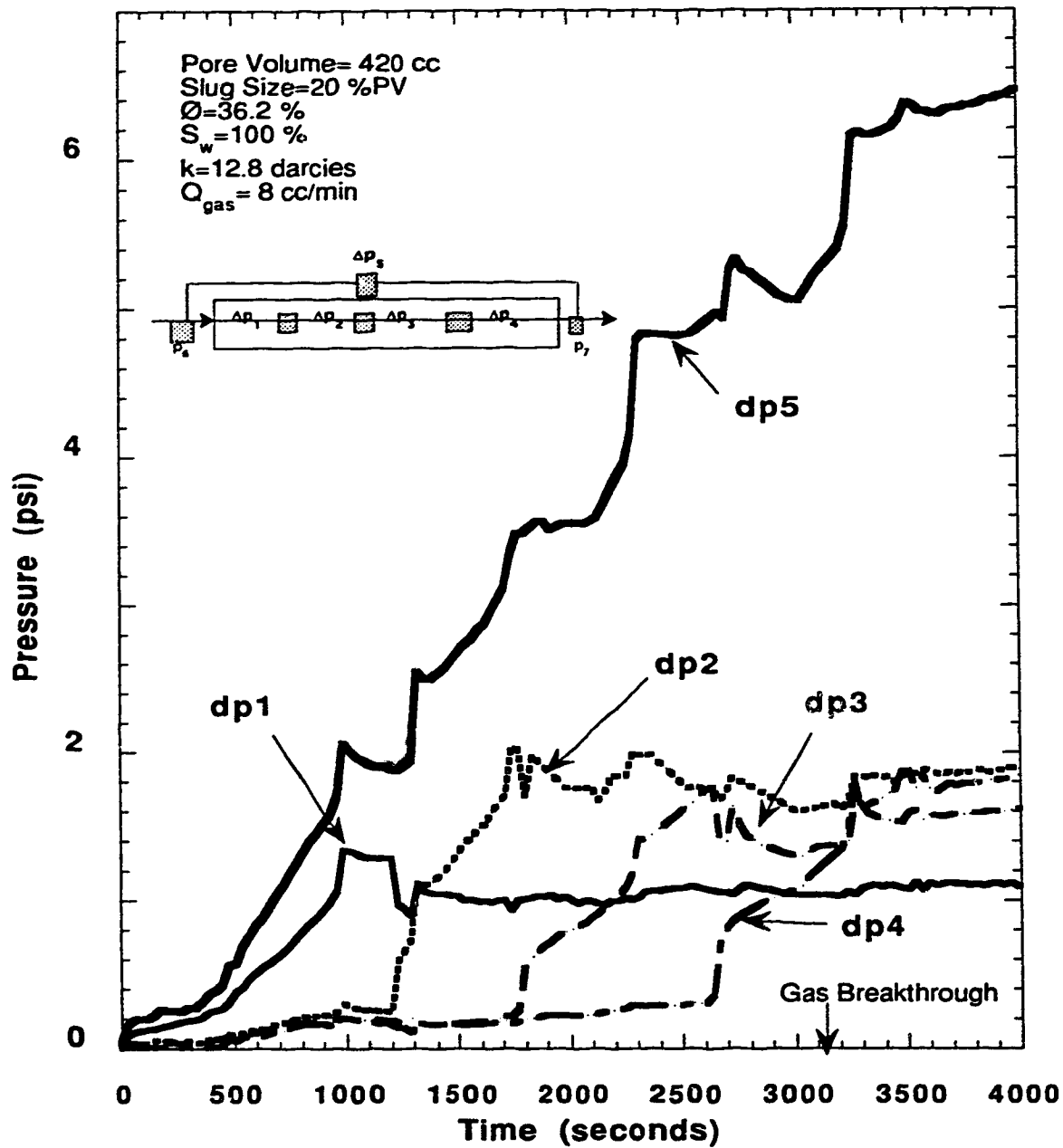


Figure 5.61- Run 19: Pressure Profile Before Gas Breakthrough Using 10% Surfactant Concentration in a Slug of 20% PV Displaced by a Gas flow Rate of 8 cc/min.

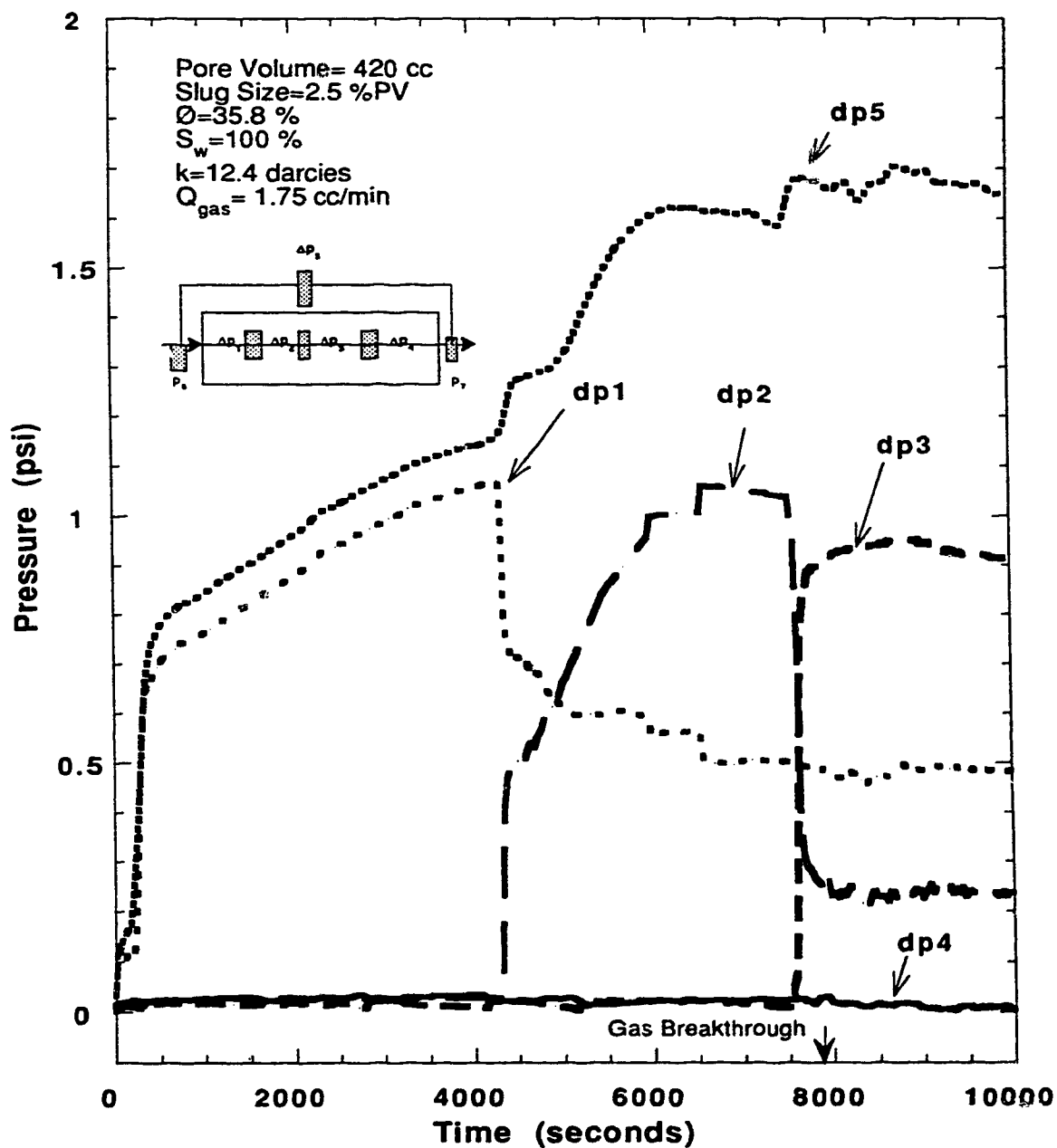


Figure 5.62- Run 37: Pressure Profile Before Gas Breakthrough Using 10% Surfactant Concentration in a Slug of 2.5% PV Displaced by a Gas flow Rate of 1.75 cc/min.

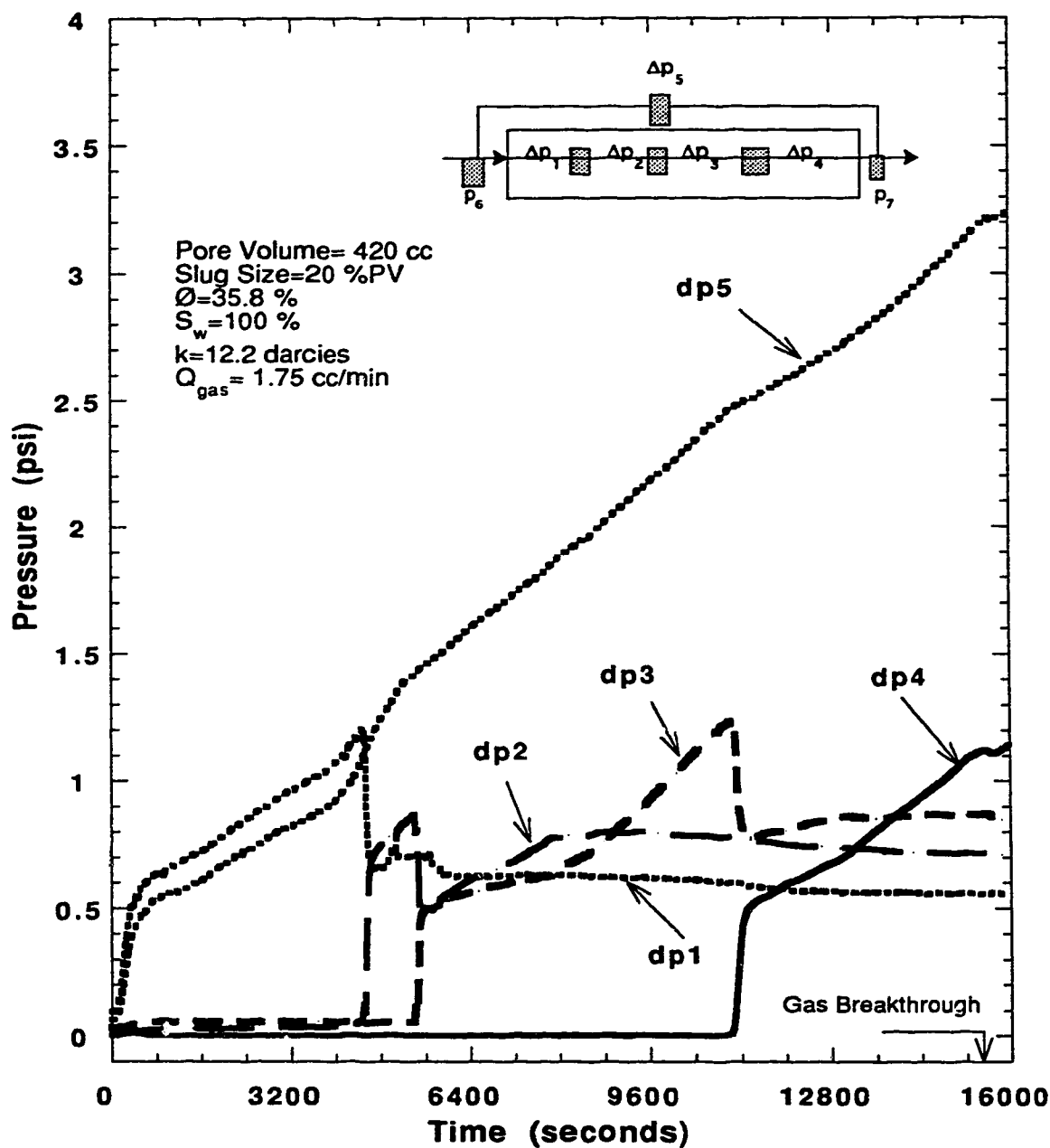


Figure 5.63- Run 38: Pressure Profile Before Gas Breakthrough Using 10% Surfactant Concentration in a Slug of 20% PV Displaced by a Gas Flow Rate of 1.75 cc/min.

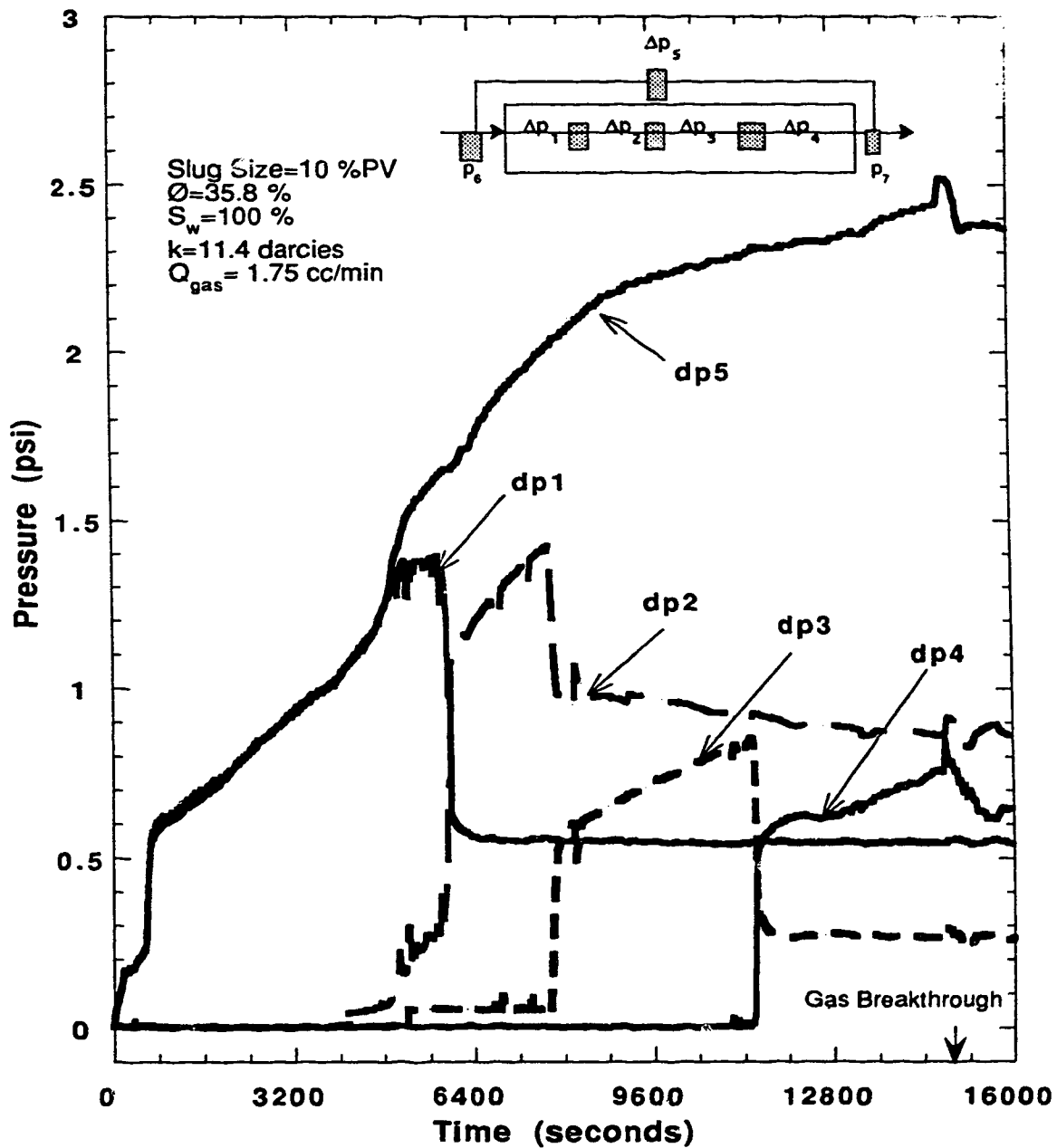


Figure 5.64- Run 40: Pressure Profile Before Gas Breakthrough Using 10% Surfactant Concentration in a Slug of 10% PV Displaced by a Gas flow Rate of 1.75 cc/min.

5.7 Reproducibility Of Results

Several runs were repeated to test experimental reproducibility. Results in Tables 5.35, 5.36 and 5.37 for Runs 21 (Repeat of Run 24), 33-R (Repeat Run 33) and 41 (Repeat of Run 6), respectively, show that experiments where no oil was involved could be repeated within $\pm 2.5\%$. And when oil was involved, Runs 33-R and 41, the repeatability was ± 8.9 and $\pm 18.3\%$, respectively. The lack of reproducibility may be due to gas flowing through different paths in different experiments⁽³⁹⁾ and the surfactant sensitivity to the oil used.

The pressure profiles for Runs 21, 33-R and 41 are shown in Figures 5.65, 5.66 and 5.67, respectively. For Run 21, in which no oil was involved, the pressure profile was reproduced. The pressure profile for Run 33-R was very different from that for Run 33.

Experimental Data for Run 21

Pore Volume (cc):	420	Surfactant Name:	Dowfax-8390
Porosity (%):	35.8	Surfactant Concentration (%):	10
Absolute Perm. (darcies):	12.6	Slug size (% PV):	10
Oil Saturation:	0	Gas Flow Rate (cc/min):	8
Totalizer Reading at B.T. (cc):	400	Gas Breakthrough Time (min)	50.15
		Cumulative Recovery at B.T. (% PV):	79.3

Sample Number	Time (sec)	Sample Volume (cc)	Cumulative Volume (cc)	Totalizer Reading (cc)	Concentration (Vol%)
1	0	0	0	0	0
2	475	50	50	63	0
3	895	45	95	120	0
4	1336	45	140	180	0
5	1728	50	190	230	0
6	2154	45	235	290	0
7	2564	48	283	343	0
8	3009	50	333	400	0.57
9	7210	25	358	960	3.87
10	18626	7	365	2483	23.20

Table 5.35 : Experimental Data for Run 21 Using 10% Dowfax-8390 in a Slug of 10% PV. (Repeat of Run 24)

Experimental Data for Run 33-R

Pore Volume (cc):	420	Surfactant Name:	Dowfax-8390
Porosity (%):	35.8	Surfactant Concentration (%):	10
Absolute Perm. (darcies):	12.2	Slug size (% PV):	10
Oil Saturation:	29.8	Gas Flow Rate (cc/min):	1.75
Totalizer Reading at B.T. (cc):	95	Gas Breakthrough Time (min)	53.85
		Cumulative Recovery at B.T. (% PV):	19.76

Sample Number	Time (sec)	Sample Volume (cc)	Cumulative Volume (cc)	Totalizer Reading (cc)	Concentration (% by Vol.)
1	0	0	0	0	0
2	1961	45	45	59	0
3	3231	38	83	95	0.5
4	7682	41	124	226	0.7
5	20826	36	160	610	1.8

Table 5.36 : Experimental Data for Run 33-R (Repeat of Run 33) Using 10% Dowfax-8390 in a Slug of 10% PV, Run Conducted in Presence of Oil.

Pore Volume (cc):
 Porosity (%):
 Absolute Perm. (darcies):
 Oil Saturation:
 Totalizer Reading at B.T. (cc):

420
 35.8
 11.8
 33.33
 106

Surfactant Name:
 Surfactant Concentration (%):
 Slug size (% PV):
 Gas Flow Rate (cc/min):
 Gas Breakthrough Time (min):
 Cum. Recovery at B.T. (%PV):

Dowfax-8390
 1
 10
 8
 13.28
 17.86

Sample No.	Time (sec)	Sample Volume (cc)	Cumulative Volume (cc)	Totalizer Reading (cc)	Concentration (% Vol)
1	0	0	0	0	0
2	422	45	45	55	0
3	797	30	75	106	0
4	1614	40	115	215	0.55
5	3440	24	139	460	0.97
6	20553	40	179	2740	0.55

Table 5.37 : Experimental Data for Run 41, Repeat of Run 6



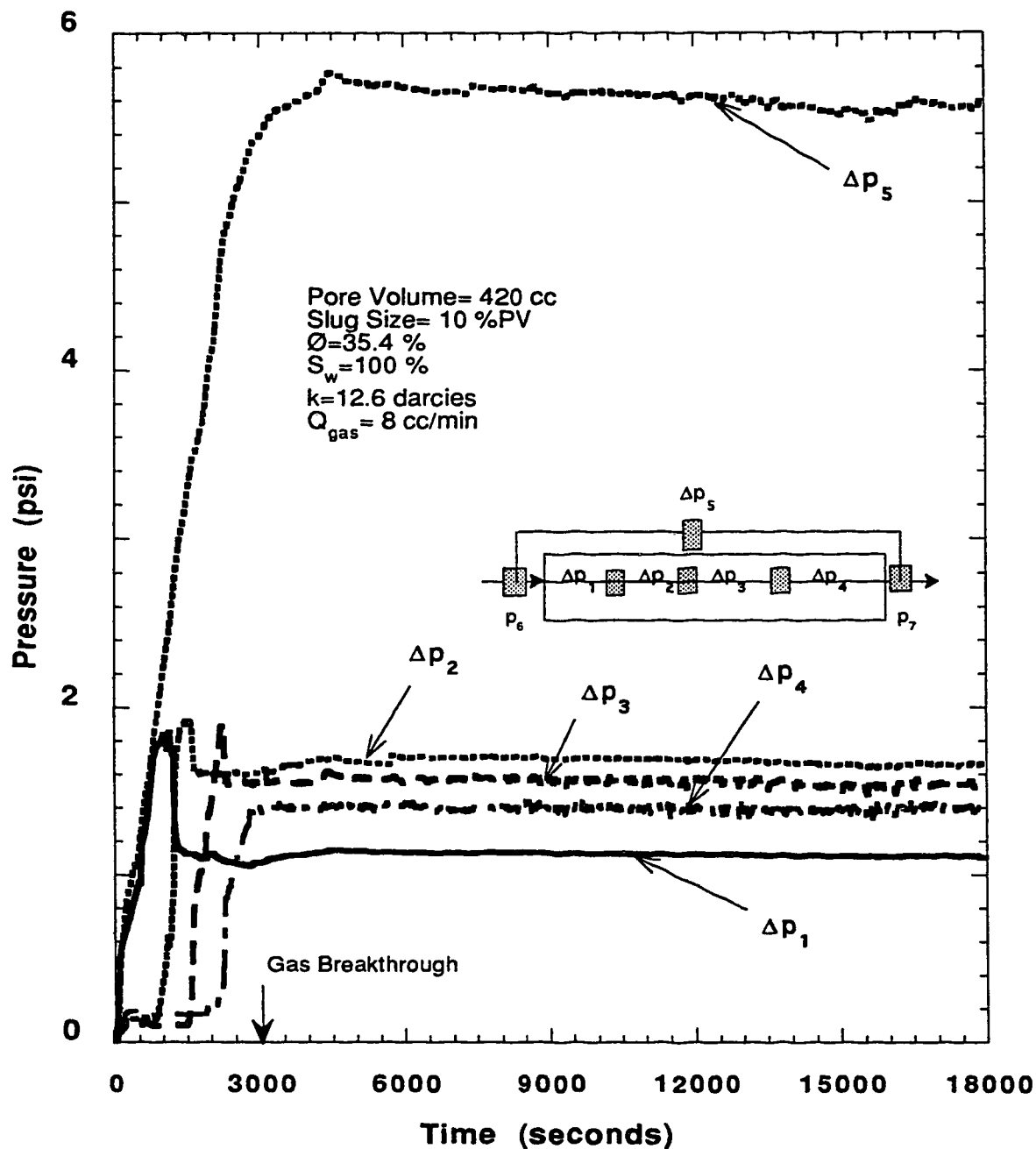


Figure 5.65- Run 21, Repeat of Run 24: Pressure Profile Using 10% Surfactant concentration in a Slug size of 10% PV Displaced by a Gas Flow Rate of 8 cc/min.

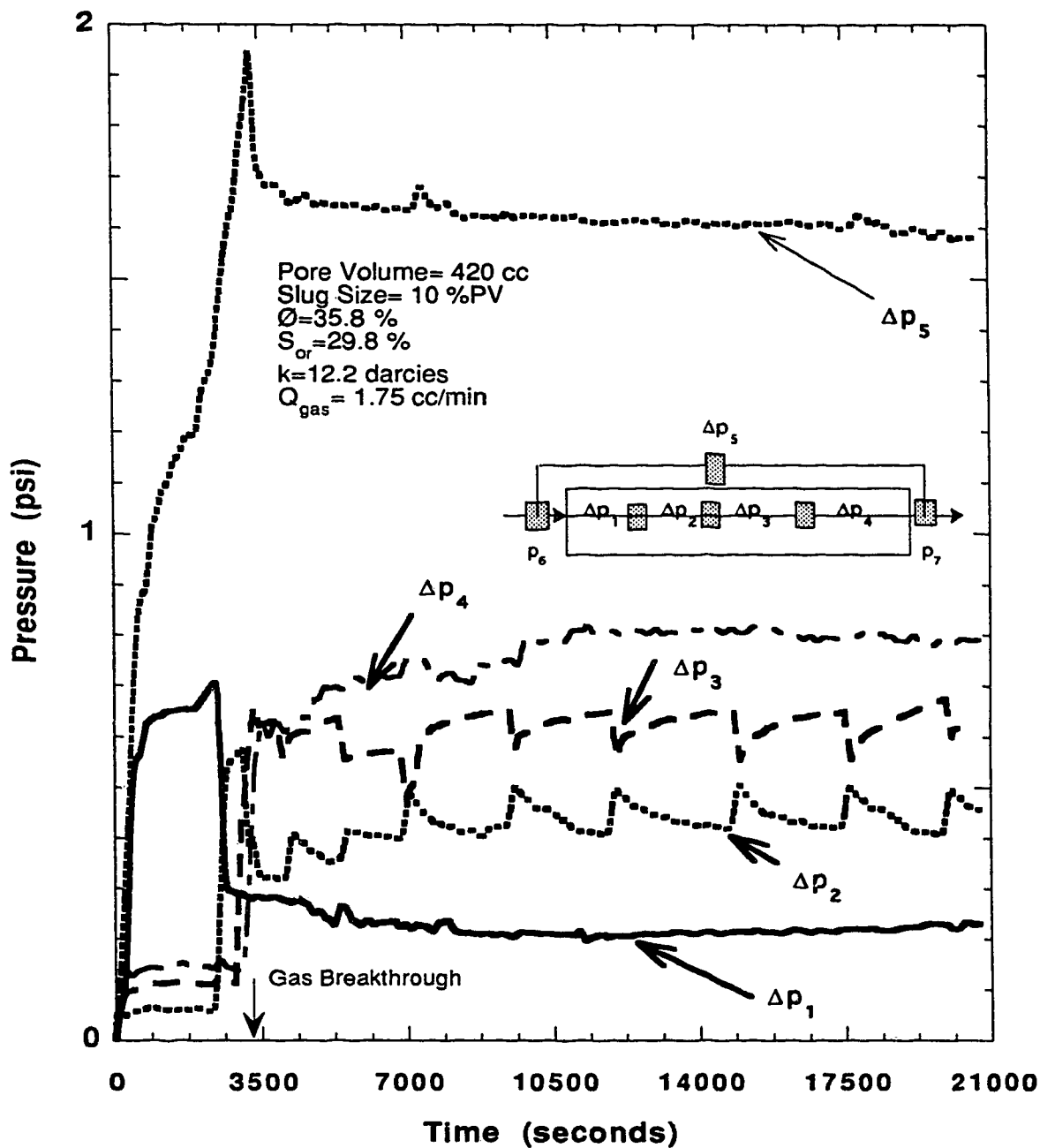


Figure 5.66- Run 33-R, Repeat of Run 33: Pressure Profile Using 10% Surfactant concentration in a Slug size of 10% PV Displaced by a Gas Flow Rate of 1.75 cc/min.

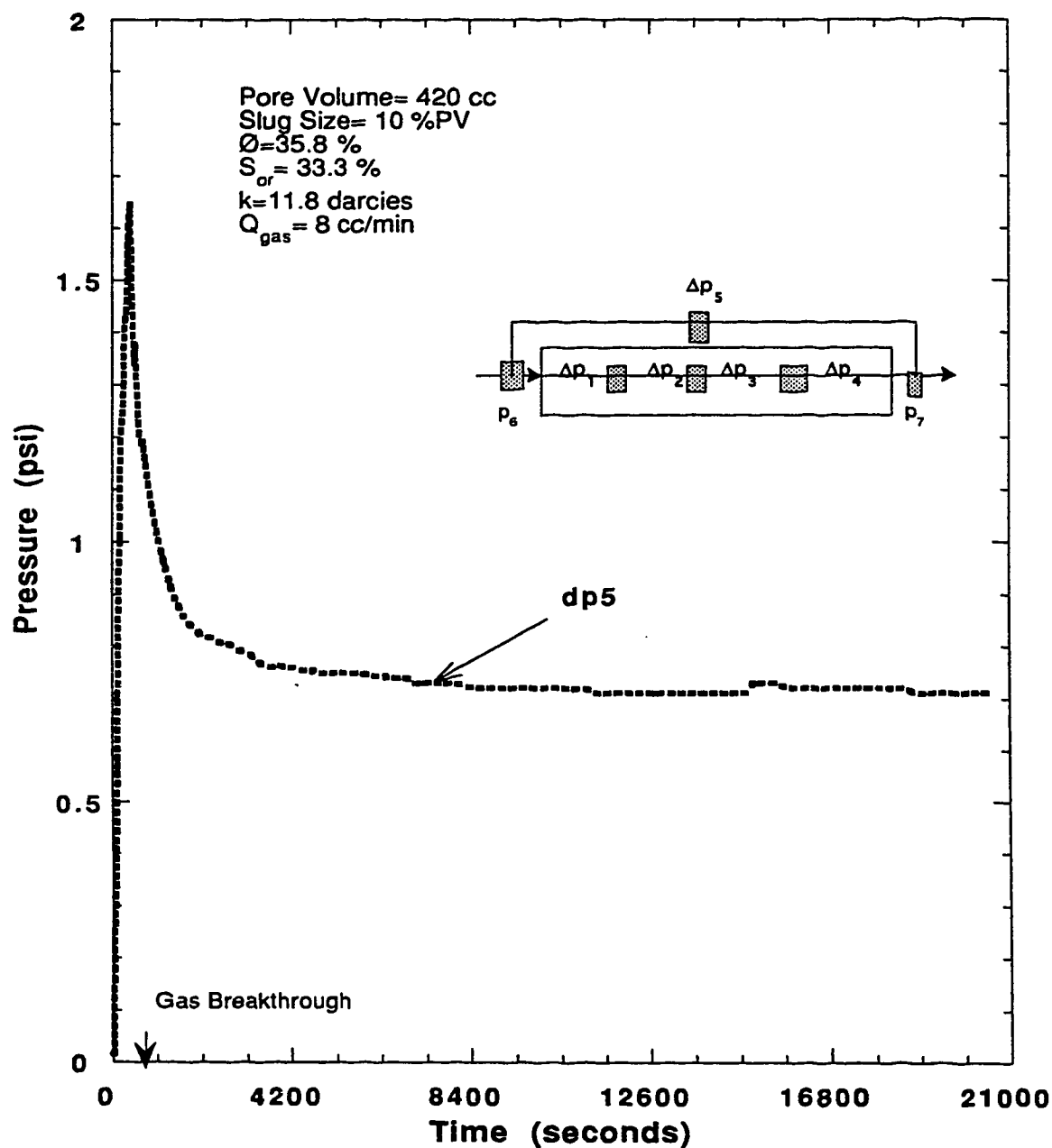


Figure 5.67- Run 41: Repeat of Run 6, Pressure Profile Using 1% Surfactant Concentration in a Slug size of 10% PV Displaced by a Gas Flow Rate of 8 cc/min.

6. Conclusions

Foam flooding experiments were performed to investigate the foam flow mechanism. Foam was formed in situ by injecting nitrogen into sand packs having a foaming surfactant to help in creating foam. The following conclusions are based on the experimental results obtained in this study:

1. Addition of surfactant caused a delay in gas breakthrough. This delay increased the displacement efficiency, resulting in a higher liquid recovery at gas breakthrough.
2. The presence of oil had a deleterious effect on all three surfactants tested. As a result, Dowfax-8390 did not lower the residual oil saturation significantly. Moreover continuous surfactant injection was not any more effective in lowering the residual oil saturations than surfactant slug injection
3. Total foam mobility was found to decrease with increasing surfactant slug size.
4. Two foam flow behaviours were identified: one when no oil is present and one when oil is present. When oil is not present, the foam propagated as a front; that is, there was no in situ mobilization of the lamellae. When oil was present, the foam was broke and reformed.
5. Although the three surfactants tested gave essentially similar results, Dowfax-8390 was a little better in that it gave a higher pressure gradient and a higher liquid recovery at gas breakthrough.
6. Foam was found to stay in the porous medium after the sand pack was left for eight days.
7. No significant effect of the gas flow rate on the cumulative volume of liquid produced at gas breakthrough was observed. However, the higher rate produced higher pressure gradients at the steady state.
8. An optimal surfactant slug size for reducing gas phase mobility was found in water-gas displacement. This slug size of 20% pore volume gave the highest recovery of water at gas breakthrough. In experiments involving oil, there was no optimal slug size in the range tested, 2.5 to 25% pore volume.

7. Recommendations

1. Surfactant selection criteria should be developed to screen different surfactants before one embarks on doing experiments. The surfactants selected should generate strong foam and should be capable of reducing oil-water interfacial tension values significantly.
2. Accurate in situ fluid saturation measurements should be utilized to have a better idea of the fluid distribution and a better definition of the foam front.
3. Experiments should be conducted to investigate foam stability and the parameters affecting it such as liquid viscosity, Marangoni effect and disjoining pressure.
4. Experiments should be conducted to investigate lamellae generation and collapse and their relation to foam texture.
5. Experiments should be undertaken to investigate foam mobility as a function of population balance or bubble size distribution.
6. A population balance method for modeling foam flow in porous media seems to have the simplicity of a black oil simulator and holds promise for future foam modeling. For these reasons, the population balance method should be exploited further.

References

1. Bikerman, J. J.: Foams, Springer-Verlag, New York, 1973.
2. Castanier, L.M. and Brigham, W.E.: "An Evaluation of Field Projects of Steam With Additives", *Society of Petroleum Engineers Reservoir Engineering*, Feb. 1991, pp. 62-68.
3. Hanssen, J.E., Holt, T. and Surguchev, L.M.: "Foam Processes: An Assessment of Their Potential in North Sea Reservoirs Based on a Critical Evaluation of Current Field Experience", paper SPE/DOE 27768 presented at the 9th Symposium on Improved Oil Recovery, Tulsa, OK, April 17-20, 1994.
4. Holbrook, O.C.: "Gas Drive Oil Recovery Process", U.S. Pat. 2 866 507 (1958).
5. Heller, J.P.: "Reservoir Application of Mobility Control Foams in CO₂ Floods", paper SPE/DOE 12644 presented at the 4th SPE/DOE Symposium on Enhanced Oil Recovery, Tulsa, OK, April 15-18, 1984.
6. Krause, R.E., Lane, R.H., Kuehne, D.L. and Bain, G.F.: "Foam Treatment of Producing Wells to Increase Oil Production at Prudhoe Bay", paper SPE/DOE 24191 presented at the 8th Symposium on Enhanced Oil Recovery, Tulsa, OK, April 22-24, 1992.
7. Minssieux, L.: "Oil Displacement by Foams in Relation to Their Physical Properties in Porous Media", *Journal of Petroleum Technology*, Jan. 1974, pp. 100-108.
8. Khatib, Z.I., Hirasaki, G.J. and Falls, A.H.: "Effects of Capillary Pressure on Coalescence and Phase Mobilities in Foams Flowing Through Porous Media", *Society of Petroleum Engineers Reservoir Engineering*, Aug. 1988, pp. 919-925.
9. Duerksen, J.H.: "Laboratory Study of Foaming Surfactants as Steam-Diverting Additives", *Society of Petroleum Engineers Reservoir Engineering*, Jan. 1986, pp. 44-52.
10. Marsden, S.S. and Khan, S. A.: "The Flow of Foam Through Short Porous Media and Apparent Viscosity Measurements", *Society of Petroleum Engineers Journal*, March 1966, pp. 17-23.
11. Falls, A.H., Musters, J.J. and Ratulowski, J.: "The Apparent Viscosity of Foams in Homogeneous Bead Packs", *Society of Petroleum Engineers Reservoir Engineering*, May 1989, pp. 155-164.
12. Marsden, S. S., Earlich, J.J., Albrecht, R.A. and David, A.: "Use of Foam in Petroleum Operations", The Proceedings of the 7th World Petroleum Congress, Mexico City, April 2-7, 1966, pp. 235-242.

13. Hirasaki, G.J. and Lawson, J.B.: "Mechanisms of Foam Flow in Porous Media: Apparent Viscosity in Smooth Capillaries", *Society of Petroleum Engineers Journal*, April 1985, pp. 176-190.
14. De Vries, A.S. and Wit, K.: "Rheology of Gas/Water Foam in the Quality Range Relevant to Steam Foam", *Society of Petroleum Engineers Reservoir Engineering*, May 1990, pp. 185-192.
15. Friedmann, F. and Jensen, J.A.: "Some Parameters Influencing the Formation and Propagation of Foam in Porous Media", paper SPE 15087 presented at the 56th California Regional Meeting of the SPE, Oakland, CA., April 2-4, 1986.
16. Ettinger, R.A. and Radke, C.J.: "Influence of Texture on Steady Foam Flow in Berea Sandstone", *Society of Petroleum Engineers Reservoir Engineering*, Feb. 1992, pp. 83-90.
17. Farouq Ali, S.M. and Seiby, R.J.: "Function, Characteristics of EOR Foam Behavior Covered in Laboratory Investigations", *Oil and Gas Journal*, Feb. 3, 1986, pp. 57-63.
18. Raza, S.H.: "Foam in Porous Media: Characteristics and Potential Applications", *Society of Petroleum Engineers Journal*, Dec. 1970, pp. 328-336.
19. Mast, R.F.: "Microscopic Behavior of Foam in Porous Media", paper SPE 3997, presented at the 47th Annual Fall Meeting of the SPE, San Antonio, TX, Oct. 8-11, 1972.
20. Maini, B.B. and Ma, V.: "Relationship Between Foam Stability Measured In Static Tests and Flow Behavior of Foams in Porous Media", paper SPE 13073 presented at the 59th Annual Technical Conference and Exhibition, Houston, TX, Sept. 16-19, 1984.
21. Chiang, J.C., Sanyal, S.K., Castanier, L.M., Brigham, W.E. and Sufi, A.: "Foam as a Mobility Control Agent in Steam Injection Processes", paper SPE 8912 presented at the 50th Annual California Regional Meeting, Los Angeles, CA, April 9-11, 1980.
22. Owete, S.O. and Brigham, W.E., "Flow Behavior of Foam: A Porous Micromodel Study", *Society of Petroleum Engineers Reservoir Engineering*, Aug. 1987, pp. 315-323.
23. Ross, S.: "Mechanisms of Foam Stabilization and Antifoaming Action", *Chemical Engineering Progress*, Vol. 63, No. 9, Sept. 1967, pp. 41-47.
24. Derjaguin B.V. and Titiievskaja, A.S., *Proceedings of the 2nd International Congress: Surface Activity*, Butterworths, London, 1957 Vol 1, pp. 211-219.
25. Jimenez, A. and Radke, C.: "Dynamic Stability of Foam Lamellae Flowing Through a Periodically Constricted Pore", paper presented at the Symposium on Advances in Oil Field Chemistry 3rd Chemical Congress of the North American Continent, Toronto, Ont, June 5-11, 1988.

26. Penny, W.G. and Blackman, M.: Ministry of Home Security, Great Britain Note 282 (1943).
27. Grove, C.S., Wise, G.E., Marsh, W.C. and Gray, B.J.: "Viscosity of Fire-Fighting Foam" *Industrial and Engineering Chemistry*, May 1951, pp. 1120-1122.
28. Sibree, T.O.: "The Viscosity of Froth", *Trans. Faraday Soc.* (1943), Vol 31, 325.
29. David, A. and Marsden, S.S.: "The Rheology of Foam", paper SPE 2544 presented at the 44th Annual Fall Meeting, Denver, CO, Sept. 28-Oct. 1, 1969.
30. Raza, S.H. and Marsden, S.S.: "The Streaming Potential and the Rheology of Foam", *Society of Petroleum Engineers Journal*, Dec. 1967, pp. 359-367.
31. Mooney, M., "Explicit Formulas for Slip and Fluidity", *Journal of Rheology*. (1931), Vol. 2, No. 2, pp. 210-222.
32. Falls, A.H., Hirasaki, G.J., Patzek, T.W., Gauglitz, D.A., Miller, D.D. and Ratulowski, T.: "Development of a Mechanistic Foam Simulator: The Population Balance and Generation by Snap-off", *Society of Petroleum Engineers Reservoir Engineering*, Aug. 1988, pp. 884-892.
33. Ransohoff, T.C. and Radke, C.J.: "Mechanisms of Foam Generation in Glass-Bead Packs", *Society of Petroleum Engineers Reservoir Engineering*, May 1988, pp. 573-585.
34. Chambers, K.T. and Radke, C.J.: "Capillary Phenomena in Foam Flow Through Porous Media" in Interfacial Phenomena in Petroleum Recovery, Science Series, Morrow, N.R. Ed; Marcel Dekker Inc., New York, 1991, Ch. 6 pp.191-255.
35. Roof, J.G.: "Snap-off Of Oil Droplets in Water-Wet Pores", *Society of Petroleum Engineers Journal*, March 1970, pp. 85-90.
36. Kovscek, A.R. and Radke, C.J.: "Fundamentals of Foam Transport in Porous Media", Topical Report, Prepared fore US. Department of Energy Assistant Secretary for Fossil Energy, Oct. 1993.
37. Friedmann, F., Chen, W.H. and Gauglitz, P.A.: "Experimental and Simulation Study of High-Temperature Foam Displacement in Porous Media: I Incompressible Foam", *Society of Petroleum Engineers Reservoir Engineering*, Feb. 1991, pp. 37-45.
38. Rossen, W.R.: "Theory of Mobilization Pressure Gradient of Flowing Foams in Porous Media", *Journal of Colloid and Interface Science*, Vol 136, No. 1, April 1990.
39. Persoff, P., Radke, C.J., Pruess, K., Benson, S.M. and Witherspoon, P.A.: "A Laboratory Investigation of Foam Flow in Sandstone at Elevated Pressure,"

Society of Petroleum Engineers Reservoir Engineering, June 1991, pp. 365-372.

40. Fried, A.N.: "The Foam-Drive Process for Increasing the Recovery of Oil", U.S. Dept. of the Interior, Bureau of Mines, Report of Investigations # 5866, 1961.
41. Holm, L.W.: "The Mechanism of Gas and Liquid Flow Through Porous Media in the Presence of Foam", *Society of Petroleum Engineers Journal*, Dec. 1968, pp. 359-369.
42. Islam, M.R. and Farouq Ali, S.M.: "Numerical Simulation of Foam Flow in Porous Media", *Journal of Canadian Petroleum Technology*, July-Aug. 1990, pp. 47-57.
43. Islam, M.R, Selby, R.J. and Farouq Ali, S.M.: "Mechanics of Foam Flow in Porous Media and Applications", *Journal of Canadian Petroleum Technology*, July-Aug., 1989, pp. 88-96.
44. Bernard, G.G. and Holm, L.W.: "Effect of Foam on Permeability of Porous Media to Gas", *Society of Petroleum Engineers Journal*, Sept. 1964, pp. 267-274.
45. Bernard, G.G., Holm, L.W. and Jacobs, W.L.: "Effect of Foam on Trapped Gas Saturation and on Permeability of Porous Media to Water", *Society of Petroleum Engineers Journal*, Dec. 1965, pp. 295-300.
46. Holm, L.W. and Garrison, W.H.: "CO₂ Diversion with Foam in an Immiscible CO₂ Field Project", *Society of Petroleum Engineers Reservoir Engineering*, Feb. 1988, pp. 112-118.
47. Huh, D.G. and Handy, L.L.: "Comparison of Steady- and Unsteady-State Flow of Gas and Foaming Solution in Porous Media", *Society of Petroleum Engineers Reservoir Engineering*, Feb. 1989, pp. 77-84.
48. Radke, C.J. and Gillis, J.V.: "A Dual Gas Tracer Technique for Determining Trapped Gas Saturation During Steady Foam Flow in Porous Media", SPE 20519, presented at the 65th SPE Annual Technical Conference., New Orleans, LA, Sept. 23-26, 1990.
49. Flumerfelt, R.W. and Prieditis, J.: "Mobility of Foam in Porous Media", in Surfactant Based Mobility Control Progress in Miscible-Flood Enhanced Oil Recovery, Smith, D.H. Ed; ACS Symposium Series No. 373; American Chemical Society, Washington DC, 1988, Ch. 15, pp. 295-325.
50. Holm, L.W.: "The Mechanism of Gas and Liquid Flow Through Porous Media in the Presence of Foam", paper SPE 1848 presented at the 42nd Annual Fall Meeting of the SPE, Houston, TX, Oct. 1-4, 1967.
51. Heller, J.P., Lien, C.L. and Kuntamukkula, M.S.: "Foam-Like Dispersions for Mobility Control in CO₂ Floods", paper SPE 11233 presented at the 57th

- Annual Fall Technical Conference and Exhibition of the SPE, New Orleans, LA, Sep. 26-29, 1982.
52. Wang, G.C.: "A Laboratory Study of CO₂ Foam Properties and Displacement Mechanism", SPE/DOE 12645, 4th Symposium on EOR, Tulsa, OK, April 15-18, 1984, pp. 169-176.
 53. MacDonald, T. A.: 1988. "Foam Flow in Porous Media", M.Sc. Thesis, University of Alberta.
 54. Chen, H. L., Ke, M.J., Chuang, T.K. and Flumerfelt, R. W.: "Experimental Studies of Capillary Pressure Effects on Foams in Porous Media;" paper SPE 20069 presented at the 60th California Regional meeting, Ventura, CA, April 4-6, 1990.
 55. Dilgren, R.E. and Owens, K.B.: "Surfactant-Enhanced Steam Drives for Heavy Oil Recovery", paper SPE 10774 presented at the California Regional Meeting, San Francisco, CA, March 24-26, 1986.
 56. Chou, S.I., "Conditions for Generating Foam in Porous Media", paper SPE 22628 presented at the 66th Annual Technical Conference and Exhibition of the SPE, Dallas, TX, Oct. 6-9, 1991.
 57. Kuhlman, M.I.: "Visualizing the Effects of Light Oil on CO₂ Foams", *Journal of Petroleum Technology*, July 1990, pp. 902-908.
 58. Manlowe, D.J. and Radke, C.J.: "A Pore-Level Investigation of Foam/Oil Interactions in Porous Media", *Society of Petroleum Engineers Reservoir Engineering*, Nov. 1990, pp. 495-502.
 59. Hudgins, D.A. and Chung, T.H.: "Long-Distance Propagation of Foams", paper SPE/DOE 20196 presented at the 7th Symposium on Enhanced Oil Recovery, Tulsa, OK, April 22-25, 1990.
 60. Schramm, L.L., Turta, A.T. and Novosad, J.J.: "Microvisual and Coreflood Studies of Foam Interactions With a Light Crude Oil", SPE/DOE 20197, 7th Symposium on Enhanced Oil Recovery, Tulsa, OK, April 22-25, 1990, pp. 249-258.
 61. Isaacs, E.E., Jian, L., Green, K. and Maunder, J.D.: "Use of Foam-Forming Surfactants to Enhance the Recovery of Heavy Oils", *AOSTRA Journal of Res.* (1988), Vol 4 pp. 267-276.
 62. Robin, M.: "Laboratory Evaluation of Foaming Additives Used to Improve Steam Efficiency", paper SPE 16729 presented at the 62nd Annual Technical Conference and Exhibition, Dallas, TX, Sept. 27-30, 1987.
 63. McPhee, C.A., Tehrani, A.D. and Jolly, R.P.: "Foam Flooding of Cores Under North Sea Reservoir Conditions;" paper SPE 17360 presented at the SPE/DOE Enhanced Oil Recovery Symposium, Tulsa, OK, April 17-20, 1988.

64. Sanchez, J.M., Schechter, R.S. and Monslave, A.: "The Effect of Trace Quantities of Surfactant on Nitrogen/Water Relative Permeabilities;" paper SPE 15446 presented at the 61st Annual Tech. Conference and Exhibition, New Orleans, LA, Oct. 5-8, 1986.
65. Kanda, M. and Schechter, R.S.: "On the Mechanism of Foam Formation in Porous Media", paper SPE 6200 presented at the 51st Annual Fall Technical Conference and Exhibition of the SPE, New Orleans, LA, Oct. 3-6, 1976.
66. Huh, D.G., Cochrane, T.S. and Kovarik, F.S.: "The Effect of Microscopic Heterogeneity on CO₂/Foam Mobility: Part I -A Mechanistic Study", paper SPE 17359, presented at the SPE/DOE Enhanced Oil Recovery Symposium, Tulsa, OK, April 17-20, 1988.
67. Rossen, W.R., Zhou, Z.H. and Mamun, C.K.: "Modeling Foam Mobility in Porous Media", paper SPE 22627, presented at the 66th Annual Technical Conference and Exhibition of the SPE, Dallas, TX, Oct. 6-9, 1991.
68. Rossen, W.R., Zeilinger, S.C., Shi, J. and Lim, U.: "Mechanistic Simulation of Foam Processes in Porous Media", paper SPE/28940, presented at the 69th Annual Technical Conference and Exhibition of the SPE, New Orleans, LA, Sept. 25-28, 1994.
69. Zhou, Z. and Rossen, W.R.: "Applying Fractional-Flow Theory to Foam Processed at the Limiting Capillary Pressure", paper SPE/DOE 24180, presented at the 8th Symposium on Enhanced Oil Recovery, Tulsa, OK, April 22-24, 1992.
70. Fisher, A.W., Foulser, R.W.S. and Goodyear, S.G.: "Mathematical Modeling of Foam Flooding", paper SPE/DOE 20195, presented at the 7th Symposium on Enhanced Oil Recovery, Tulsa, OK, April 22-25, 1990.
71. Patzek, T.W. and Koinis, M.T.: "Kern River Steam-Foam Pilots", *Journal of Petroleum Technology*, April 1990, pp. 496-503.
72. Marfoe, C.H. and Kazemi, H.: "Numerical Simulation of Foam Flow in Porous Media", paper SPE 16709, presented at the 62nd Annual Technical Conference and Exhibition of the SPE, Dallas, TX, Sept. 27-30, 1987.
73. Pope, G.A.: "The Application of Fractional Flow Theory to Enhanced Oil Recovery", *Society of Petroleum Engineers Journal*, June 1980, pp. 191-205.
74. Chou, S.I., "Percolation Theory of Foam in Porous Media", 7th Symposium on EOR, Tulsa, OK, April 22-25, 1990.
75. Kovscek, A.R., Radke, C.J.: "A Comprehensive Description of Transient Foam Flow in Porous Media", paper presented at the DOE/NIPER Symposium on Field Application of Foams for Oil Production, Bakersfield, CA, Feb. 11-12, 1993.
76. Patzek, T.W.: "Description of Foam Flow in Porous Media by the Population Balance Method", American Chemical Society, 1988.



Appendix A: Tabulated Experimental Results

Experimental Data for Run 20

Pore Volume (cc):	420	Surfactant Name:	Dowfax-8390
Porosity (%):	35.7	Surfactant Concentration (%):	10
Absolute Perm. (darcies):	12.3	Slug size (% PV):	5
Oil Saturation:	0	Gas Flow Rate (cc/min):	8
Totalizer Reading at B.T. (cc):	232	Gas Breakthrough Time (min):	28.97
		Cumulative Recovery at B.T. (% PV):	52.6

Sample Number	Time (sec)	Sample Volume (cc)	Cumulative Volume (cc)	Totalizer Reading (cc)	Concentration (Vol%)
1	0	0	0	0	0
2	480	57	57	67	0
3	919	55	112	124	0
4	1377	56	168	184	0
5	1738	53	221	232	0
6	3286	46	267	440	0.29
7	11218	41	308	1496	0.58
8	18418	15	323	2457	1.99

Table 5.16 : Experimental Data for Run 20 Using 10% Dowfax-8390 in a Slug of 5% PV.

Experimental Data for Run 22

Pore Volume (cc):	415	Surfactant Name:	Dowfax-8390
Porosity (%):	35.4	Surfactant Concentration (%):	10
Absolute Perm. (darcies):	12.5	Slug size (% PV):	25
Oil Saturation:	0	Gas Flow Rate (cc/min):	8
Totalizer Reading at B.T. (cc):	435	Gas Breakthrough Time (min)	54.32
		Cumulative Recovery at B.T. (% PV):	84.82

Sample Number	Time (sec)	Sample Volume (cc)	Cumulative Volume (cc)	Totalizer Reading (cc)	Concentration (Vol %)
1	0	0	0	0	0
2	492	50	50	66	0
3	959	56	106	128	0
4	1393	49	155	188	0
5	1821	50	205	243	0
6	2296	50	255	309	0
7	2779	50	305	371	0
8	3259	47	352	435	29.53
9	5259	21	373	703	33.38
10	18715	28	401	2497	43.26

Table 5.17 : Experimental Data for Run 22 Using 10% Dowfax-8390 in a Slug of 25% PV.

Experimental Data for Run 23

Pore Volume (cc): 420
 Porosity (%): 35.8
 Absolute Perm. (darcies): 12.3
 Oil Saturation: 0
 Totalizer Reading at B.T. (cc): 160
 Surfactant Name: Dowfax-8390
 Surfactant Concentration (%): 0
 Slug size (% PV): 2.5
 Gas Flow Rate (cc/min): 8
 Gas Breakthrough Time (min): 19.62
 Cumulative Recovery at B.T. (% PV): 35

Sample Number	Time (sec)	Sample Volume (cc)	Cumulative Volume (cc)	Totalizer Reading (cc)	Concentration (Vol%)
1	0	0	0	0	0
2	547	55	55	73	0
3	997	65	120	133	0
4	1177	27	147	160	0
5	2521	40	187	335	0.57
6	9727	34	221	1298	1.73
7	17395	21	242	2319	2.04

Table 5.18 : Experimental Data for Run 23 Using 10% Dowfax-8390 in a Slug of 2.5% PV.

Experimental Data for Run 24

Pore Volume (cc):	415	Surfactant Name:	Dowfax-8390
Porosity (%):	35.4	Surfactant Concentration (%):	10
Absolute Perm. (darcies):	12.1	Slug size (% PV):	10
Oil Saturation:	0	Gas Flow Rate (cc/min):	8
Totalizer Reading at B.T. (cc):	395	Gas Breakthrough Time (min):	49.3
		Cumulative Recovery at B.T. (% PV):	77.3

Sample Number	Time (sec)	Sample Volume (cc)	Cumulative Volume (cc)	Totalizer Reading (cc)	Concentration (Vol%)
1	0	0	0	0	0
2	533	50	50	72	0
3	988	54	104	132	0
4	1901	100	204	255	0
5	2346	50	254	314	0
6	2789	50	304	372	0
7	2956	17	321	395	0.27
8	7391	34	355	987	1.11
9	16420	18	373	2189	10.90
10	22322	6	379	2978	27.95

Table 5.19 : Experimental Data for Run 24 Using 10% Dowfax-8390 in a Slug of 10% PV.

Experimental Data for Run 40

Pore Volume (cc):	420	Surfactant Name:	Dowfax-8390
Porosity (%):	35.8	Surfactant Concentration (%):	10
Absolute Perm. (darcies):	11.4	Slug size (% PV):	10
Oil Saturation:	0	Gas Flow Rate (cc/min):	1.75
Totalizer Reading at B.T. (cc):	429	Gas Breakthrough Time (min)	244.12
		Cumulative Recovery at B.T. (% PV):	78.57

Sample Number	Time (sec)	Sample Volume (cc)	Cumulative Volume (cc)	Totalizer Reading (cc)	Concentration (Vol%)
1	0	0	0	0	0
2	2253	50	50	67	0
3	4513	50	100	130	0
4	6780	50	150	196	0
5	9012	50	200	263	0.29
6	11189	50	250	327	0.58
7	13371	50	300	391	0.58
8	14647	30	330	429	1.17
9	30217	15	345	882	2.71

Table 5.22 : Experimental Data for Run 40 Using 10% Dowfax-8390 in a Slug of 10% PV.

Experimental Data for Run 27

Pore Volume (cc):	420	Surfactant Name:	Dowfax-8390
Porosity (%):	35.8	Surfactant Concentration (%):	10
Absolute Perm. (darcies):	12.4	Slug size (% PV):	5
Oil Saturation:	28.6	Gas Flow Rate (cc/min):	8
Totalizer Reading at B.T. (cc):	108	Gas Breakthrough Time (min)	13.42
		Cumulative Recovery at B.T. (% PV):	21.67

Sample Number	Time (sec)	Sample Volume (cc)	Cumulative Volume (cc)	Totalizer Reading (cc)	Concentration (Vol%)
1	0	0	0	0	0
2	518	50	50	70	0
3	805	41	91	108	0
4	3099	45	136	414	0
5	5392	45	181	720	1.11
6	14961	25	206	1995	1.11
7	17588	1	207	2349	NES*

Table 5.25 : Experimental Data for Run 27 Using 10% Dowfax-8390 and a Slug of 5% PV Run Conducted in Presence of Oil.

* Not enough sample to measure concentration

Experimental Data for Run 29

Pore Volume (cc):	420	Surfactant Name:	Dowfax-8390
Porosity (%):	35.8	Surfactant Concentration (%):	10
Absolute Perm. (darcies):	12.3	Slug size (% PV):	10
Oil Saturation:	30.1	Gas Flow Rate (cc/min):	8
Totalizer Reading at B.T. (cc):	113	Gas Breakthrough Time (min)	13.97
		Cumulative Recovery at B.T. (% PV):	22.62

Sample Number	Time (sec)	Sample Volume (cc)	Cumulative Volume (cc)	Totalizer Reading (cc)	Concentration (Vol%)
1	0	0	0	0	0
2	545	50	50	74	0.00
3	838	38	88	113	0.00
4	1547	34	122	210	0.00
5	4999	25	147	667	0.28
6	10189	18	165	1358	0.84

Table 5.26 : Experimental Data for Run 29 Using 10% Dowfax-8390 in a Slug of 10% PV, Run Conducted in Presence of Oil.

Experimental Data for Run 30

Pore Volume (cc):	425	Surfactant Name:	Dowfax-8390
Porosity (%):	36.2	Surfactant Concentration (%):	10
Absolute Perm. (darcies):	12.4	Slug size (% PV):	2.5
Oil Saturation:	28.7	Gas Flow Rate (cc/min):	8
Totalizer Reading at B.T. (cc):	88	Gas Breakthrough Time (min)	10.72
		Cumulative Recovery at B.T. (% PV):	19.3

Sample Number	Time (sec)	Sample Volume (cc)	Cumulative Volume (cc)	Totalizer Reading (cc)	Concentration (Vol%)
1	0	0	0	0	0
2	424	52	52	59	0
3	643	30	82	88	0
4	2365	45	127	318	0.28
5	9899	10	137	1320	2.29
6	17561	10	147	2340	1.99

Table 5.27 : Experimental Data for Run 30 Using 10% Dowfax-8390 in a Slug of 2.5% PV, Run Conducted in Presence of Oil.

Experimental Data for Run 31, 10% Dowfax-8390 And A Slug Of 25% PV

Pore Volume (cc):	415	Surfactant Name:	Dowfax-8390
Porosity (%):	35.4	Surfactant Concentration (%):	10
Absolute Perm. (darcies):	12.4	Slug size (% PV):	25
Oil Saturation:	28.9	Gas Flow Rate (cc/min):	8
Totalizer Reading at B.T. (cc):	85	Gas Breakthrough Time (min)	10.63
		Cumulative Recovery at B.T. (% PV):	19.28

Sample Number	Time (sec)	Sample Volume (cc)	Cumulative Volume (cc)	Totalizer Reading (cc)	Concentration (Vol%)
1	0	0	0	0	0
2	435	50	50	60	0
3	638	30	80	85	0
4	1375	56	136	185	0.30
5	4738	32	168	633	0.57
6	12259	30	198	1636	2.34
7	18587	20	218	2480	3.27

Table 5.28 : Experimental Data for Run 31 Using 10% Dowfax-8390 in a Slug of 25% PV, Run Conducted in Presence of Oil.

Experimental Data for Run 32

Pore Volume (cc):	425	Surfactant Name:	Dowfax-8390
Porosity (%):	36.2	Surfactant Concentration (%):	10
Absolute Perm. (darcies):	12.5	Slug size (% PV):	2.5
Oil Saturation:	28.4	Gas Flow Rate (cc/min):	1.75
Totalizer Reading at B.T. (cc):	104	Gas Breakthrough Time (min)	57.92
		Cumulative Recovery at B.T. (% PV):	20.7

Sample Number	Time (sec)	Sample Volume (cc)	Cumulative Volume (cc)	Totalizer Reading (cc)	Concentration (Vol%)
1	0	0	0	0	0
2	2169	50	50	65	0
3	3475	38	88	104	0
4	5001	25	113	148	0
5	13988	17	130	410	0.84
6	16098	5	135	470	0.28

Table 5.29 : Experimental Data for Run 32 Using 10% Dowfax-8390 in a Slug of 2.5% PV, Run Conducted in Presence of Oil.

Experimental Data for Run 33

Pore Volume (cc):	415	Surfactant Name:	Dowfax-8390
Porosity (%):	35.4	Surfactant Concentration (%):	10
Absolute Perm. (darcies):	12.3	Slug size (% PV):	10
Oil Saturation:	28.9	Gas Flow Rate (cc/min):	1.75
Totalizer Reading at B.T. (cc):	109	Gas Breakthrough Time (min)	63
		Cumulative Recovery at B.T. (% PV):	21.69

Sample Number	Time (sec)	Sample Volume (cc)	Cumulative Volume (cc)	Totalizer Reading (cc)	Concentration (Vol%)
1	0	0	0	0	0
2	1945	45	45	56	0
3	3780	45	90	109	0.41
4	4271	15	105	127	0.28
5	8130	28	133	236	0.55
6	18596	25	158	542	0.84
7	21426	4	162	625	1.41

Table 5.30 : Experimental Data for Run 33 Using 10% Dowfax-8390 in a Slug of 10% PV, Run Conducted in Presence of Oil.

Experimental Data for Run 36

Pore Volume (cc):	415	Surfactant Name:	Dowfax-8390
Porosity (%):	35.4	Surfactant Concentration (%):	10
Absolute Perm. (darcies):	12.4	Slug size (% PV):	20
Oil Saturation:	31.3	Gas Flow Rate (cc/min):	1.75
Totalizer Reading at B.T. (cc):	95	Gas Breakthrough Time (min)	54.12
		Cumulative Recovery at B.T. (% PV):	21.21

Sample Number	Time (sec)	Sample Volume (cc)	Cumulative Volume (cc)	Totalizer Reading (cc)	Concentration (Vol%)
1	0	0	0	0	0
2	1151	30	30	36	0
3	2252	30	60	67	0.28
4	3247	28	88	95	2.12
5	6121	45	133	180	3
6	12372	30	163	360	1
7	25728	8	171	750	0.51

Table 5.31 : Experimental Data for Run 36 Using 10% Dowfax-8390 and a Slug of 20% PV, Run Conducted in Presence of Oil.

Appendix B: Data For the Surfactants Used

Surfactant Name: Dowfax 8390

181

Supplier: Dow chemical company
Midland, MI 486674, U.S.A.

Chemical Name: no data available

Formula: no data available

Hazardous decomposition products: sulfur dioxide

Incompatibility (Keep away from):
acids

Toxic and hazardous ingredients: no data available

Form: liquid

Appearance: amber to light brown liquid

Odor: disinfectant-type

Colour: light brown

Specific Gravity (water=1): 1.03-1.13

Boiling Point: 100 °C

Melting Point: no data available

Solubility in water (by weight %): completely miscible

Volatile (by weight %): no data available

Evaporation rate: no data available

Vapor pressure (mm Hg at 20 °C): 17.8 mmHg

Vapor density (air = 1): no data available

pH (5 %): no data available

Stability: Product is stable under normal conditions

Viscosity SUS at 100 °F: no data available

Surfactant Name: Witcolate 1276

182

Supplier: Oleochemicals/Surfactant
3200 Brookfield St., Houston, TX, 77045

Chemical Name: alkyl ether sulfate, ammonium salt

Formula: no data available

Hazardous decomposition products:

carbon monoxide and carbon dioxide from burning.
oxides of sulfur

Incompatibility (Keep away from):

avoid contact and/or mixing with strong bases. Contact with strong base
will liberate amine

Toxic and hazardous ingredients:

2 - propanol or ethanol

Note: This product may contain trace amounts of 1,4 - Dioxane. See

COMMENTS section further details

Form: liquid

Appearance: clear liquid

Odor: bland

Colour: light yellow

Specific Gravity (water=1): 1.01

Boiling Point: no data available

Melting Point: less than 10 °F

Solubility in water (by weight %): soluble at 25 °C

Volatile (by weight %): 40-46

Evaporation rate: not applicable

Vapor pressure (mm Hg at 20 °C): no data available

Vapor density (air = 1): no data available

pH (5 %): 7.5 to 8

Stability: Product is stable under normal conditions

Viscosity SUS at 100 °F: no data available

Surfactant Name: Witcolate 1247H

183

Supplier: Oleochemicals/Surfactant
3200 Brookfield St., Houston, TX, 77045

Chemical Name: alcohol ether sulfate, ammonium salt

Formula: no data available

Hazardous decomposition products:

carbon monoxide and carbon dioxide from burning.
oxides of sulfur

Incompatibility (Keep away from):

strong oxidizers such as hydrogen peroxide, bromine and chromic acid.

Toxic and hazardous ingredients:

2 - propanol

Note: This product may contain trace amounts of 1,4 - Dioxane. See
COMMENTS section further details

Form: liquid

Appearance: clear liquid

Odor: bland

Colour: light amber

Specific Gravity (water=1): 1.06

Boiling Point: no data available

Melting Point: no data available

Solubility in water (by weight %): soluble at 25 °C

Volatile (by weight %): 30-34

Evaporation rate: not available

Vapor pressure (mm Hg at 20 °C): 31

Vapor density (air = 1): no data available

pH (5 %): 7 to 8.5

Stability: Product is stable under normal conditions

Viscosity SUS at 100 °F: no data available